UNIVERSITY OF SOUTHAMPTON

OLIGOMERIC LIQUID CRYSTALS

by

Peter Jeremy Barnes

A dissertation submitted in partial
fufilment of the requirements for
the degree of Doctor of Philosophy
at the University of Southampton

Department of Chemistry

May 1994

UNIVERSITY OF SOUTHAMPTON

ABSTRACT

FACULTY OF SCIENCE

Doctor of Philosophy

OLIGOMERIC LIQUID CRYSTALS

by Peter Jeremy Barnes

The work presented in this Thesis is concerned with the synthesis and characterisation of liquid crystalline dimers and trimers. The role of the alkyl spacer and the mesogenic groups are shown to have a critical influence on the mesogenic behaviour of these oligomers. Chapter 1 provides a general account of the liquid crystal phase together with some structure-property relationships and the experimental techniques used to characterise their liquid crystalline behaviour. Chapter 2 introduces the reader to order parameters and distribution functions which provides a background for the technique of nuclear magnetic resonance spectroscopy, NMR, as used to determine the orientational order parameters within the liquid crystal phase. In Chapter 3 the odd-even behaviour of some methylene linked cyanobiphenyl dimers has been examined alongside that of analogous ether linked dimers by NMR spectroscopy using anthracene-d_{10} as a solute. The odd-even behaviour of these dimers is shown to depend critically on molecular geometry. Dimers containing both an oxy and a methylene link have been similarly examined. A smectic phase, exhibited by odd dimers containing a methylene link, is characterised in 1,7-bis(4'-cyanobiphenyl-4-yl)heptane, using a variety of techniques. The diminished odd-even effect of a homologous series of carbonate linked cyanobiphenyl dimers is reported in Chapter 4. Chapter 5 details the use of deuterium NMR spectroscopy to determine the order parameters of the specifically deuteriated mesogenic groups in two short length cyanobiphenyl terminated liquid crystal trimers whose mesogenic groups are predicted to be ordered to different extents. Chapter 6 reports the mesogenic behaviour of four novel homologous series of non-symmetric trimers which contain two alkyl spacers of different lengths. Finally, Chapter 7 describes the synthesis and transitional properties of two series of cyanobiphenyl terminated liquid crystal trimers containing a naphthyl moiety as the central mesogenic core.

Inspiration of the day

'If I can do it.....'

Anon.

CONTENTS

Acknowledgements

I would like to thank my supervisor, Professor G.R. Luckhurst for his continued guidance, enthusiasm and faith. All of which have helped me tremendously with my studies and seen me through to completing this Thesis.

I must also thank Dr. Andrew Douglass for the synthesis of the compound CB7CB and Chris Dunn for carrying out the ESR experiments that are presented in Chapter 3.
On a slightly less academic level I want to mention Dr. Andrew Douglass and Dr. Ian Fletcher (who both managed to pip me to the post), Flavio dos Santos, Andrew Blatch, Chris Dunn and all the other members of the liquid crystal group who have made my time at the university so memorable. I also want to thank my friends outside of the Chemistry Department notably Dan, Jill, Melissa and Adam together with the rest of the London crowd who have all been great over the past few years and of course my parents who have, at least most of the time, been a tower of supportive encouragement.

Finally I am grateful to my industrial sponsors, Merck Ltd., Poole and to the SERC for the award of a CASE studentship.

CHAPTER 1

Introduction to liquid crystals

1.The liquid crystalline state

Some solids, mainly organic in nature, do not melt directly into the isotropic liquid, under certain circumstances they form a turbid liquid which is birefringent, a property typically exhibited by crystalline solids, but they flow under shear, a property typically exhibited by liquids. These 'positionally disordered' crystals or 'orientationally disordered' liquids are called liquid crystals, a term first coined by Lehmann in 1904 [1] to embody this duality of properties. There are two main types of liquid crystal namely thermotropic and lyotropic. The former are formed through thermal effects; either by heating a solid or cooling a liquid phase.The latter are usually composed of two or more components, for example, soap and water, here, solute molecules interact with a solvent to form aggregates which, at certain compositions, form lyotropic liquid crystal phases [2] i.e. they differ in the nature of the anisotropic unit; single molecules for thermotropic liquid crystals and micelles/aggregates for lyotropic.

In this Thesis the work is concerned solely with thermotropic liquid crystals. This fascinating class of materials was first documented by Reinitzer in the late nineteenth century when he noted the two-stage melting of cholesteryl benzoate [3]. Research into the nature of this new state of matter flourished up until the Second World War when the scientists of the time thought that all the problems concerning liquid crystals had been solved and so directed their talents to other areas. It was not until the late fifties/early sixties that scientists began to re-examine the liquid crystal

phenomenon. Microscopic theories were quickly established as was the ability of liquid crystals to detect extremely small changes in temperature, mechanical stress, electromagnetic radiation and chemical environment. From these potential applications came the discovery that a thin layer of liquid crystal material was capable of switching from a clear to cloudy state when an electrical voltage was applied. This early display paved the way for the wealth of electro-optic devices, knowledge and research that continues to fascinate scientists today.

In this introductory Chapter we will describe some of the forms a liquid crystal phase can adopt and then give an account of some of the structure-property relationships that pertain to liquid crystal formation. This is followed by a discussion of some of the techniques used to characterise these intriguing materials.

2. The liquid crystal phases

The thermotropic class of liquid crystals can be further broken down according to the long range spatial and angular arrangements of the molecules with respect to one another. Three basic types† of mesophase exist: nematic, cholesteric and smectic, although the nematic and cholesteric phases are very closely linked. The constituent molecules of all three types have the fundemental requirement of shape anisotropy. In most liquid crystals this means rod-like molecules whose long axes tend to lie parallel even when separated by large molecular distances. However discotic liquid crystals are also known [5]. Discotic mesophases are formed by molecules with a disc-like structure, they exhibit nematic phases although the discs can also stack together in columns which then arrange themselves to form additional liquid crystalline phases, the so-called columnar phases. The majority of the work described in this Thesis is concerned with the nematic phase.

†A fourth, the biaxial nematic phase, has been predicted to exist for thermotropic liquid crystals, but as yet has not been experimentally confirmed unambiguously [4].

2.1 The nematic phase (N)

The simplest and most disordered of the liquid crystal phases is the optically uniaxial nematic phase, a name derived from the Greek word for thread which recalls one of their optical textures. In low molecular mass liquid crystals, the viscosity of this phase is usually low and it flows like a liquid, however, for nematic glasses and some polymers it is solid like. It is commonly bounded by a smectic or crystalline phase at low temperatures and an isotropic liquid at high temperature. The nematic consists of elongated molecules whose centres of mass are randomly arranged, except at short range, throughout the sample but the long axes of the molecules, over a long range, line up parallel to a preferred direction in space, called the director, n. The ability of a small electric or magnetic field to orient these directors uniformly thus producing true macroscopic order is a property which is utilised in most of the electro-optic display devices currently available [6].

2.2 The cholesteric phase

Closely related to the nematic is the cholesteric phase. Indeed the two are not discernible on a molecular scale, but they differ significantly in that the director is not randomly arranged in space but undergoes a helical distortion. The cholesteric or, more properly, the chiral nematic phase is exhibited only by chiral molecules or compounds doped with some chiral material. The structure may be simplistically envisaged as composed of regions of nematic liquid crystal, the direction of an individual region is rotated through a microscopic angle with respect to the director in adjacent regions. As a succession of regions is passed through, the director turns through 360° and the distance traversed represents the pitch length of the helix. When the pitch is of the order of the wavelength of visible light Bragg scattering occurs and the phase becomes coloured. Changing the temperature when the system is coloured will alter the pitch of the helix, normally because of pretransitional

behaviour prior to the transition to a smectic A phase, and hence the colour. This thermochromic property has found numerous applications [7]. The helical structure can be removed by the action of an electric or magnetic field which aligns the director parallel to the field as long as $\Delta\chi$ and $\Delta\varepsilon > 0$. Since the cholesteric phase is only formed by optically active species, a racemic mixture will give a nematic mesophase.

2.3 The smectic mesophase

The smectic phase, named after the Greek word for soap because of their soap-like consistency, possess some degree of translational order as well as the long range orientational order which is typical of all liquid crystals. From a structural point of view, all smectics are layered with a well-defined interlayer spacing, which can be measured by X-ray diffraction [8]. This extra degree of order gives rise to three main types which are identified by the letters A, B and C; this is a purely chronological nomenclature with no structural implications. Further in this classification there are at least eight other recognised polymorphic smectic modifications (designated D-K, although the S_D phase does not possess the stratified molecular arrangement common to other smectics) with several more variations as yet not fully characterised or documented, but these are beyond the bounds of this text and will not be discussed.

2.3.1 Smectic A

This is the simplest smectic structure with a layer thickness close to the full length of the constituent molecules first recognised by Friedel [9]. Within each layer, the centres of mass of the molecules show no long range order, and each layer can be regarded as a two dimensional nematic. The system is optically uniaxial with the optical axis normal to the planes of the layers. Further sub-divisions such as S_{A2},

S_{Ad} and $S_{\tilde{A}}$ have been recognised. These structures are usually exhibited by polar molecules, and result from specific molecular interactions which can mean that the basic structural unit within the smectic A phase is a dimer.

2.3.2 Smectic C

The smectic C phase contrasts with the smectic A phase by being optically biaxial, this feature can be interpreted by regarding the director as being tilted with respect to the normal of the layers. These layers are free to slide over one another as in the smectic A phase, i.e. there is no long range correlation except for a monodomain sample, even of the tilt direction, between the layers. The tilt angle in the smectic C phase has been shown to vary with temperature in a uniform way, for example, in terephthalyl-idene-bis-4-n-butylaniline or TBBA (a di-Schiffs base) the tilt angle changes gradually from 0° to 25° within the smectic C range because the phase is formed from a smectic A, however, a S_C-S_A transition can sometimes be first order. In contrast when the smectic C is formed from a nematic the tilt angle spontaneously jumps to a large (~30°) value which is insensitive to temperature. Again, further sub-divisions of the smectic C phase exist but these will not be discussed.

2.3.3 Smectic B

The smectic B (or hexatic B) phase has the constituent molecules arranged within the layers in a hexagonally close-packed array with the molecular long axes perpendicular to the layer planes. The structure is similar to that of the S_A phase except with hexagonal packing of the molecules within the layers. However, in spite of the absence of positional long range ordering within the smectic layers it is found that the orientation of the hexagonal lattice is maintained within each layer and across adjacent layers, this is referred to as bond orientational order.

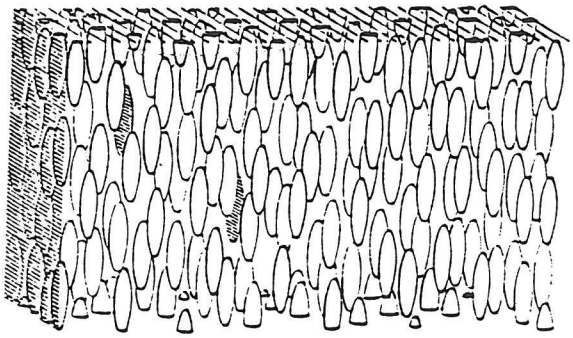

Nematic

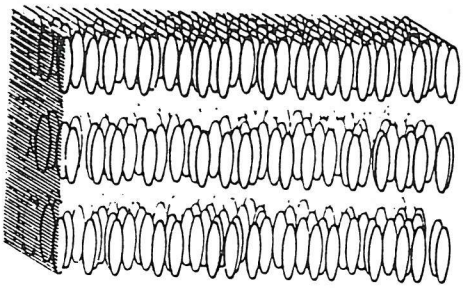

smectic A

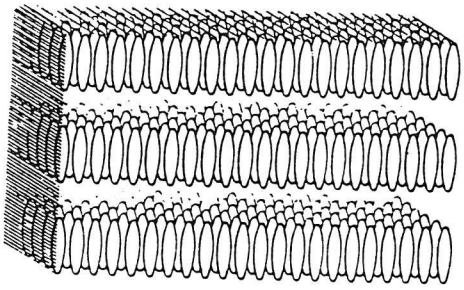

smectic B

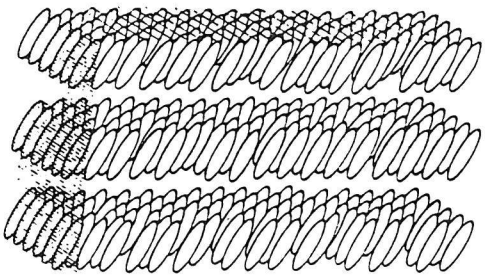

smectic C

Schematic representation of smectic A,B and C phases.

In some cases the close-packed arrangement within a given layer has been shown to be very long range with the hexagonal net extending over a large number of layers thus making it structurally solid-like and not a true liquid crystal phase. However, this crystal B phase exhibits shear and flow properties under stress, precisely reversible phase transitions, does not undergo supercooling and, for homologous series, shows regular trends, all the characteristics usually associated with true liquid crystals.

3. Structure-property relationships in low molar mass liquid crystals

There are two features principally responsible for the formation of liquid crystals. One of these, anisotropy of molecular shape, is a fundamental requirement of all mesogens. It was noted earlier that a rod-like shape is the most common form of anisotropy but plate-like mesogens that form discotic phases are also known [10]. Indeed liquid crystals exist in a wide variety of exotic shapes including; star-shaped [11], phasmidic [12], and even a 'Wheel of Mainz' type structure [13].

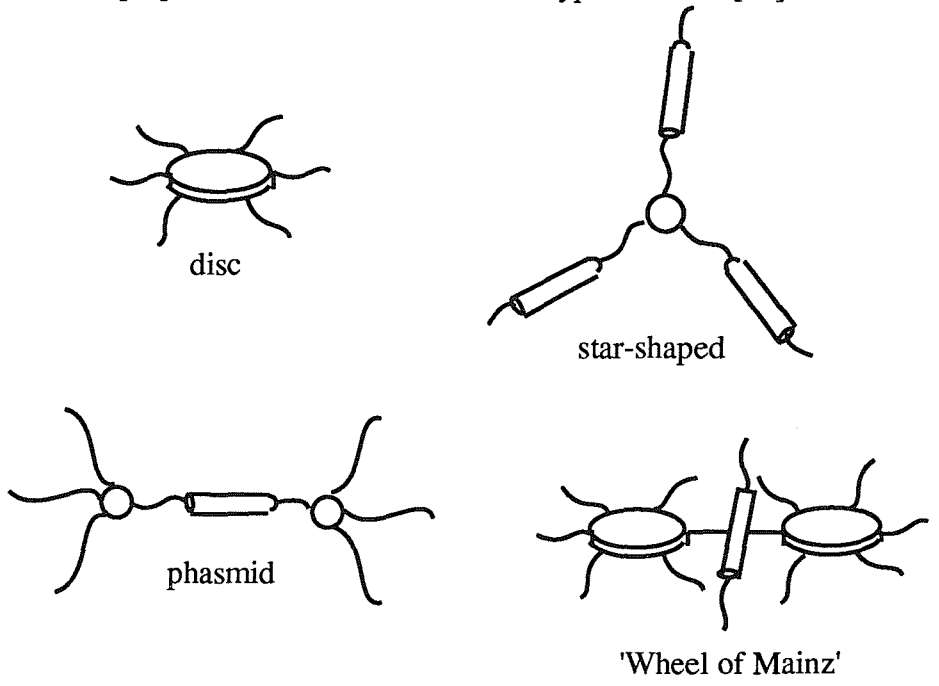

Anisotropy of the force field responsible for intermolecular interactions is the other feature that contributes to the formation of a mesomorphic phase [14]. This second feature is particularly operative in low molecular weight mesogens, which generally contain groups with large dielectric anisotropies.

Molecules of the requisite rod or lath-like structure must possess some degree of rigidity if a liquid crystal phase is to be formed and it is for this reason that many liquid crystals are built from an aromatic base [15,16]. Good thermal stability coupled with the relative ease of preparation means that an aromatic ring system is frequently an integral part of most thermotropic liquid crystals.

However, the high melting points of some multiphenyl systems can hide any potential mesophases.

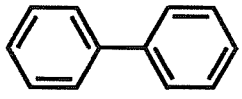

C 71°C I

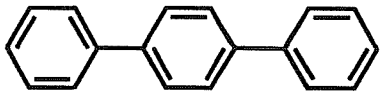

C 212°C I

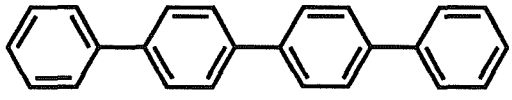

C 300°C I

The inclusion of flexible chains along the long axis of the molecule is a standard technique used to lower the transition temperatures and hopefully access any 'hidden' mesophase without unduly disrupting the anisotropy of molecular shape [17]. We can see that the addition of alkyl chains has lowered the transition temperatures and promoted liquid crystal behaviour for all the previously non-mesogenic multi-phenyl systems.

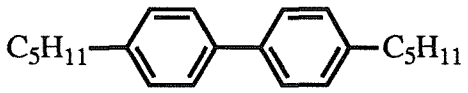

C 26°C S 47.6°C S 52.2°C I

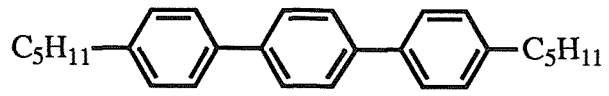

C 192°C S 213°C I

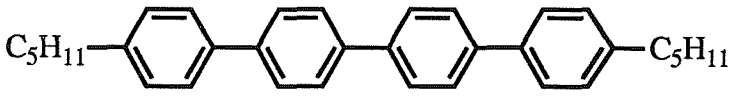

C 297°C S 352°C I

In general, any structural feature such as increased core length, terminal groups or linking groups which give reasonable rigidity to an almost linear molecule should be conducive to liquid crystal formation. Even small, non-flexible,lateral groups such as fluorine can often be accommodated [18], however, lateral inclusion invariably lowers T_{NI} and suppresses smectogenic behaviour. This property is utilised in display applications where low transition temperatures are desirable and the possible occurrence of smectic phases is a disadvantage [19,20]. Theoretically, any rod-like particles devoid of intermolecular forces other than insurmountable repulsions upon contact, predict the formation of a nematic phase above a number density that depends on the axial ratio of the particles. All such mesogens have a characteristic geometric molecular shape (described as rod-like) which gives rise to anisotropic intermolecular forces with the interactions between the ends of the molecules being weaker than the lateral associations.

An efficiently conjugated aromatic group is not, however, a prerequisite for useful nematogenic properties, indeed, the first liquid crystal, cholesteryl benzoate, studied was largely alicyclic [3]. Replacing one of the phenyl rings in in a biphenyl based liquid crystal with its saturated analogue not only maintains a useful nematic range by increasing T_{NI} [21] but produces a lower viscosity and birefringence Δn while maintaining a relatively large dielectric anisotropy $\Delta\varepsilon$. These properties make the materials suitable for use in display devices since low viscosity enhances response times, moderate to low Δn reduces the thickness and uniformity constraints while a

large $\Delta\varepsilon$ ensures strong interaction between the liquid crystal and the applied electric field. Here perhaps it is more plausible to think of the cyclohexane ring not as a central linking unit but as a terminal group because a frequently used end group such as a cyano terminus can adopt an axial or equatorial conformation where on a phenyl group it cannot. Furthermore, replacing the second phenyl ring with cyclohexane gives a molecule with an enantiotropic nematic phase at around room temperature. This gives lower Δn and a negative permittivity anisotropy $\Delta\varepsilon$ both of which are useful for producing high contrast guest-host and cholesteric-nematic phase change displays [22].

The transition temperatures and the thermal persistence of the liquid crystal phase is frequently enhanced by incorporating a third aromatic ring, for example

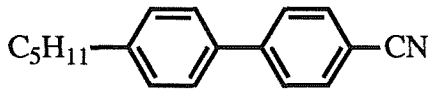

C 22.5°C N 35°C I

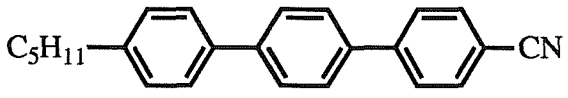

C 130°C N 239°C I

or a linking unit thus [23],

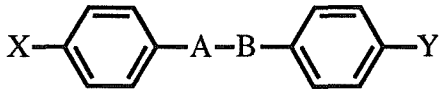

The linking unit A-B frequently contains multiple bonds about which freedom of rotation is restricted so preserving the rigidity and elongation of the molecule. These multiple bonds can also conjugate with the phenyl rings enhancing the anisotropic polarisability, such linking units include,

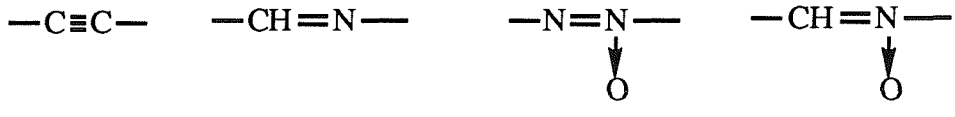

The ester linkage is also effective since resonance confers double bond character on the C-O linkage thus restricting rotation. But these are probably not of major importantance in stabilising liquid crystal phases in comparison with shape anisotropy.

It should be noted however, that apart from the tolanes,

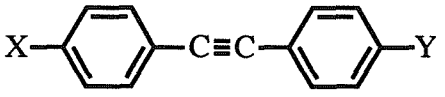

molecules containing a linking group are not completely linear and in some cases the possibility of isomerisation can reduce the ability of a molecule to form a liquid crystal. For example only trans stilbene exhibits a liquid-crystalline phase whereas the cis does not.

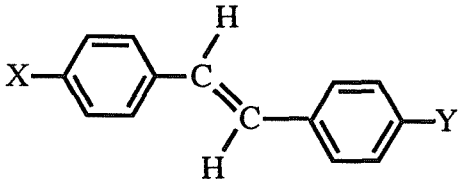

trans

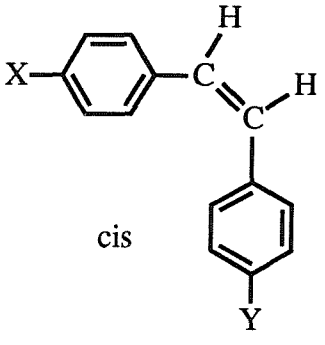

cis

Increasing the length of the terminal alkyl/alkyloxy chains increases the smectogenic tendencies relative to the nematic tendencies of a system. Eventually there can become a stage when nematic properties are extinguished and the compounds are purely smectogenic, for example, the 4-(4'-n-alkyloxy-benzilidene)aminobiphenyls, see figure 1.

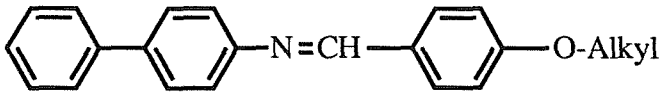

Increasing the number of rings and linking units has a similar effect resulting in a much greater thermal persistence of the phase. For the system,

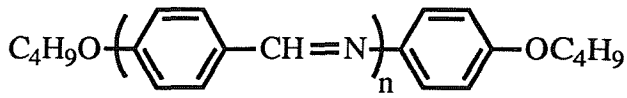

when n is 1 the nematic phase is monotropic the isotropic-nematic temperature, T_{IN} is 121°C and when n is 2, T_{NI} is 298°C. It is generally accepted that to enhance thermal stability both molecular elongation and rigidity need to increase, although a liquid crystal phase may be obtained at lower temperatures by the introduction of some flexibility into the molecule.

For molecules of the general structure,

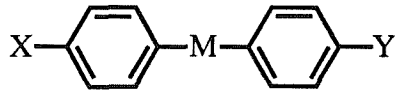

it is possible to construct an average order of efficiency for the central groups M in increasing the nematic-isotropic transition temperatures [24]. The general order is

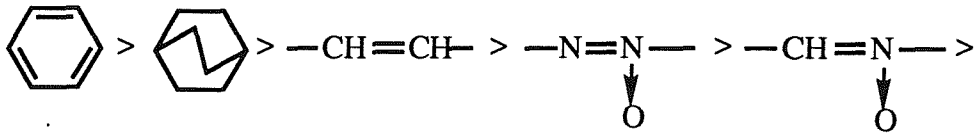

—C≡C— > —N=N— > —CH=N— > —CO.O— > none.

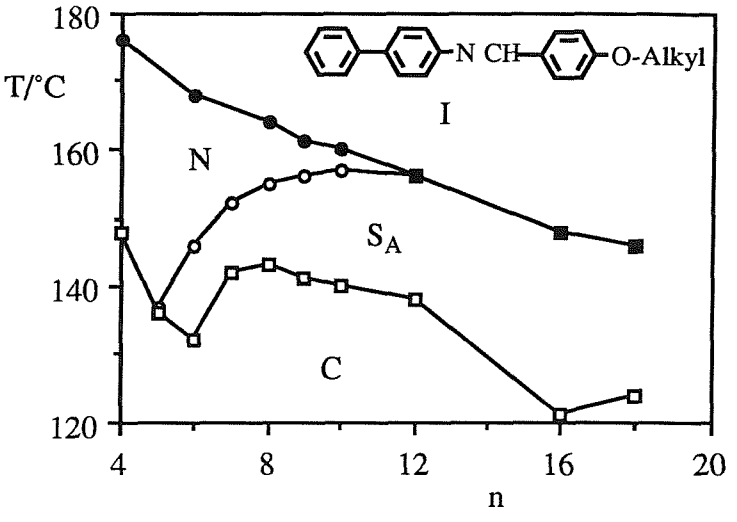

Figure 1. The dependence of the transition temperatures on the number of methylene units, n, in the terminal alkyl chain for the 4-(4'-n-alkyloxy-benzilidene)aminobiphenyls. Showing that as n increases the nematic range is steadily reduced until the liquid crystal phase becomes purely smectic A when n is 12.

Stereochemical considerations are important and affect the position in the order e.g. stilbenes are planar, azoxybenzenes are slightly twisted, Schiffs' bases are considerably twisted and the aromatic rings in tolanes lie orthogonal to one another. Indeed most linking groups bend the molecule thus reducing the tendency to form liquid crystal phases and possibly lowering the melting point also.

It is interesting to note, although not directly relevant to this project, that the inclusion of heteroatoms into the molecule has been studied and a recent review of heteroatomic rings as linking groups has been published [25]. It was found that the general order for T_{NI} enhancement in the system,

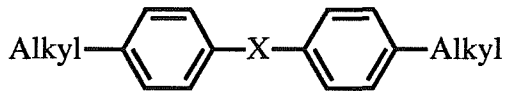

is

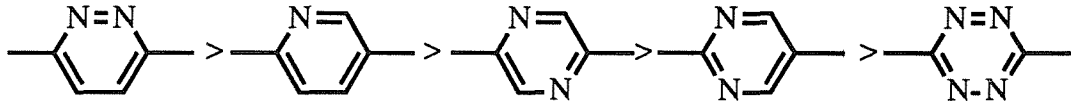

The order of effectiveness of terminal heteroatomic rings varies from system to system and a clear picture does not result from these studies, but in some cases conjugative interactions and twisting of the structure do follow an expected pattern. The addition of large lateral substituents onto the rigid aromatic rings and linking groups serves to broaden the molecule thus lowering the length to breadth ratio and causing T_{NI} to fall. The extent of the lowering of the transition temperature can be related to the size of the substituent [26]. However, for alkyl chains the effect is not so dramatic as might have been anticipated presumably because the lateral chain lies more or less parallel to the long axis of the basic molecule [27]. For example,

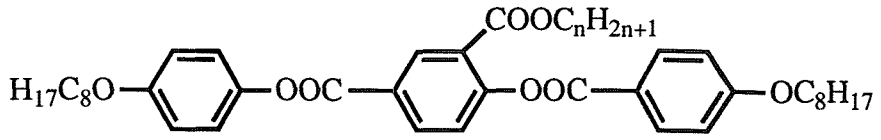

in this series the high T_{NI} of the 3 ring system tolerates the chain and as n increases, a nematic phase is maintained for all n studied from 1 to 12, and for

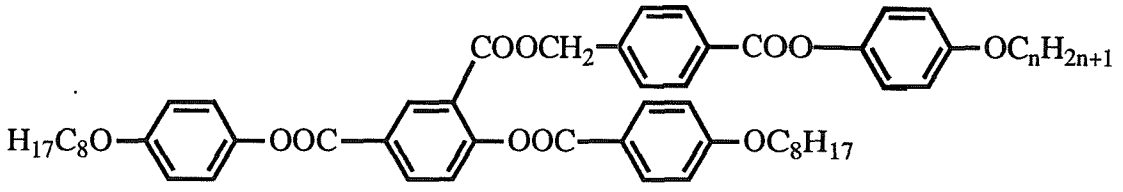

The clearing temperatures are nearly independent of the length of the alkoxy chain [28].

n	T_{CN}/°C	T_{NI}/°C
1	121	152
2	120	153
3	110	153
4	108	152
5	99	151
6	99	149
7	103	148

General accounts of the effects of lateral substituents have been well documented by Gray [29] and Demus [30].

4. Liquid crystalline polymers

The title of this Thesis is oligomeric liquid crystals, here, the term oligomer is used to describe molecules containing upto three mesogenic groups as opposed to monomers with just one and polymers which can contain many hundred mesogenic units. Oligomeric liquid crystals exhibit properties similar to polymeric liquid crystal systems and so perhaps at this juncture it is pertinent to mention some thermotropic polymeric structures and properties.

Polymers are often formed from one or more bifunctional monomers. Everyday examples include:- polythene-made from ethene, polyurethane-made from a diol and a di-isocyanate and nylon- made from a di-amine and a di-acid. By introducing highly anisotropic units into the polymeric structure, either in the main chain, as a side chain, or both, liquid crystal polymers can result.

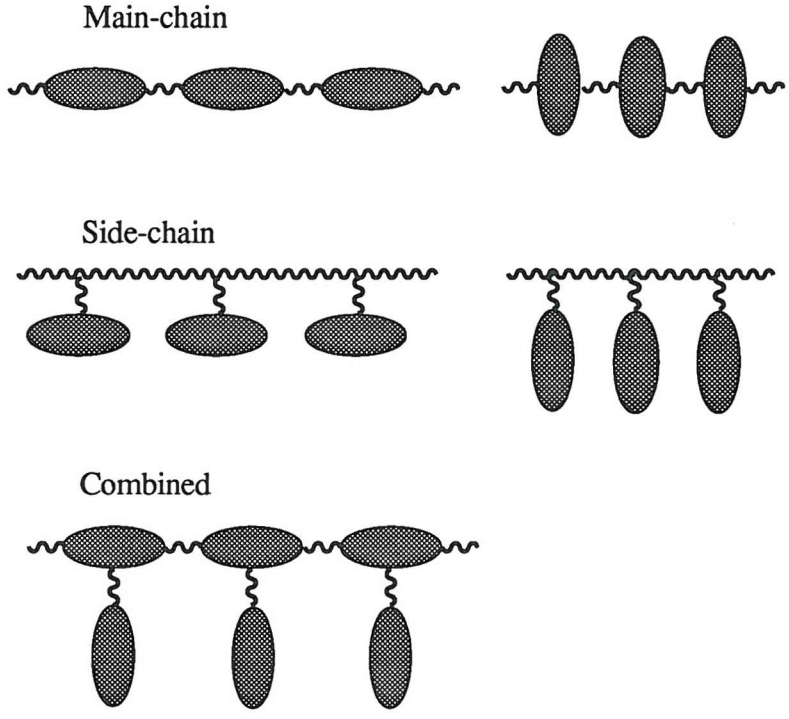

Polymers formed from their liquid crystal state, induced through heat or by a solvent, become highly organised as they are processed. This orientation can lead to polymers of high modulus and tensile strength [31]. A well known example of this

is the polyamide commercially known by one company as Kevlar which, weight for weight, is stronger than steel.

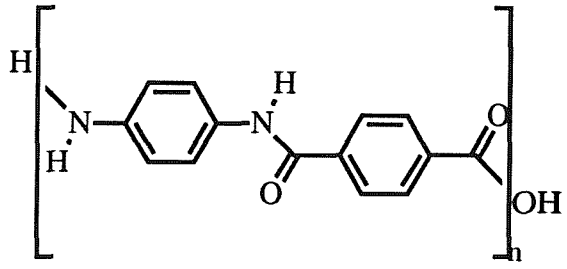

These liquid crystal polymers tend to have very high transition temperatures, sometimes above their decomposition temperature, and very viscous mesophases. The introduction of non-linearity [32] often lowers the crystallisation point . For example the inclusion of a rigid 2,6-dihydroxynaphthalene group into the structure introduces a step that lowers the melting point sufficiently to access the liquid crystal phase,

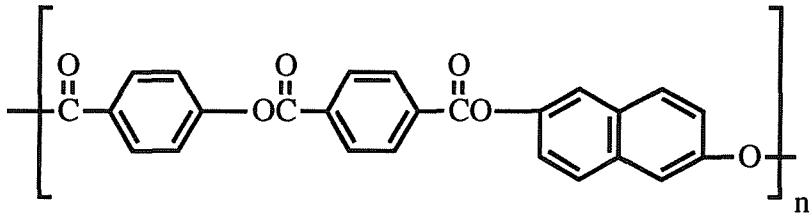

The attachment of lateral substituents to the mesogenic moieties in the polymer backbone can also act to lower transition temperatures by broadening the structure and hence diffusing intermolecular associations. This reduces the melting points of such materials allowing liquid crystals phases to be observed [33, 34].

An excessive number of side groups, however, or too much non-linearity disrupts the ability of the polymer to form a liquid crystal and so a happy medium has to be struck. This can often be achieved with copolymer techniques.

It has been demonstrated by a number of investigators [35-38] that the introduction of flexible spacers between the mesogenic moieties in the polymer backbone not

only lowers the melting and clearing temperatures but can produce improved liquid-crystalline properties.

These semi-flexible main-chain polymers possess transition temperatures and transitional entropies that depend critically on both the length and parity of the flexible spacer. Hence, for a series of polymers in which only the length of the flexible spacer is varied, a pronounced odd-even effect in the transitional properties is seen. Figure 2 shows the dependence of T_{NI} and $\Delta S_{NI}/R$ upon the length of the flexible spacer for the α,ω-(4,4'-(2,2'-dimethyl-azoxyphenyl))alkanedioates [39].

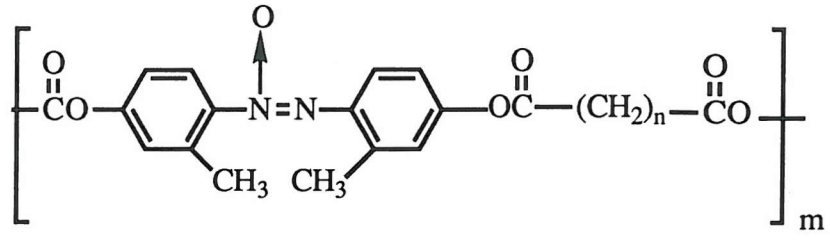

A qualitative explanation of this odd-even effect is given later in this Chapter.
The ability of liquid crystal polymers to respond to electric and magnetic fields means that they can be oriented in their liquid crystal phases and then frozen on cooling thus retaining this orientation. Hence, the possibility of memory storage devices capable, when addressed by a laser, of storing vast amounts of information indefinitely.

(a).

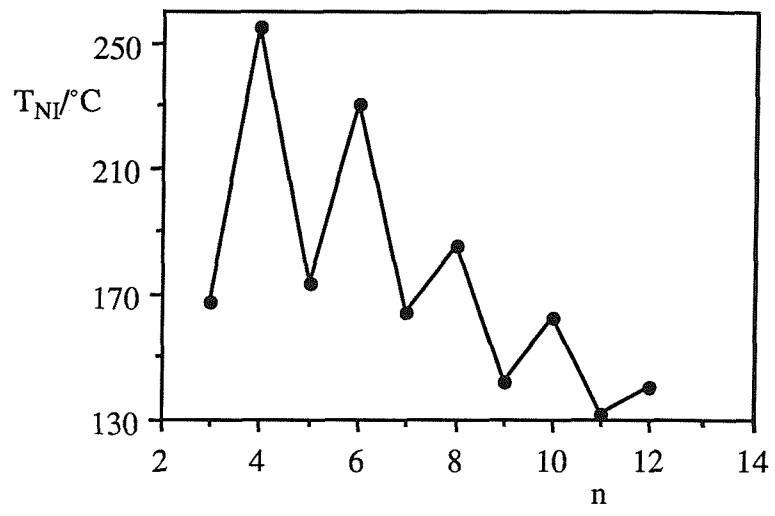

(b).

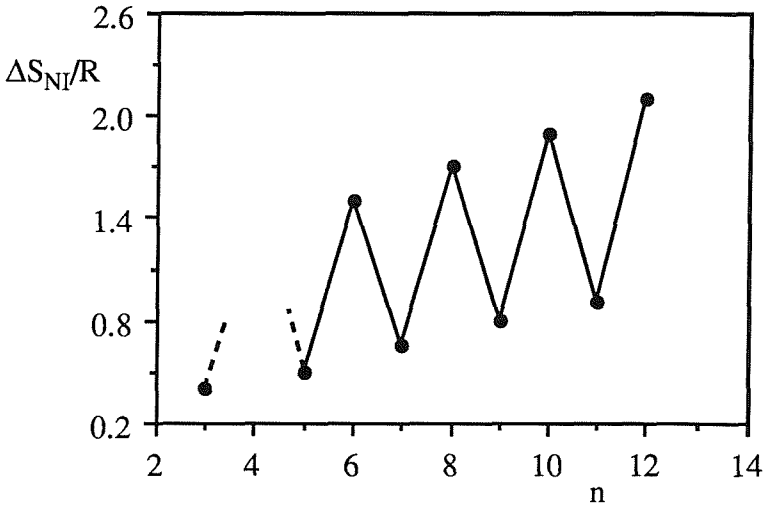

Figure 2. The dependence of (a). The nematic-isotropic transition temperatures and (b). The nematic-isotropic entropies of transition on n, the number of methylene groups in the flexible spacer for the poly α,ω-[4,4'-(2,2'-dimethylazophenyl)]alkanedioates.

5. Dimeric liquid crystals

A dimeric liquid crystal consists of two mesogenic groups connected by a flexible spacer. The most common form of which, is two mesogenic groups joined through their long axes by a flexible alkyl/alkyloxy chain.

The first dimer compounds to be synthesised were the α,ω-bis(4-alkoxyphenyl-4'-azophenyl)alkanedioates, prepared by Vorlander as long ago as 1927 [40].

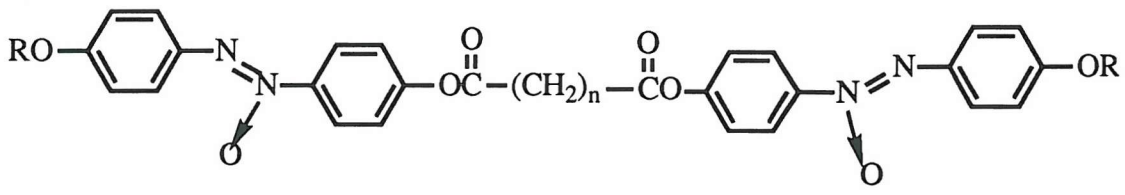

These materials were found to be nematogenic with a very pronounced regular alternation in the clearing temperatures as n was varied. This phenomenon, thought interesting but worthless at the time, was largely ignored until Griffin and Britt prepared the α,ω-bis(4-alkoxybenzoyloxy-4'-phenoxy)alkanes some 50 years later [41].

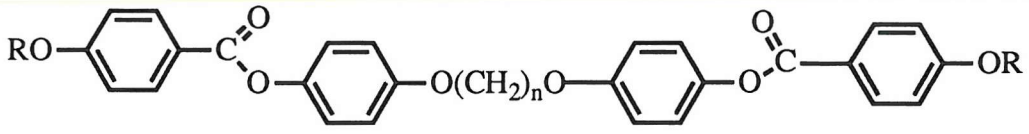

Many variations on this theme quickly followed,

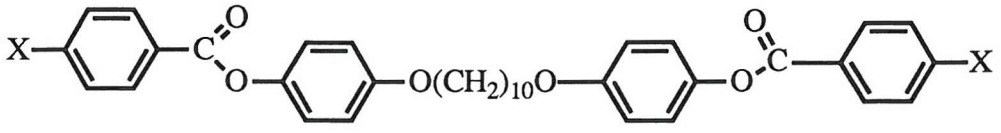

α,ω-bis(4-substituted-4'-phenoxycarbonyl)phenoxydecanes [42]

Jin et al studied the the nematic behaviour for a range of terminal substituents, X, including methyl, chloro, cyano and nitro groups and the effect of the substituents upon the thermal stability of the nematic phase was found to be in accord with the behaviour of analogous nematogens with a single semi-rigid core. Other typical dimers include;

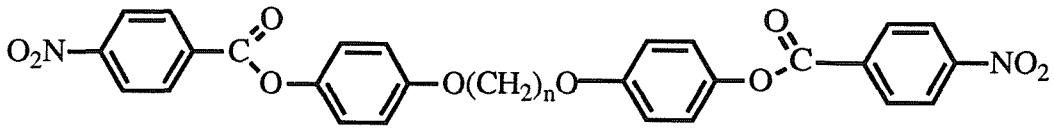

α,ω-bis(4-nitrobenzoyloxyphen-4'-oxy)alkanes [43]

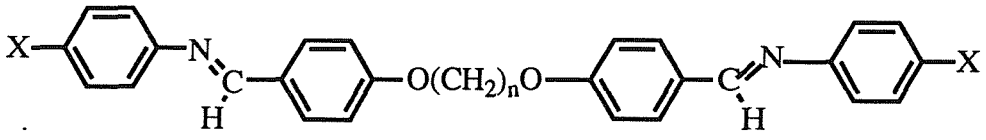

α,ω-bis(4-substituted-anilinebenzylidene-4'-oxy)alkanes [44]

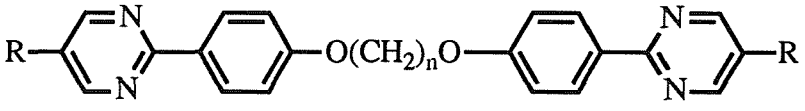

α,ω-bis(5-n-alkyl-2-(4-hydroxyphenol)-pyrimidines [45]

In short, dimers and indeed trimers and polymers can be prepared by introducing extra functionality into the monomeric compounds while maintaining the the appropriate anisotropic rules for mesogenicity briefly described earlier in this chapter. Indeed, liquid crystallinity can be enhanced by the dimerisation of two monomers, an example of which is the well studied α,ω-bis(4-cyanobiphenyl-4'-oxy)alkanes series [46]

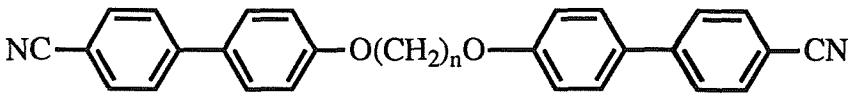

which can be built up from

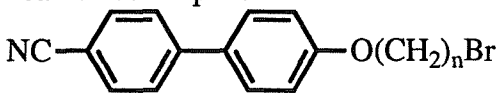
and
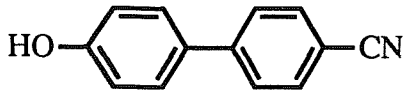

	Monomers		Dimers	
n	T_{CI}/°C	T_{IN}/°C	T_{CN}/°C (T_{CI}/°C)	T_{NI}/°C (T_{IN}/°C)
3	107	40	(185)	(170)
4	66	63	209	250
5	84	65	137	186
6	70	65	187	221
7	79	66	137	181
8	84	65	175	201
9	74	72	133	172
10	77	68	164	184
11	78	68	123	164
12	77	69	152	169

Dimers can also exist as what is known as an asymmetric dimer, where the two mesogenic units are different. For example the α-(4-cyanobiphenyl-4'-oxy)-ω-(4-n-alkylanilinebenzylidene-4'-oxy)hexanes [47]:

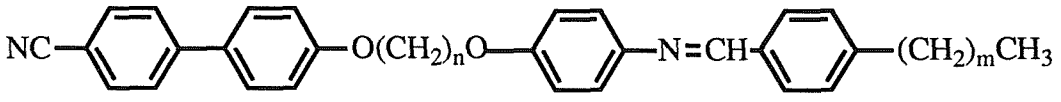

these have a cyanobiphenyl group as one mesogenic unit and a Schiffs base group as the other, connected together by an alkoxy chain.

Asymmetric series such as these exhibit rich polymorphism coupled with a strange phase structure thought to be due to the association between the electron donating cyanobiphenyl group and the electron acceptor properties of the Schiffs base group. Hogan et al [47] and later Attard et al [48] proposed that the unusual phase behaviour and layer spacings, obtained from X-ray data, for such systems was due to an intercalated structure resulting from charge transfer interactions between the different units.

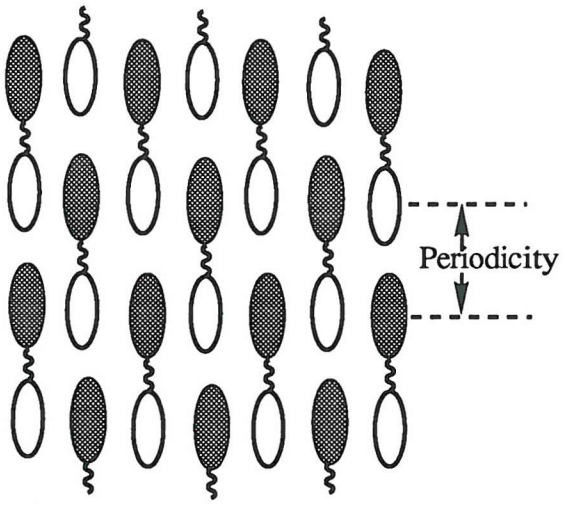

Some dimers, however, exhibit interdigitated structures depending on their chain lengths.

Changing the nature of the spacer has also been investigated as a means of lowering the crystal to liquid crystal transition temperatures. It has been found that the use of an oligosiloxane spacer has the desired effect of lowering the transition temperatures, because of its high flexibility and low crystallinity [49,50]. Apparently the low temperature fluidity of these materials can be attributed to the effect of the bulky structure, flexibility and the irregular conformations of the oligodimethyl siloxane spacer between the rigid mesogenic groups.

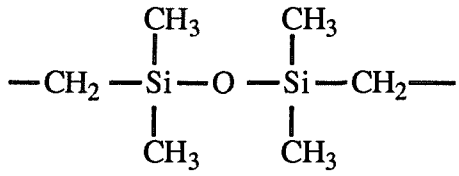

The methyl groups in these dimethylsiloxane units rotate with unusual ease around the Si-O bond temperatures as low as -195°C [51]

From the evidence described here it appears that there may be a continuum of liquid-crystalline behaviour from dimers to polymers through low molar mass oligomeric structures. Preliminary studies of trimeric liquid crystals i.e. materials containing three mesogenic groups, show pronounced odd-even effects. Hence it may be concluded that oligomeric molecules containing rigid mesogenic groups connected through flexible spacers provide an interesting class of mesogens both as models for polymeric systems and as exciting liquid crystals in their own right.

6. A qualitative interpretation of the odd-even effect

It is found that the liquid-crystalline properties of oligomers and polymers containing a flexible alkyl chain depend critically on the length of that chain. For example the nematic-isotropic transition temperatures, T_{NI}, for members of a homologous series of dimers with an even number of methylene groups fall on one smooth curve while T_{NI} for those with an odd number fall on another. This odd-even effect, which is much greater than that seen in monomeric materials, is also exhibited by other properties which include the entropy change at the nematic-isotropic transition $\Delta S_{NI}/R$ and the orientational order at the transition. The entropy exhibits a continuous alternation which is not attenuated, unlike T_{NI} the strong alternation in $\Delta S_{NI}/R$ implies a dramatic variation in the orientational order of the mesogenic groups with the number of methylene groups in the alkyl chain, such a

variation has been observed using deuterium NMR spectroscopy. All of these alternations are reduced quite dramatically when the chain is terminal. The dramatic odd-even effects can, perhaps be understood qualitatively by considering two members of a dimeric series, one with an odd number of methylene links, the other even.

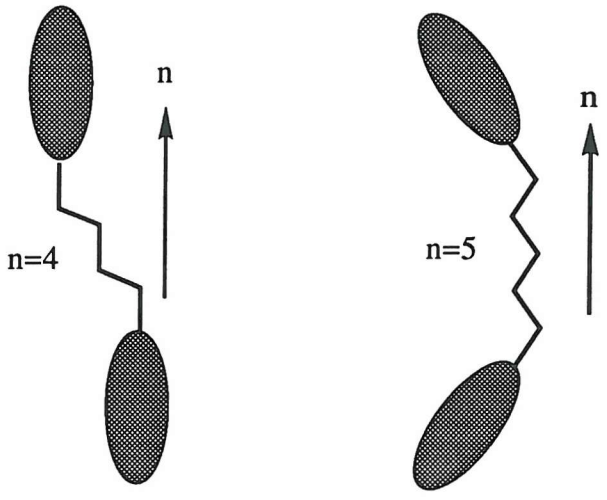

The tetrahedral character of the sp^3 carbon atoms dictates that the bonds connecting consecutive methylene units within a chain are bent with respect to one another. When the lowest energy all-trans conformations of the dimers are considered the mesogenic groups lie colinear in the even membered spacers but are always at an angle to one another for odd spacers. Even allowing for some gauche links, which are thermally populated at temperatures close to T_{NI}, the major axes of the rigid mesogenic groups for odd n are not expected to be parallel and the molecule is, on average, more bent than its even counterpart. Since the order in the liquid-crystalline phase is favoured by the ability of the component molecules to pack efficiently, the pentamethylene spacer in the angular all-trans conformation prevents formation of an extended, rod-like structure with favourable steric packing. This theory is apparently supported by the higher order parameters of the nematogens with even membered alkyl chains. Calculations performed with this simple geometric view in mind however, predict that the even dimers behave like a rod-like monomer whilst

the odd have a much lower order/entropy [52]. Whereas for real systems, the odd behaves like a monomer and the even has a much higher order/entropy. A theory has therefore been proposed that within the isotropic phase, there is a proportion of linear conformers in both odd and even dimers [53]. The concentration of these linear conformers is greatest for the even dimers. At the nematic-isotropic transition this concentration of linear conformers in even dimers is sufficiently high to promote the conversion of some of the remaining bent conformers to linear, resulting in a strong first order transition. In the odd dimers, there is insufficient of the linear component for the change in the orientational partition function at the transition to the nematic phase to produce a significant jump in the concentration of the linear conformers, hence for odd dimers the transition is weakly first order.

7. Characterisation of liquid crystals

7.1 Optical microscopy

The polarising microscope with integral hot-stage is often the first port of call for the chemist clutching a potential liquid crystal. The birefringent nature of liquid-crystalline materials produces a mobile, multi-coloured pattern when viewed through crossed polars. Characteristic shapes within this pattern are also used as an indication of the nature of the liquid crystal phase type. The use of an efficient hot-stage can be used as an indication of the purity of a material either by the sharpness of transition or, if the transition temperatures of the pure material are known, by comparison.

A further advantage of examining liquid-crystalline mesophases by optical microscopy is that the specimen can be oriented in a variety of ways by the prior preparation of the microscope slide surface. For polar mesogens such as cyanobiphenyl and Schiffs' base derivatives obtaining homeotropic alignment to

help with phase identification can be quite straight forward and useful. With such compounds homeotropic alignment, where the director is oriented parallel to the viewing direction is often achieved by allowing a liquid crystal to seep between a clean slide and cover slip under capillary action. Surfactants offer a more time consuming but often more successful method. Through crossed polars, an optically uniaxial, homeotropic texture is seen as black. A homeotropic texture that flashes with multicoloured light when mechanically stressed is taken to be indicative of a nematic phase. If there is a smectic A phase, S_A, below the homeotropic nematic then there is no change optically on passing through the transition, however the preparation will no longer flash when subjected to stress because of the relatively viscous nature of the smectic regime. A smectic C phase, S_C, below a homeotropic nematic would adopt a schlieren texture at the transition because the tilt of the director disrupts the homeotropic arrangement. In an unaligned sample the focal conic textures of S_A and the S_C phases are frequently very similar and cannot serve to distinguish between the two phase identities.

Occasionally a smectic phase can appear schlieren as if a nematic. Liquid crystals have point singularities. These correspond to strong distortions in the director field with a discontinuity in the ordering of the molecules occuring at a single point. Through a polarising microscope these singularities can be seen as points with brushes emanating from their centres.

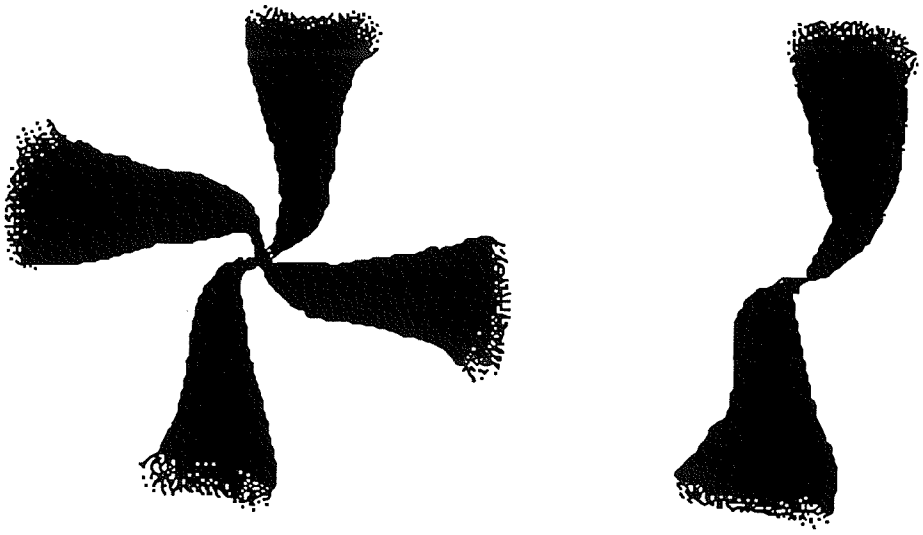

Nematic phases exhibit singularities that have both two and four brushes emanating from their centres, whereas, smectic phases only exhibit singularities that have four schlieren brushes. This gives us a way to identify nematics from smectics, although it should be noted that for less common smectics such as antiferroelectric and intercalated structures both two and four brushes are observed.

For compounds that, on initial inspection appear to display no mesogenic behaviour but whose molecular structure might indicate a modicum of liquid-crystallinity, two methods of investigation can be explored under the microscope; droplets and liquid crystal mixtures. Small droplets may be supercooled way below the freezing point of the bulk sample, allowing any mesophase otherwise hidden by the high melting point of the sample to be seen. This can sometimes indicate that just a subtle change in the molecular structure would support enantiotropic behaviour.

Liquid crystal mixtures allow virtual transitions of materials to be determined by dissolution in a standard liquid crystal, preferably of similar make-up, and then plotting the transition temperatures of the mixture against a series of concentrations of the liquid crystal employed. The eutectic point is then the virtual transition temperature of the material.

Contact preparations are made in a similar manner to homeotropic preparations by drawing two materials together under the cover slip by capillary action.The materials

are allowed to make contact while in their liquid phases, with care to avoid excessive mixing. The concentration gradient where where the two samples meet can now be examined optically. Contact preparations are used in several ways; (i) to determine phase-type by miscibility, (ii) to determine helical twist sense in helical chiral phases and (iii) by using an electron rich compound as one material, a liquid crystal phase can sometimes be induced in the other. This technique is also often used when introducing solvent to an amphitropic material, one which exhibits both thermotropic and lyotropic phases.

7.2 Differential scanning calorimetry

Another tool essential to preparative liquid crystal science is differential scanning calorimetry or DSC. This method is popularly regarded as complimentary to optical microscopy because an optically subtle phase change missed by the microscopist is often picked up on the DSC. A DSC apparatus utilises the latent heat absorbed or evolved from a material as a transition is passed through. It gives not only the transition temperatures but, through enthalpy and entropy derivations, can give the order of a phase. Technically a DSC records the energy necessary to establish zero temperature difference between a substance and a reference material against either time or temperature as the two specimens are subjected to identical temperature regimes in an environment heated or cooled at a controlled rate. The DSC curve as recorded represents the heat applied per unit time as ordinate against either time or temperature as abscissa.

The power compensated DSC, as used for the analysis of the compounds in this Thesis, works by having two microfurnaces, one for the sample and one for the reference, linked in one loop which provides the temperature change at the (operator) preselected rate and in another loop which ensures that the temperature of the two pan holders is always the same. Thus, if a melting event occurs, more energy has to

be provided to the sample in order to keep the temperature of the sample and reference the same at the same heating rate.

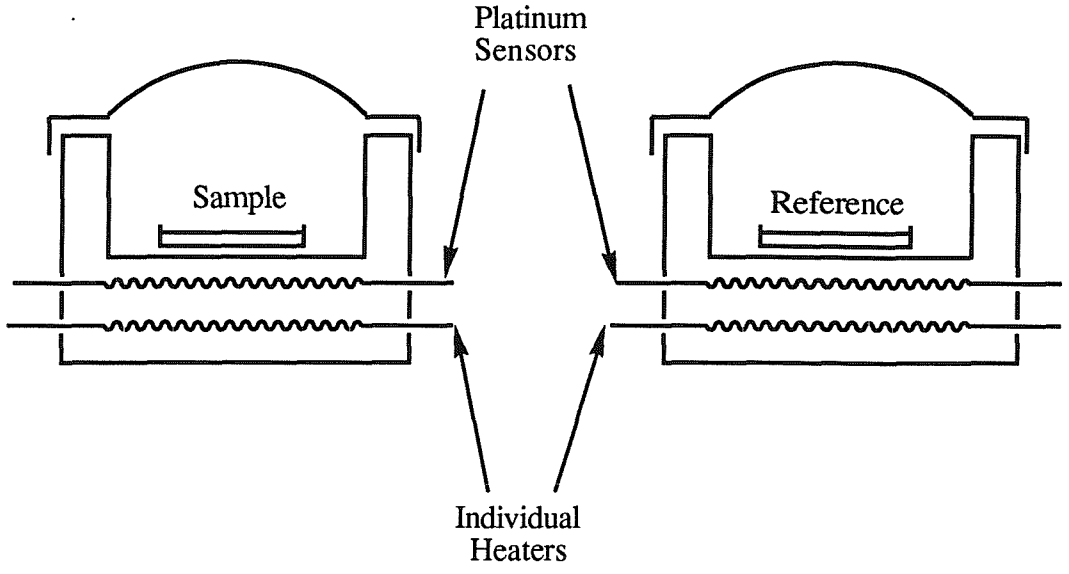

This extra energy is measured by the instrument and is directly proportional to the energy change of the system. Therefore, once the instrument has been calibrated with a sample of known ΔH, the attached computer processor can calculate the ΔH for the event in question.

There are two main types of thermal event measured by the DSC, namely first and second order transitions. The Gibbs Free Energy (G) can be expressed as:

$$G = H - TS$$

where H is the enthalpy, T is the temperature and S is the entropy. The first derivative of G with respect to T gives, for a pure compound, the entropy:

$$\left(\frac{\partial G}{\partial T}\right)_p = -S$$

While the second derivative is related to the heat capacity at constant pressure:

$$\left(\frac{\partial^2 G}{\partial T^2}\right)_p = -\frac{C_p}{T}$$

Two types of behaviour are commonly observed at a phase transition and these are related to the behaviour of the function $\partial G/\partial T$ (i.e. S) with temperature [54]. If at a phase transition, $\partial G/\partial T$ shows a discontinuity, then the transition is said to be first order. The change in enthalpy associated with such transitions ($\Delta H = \Delta S/T$) is usually referred to as the latent heat of the transition. It is also possible for the phase transitions to occur without a change in entropy, and therefore enthalpy, but with some discontinuity in the second derivative of G ($\partial^2 G/\partial T^2$) with respect to T. Such transitions are referred to as second order and are accompanied by a discontinuity in the heat capacity.

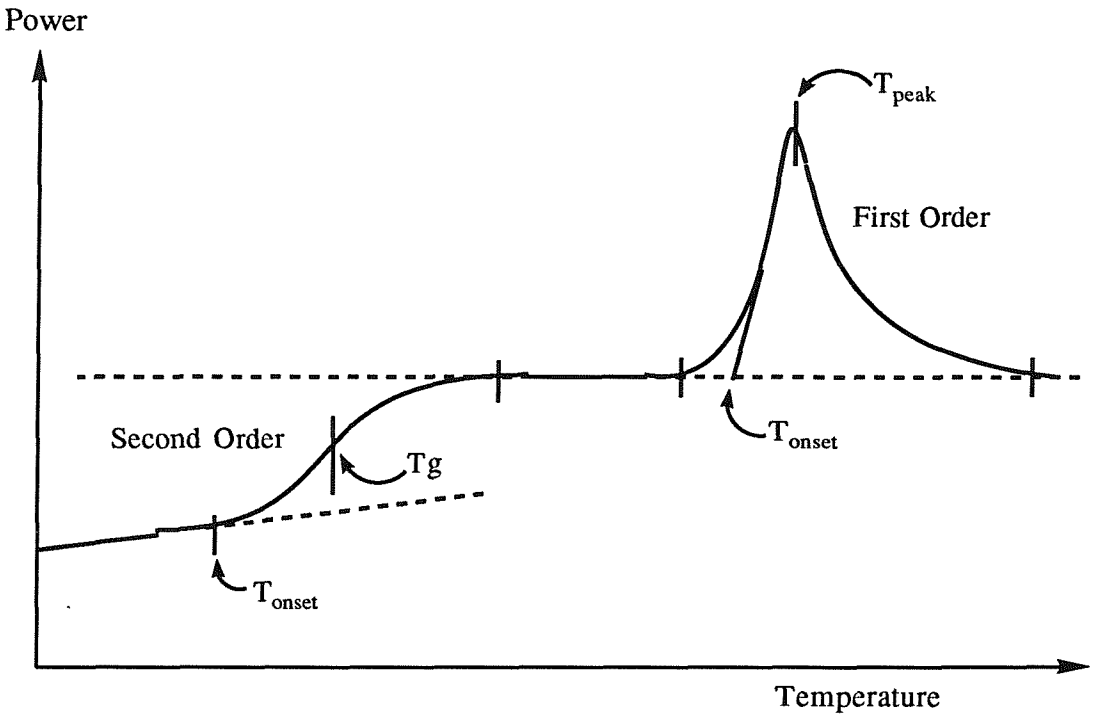

The melting transition is always first order and is very often the strongest. This large enthalpy change comes about as the 3-dimensional orientational order of the crystal is reduced to either 2-dimensional order (smectic phase) or 1-dimensional order (nematic phase). The order and strength of a transition can occasionally give an indication as to the identity of a phase. As stated earlier the melting transition and also the mesophase→isotropic transition are always first order. Some liquid crystal transitions can be second order. For example, an S_C - S_A transition is often second

order because it involves only a change in the director orientation and not an intrinsic change in order of the system, however, some N - S_A phase can become second order especially when the nematic phase is long. Polymeric liquid crystals often exhibit a glass transition which occurs when intermolecular motion becomes hindered and essentially stops before crystallisation can occur, hence they are always second order.

7.3 X-ray diffraction

X-ray diffraction is another technique often employed in the analysis of liquid crystals, it is especially useful in the elucidation of phase type. When an X-ray beam is incident upon an atom interference can arise within the atom itself, consequently the scattering power of the atom decreases with increasing scattering angle. The forward scattered amplitude is directly proportional to the atomic number of the atom. The coherently scattered X-rays from different atoms cannot be refocussed to produce an image of the structure but do give rise to an interference pattern whose form is related to the scattering structure, and hence is related to phase type in the case of liquid crystals. A discussion of this relationship is beyond the bounds of this text, however, further details are available in the literature [55].

References

[1] Lehmann O., 1904, *Fluessige Kristalle*, Engelmann, Leipzig.

[2] Tanford C., *The Hydrophobic Effect*, 1980, Wiley Interscience, New York.

[3] Reinitzer F., 1888, *Montash. Chem.*, **9** 421.

[4] Grinstein G., Toner J., 1983, *Phys. Rev. Lett.*, **51**, 2386.

[5] Chandrasekhar S., Sadashiva B.K., Suresh K.A., 1977, *Pramana* , **9**, 471. 1978 *Chem Abstr.* **88**, 30566y.

[6] Badadur B., 1984, *Mol. Cryst. Liq. Cryst.*, **1**, 109.

[7] Fergason J., 1964, *Scient. Am.*, **211**, 77.

[8] Sackmann H., 1984, *Prog. Colloid. Polym. Sci.*, **69**, 73.

[9] Freidel E., C-r. Hebd. Sean., 1925, *Acad. Sci. Paris*, **180**, 269.

[10] Destrade C., Foucher P., Gasparoux H., Nguyen Huu Tinh, Levelut A.M., Malthete J., 1984, *Mol. Cryst. Liq. Cryst.*, **106**, 121.

[11] Demus D., 1989, *Liq. Crystals*, **5**, 75.

[12] Malthete J., Nguyen Huu Tinh, Levelut A.M., 1986, *J. Chem. Soc. Commun.*, 1548.

[13] Kreuder W., Ringsdorf H., Hermann-Schonherr O., Wendorff J.H., 1987, *Angew. Chem. Int. Ed. Engl.*, **26**, 1249.

[14] Chandrasekhar S., 1985, *Mol. Cryst. Liq. Cryst.*, **124**, 1.

[15] Demus D., Zaschke H., 1984, *Flussige Kristalle in Tabellen* , Vol.II, Leipzig.

[16] Kelker H., Hatz R., Schumann C., 1980, *Handbook of Liquid Crystals*, Verlag Chemie, Weinheim, Deerfield.

[17] Demus D., Demus H., Zaschke H., 1974, *Flussige Kristalle in Tabellen* , Leipzig. P230.

[18] Osman M.A., 1985, *Mol. Cryst. Liq. Cryst.*, **128**, 45.

[19] Balkwill P., Bishop D., Pearson A., Sage I., 1985, *Mol. Cryst. Liq. Cryst.*. **123**, 1.

[20] Chan L.K.M., Gray G.W., Lacey D., 1985, *Mol. Cryst. Liq. Cryst.*, **123**, 185.

[21] Pohl L., Eidenschink R., Krause J., 1977, *Phys. Lett.*, **60A**, 421.

[22] Pohl L., Eidenschink R., Krause J., 1978, *Phys. Lett.*, **65A**, 169.

[23] Destrade C., Nguyen Huu Tinh, Gasparoux H., 1980, *Mol. Cryst. Liq. Cryst.*, **59**, 273.

[24] Gray G.W., 1979, *Molecular Physics Of Liquid Crystals*, Chapter 1, Academic Press.

[25] Gray G.W., 1976, *Advances in Liquid Crystals*, (G.H. Brown ed.) vol.1, P.1, Academic Press Inc. N.Y.

[26] Weissflog W., Demus D., 1985, *Mol. Cryst. Liq. Cryst.*, **129**, 235.
[27] Demus D., Hauser A., Selbmann Ch., Weissflog W., 1984, *Cryst. Res. Technol.*, **19**, 271.
[28] Weissflog W., 1989, *Liq. Crystals*, **5(1)**, 75.
[29] Gray G.W. and Windsor P.A. 1974, *Liquid Crystals and Plastic Crystals*, vol.1, Ellis Horwood, Chichester, England.
[30] Demus D., 1989, *Liq. Crystals.*, **5(1)**, 111.
[31] For example see: White J.L., Fellers J.F., 1978, *J. Appl. Polym. Sci.*, **33**, 137.
[32] Irwin R.S., 1980, *US Pat 4*, **188**, 476.
[33] Blumstein A., 1985, *Polym. J.*, **17**, 277.
[34] Lenz R.W., 1985, *Faraday Discuss. Chem. Soc.*, **79**, 21.
[35] Jo B.W., Jin J-I., Lenz R.W., 1982, *Eur. Polym.*, **18**, 233.
[36] Jin J-O., Oh H.T., Park J.H., 1986, *J. Chem. Soc. Perkin. Trans.*, **11**, 343.
[37] Griffin A.C., Havens S.J., 1981, *J. Polym. Sci.*, **19**, 951.
[38] Creed D., Griffin A.C., 1987, *Mol. Cryst. Liq. Cryst.*, **149**, 185.
[39] Blumstein A., Thomas O., 1982, *Macromolecules*, **15**, 1264.
[40] Vorlander D., 1927, *Z. Phys. Chem.*, **126**, 449.
[41] Griffin A.C. and Britt T.R., 1981, *J.Am. Chem. Soc.*, **103**, 4957.
[42] Jin J-I., Chung Y.S., Lenz R.W., Ober C., 1983, *Bull. Korean Chem. Soc.*, **4(3)**, 143.
[43] Jin J-I., Kang J.S. Jo B.W., Lenz R.W., 1983, *Bull. Korean Chem. Soc.*, **4(4)**, 176.
[44] Jin J-I., Park J.H., 1984, *Mol. Cryst. Liq. Cryst.*, **110**, 293.
[45] Krone V., Ringsdorf H., 1987, *Liq.Crystals*, **2**, 411.
[46] Emsley J.W., Luckhurst G.R., Shilstone G.N. and Sage I., 1984, *Mol. Cryst. Liq. Cryst. Lett.*, **102**, 223.
[47] Hogan J.L., Imrie C.T., Luckhurst G.R., 1988, *Liq. Crystals*, **3**, 645.
[48] Attard G.S., Garnett S., Hickman C.G., Imrie C.T., Taylor L., 1990, *Liq. Crystals*, **7**, 495.
[49] Aquilera C., Bernai L., 1984, *Polym. Bull.*, **12**, 383.
[50] Jin J-I., 1980, *Br. polym. J.*, **12(4)**, 132.
[51] Jon L.K., Robert U., 1969, *Macromolecules*, **2**, 525.
[52] Emsley J.W., Luckhurst G.R., Shilstone G.N., 1984, *Molec. Phys.*, **53**, 1023.
[53] Ferrarini A., Luckhurst G.R., Nordio P.L., Roskilly S.J., 1993, *Chem. Phys. Lett.*, **214**, 409.
[54] Wunderlich B., Grebowicz J., 1984, *Advances in Polymer Science*, Springer-Verlag, Berlin, Heidelberg.
[55] Guinier A., 1963, *'X-Ray Diffraction'*, Published by W.H. Freeman.

CHAPTER 2

Order parameters, distribution functions and nuclear magnetic resonance of liquid crystals

This Chapter introduces the reader to the concept of distribution functions and their relationship with orientational order parameters. We will then go on to discuss how we can measure the order parameters of liquid crystalline materials using nuclear magnetic resonance spectroscopy.

1. Order Parameters and Distribution Functions

In order to gain an understanding of the inherent link between the microscopic structure and the known properties of a system it is necessary to formulate a relationship built upon the concept of a distribution function, an essential part of any such theory.

From statistical mechanics, the definition of the distribution function is based on a macroscopic system characterised by a constant number of particles (N), temperature (T) and volume (V), known as a canonical ensemble. For a system of N rigid particles of arbitrary shape the microscopic states of the canonical ensemble are defined by the positions and orientations of the constituent particles. In cartesian coordinates the position of each particle is given by r(x,y,z) and three Euler angles (α,β,γ) Ω which denote the molecular orientation with respect to the space fixed laboratory axes (see figure 1).

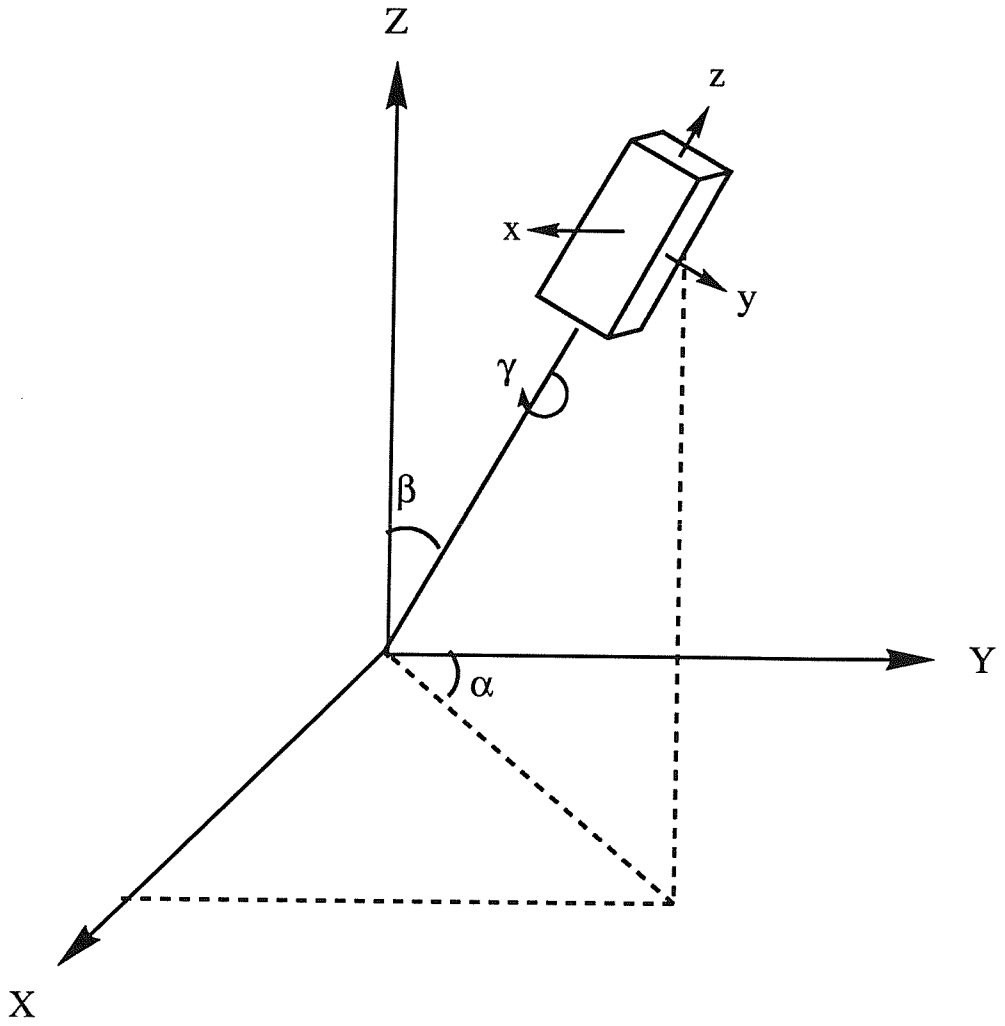

Figure 1. The Euler angles α,β and γ, relating a molecular frame (x,y,z) to a laboratory frame (X,Y,Z).

The sum over configurational partition functions for N molecules in the ensemble is given by:

$$Q = (1/N!) \int \{dX^N\} \exp [-U(\{X^N\})/kT], \qquad (1)$$

where $U(\{X^N\})$ is the potential energy of N particles and X^N denotes the six variables ($\underline{r}$, Ω) for each of them, the curly brackets represent collectively N variables. Thus $\{X^N\} = X_1, X_2.....X_N$, similarly $\{dX^N\} = dX_1\, dX_2\, ...dX_N$. The volume element dX is equivalent to $d\underline{r}\ d\Omega$ where $d\underline{r} = dr_x dr_y dr_z$ and $d\Omega = d\alpha \sin\beta d\beta d\gamma$. We have replaced the multi-dimensional integral over the volume elements that appear by a single integral to simplify the notation. For the spatial variable the integration is over the sample volume V and the orientational variables are taken over the usual domains, which are $0<\alpha<2\pi$, $0<\beta<\pi$, $0<\gamma<2\pi$.

The n particle distribution function defining the probability of finding n particles out of a total N with coordinates in the range,

$$X_1 \text{---} X_1 + dX_1,\ X_2 \text{---} X_2 + dX_2,\ .....X_n \text{---} X_n + dX_n,$$

is given by,

$$P^{(n)}(\{X^n\}) = N!/((N-n)!Z_N) \int \{dX^N{}_{n+1}\} \exp[-U(\{X^N\})/kT, \qquad (2)$$

where $\{dX^N{}_{n+1}\}$ is $dX_{n+1}\ .....dX_n$. $P^{(n)}$ is normalised to the n-plets that can be formed by choosing n particles out of N i.e.

$$\int P^{(n)}(\{X^n\})\{dX^n\} = N!/(N-n)! \,. \qquad (3)$$

The distribution function defined in equation (3) can be used to derive an average property which depends on the position and orientation of n-particles at a constant temperature and volume.

$$<A\{X^n\}> = \{(N-n)!/N!\}\int \{dX^n\}A(\{X^n\})P^{(n)}(\{X^n\}) \tag{4}$$

In a number of techniques including NMR we concern ourselves with one and two average particle properties which necessarily require the single and pair distribution functions. Also for a uniform or homogeneous system such as an isotropic liquid or a nematic phase the physical properties are invariant under translation and therefore the interaction energy $U(\{X^N\})$ depends only on relative distances. Therefore, we can write the distribution function in terms of the orientational contribution such that

$$P^{(n)}(r_1, \Omega_1) = \rho f(\Omega_1), \tag{5}$$

and

$$P^{(2)}(r_1, \Omega 1, r_2, \Omega_2) = \rho^2 f(\Omega_1) f(\Omega_2) g^2(r_{12}, \Omega_1, \Omega_2), \tag{6}$$

where ρ is the number density and $g^2(r_{12}, \Omega_1, \Omega_2)$ is the pair correlation function. We now consider the special case of cylindrically symmetric molecules comprising a uniaxial phase. Since we are interested in single particle properties the relevant quantity is the single particle orientational distribution function $f(\omega)$

$$f(\omega) = f(\alpha, \beta) \tag{7}$$

The detailed form of $f(\alpha, \beta)$ is of course unknown, never the less we can impose constraints on $f(\alpha, \beta)$ by utilising the symmetry of the phase and constituent

molecules. We know, for example, from experiment that the nematic phase has D_{3h} symmetry or higher about the director. Therefore, the distribution function is independent of α and not altered by rotation about the laboratory Z axis. In addition if the phase is apolar i.e. has a plane of symmetry orthogonal to the director, then

$$f(\beta) = f(\pi-\beta) \tag{8}$$

The distribution is now normalised so that

$$\int_0^{\pi} d\beta \sin\beta f(\beta) = 1 \tag{9}$$

since there is a certainty of finding the molecule in the range 0 to π. The exact form of the singlet orientational distribution function is unknown, however, $f(\beta)$ can be expanded in terms of a set of quantities which are known functions of β [1]. These functions are the Legendre polynomials which form a complete orthogonal basis set spanning the whole of orientational space. The expansion is given by:

$$f(\beta) = \sum_L f_L P_L(\cos\beta) \tag{10}$$

$P_L(\cos\beta)$ are the Legendre polynomials and β is the angle made by the molecular symmetry axis with the director. The phase symmetry dictates that L has to be even since $P_L(\cos\pi-\beta) = (-1)^L P_L(\cos\beta)$. The coefficients f_L in the expansion of $f(\beta)$ can be obtained through the orthogonality properties of the Legendre polynomials. This is achieved by multiplying both sides of equation (10) by $P_{L'}(\cos\beta)$ and integrating over all β such that

$$\int_0^{\pi} d\beta \sin\beta f(\beta) P_{L'}(\cos\beta) = \sum_L f_L \int d\beta \sin\beta P_L(\cos\beta) P_{L'}(\cos\beta). \tag{11}$$

The average quantity on the left hand side of equation (11) defines the infinite set of orientational order parameters P_L. Therefore

$$\bar{P}_{L'} = \sum f_L \frac{2}{(2L+1)} \delta_{LL'} \qquad (12)$$

Equation (12) contains only one non-zero term which is obtained when L = L'. The singlet orientational distribution is now given by

$$f(\beta) = \sum_L \frac{(2L+1)}{2} \bar{P}_L P_L(\cos\beta) \; ; \quad L \text{ is even} \qquad (13)$$

Thus $f(\beta)$ can be described by an infinite set of order parameters given by $\bar{P}_L$ and the more order parameters we know the closer we can approach the true nature of the orientational distribution. When the condition of perfect order prevails $f(\beta)$ becomes a δ function since $\bar{P}_L$ is unity for all values of L. For a state of intermediate order we would expect the function to converge, albeit rather slowly, since in this range $\bar{P}_2 > \bar{P}_4 > \bar{P}_6$ and contributions of higher terms become negligible. If we expand $f(\beta)$ to fourth rank terms we find

$$f(\beta) = \frac{1}{2} + \frac{5}{2} \bar{P}_2 P_2(\cos\beta) + \frac{9}{2} \bar{P}_4 P_4(\cos\beta) + \ldots\ldots \qquad (14)$$

The first non-trivial term in the expansion contains the second rank order parameter $\bar{P}_2$ which is given by

$$\bar{P}_2 = (3\bar{\cos}^2\beta - 1)/2 \qquad (15)$$

This average behaves intuitively as one would expect since the limit of perfect order $\bar{P}_2=1$ and in the isotropic phase $\bar{P}_2=0$. The same limits apply for all $\bar{P}_L$ when L is

even. For a first order transition, or going from an ordered state to one in which the ordering is destroyed, the order parameter goes discontinuously to zero. Conversely, for a second order transition the order parameter goes continuously to zero.

2. Saupe Ordering Matrix

An alternative way of defining the orientational order parameters in a uniaxial phase is by expanding $f(\Omega)$ in terms of the direction cosines, l_α ($\alpha = x, y, z$), of the director in a frame fixed in the molecule. The expansion to second rank terms gives

$$f(\Omega) = (1/8\pi^2)\,(1+5\sum_{\alpha\beta} S_{\alpha\beta} l_{\alpha\beta}) \qquad (16)$$

where the traceless ordering matrix is given by

$$S_{\alpha\beta} = (3\bar{l_\alpha l_\beta} - \delta_{\alpha\beta})/2 \qquad (17)$$

and is known as the Saupe ordering matrix. In the limit of molecular cylindrical symmetry this equation is identical to equation (15) and depends only on the angle β.

$$S = (3\,\bar{\cos^2\beta} - 1)/2. \qquad (18)$$

The Saupe ordering matrix is real, symmetric i.e. $S_{\alpha\beta} = S_{\beta\alpha}$ and traceless i.e. $S_{xx} + S_{yy} + S_{zz} = 0$, which is readily discernible from equation (17) and the properties of the direction cosines. Thus we can distinguish five independent elements of the matrix which are related to the second rank modified spherical harmonics by

$$S_{zz} = \bar{C}_{2,0},$$

$$
\begin{aligned}
S_{xx\text{-}yy} &= \left(\frac{3}{2}\right)^{1/2} (\bar{C}_{2,2} + \bar{C}_{2,-2}) , \\
S_{xy} &= i\left(\frac{3}{8}\right)^{1/2} (\bar{C}_{2,-2} + \bar{C}_{2,2}) , \\
S_{xz} &= \left(\frac{3}{8}\right)^{1/2} (\bar{C}_{2,-1} + \bar{C}_{2,1}) , \\
S_{yz} &= i\left(\frac{3}{8}\right)^{1/2} (\bar{C}_{2,1} + \bar{C}_{2,-1}) ,
\end{aligned} \tag{19}
$$

For a molecule whose principal axes cannot be located i.e. has symmetry less than a two fold axis of rotation (C_2) then all five elements of the Saupe ordering matrix are required to describe the orientational ordering. In the principal axes system of S only two elements remain, S_{zz} and the biaxiality (S_{xx} - S_{yy}) . However, if there is at least a three fold symmetry axis of rotation, the number may be further reduced to a single order parameter to describe the orientational ordering of the symmetry axis namely, S_{zz}.

Having discussed distribution functions and their relationship with the orientational order parameters we now turn to the measurement of these order parameters using nuclear magnetic resonance (NMR). This experimental technique measures the partial averages of the components along the magnetic field of a number of second rank properties such as quadrupolar interaction q_i and dipolar coupling D_{ij} . The partial averaging of the second rank interactions comes about due to the rapid anisotropic molecular tumbling; the extent of the averaging is dependent upon the orientational order. Thus, the relationship between the partial average of the component along the field (or director if n || **B**) A_{zz}, the components set in a molecular frame $A_{\alpha\beta}$ and the Saupe ordering matrix is given by

$$
A_{zz} = A_0 + 2/3 \sum_{\alpha\beta} A_{\alpha\beta} S_{\alpha\beta} , \tag{20}
$$

where A_0 is the isotropic average of the second rank interaction tensor, i.e. $A_0 = 1/3 (A_{xx}+A_{yy}+A_{zz})$. In the case of the quadrupolar interaction $A_{\alpha\beta} = q_{\alpha\beta}$ and A_0 is zero because the quadrupolar interaction tensor is traceless.

3. Nuclear Magnetic Resonance (NMR)

NMR measures the very weak magnetic, and in some cases electrical, interactions of atomic nuclei with their surroundings. Its utility in the identification of molecular structure and orientation stems from the fact that the resonance signals from individual atomic nuclei can often be separately resolved. Conventional spectroscopy and relaxation time measurements can be used to probe microscopic structure and dynamics as well as long range orientational ordering. Techniques such as pulsed field gradient NMR can be used to measure diffusion over macroscopic distances and is especially useful as a probe of aggregate structures in lyotropic liquid crystals. We will, however, be solely concerned with the more routine deuterium NMR in this chapter.

In most liquid crystals, and for all the systems described in this Chapter, the molecular reorientations are anisotropic and fast on the NMR timescale (which is typically>10^{-6}s). The NMR experiment can therefore only measure partially averaged values of the second rank nuclear spin properties, access to higher rank order parameters may be gained through techniques such as fluorescence spectroscopy [2,3] and neutron scattering [4]. Proton (^{1}H) spectroscopy is often extremely complicated and not always very useful for the study of liquid crystals because all of the n protons in a material are dipolar-coupled, giving an exceedingly complex unresolved spectrum containing 2^n lines. The strategy is, therefore, to simplify the spectrum by partial deuteriation and high power decoupling. Alternatively, the spectrum of the 'single' deuterium spin can be observed directly. This spectrum is dominated by the coupling between the nuclear quadrupole

moment and the electric-field gradient at the nucleus. The chemical shift is another 'single-spin' interaction which is often measured.

4. Deuterium NMR Spectroscopy in Liquid Crystals

In this section we shall describe the dipolar and quadrupolar interaction necessary for the measurement of orientational order parameters.

The relevant interactions which contribute to the nuclear spin hamiltonian are given as

$$H = H_Z + H_J + H_D + H_Q \quad , \tag{21}$$

where the hamiltonians represent, the Zeeman interaction, indirect spin-spin coupling, the dipolar spin–spin coupling and the quadrupolar interaction. In principle any one or all of these four interactions should lead to information about the ordering of an anisotropic system. However, in the majority of NMR experiments it is the Zeeman term, which represents the interaction between the magnetic dipole moment μ and the magnetic field B, which is dominant. Other interactions such as the shielding effect, indirect spin coupling, direct spin coupling and quadrupolar interaction arise from different electric and magnetic interactions and are treated as perturbations of the Zeeman interaction. The chemical shielding results from the screening effect of surrounding electrons which generate a local field that counteracts the applied magnetic field. The indirect spin-spin coupling is the interaction between nuclei through the electronic structure of the molecule. Although both the chemical shielding effect and the indirect spin-spin coupling are anisotropic and can be potentially useful in the study of orientational order, two purely anisotropic interactions, namely the dipolar and quadrupolar interactions, are usually measured to study the molecular orientational order in liquid crystals. Here

we first discuss briefly the Zeeman interaction, and then consider the dipolar and quadrupolar interactions

4.1 Zeeman Interaction

Nuclei with a spin greater than zero possess a magnetic dipole moment μ which interacts with a magnetic field of flux density **B** to give an energy E known as the Zeeman interaction

$$E = \mu . \mathbf{B} \ . \tag{22}$$

The magnetic dipole moment of a nucleus is related to the spin angular momentum **I**, through the magnetogyric ratio γ, which is a constant characteristic of a given nucleus

$$\mu = \gamma \mathbf{I} \ . \tag{23}$$

The presence of a magnetic field quantises the spin angular momentum along the Z' direction of the field such that

$$\mu_{Z'} = \gamma I_{Z'} . \tag{24}$$

and

$$E = \mu_{Z'} B_{Z'} \tag{25}$$

by definition.

The operator equivalent of **I** is I and the spin hamiltonian for the Zeeman interaction is

$$H_{Z'} = - \gamma \mu_{Z'} I_{Z'}. \qquad (26)$$

The discrete set of energy levels of the nuclear spin can be determined from the time independent Schrodinger equation,

$$H \phi |I, m\rangle = E_m \phi |I, m\rangle, \qquad (27)$$

where $\phi |I, m\rangle$ are eigenfunctions of the spin angular momentum operator $I_{Z'}$ and E_m are the eigenvalues. Therefore,

$$I_{Z'} \phi |I, m\rangle = (m \hbar) \phi |I, m\rangle, \qquad (28)$$

the magnetic quantum number m takes the values $I, I-1, \ldots, -I$ and $\hbar = h / 2\pi$ where $\hbar$ is Plank's constant. The energies of these states are given by

$$E_m = - \hbar \gamma B_{Z'} m \ , \qquad (29)$$

The quantum of energy ($\Delta E = h\upsilon$) required to cause NMR transitions between the energy states occurs in the radiofrequency, depending on $B_{Z'}$, region of the spectrum and is given by

$$\Delta E = - \hbar \gamma B_{Z'} . \Delta m \ . \qquad (30)$$

The selection rule governing such transitions is $\Delta m = \pm 1$ and the resonance frequency is

$$\Delta E = - \hbar \omega \ , \qquad (31)$$

where $\omega = \gamma B_Z$ and is known as the Larmor frequency.

4.2 Dipolar Coupling

The dipolar coupling is an interaction through space between two magnetic moments (see figure 2) and its contribution to the spin hamiltonian can be expressed as

$$H_D = I_i \, D_{ij} \, I_j \tag{32}$$

Here, D_{ij} is the partially averaged second rank dipolar interaction tensor whose components are

$$D_{ij} = \frac{\gamma_i \gamma_j h}{4\pi^2 r_{ij}^3} S_{ij} \tag{33}$$

γ_i and γ_j are the magnetogyric ratios of the respective nuclei, r_{ij} is the vector connecting the nuclear magnetic moments and S_{ij} is the order parameter for the internuclear vector joining i and j. In strong magnetic fields the Zeeman term in the nuclear spin hamiltonian is large compared to the dipolar interaction in hydrogen and deuterium nuclei. As a consequence the spins are quantised along the field direction (Z). Therefore equation (33) can be written as

$$D_{ijzz} = -\frac{\gamma_i \gamma_j h}{4\pi^2 r_{ij}^3} S_{ij} \, . \tag{34}$$

where

$$S_{ij} = (3\cos^2 \phi_{ijz} - 1)/2. \tag{35}$$

here Sij is the Saupe order parameter and r_{ij}^3 is the vibrational averaged distance between nuclei i and j. Hence, from the measurement of the dipolar interaction, it is possible to obtain S_{ij} which defines the ordering of the internuclear vector connecting nuclei i and j with respect to the magnetic field. Given that r_{ij} and the geometry of the molecule are known, measurement of D_{ijzz} will give information about the second rank orientational order parameters for the molecules

4.3 Nuclear Quadrupolar Interaction

Deuterium has a nuclear spin of one and so possesses an electric quadrupole moment (see figure 3). This is true for all nuclei with a nuclear spin greater than one half. The quadrupole moment interacts with the electric field gradient at the nucleus, to give a quadrupole interaction tensor. For a single deuteron in a high magnetic field the Zeeman interaction far exceeds the quadrupolar interactions and the spin angular momentum is quantised along the field direction (Z). In units of frequency the spin hamiltonian of the Zeeman and quadrupolar interaction in a uniaxial liquid crystal for a single deuteron is given by

$$H_Q = -\omega I_{iZ'} + \frac{e Q V_{iZ'Z'}}{4h} (3 I_{iZ'} I_{iZ'} - 2) \qquad (36)$$

where ω is the frequency corresponding to the Zeeman interaction ($-\omega I_{iZ'}$ is the Zeeman coupling, H_Z), e is the charge on the electron, $V_{iZ'Z'}$ is the electric field gradient for the ith deuteron along the Z' direction, axial symmetry about Z' is assumed, i.e. ($V_{iX'X'} - V_{iY'Y'}$) vanishes, and that the high field approximation ensures that the off-diagonal elements in the quadrupolar interaction tensor, **q** are not important. The component of the partially averaged interaction tensor, where ~ denotes the value in the liquid crystal phase, is

$$\tilde{q}_{ipq} = e Q V_{ipq} / h \qquad (37)$$

and H_Q is

$$H_Q = H_Z + \tilde{q}_{iZ'Z'} (3 I_{iZ'} I_{iZ'} -2) /4. \quad (38)$$

Deuterium has three spin quantum numbers $m = -1, 0, +1$, the energy levels corresponding to the values are

$$E_1 = - \omega + \tilde{q}_{iZ'Z'} / 4,$$
$$E_0 = - \tilde{q}_{iZ'Z'} / 2$$
and $$E_{-1} = + \omega + \tilde{q}_{iZ'Z'} / 4. \quad (39)$$

The selection rule $\Delta m = \pm 1$ means that there are two transitions corresponding to the frequencies

$$E_0 - E_1 = \nu_1 = \omega - 3\tilde{q}_{iZ'Z'} / 4$$
$$E_{-1} - E_0 = \nu_2 = \omega + 3\tilde{q}_{iZ'Z'} / 4 . \quad (40)$$

Therefore two lines are expected in the spectrum of a single deuteron which has a splitting

$$\Delta \tilde{\nu} = 3/2 \, \tilde{q}_{iZ'Z'} \quad (41)$$

centred at a frequency ω.

In general $\tilde{q}_{iZ'Z'}$ will depend upon the average of some function that a given C-D bond in a molecule makes with respect to the field direction. The rapid and random molecular tumbling averages the quadrupolar interaction tensor to zero in isotropic liquids and the doublet collapses into a single peak at ω. In an anisotropic phase, such as a nematic, the quadrupolar tensor is only partially averaged due to the

anisotropic molecular motion. We recall from equation (20) that the partially averaged tensor parallel to the field (or strictly, the director) can be written as

$$\tilde{q}_{iZ'Z'} = 3/2 \ \Sigma \ q_{i\,\alpha\beta} S_{\alpha\beta}. \qquad (42)$$

where we have set the isotropic average to zero in accord with the traceless property of the quadrupolar interaction tensor. We can now rewrite equation (42) in terms of the components of q in the principal axis system for q (a , b , c) which is chosen such that $|q_{a\,a}| > |q_{cc}| > |q_{bb}|$, thus

$$\tilde{q}_{iZ'Z'} = q_{i\,aa} \ [S_{aa} + 1/3\,\eta_i \ (S_{bb} - S_{cc})] , \qquad (43)$$

where we have introduced the parameter η which is a measure of the asymmetry in the quadrupolar interaction tensor and is given by

$$\eta = \frac{(q_{bb} - q_{cc})}{q_{aa}}. \qquad (44)$$

The quadrupolar splitting becomes

$$\Delta\nu_i = 3/2 \ \tilde{q}_{i\,aa} \ [S_{aa} + 1/3\,\eta_i \ (S_{bb} - S_{cc})]. \qquad (45)$$

The value of the quadrupolar interaction tensor is available from single crystal studies [5] and to a good approximation a axis lies along the C-D bond (see figure 2). In many cases η is assumed to be small enough to be ignored, this is taken to be true for aliphatic deuterons.For planar aromatic systems described in this Thesis the c axis is normal to the ring axis and parallel with the y axis in the principal molecular frame x, y, z for **S**, therefore $l_{iyc}^{\,2}=1$ and $l_{izc}^{\,2}$, $l_{ixc}^{\,2}$ $l_{iyb}^{\,2}$ and$l_{iya}^{\,2}$ all equal zero. In general the principal axes for **S** and **q** are not the same and so equation (41) may be expressed as

$$\Delta\nu_i = 3/2\ \tilde{q}_{i\,aa}\ [S_{zz}\ (3/2\, l_{iza}^{\,2} - 1/2 - 1/2\,\eta_i\, l_{izb}^{\,2}) + 1/2\ (S_{xx} - S_{yy})\,(l_{ixa}^{\,2} - 1/2 - 1/2\,\eta_i\, l_{ixb}^{\,2})], \qquad (46)$$

where l_{iza}, l_{izb}, l_{ixa}, and l_{ixb} are the direction cosines relating the principal axes (x, y, z) of **S** with those (a, b, c) of **q** for the i th deuteron. From this equation it is possible to evaluate the principal elements of **S** providing the geometry of the molecule and the principal elements of the quadrupolar interaction tensor are known together with two different values of $\Delta\nu_i$ the two principal elements of the Saupe ordering matrix expressed as S_{zz}, the major element, and S_{xx}-S_{yy}, the biaxiality may be calculated from equation (46). For example, for the probe anthracene-d_{10} employed in some experiments in this Thesis, there are three non-equivalent sites of deuterium, although in many experiments only two are resolved. For the other experiments discussed in this Thesis the directly deuteriated mesogenic materials possess just one deuterium site and so two quadratic equations must be solved using values of $\Delta\nu_i$ obtained from the experimentally observed quadrupolar and the dipolar splittings in order to obtain the major order parameter S_{zz} and the biaxial order parameter $(S_{xx} - S_{yy})$.

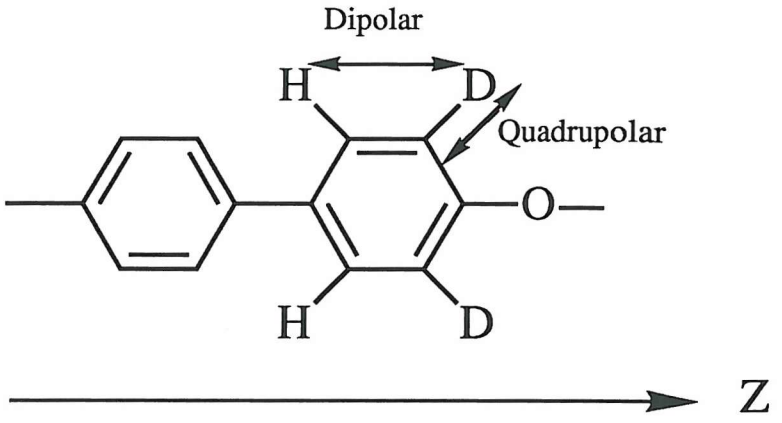

Figure 2. Diagram indicating the symmetry axes of the dipolar interaction andthe quadrupolar interaction in relation to the molecular axis Z.

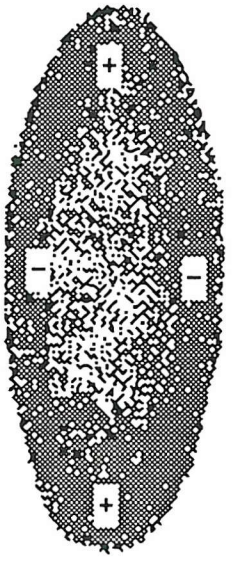

Figure 3. Diagram showing the charge distribution of a nucleus with an axial quadrupole.

References

[1] Veracini, C., 1985, *Nuclear Magnetic Resonance of Liquid Crystals*, Ed., J.W. Emsley, Reidel.

[2] Arcioni A., Tarroni R. and Zannoni C., 1988, *Polarised Spectroscopy of Order Systems*, Eds. B. Samori and E. Thulstrup, (Kluwer, Deventer) p.421.

[3] Arcioni A., Tarroni R. and Zannoni C., 1989, *Liq. Crystals*, **6**, 63.

[4] Leadbetter A.J., Richardson R.M., 1979, *'Molecular Physics of Liquid Crystals'*, Chapt. 20, Eds. G.R. Luckhurst and G.W. Gray. Academic Press.

[5] Ellis D.M., Bjorkstam J.L., 1967, *J. Chem. Phys.*, **46**,4460.

CHAPTER 3

The orientational behaviour of liquid crystal dimers which contain methylene and ether links.

1. Introduction

Attention has been focussed on dimeric liquid crystals for many years now, not least because of their structural and behavioural similarities to semi-flexible main chain polymer systems.

This continued interest and hence the vast amount of detailed research and understanding that that is stimulated by it provide a solid basis on which to conduct a study into the effect the linkage between the flexible chain and the mesogenic group has upon the orientational order and physical properties of a dimer. The pronounced odd-even effect, a familiar characteristic of many dimers [1] is a sensitive function of the nature of the linking group between the alkyl chain and mesogenic group. The nature of this effect is based fundamentally on the parity of the flexible chain, however, the magnitude is related to the composition of the molecule as a whole. Take for example a monomer in which a cyanobiphenyl group attached to an alkyl chain either through an oxy or a methylene link. The nematic-isotropic transition temperature (T_{NI}) for the ether link has a near 40°C advantage over the methylene linked analogue. The higher clearing points associated with the alkyloxy chain has previously been ascribed to the greater conjugation provided by the lone pairs of electrons on the oxygen atom effectively elongating the conjugation pathway and so enhancing the polarisability anisotropy [2]. It follows therefore that this behaviour should also be observed for dimers of similar construction.

Recently however, it has been proposed that the difference between the geometry of the links, which changes the length to breadth ratio, far outweighs any enhancement of the polarisability anisotropy of the mesogenic group afforded by the ether link [3]. The bond angle for the $C_{ar}\hat{O}C_{al}$ is near 120° whereas the $C\hat{C}C$ bond angle is approximately 109°. When considering the preferred low energy all-trans state of the alkyl chain, such a variation in bond angles causes significant difference between the relative orientation of the mesogenic groups in the dimers (see figure 1).

As the angle between the effective long axes of the flexible chain and the mesogenic group decreases so the magnitude of the odd-even effect grows. Mesogenic groups attached through an even numbered chain remain essentially parallel as the $C_{ar}\hat{O}C_{al}$ angle changes and so only a minor reduction in mesogenic tendency is observed. However, for odd conformers, the lower order associated with their greater biaxiality leads to a substantial reduction in liquid crystal forming ability. Hence the nematic-isotropic transition temperatures for a series of methylene linked dimers are predicted to alternate more than their ether linked counterparts with less attenuation as the chain length increases. This effect is proposed to hold not only for the idealised all trans state sketched in figure 1, but theoretical calculations predict that this enhanced odd-even effect to remain, at least qualitatively, for other conformations of the chain also. The increased alternation in T_{NI} for these methylene linked dimers is expected to be mirrored in the transitional entropy data. For short length alkyl chains containing an odd number of units, a very small perhaps second order isotropic-nematic transition might be expected leading to the possibility of the elusive biaxial nematic phase [3].

To examine further this methylene linkage within a dimer, four members of the α,ω–bis(4'-cyanobiphenyl-4-yl)alkane series have been prepared with n = 4,5,6 and 7 where n is the number of methylene units in the spacer. For comparison, the properties of analogous dimers containing ether linkages, namely the 4,4'-bis(4'-cyanobiphenyl-4-yloxy)-alkanes with n = 2,3,4 and 5 again where n is the number

(a).

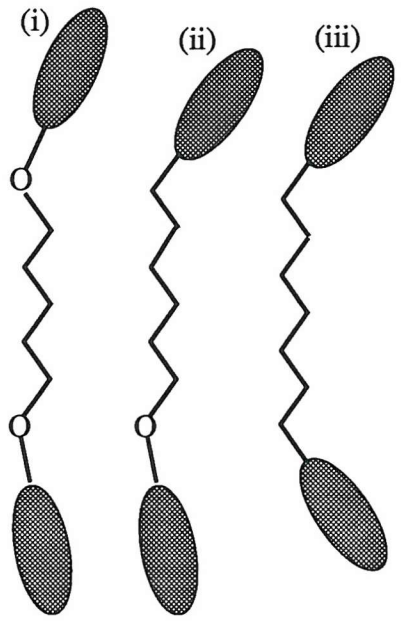

(b).

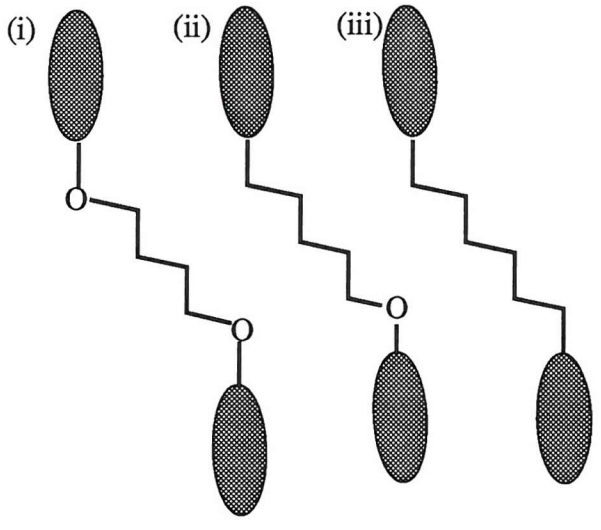

Figure 1. The change in molecular shape of the all-trans conformers of; (i) ether, (ii) oxymethylene and (iii) methylene linked dimers with (a) an odd and (b) an even number of atoms, excluding hydrogen, in the spacer chain.

of methylene linkages, are included. n.b. dimers with the same total no. of atoms in the spacer backbone.

Later in this chapter the properties of four members of the dimeric α-(4-cyanobiphenyl-4'-oxy)-ω-(4,-cyanobiphenyl-4-yl)alkane series are introduced. These will be discussed as dimers intermediate to the solely ether and methylene types of dimer mentioned previously and as interesting mesogens in their own right.

2. Experimental

Details of the synthetic method used for the preparation of the 1,7-bis(4'-cyanobiphenyl-4-yl)heptane are presented in this section and outlined in reaction scheme 1; the hexyl, pentyl and butyl homologues of this series were prepared in a similar manner. Characterisation of CB6CB is included for comparison.

2.1 *Synthesis of 1,7-bis(4'-cyanobiphenyl-4-yl)heptane*

Synthesis of 1,5-bis(4'-bromobiphenyl-4-carbonyl)pentane

A solution of freshly distilled pimeloyl chloride (0.03mol, 5.91g) and 4-bromobiphenyl (15g, 0.065 mol) in dichloromethane (30ml) was added dropwise to a stirred suspension of powdered, anhydrous aluminium trichloride (0.062mol, 7.72g) in dichloromethane (25ml) at 0°C. The resulting mixture was allowed to warm to room temperature and stirred overnight. The reaction mixture was poured into water (200ml) and extracted with dichloromethane (3x40ml). The remaining aqueous suspension was filtered, washed and the solid recrystallised from toluene.

Yield (7.95g, 52%), mp 213-214°C.

IR; υ 1673 cm^{-1} (carbonyl).

^1H NMR; ($CDCl_3$, δ) 2.1-2.3 (3H, m), 3.1-3.3 (2H, t), 7.3-8.1 (8H, m).

Synthesis of 1,7-bis(4'-bromobiphenyl-4-yl)heptane

Triethylsilane (0.065mol, 7.54g) was added dropwise to a stirred solution of 1,4-bis(4'-bromo-biphenyl-4-carbonyl)butane (0.013mol, 7.67g) in trifluoroacetic acid (0.20mol, 23.26g) and dichloromethane (20ml) at 0°C [4]. The reaction mixture was allowed to reach room temperature and stirred for 48 h. The white solid was then filtered off, washed thoroughly with water and recrystallised from toluene. Yield (3.58g, 47%), mp 147-148°C.

IR; no evidence of carbonyl stretch.
^{1}H NMR; ($CDCl_3$, δ) 1.3–1.5 (2H, m), 1.6-1.8 (4H, m), 2.5-2.7 (4H, t), 7.3-7.8 (16H, m) ppm.

Synthesis of 1,7-bis(4'-cyanobiphenyl-4-yl)heptane

The cyanation was carried out using a modified method developed by Coates and Gray [5]. Cuprous cyanide (0.011mol, 1.02g) was dissolved in dry N-methyl pyrrolidone (15ml). Approximately 10% of the solvent was then distilled off under vacuum and discarded to remove any moisture in the CuCN and any remaining in the NMP. This was then added to a solution of 1,7-bis(4'-bromobiphenyl-4-yl)heptane (0.0038mol, 2.14g) in NMP (15ml) that had been treated in a similar way. The reaction mixture was stirred at 200°C for 4 h. This was then cooled to 80°C and a solution of ferric chloride (5g) in water (10ml) and hydrochloric acid (4ml) was added to solubilise any copper complexes formed. After stirring for a further 30 min the mixture was allowed to cool overnight, poured into water (100ml), filtered and the solid was washed with water (200ml). The product was purified by column chromatography (dichloromethane/ silica 60) and recrystallised from toluene. Yield (1.08g, 47%).
1,7-bis(4'-cyanobiphenyl-4-yl)heptane

IR; υ 2224 cm^{-1} (cyanide).

^1H NMR; ($CDCl_3$, δ) 1.4 (6H, m), 1.7 (4H, m), 2.7 (4H, t), 7.3 (4H, d, J = 8 Hz), 7.5 (4H, d, J = 8 Hz), 7.7 (8H, m) ppm.

^{13}C NMR; ($CDCl_3$, δ) 29.24, 29.37, 31.35, 35.63, 110.59, 119.03, 127.11, 127.48, 129.22, 132.58, 136.48, 143.73, 145.59 ppm.

MS (EI, 70eV) 454 (M^+, 27%), 192 ($C_{14}H_{10}N$, 100%).

1,6-bis(4'-cyanobiphenyl-4-yl)hexane

Yield (0.85g, 55%).

IR; υ 2224 cm^{-1} (cyanide).

^1H NMR; ($CDCl_3$, δ) 1.4 (4H, m), 1.7 (4H, m), 2.7 (4H, t), 7.3 (4H, d, J = 8 Hz), 7.5 (4H, d, J = 8 Hz), 7.7 (8H, m) ppm.

^{13}C NMR; ($CDCl_3$, δ) 29.25, 31.38, 35.71, 110.72, 119.72, 127.21, 127.59, 129.29, 132.67, 136.65, 143.73, 145.71 ppm.

MS (EI, 70eV) 440 (M^+, 46%), 192 ($C_{14}H_{10}N$, 100%).

Reaction Scheme 1

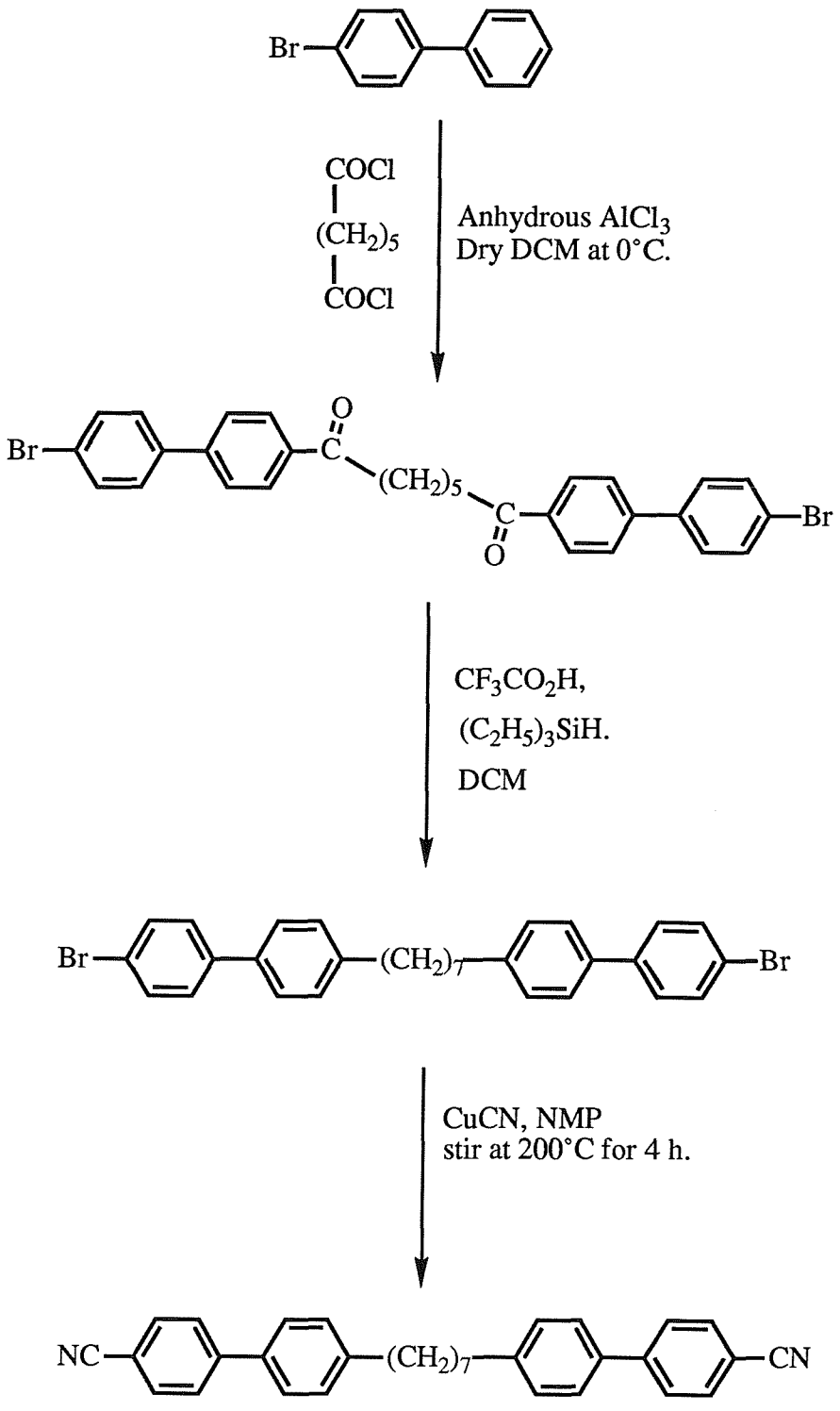

Reaction Scheme 2

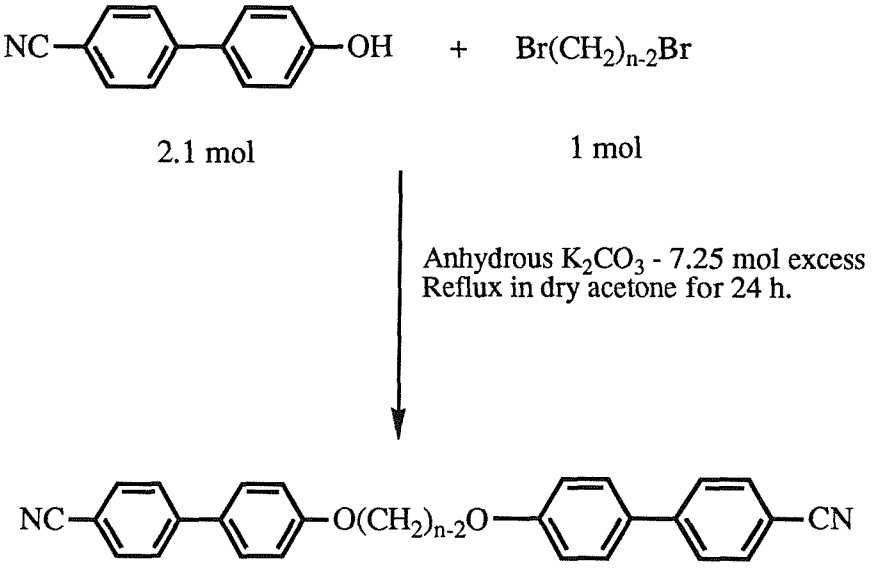

3. Results and Discussion

3.1 Transitional properties

For ease of notation and the α,ω-bis(4'-cyanobiphenyl-4-yl)alkanes will be referred to as the methylene linked dimers or simply CBnCB. The α,ω-bis(4'-cyanobiphenyl-4-yloxy)alkanes will be referred to as the ether linked dimers or CBO(n-2)OCB, where n in each case describes the number of atoms in the spacer chain.

The transitional data for the α,ω-bis(4'-cyanobiphenyl-4-yl)alkanes with n=4,5,6 and 7 are given in table 1.All are enantiotropic with the exception of CB5CB which has a short-range monotropic mesophase region. The odd members of the series examined here both exhibit a smectic phase. Members of the well-known [1] α,ω-bis(4'-cyanobiphenyl-4-yloxy)alkanes of corresponding length are listed in table 2 for comparison.

When studying the data it is immediately apparent that the magnitude of the odd-even effect is greatly enhanced in the absence of ether linkages, as predicted by theory [3]. Attenuation of this effect with increasing chain length is still observed. The differences between the nematic-isotropic transition temperatures between odd and even conformers on ascending the CBnCB series is 184°,139° and 115°C, whereas for the CBO(n-2)OCB series they are 95°, 80° and 64°C. This trend can, to a large extent, be interpreted as a reduction in the liquid crystalline behaviour of odd methylene linked dimers as compared to the ether linked analogues. The difference in the transition temperatures for chains containing an even number of units between the two series is a fraction ($\approx 1/4$) of the difference observed for the odd conformers reinforcing the idea that the geometry of the mesogenic group-chain bond has a much greater influence over the odd rather than the even dimers. The mesogenic groups in even dimers are capable of aligning in a parallel arrangement,

Table 1. The transitional data of the α,ω-bis(4'-cyanobiphenyl-4-yl)alkanes. The published data for CB7CB are included for comparison [6].

	CB4CB	CB5CB	CB6CB	CB7CB	CB7CB [6]
T_{NI}/°C	275	(91)	230	115	114.1
ΔH_{NI}/kJ mol^{-1}	10.07	0.24	10.91	1.09	0.67
ΔS_{NI}/R	2.21	0.08	2.61	0.34	0.21
T_{CN}/°C	225	144†	183	101	104.5
ΔH_{CN}/kJ mol^{-1}	33.11	38.80	36.00	23.84	24.60
ΔS_{CN}/R	8.16	11.19	9.50	7.67	8.00
T_{SN}/°C		(87)		102	
ΔH_{SN}/kJ mol^{-1}		1.32		0.97	
ΔS_{SN}/R		0.44		0.31	

The uncertainties in the transition temperatures are ±1°C, and the enthalpies and entropies of transition ±5%.

( ) indicates a monotropic transition. † indicates a crystal-isotropic transition.

Table 2. the transitional data of the α,ω-bis(4'-cyanobiphenyl-4-yloxy)alkanes that contain a comparable numbers of units in the spacer chain to the methylene linked dimers detailed in table 1.

	CBO2OCB	CBO3OCB	CBO4OCB	CBO5OCB
T_{NI}/°C	265	(170)	250	186
ΔH_{NI}/kJ mol^{-1}	7.91	1.99	8.47	2.53
$\Delta S_{NI}/R$	1.77	0.54	1.95	0.66
T_{CN}/°C	205	†185	209	137
ΔH_{CN}/kJ mol^{-1}	37.4	45.5	41.7	30.2
$\Delta S_{CN}/R$	9.4	12.0	10.4	8.8

The uncertainties in the transition temperatures are ±1°C, and the enthalpies and entropies of transition ±5%.

( ) indicates a monotropic transition. † indicates a crystal-isotropic transition.

for odd dimers this is not possible without the unfeasible distortion of the bond angles.

This odd-even effect enhancement is also displayed in the unattenuated entropy of transition data. CB6CB exhibits the largest entropy at $\Delta S/R=2.61$ and CB5CB the smallest at $\Delta S/R=0.09$. These thermal data are shown in figures 2 and 3 together with the data predicted from theory. The agreement of the theory with experimental findings in both the thermal and entropic data is good. The entropy of transition for the odd members of the CBnCB series is predicted to be very small to the point of becoming second order and thus indicating the possibility of a biaxial nematic for $n_{odd}<7$. CB5CB provides only a short, unusually monotropic ($\approx 50°$ below T_{NI}) mesophase region (figure 4). A narrow nematic band is followed by a phase optically similar to that seen in CB7CB. The entropy is, as expected, extremely low for a dimer at $\Delta S/R=0.08$, lending support to the possible existence of a biaxial nematic. Unfortunately due to the transience of these phases further studies, such as deuterium NMR, to elucidate their identity were unsuccessful.

As the number of units in the flexible chain is reduced, so the average molecular biaxiality is increased. For the dimers described in this chapter this effect grows as a function of two factors:-

(i) As the angle between the para-axis of the mesogenic group and the flexible chain decreases.

(ii) As the length of the flexible chain decreases.

Considering the dimers examined in this study, it may be presumed that the methylene dimers are the more biaxial. This biaxiality increasing as the number of methylene units is decreased. We will now endeavour to consolidate this theory of the increased biaxiality of methylene linked dimers on an empirical level with the aid of deuterium NMR spectroscopy.

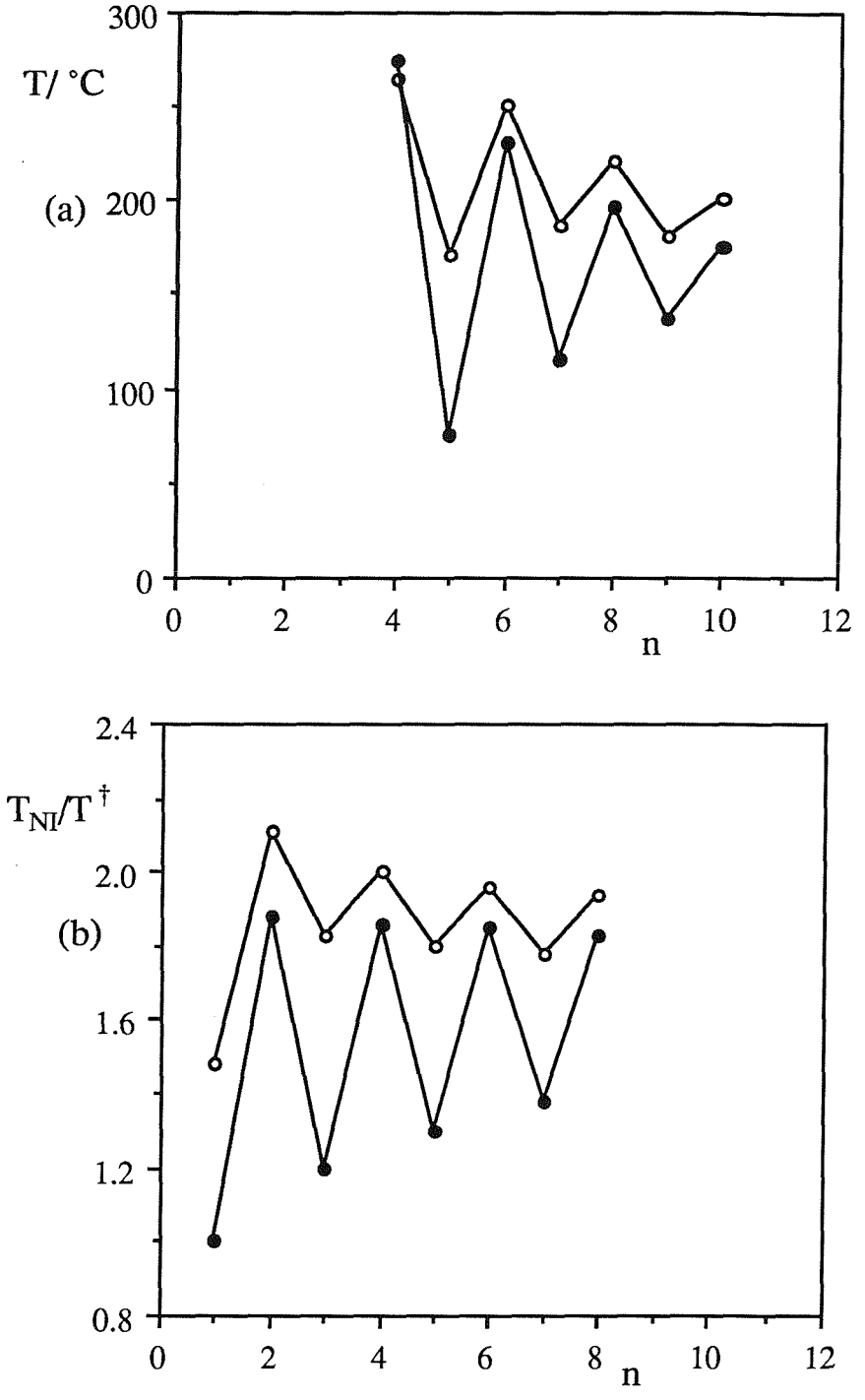

Figure 2. (a) The nematic-isotropic transition temperatures for the methylene (●) and ether (O) linked dimers. n is the number of atoms in the spacer (excluding hydrogen). (b) The predicted transition temperatures from theory; † the values are scaled to that of CB1CB.

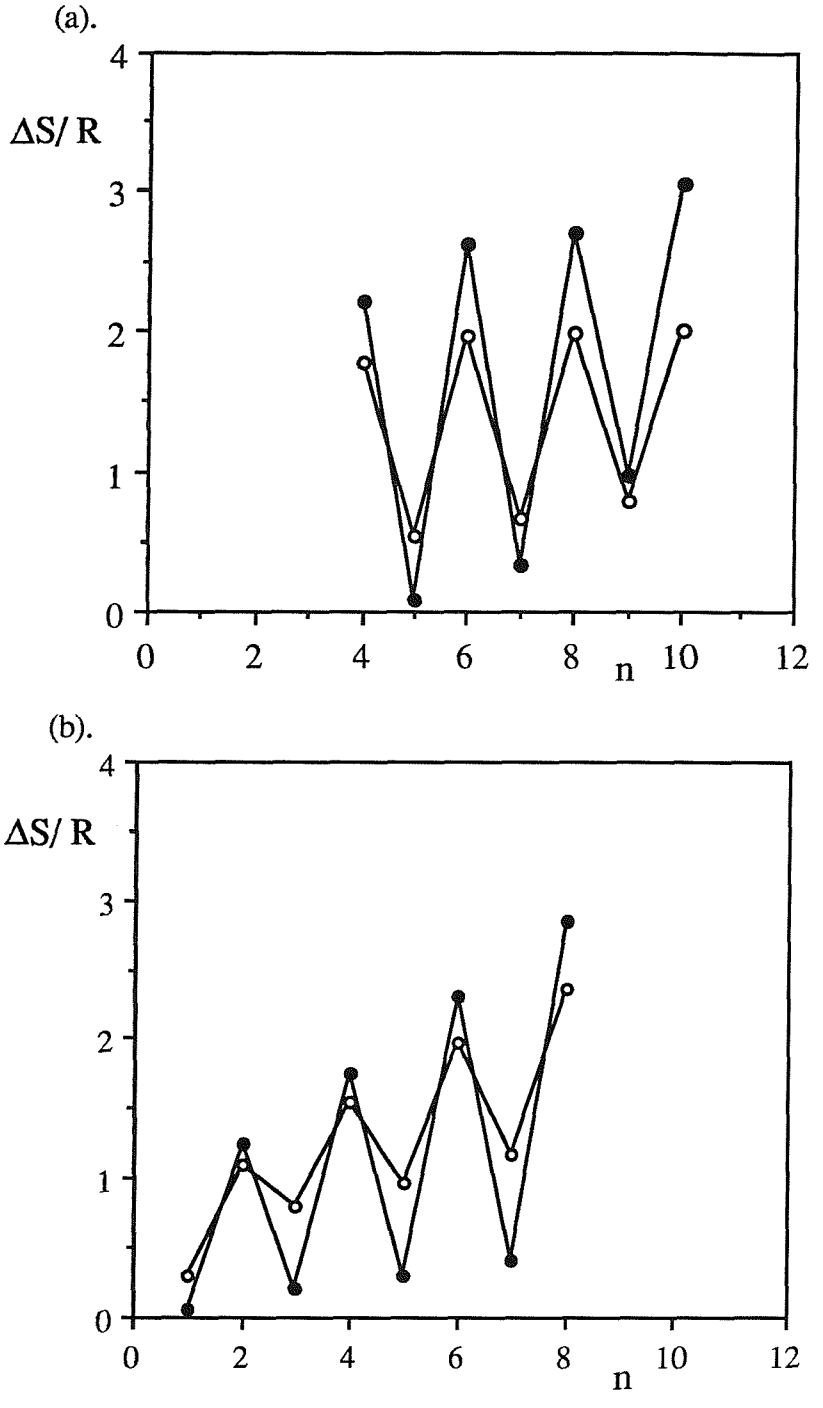

Figure 3. (a) The nematic-isotropic transitional entropies for the methylene (●) and ether (O) linked dimers. n is the number of atoms in the spacer (excluding hydrogen). (b) The predicted transitional entropies from theory.

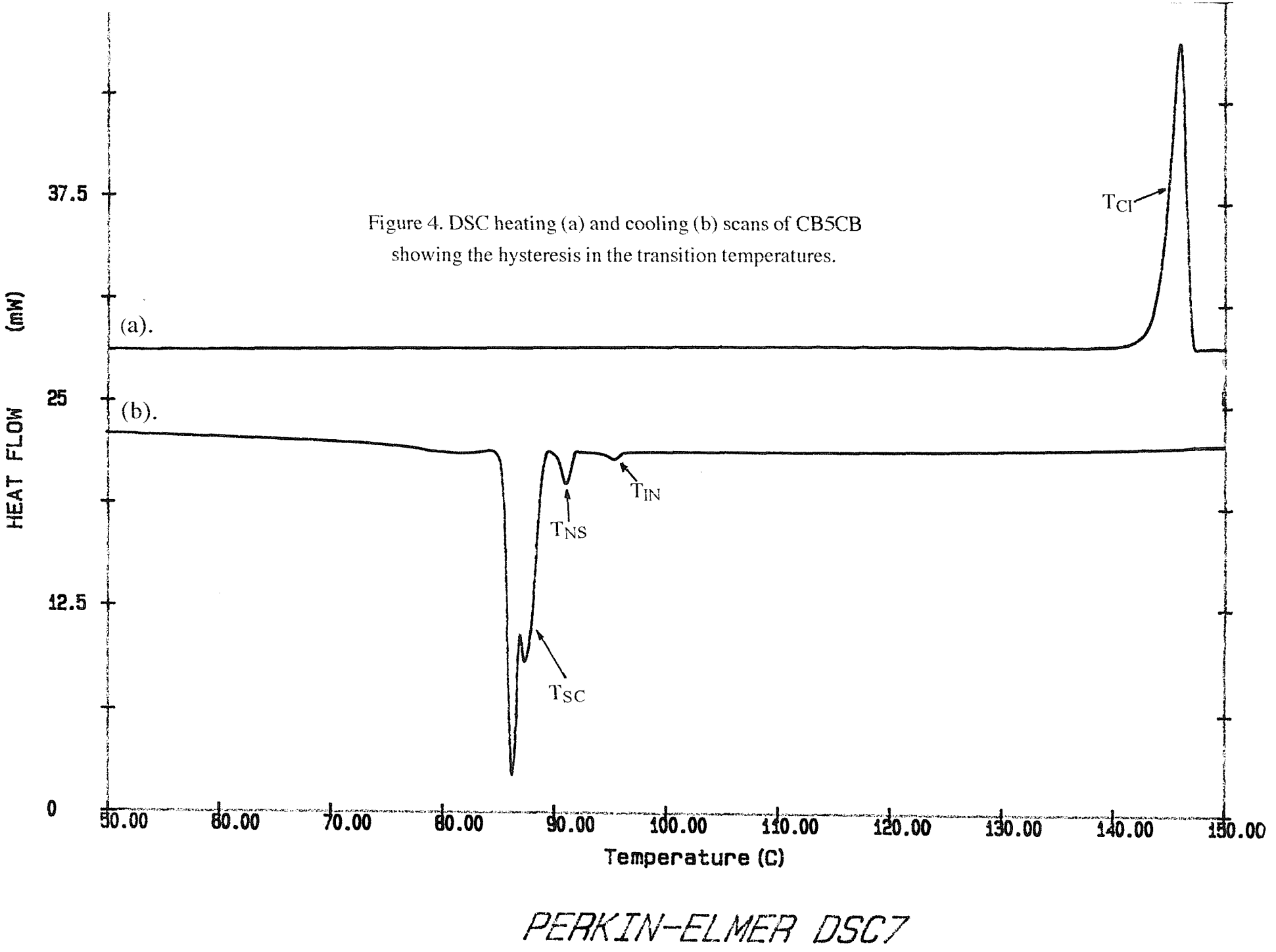

Figure 4. DSC heating (a) and cooling (b) scans of CB5CB showing the hysteresis in the transition temperatures.

3.2 Deuterium NMR spectroscopy

The enhanced odd-even effect observed in both the nematic-isotropic transition temperatures and the entropy of transition for the methylene linked dimers should be reflected in the orientational order of these molecules. To test this prediction , the Saupe ordering matrix of the solute anthracene-d_{10} has been determined for two methylene dimers with spacer lengths of 6 and 7. Unfortunately the order parameters of the methylene linked dimers CB4CB and CB5CB could not be measured. The transition temperatures of CB4CB were too high for our equipment and CB5CB possesses such a small monotropic mesophase range that crystallisation of the sample occurs before the equilibration of the temperature within the confines of the NMR spectrometer despite flash cooling. This is rather disappointing since CB5CB is predicted to be the most likely dimer to form a biaxial nematic phase.

From the NMR spectra in figure 5 of CB6CB and CB7CB at the nematic-isotropic transition, we can see that a small biphasic region exists caused by the effect of the solute anthracene-d_{10}. In this region the quadrupolar splittings and hence the orientational order of the solute are essentially independent of temperature. This allows accurate determination of the order parameters of the solute at the transition. This point in each sample was designated zero on a shifted temperature scale which allowed direct comparison between samples with the elimination of absolute temperature. These transitional data are listed in table 3. The major order parameters S_{ZZ}^{NI} show a difference between odd and even dimers of 0.25. This is approximately twice that observed for the ether linked dimers. This difference in order between the methylene and ether linked dimers of comparable length is in keeping with the entropy data. This fits in well with qualitative theoretical predictions but it should be noted that we find S_{ZZ}^{NI} for the even spacer to be greater for the methylene link than the ether linked dimer by 0.08 while S_{ZZ}^{NI} for the odd spacer with the methylene link

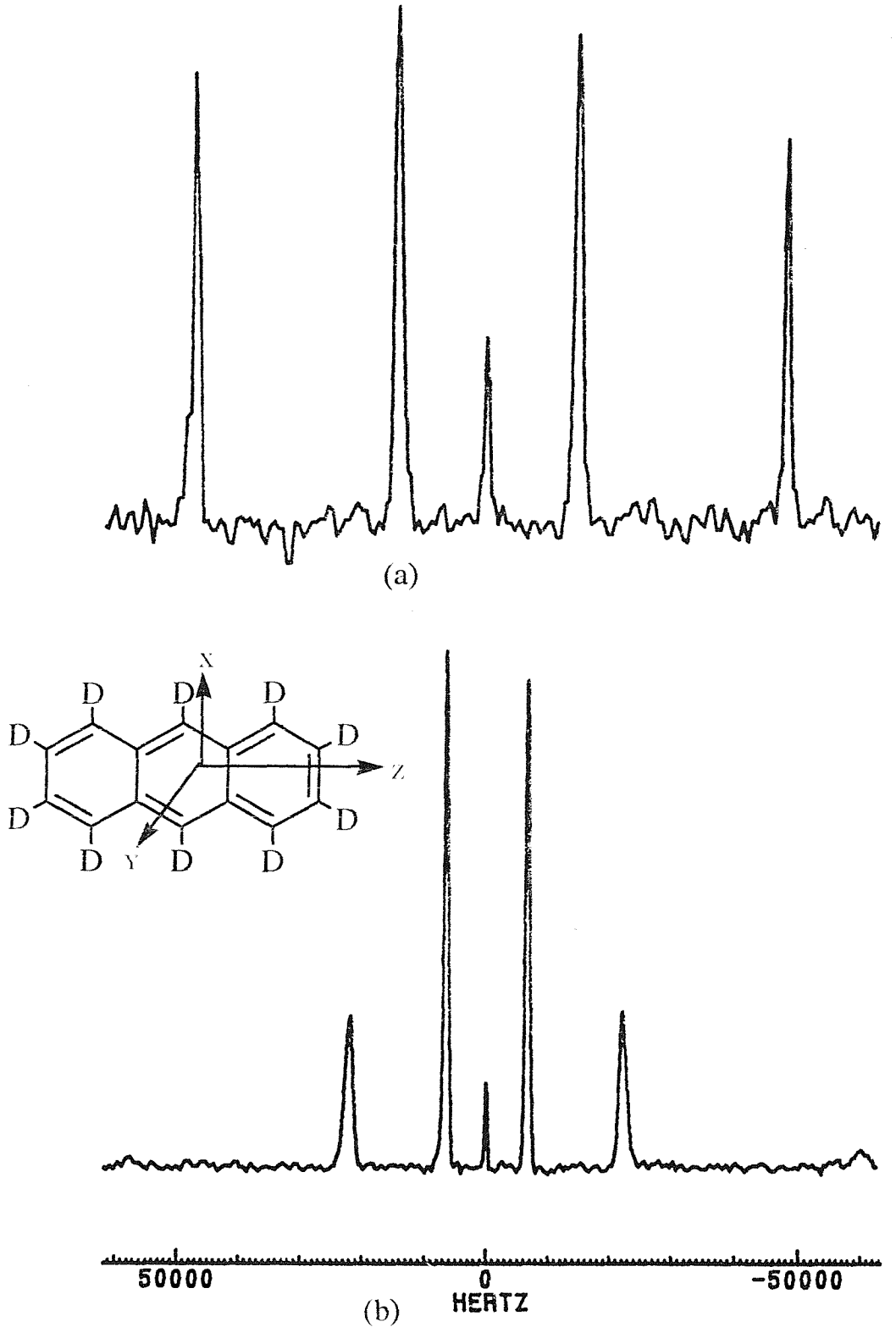

Figure 5. The deuterium NMR spectra of anthracene-d_{10} dissolved in (a) CB6CB and (b) CB7CB at the nematic-isotropic transition; the molecular structure of anthracene-d_{10} and the principal axes of the Saupe ordering matrix are also shown.

Table 3. The major (S_{zz}) and biaxial (S_{xx}-S_{yy}) order parameters of anthracene-d_{10} dissolved in CB6CB, CB7CB, CBO4OCB and CBO5OCB at the nematic-isotropic transition and at T_{NI}-15°C.

	CB6CB	CB7CB	CBO4OCB	CBO5OCB
S_{zz}^{NI}	0.479	0.224	0.398	0.268
$S_{zz}^{NI-15^\circ}$	0.531	0.334	0.480	0.406
S_{xx-yy}^{NI}	0.249	0.122	0.228	0.161
$S_{xx-yy}^{NI-15^\circ}$	0.240	0.129	0.232	0.192

The uncertainties in the measurement of S_{zz} and (S_{xx}-S_{yy}) are ±3%.

is less than that found for the ether link by 0.04, a trend also found in the experimental $\Delta S/R$ values. Theory, however, predicts that changes in $\Delta S/R$ are greatest for the odd rather than the even spacer on going from an ether to a methylene link.

The qualitative trends of the biaxial order parameters (S_{xx}^{NI}-S_{yy}^{NI}) follow those observed for S_{zz}^{NI} i.e greater for dimers with even rather than odd and also greater for ether rather than methylene linked dimers. This appears contrary to the intuitive expectation stated earlier that molecular biaxiality will be largest for short length odd methylene linked dimers. Similar behaviour has, however, been observed for the order parameters of a different solute in ether linked dimers [7]. We will return to this point later in the discussion. The temperature dependence of S_{zz} and (S_{xx}-S_{yy}) for anthracene-d_{10} dissolved in the four dimers is shown in figure 6. The order parameters are plotted against T_{NI}-T, a convenient way of comparing data sets, where T_{NI} is taken to be the temperature at which the system just becomes completely nematic i.e. when the central isotropic peak just vanishes. Looking first at S_{zz} it is seen that the differing behaviour of the dimers at the nematic-isotropic transition continues throughout the nematic range. The difference in the solute ordering between each dimer solvent is found to be almost independent of temperature. The initial rate of increase of S_{zz} does however grow as S_{zz}^{NI} gets smaller. This is to be expected, since the smaller value of the order parameter has to increase more rapidly at low shifted temperatures in order to achieve the limiting high values at lower temperatures. The jump observed for the solute ordering in CB7CB is ascribed to the transition to a smectic phase which is observed optically. The exact identity of this phase will be discussed later in this chapter.

The temperature dependence of the biaxial order parameters, (S_{xx}-S_{yy}), for the solute does not follow such a uniform path. For the even methylene linked dimer, (S_{xx}-S_{yy}) decreases with decreasing temperature, while for the odd dimer the order parameter first increases then decreases as the temperature is lowered. This rate of decrease is accelerated as the smectic phase is encountered. The odd ether linked

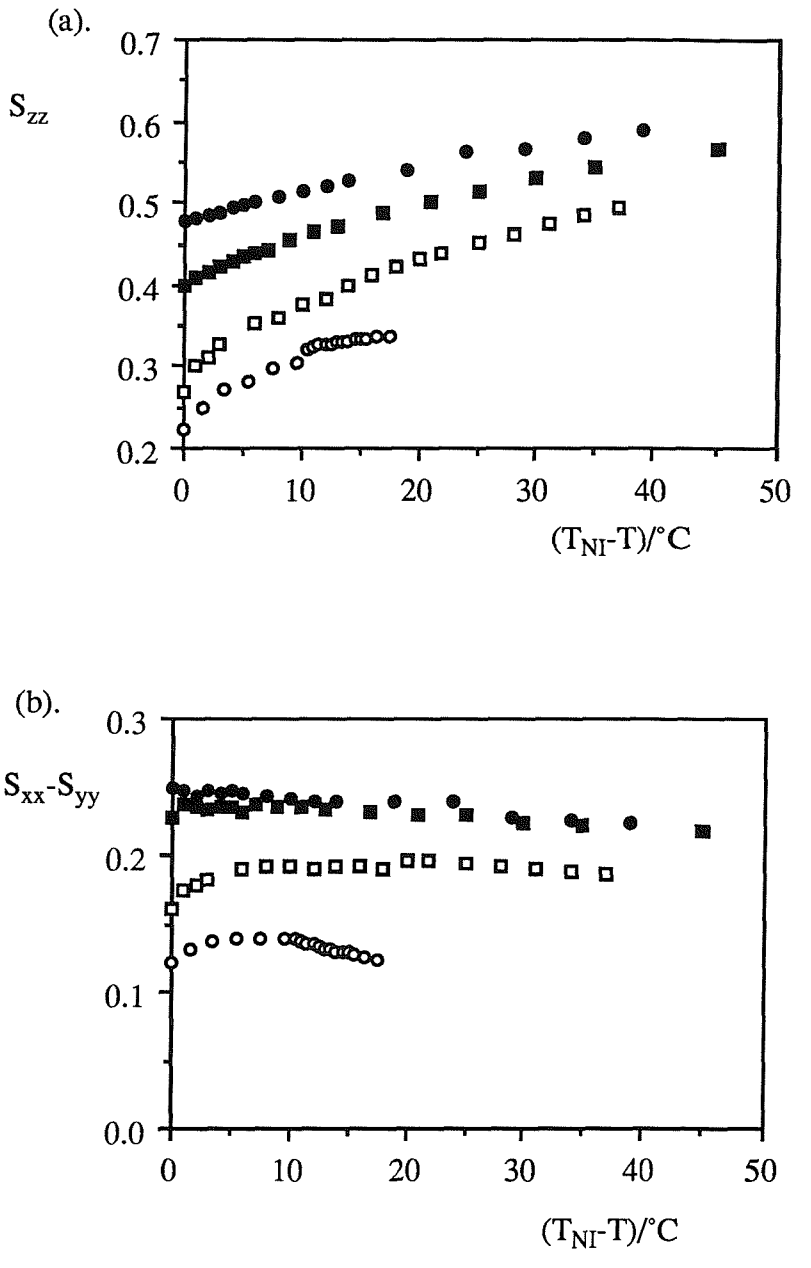

Figure 6. The dependence of (a) the major (S_{zz}) and (b) the biaxial (S_{xx}-S_{yy}) order parameters of anthracene-d_{10} dissolved in CB6CB (●), CB7CB (○), CBO4OCB (■) and CBO5OCB (□) on the shifted temperature (T_{NI}-T).

dimer shows the same qualitative behaviour but with the absence of a smectic phase (S_{xx}-S_{yy}) traces a smoother curve without the sudden drop. Following an initial jump in the biaxial order parameter close to T_{NI} for the even ether linked dimer, a slow decrease of (S_{xx}-S_{yy}) with decreasing temperature is maintained effectively shadowing that of the methylene linked counterpart.

Such behaviour can be readily understood if we consider that the major and biaxial order parameters of the anthracene solute are intrinsically linked. Theory predicts [8,9] that when S_{zz} is less than about 0.4 then (S_{xx}-S_{yy}) will increase with increasing S_{zz}. Conversely (S_{xx}-S_{yy}) will begin to decrease when the increasing S_{zz} is greater than 0.4 or thereabouts. It follows therefore that if S_{zz} increases upto and beyond 0.4 then (S_{xx}-S_{yy}) will reflect this with the locus of a gentle hump. This is seen for the solute dissolved in the odd ether linked dimer. CB6CB shows a steadily decreasing trend for (S_{xx}-S_{yy}) since S_{zz} does not drop below 0.4. This partnership between the major and the biaxial order parameter can be visualised more clearly if one is plotted against the other, point for point, thus eliminating the temperature. Figure 7 shows such a plot. The trends highlighted earlier concerning this limiting value of S_{zz}=0.4 are clearly demonstrated. The major order parameter for anthracene dissolved in CB7CB steadily increases with decreasing temperature but does not reach 0.4 and yet a maximum is observed. This unexpected result coupled with a discontinuous change in slope is attributed to the transition from the nematic to a smectic phase.

The presentation of the order parameters of the anthracene probe given in figure 6 should give an estimate of the biaxiality in the molecular interactions. The even dimers possess similar levels of biaxiality with the methylene linked CB6CB attaining a slightly larger value. The odd dimers show quite a significant reduction in this biaxiality. The methylene linked mesogen CB7CB, the dimer expected to show the greatest molecular biaxiality, has the lowest value of all four.

These apparently anomalous findings can be rationalised, at least qualitatively, if we draw upon the concept of global (G) and local (L) directors [10]. The anthracene

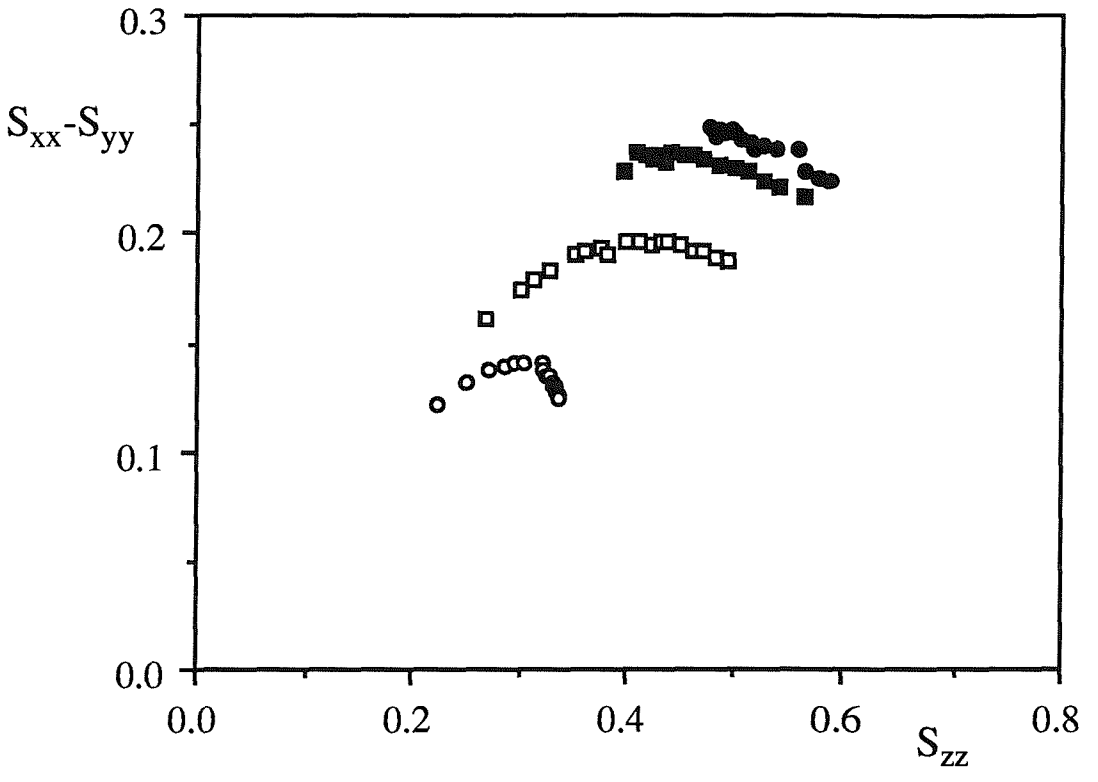

Figure 7. The variation of the biaxial order parameter (S_{xx}-S_{yy}) with the major order parameter S_{zz} for anthracene-d_{10} dissolved in CB6CB (●), CB7CB (O), CBO4OCB (■) and CBO5OCB (□).

probe molecule is assumed to be aligned parallel to the local director which for our molecules is associated with the aromatic cyanobiphenyl mesogenic unit. In even dimers both mesogenic groups can align parallel to a common direction making the local and global directors coincident. The chain constraints dictate that for odd dimers the long axes of the terminal mesogenic groups will on average be inclined to the global director so creating an angle ß between the local and global directors. This idea is caricatured in figure 8. The orientational order of the system in our NMR experiment is measured along the direction of the global or macroscopic director. An inclination or tilt of the mesogenic groups with respect to the global director serves to reduce the observed order parameters by the same factor [10]

$$S_{ZZ}^{G} = S_{ZZ}^{L} P_2(\cos ß),$$

and

$$(S_{XX}^{G} - S_{YY}^{G}) = (S_{XX}^{L} - S_{YY}^{L}) P_2(\cos ß).$$

This reduction in order parameters between odd and even dimers by the factor of $P_2(\cos ß)$ can be crudely tested if we assume that the local order at the same shifted temperature is independent of the spacer parity, as well as the nature of the link between the flexible chain and the mesogenic group. The nature of the link, however, must be the same when comparing odd and even dimers. The validity of these equations and hence this rather simple model, can be explored via the ratios $S_{ZZ}^{odd} / S_{ZZ}^{even}$ and $(S_{XX}-S_{YY})^{odd}/(S_{XX}-S_{YY})^{even}$. These should be equal to each other at the same shifted temperature and essentially independent of temperature provided the angle between the local and global directors for the odd dimers does not change. These ratios are plotted in figure 9 for the methylene and ether linkages. Angular bands of ß have been evaluated. From the molecular geometry it is expected that ß will be approximately 25° for the ether linked and 35° for the methylene linked dimers. It is seen that ß lies between 18° and 28° for the ether linked dimers and between 31° and 37° for the methylene linked dimers. This highly satisfactory result

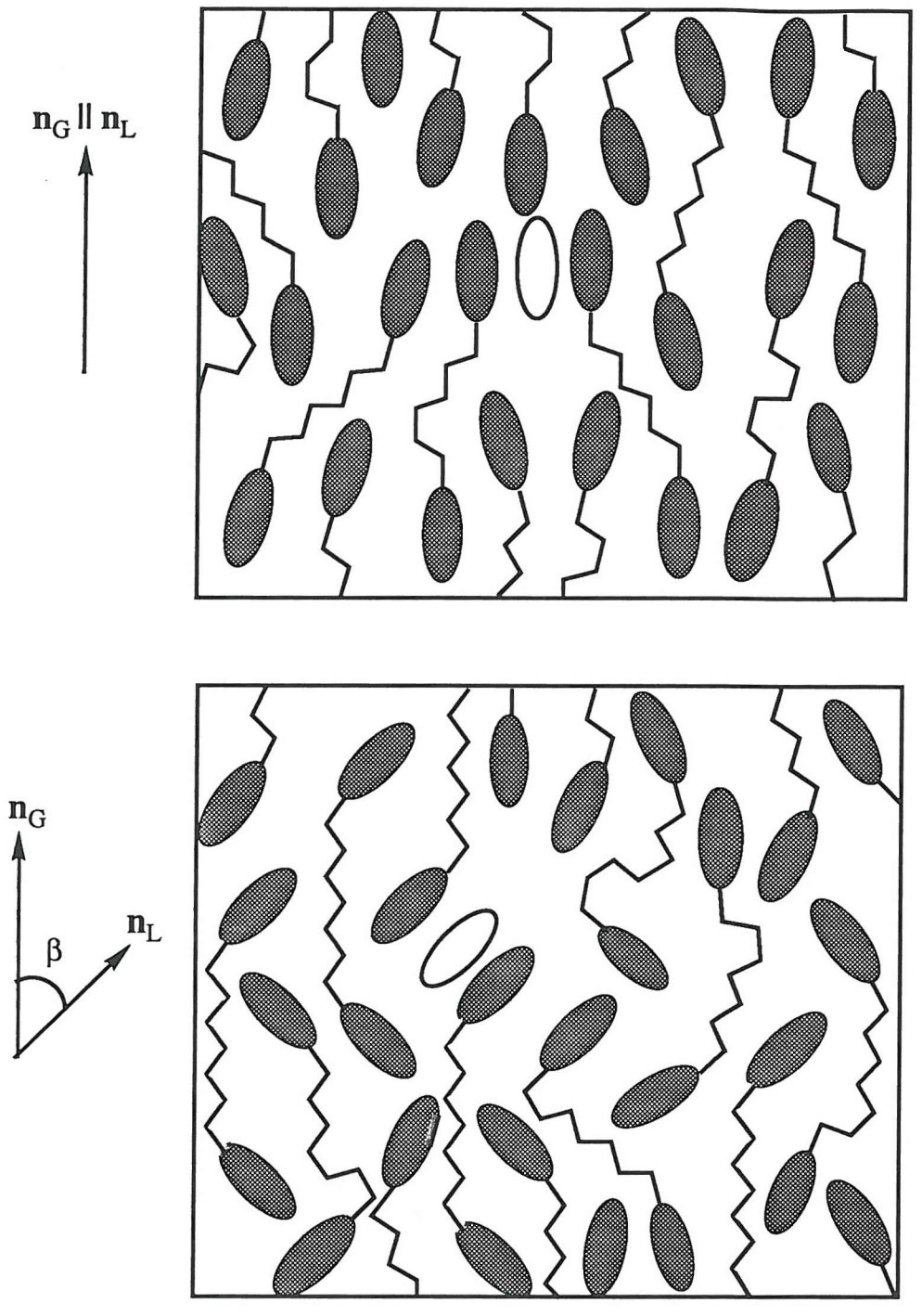

Figure 8. Caricature of the molecular organisation of a nematic phase composed of dimers with (a) even and (b) odd spacers showing the possible location of a rigid probe molecule. The angles between the local and global directors are shown at the side.

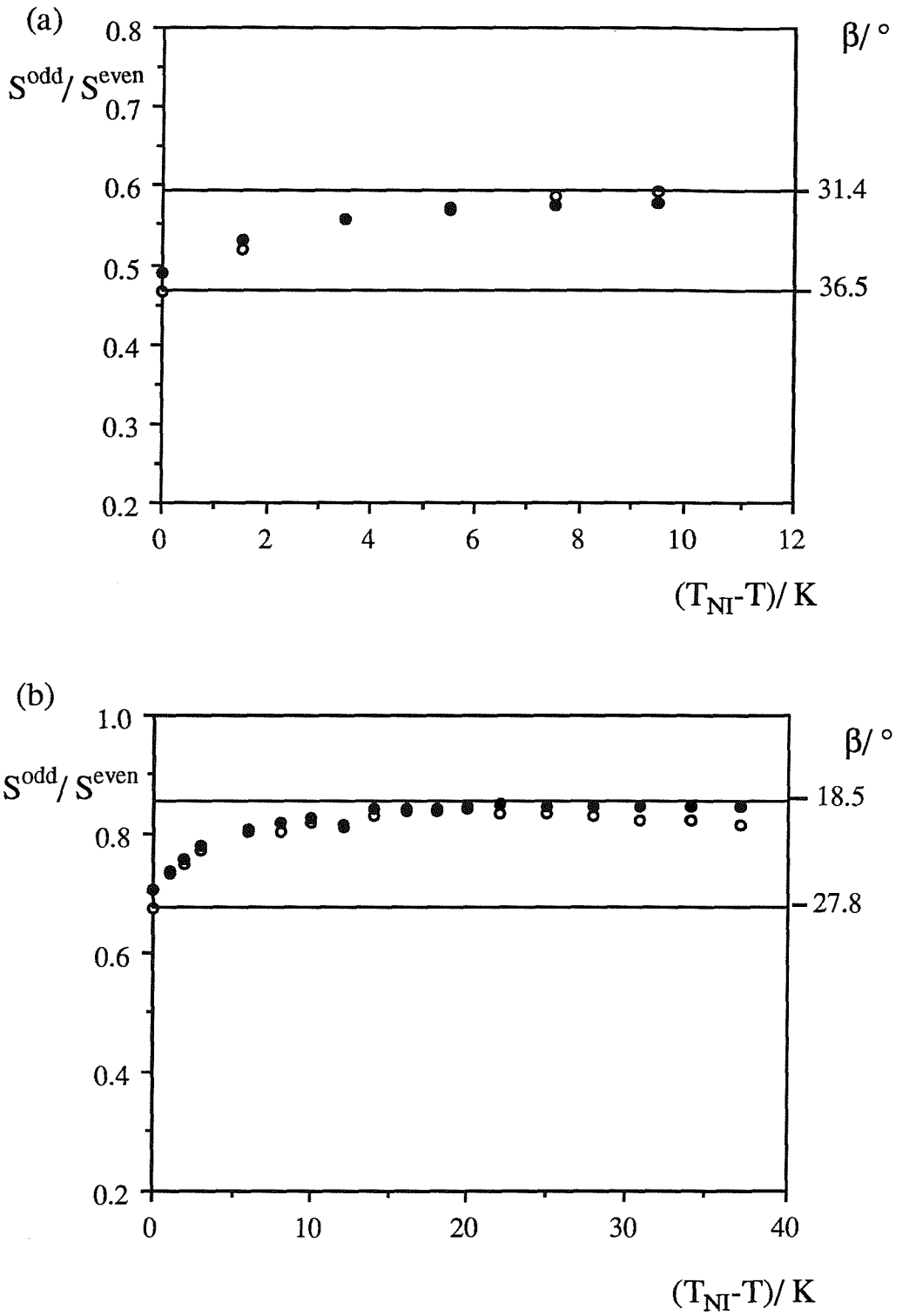

Figure 9. The dependence of the ratios $S_{zz}^{odd}/S_{zz}^{even}$ (O) and $(S_{xx} - S_{yy})^{odd}/(S_{xx} - S_{yy})^{even}$ (●) on the shifted temperature for (a) CB6CB and CB7CB and (b) CBO4OCB and CBO5OCB.

emphasises the greater biaxiality of methylene linked dimers although this indirect measurement is not strictly temperature independent as was assumed. The slight temperature dependence is, however, consistent with the tendency of the mesogenic groups in the odd dimers to become more parallel as the orientational order of the nematic phase increases. This is seen in nematic-smectic A transitions which are normally first order, but, for large nematic phases the transition becomes second order [11]. This tells us that the nematic becomes more ordered as lower temperature transition is approached.

4. Non-symmetric dimers

The smectic phase observed in CB7CB and CB5CB has also been seen in another dimer of similar construction, namely, 1-(4'-cyanobiphenyl-4-yloxy)-6-(4'-cyanobiphenyl-4-yl)hexane [12], a non-symmetric dimer containing both an ether and a methylene link. This will be abbreviated to CB6OCB, again where the 6 refers to the number of methylene units in the chain. CB6OCB differs from CB7CB only in the replacement of a methylene group with an oxygen atom.

The appearance of this unusual smectic phase with a larger enantiotropic range than the wholly methylene linked analogue prompted the synthesis and examination of other members of this oxy-methylene series to see if they too show similar smectic phases.

4.1 Experimental

Synthesis of α-(4-cyanobiphenyl-4'-oxy)-ω-(4-cyanobiphenyl-4'-yl)alkanes

The method for the preparation of the butyl homologue is detailed below, however, the same synthetic method as outlined in reaction scheme 3 applies to each of the CB(n-1)OCB dimers described in this Chapter.

Synthesis of 4-bromo-4'-(ω-bromobutanoyl)biphenyl

When the ω-bromoalkanoyl chloride was unavailable commercially, it was prepared by stirring the ω-bromoalkanoic acid (10g) with freshly distilled oxalyl chloride (20ml) for 2 h. After removal of the oxalyl chloride under reduced pressure the ω-bromoalkanoyl chloride was purified by distillation. Quantitative yields were obtained.

A solution of ω-bromobutanoyl (0.06 mol, 11.1g) and 4-bromobiphenyl (0.06 mol, 14g) in dry dichloromethane (30ml) was added dropwise to a stirred suspension of freshly crushed, anhydrous aluminium trichloride (0.06mol, 8g) in dry dichloromethane (DCM) at 0°C. The resulting deep red mixture, resulting from the aluminium complex, was allowed to warm to room temperature and stirred overnight. The mixture was then carefully added to water (200ml) and extracted with DCM (3x100ml). The combined organic fractions were dried over anhydrous calcium chloride and the DCM removed under reduced pressure. The crude product was passed through a flash silica column using a mixture of DCM and petroleum ether (50:50) as eluent. The desired product was recrystallised from ethanol and dried. Yield 85%.

I.R.; υ carbonyl stretch at 1681cm^{-1}.

^{1}H NMR; ($CDCl_3$, δ), 1.6-2.0 (m, 1H), 3.0-3.2 (t, 1H), 3.4-3.6 (t, 1H), 7.4-8.0 (m, 4H).

Synthesis of 1-bromo-4-(4,4'-bromobiphenyl)butane

The carbonyl group was reduced to a methylene unit using the mild triethylsilane in trifluoroacetic acid method [4] . Triethylsilane (0.07 mol, 11ml) was added dropwise to a stirred solution of 4-bromo-4'-(ω-bromobutanoyl)biphenyl (0.03 mol, 11.5g) in trifluoroacetic acid (0.22 mol, 17ml) ensuring that the temperature did not rise above 40°C. After 2 h the resulting white suspension was shaken thoroughly with water (200ml). This was then extracted with DCM (3x100ml), and the solvent removed to leave a white solid which was recrystallised from ethanol. Yield 80%.

I.R.; loss of carbonyl stretch

^{1}H NMR; ($CDCl_3$, δ), 1.7-2.1 (m, 2H), 2.7-2.9 (t, 1H), 3.4-3.6 (t, 1H), 7.1-7.7 (m, 4H).

Synthesis of 1-(4-cyanobiphenyl-4'-oxy)-4-(4-bromobiphenyl-4'-yl)butane

A mixture of 1-bromo-4-(4-bromobiphenyl-4'-yl)butane (0.012 mol, 4.4g), 4-hydroxy-4'-cyanobiphenyl (0.012 mol, 2.4g), anhydrous potassium carbonate (0.05 mol, 7g) and dry butanone (40ml) was stirred under reflux for 8 h. The reaction mixture was then filtered hot and the remaining solid was washed with a further 20ml of hot butanone. The solvent was removed and the crude product was recrystallised from ethanol. Yield 70%.

I.R.; υ cyano stretch at 2216 cm^{-1}.

^{1}H NMR; ($CDCl_3$, δ), 1.8-2.0 (m, 2H), 2.7-2.9 (t, 1H), 3.9-4.1 (t, 1H), 6.9-7.7 (m, 8H).

Synthesis of 1-(4-cyanobiphenyl-4'-yloxy)-4-(4-cyanobiphenyl-4'-yl)butane

1-(4-cyanobiphenyl-4'-yloxy)-4-(4-bromobiphenyl-4'-yl)butane (0.006 mol, 2.9g) was dissolved in dry N-methyl pyrrolidone (NMP, 15ml) and approximately 10% of the solvent containing any remaining azeotroped water was distilled off and discarded. This was then added to a solution of cuprous cyanide (0.0084 mol, 1.5g) in NMP treated in a similar manner, and the combined reaction mixture was stirred at 200°C for 4 h. The mixture was then cooled to 80°C and a solution of ferric chloride (5g) in water (20ml) and hydrochloric acid (5ml) was added to destroy any copper complexes produced. The resulting black mixture was stirred for a further 30 min and left to cool overnight. After addition to water (200ml) the organic component was extracted with DCM (3x100ml) and then washed with water to remove any remaining NMP and dried over anhydrous $CaCl_2$. The DCM was removed and the crude brown product was passed through a flash silica column using petroleum ether and DCM (50:50) as eluent. The pure desired product was recrystallised from ethanol to give white crystals in 65% yield.

I.R.; υ carbonyl stretch at 2216 cm^{-1}.

^1H NMR; ($CDCl_3$, δ), 1.8-2.0 (m, 2H), 2.7-2.9 (t, 1H), 3.8-4.0 (t, 1H), 6.8-7.7 (m, 8H).

MS (EI, 70eV); 178, 194 (100%), 427 (M^+).

The dimer CB6OCB-d_2 was synthesised in a similar manner to the previous reaction scheme with the substitution of 4-hydroxy-4'-cyanobiphenyl-d_2, whose preparation has been described elsewhere in this Thesis, for 4-hydroxy-4'-cyanobiphenyl in the third step of the synthesis.

I.R.; υ cyano stretch at 2210 cm^{-1}.

^1H NMR; ($CDCl_3$, δ), 1.3-1.8 (m, 4H), 2.6-2.8 (t, 1H), 3.7-3.9 (t, 1H), 6.8-7.6 (m, 7H).

Reaction Scheme 3

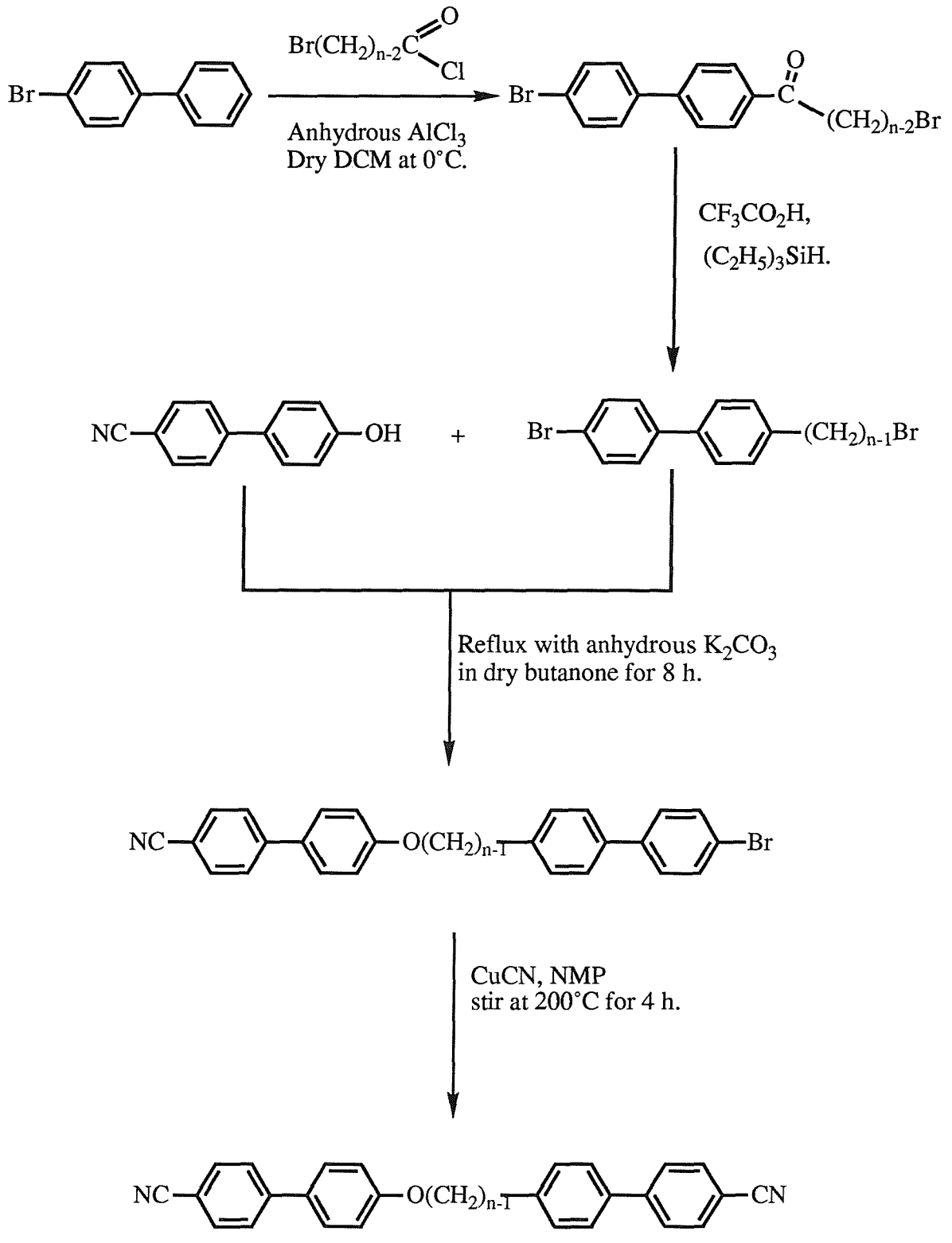

4.2 Results and discussion

The transitional given in table 4 data for these non-symmetric dimers confirms that they are indeed more mesogenic than the solely methylene linked dimers indeed CB4OCB is more mesogenic than the ether linked CBO3OCB which is a surprising result.

In general, however, the thermal data for this class of compounds lies, as might be expected between that of the methylene and ether linked symmetric dimers. T_{NI} for even numbered chains in the series have a lower transition temperature than analogous ether and methylene linked dimers, this is thought to be due to the lack of symmetry in the molecule which disrupts the high temperature ordering. The variation of $\Delta S/R$ with the number of units in the spacer, is generally believed to be a much more accurate measure of the order within a system. Figure 10 shows such variation. It is seen that the transitional entropy for the CB(n-1)OCB series alternates in a very regular fashion between that observed for the ether and methylene linked dimers of comparable length.

To study this intermediate class of liquid crystal dimers further, the Saupe ordering matrix of anthracene-d_{10} has been determined for four members of the CB(n-1)OCB series with n= 3,4,5 and 6.

The plots of Szz against shifted temperature for each of the oxy-methylene dimers as solvent are shown in figure 11. It is immediately apparent that, as the entropy data suggest, the orientational order within this class of molecules lies intermediate to the ether and the methylene linked systems as far as comparison allows. The unusual smectic phase observed in supercooled CB4OCB unfortunately did not withstand the bulk sample effects in the NMR spectrometer and crystallised before the phase could be reached.

The results are nonetheless very interesting. The fact that the non-symmetric dimers, CB3OCB and CB4OCB, lie approximately between the ether and

Table 4. The transitional data of the α-(4-cyanobiphenyl-4'-yloxy)-ω-(4-cyanobiphenyl -4'-yl)alkanes. Order parameter data is given for the anthracene-d_{10} probe and the pure phase for CB6OCB.

	CB3OCB	CB4OCB	CB5OCB	CB6OCB	CB6OCB -d_2
T_{NI}/ °C	263	124	227	155	154
ΔH_{NI}/ kJ mol^{-1}	10.65	0.83	9.94	1.82	1.86
ΔS_{NI}/ R	1.87	0.25	2.39	0.53	0.50
S_{zz}^{NI}	0.430	0.172	0.451	0.203	0.207
$S_{xx}^{NI} - S_{yy}^{NI}$	0.231	0.079	0.220	0.154	0.033
T_{CN}/ °C	163	112	170	95	94
ΔH_{CN}/ kJ mol^{-1}	36.00	34.5	33.45	31.4	32.1
ΔS_{CN}/ R	7.25	10.69	9.08	10.2	10.5
T_{SN}/ °C		(89.5)		108	106
ΔH_{SN}/ kJ mol^{-1}		0.24			
ΔS_{SN}/ R		0.08			

The uncertainties in the transtition temperatures are ±1°C, and the entropies of transition ±5%. ( ) indicates a monotropic transition.

(a).

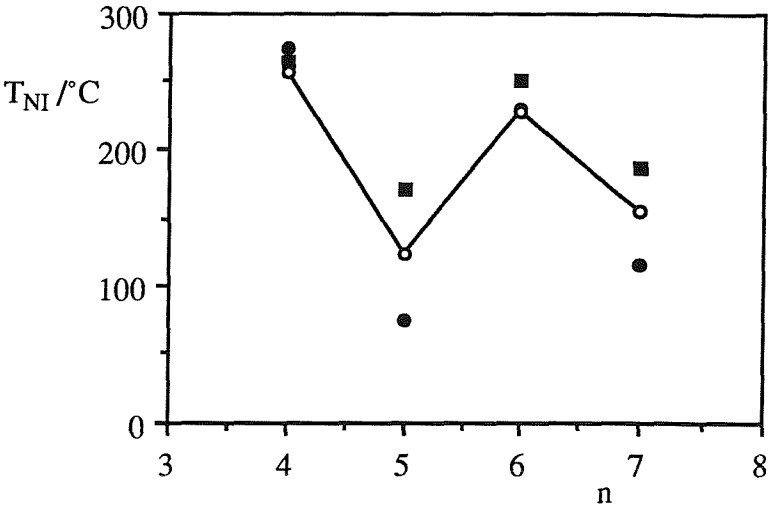

(b).

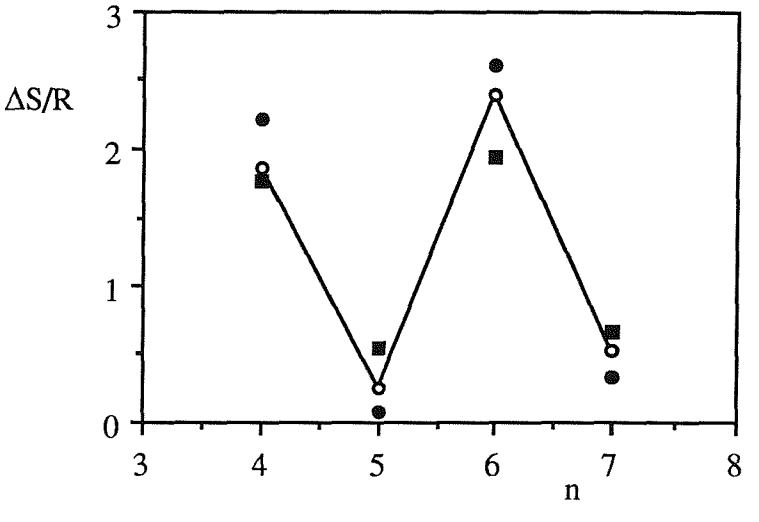

Figure 10. The variation of nematic-isotropic transition temperature (a) and entropy of transition (b) with the number of units in the spacer chain for the CB(n-1)OCB series (O). The values for CBO(n-2)OCB (■) and CBnCB (●) of similar length are given for comparison.

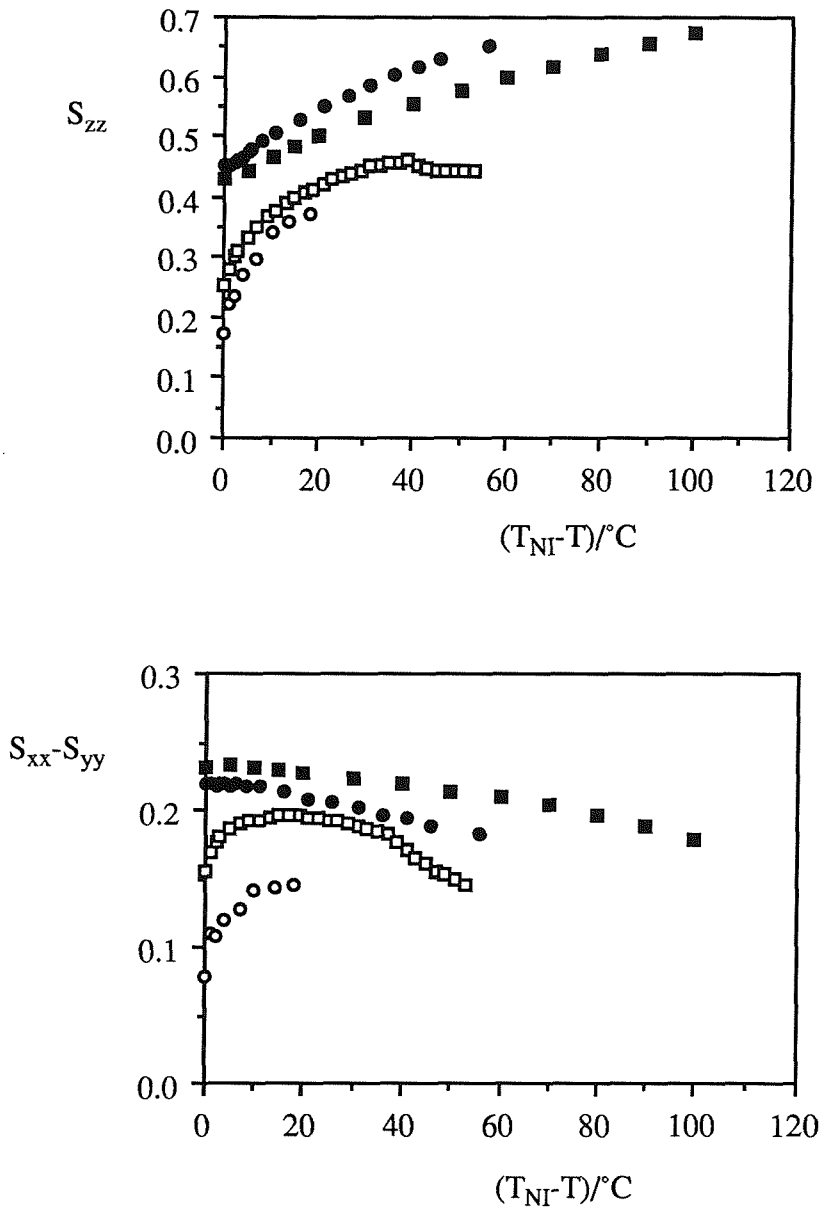

Figure 11. The dependence of the major (S_{zz}) and biaxial ($S_{xx}-S_{yy}$) order parameters of anthracene-d_{10} dissolved in CB3OCB (■), CB4OCB (O), CB5OCB (●) and CB6OCB (□) on the shifted temperature ($T_{NI}-T$).

methylene linked dimers in terms of transition temperature and entropy allows us to make intuitive predictions as to the order within CB4CB and CB5CB respectively assuming that this intermediacy still holds. The dimers with even chains namely CB3OCB and CB5OCB possess very high orientational order. When the major order parameters of anthracene dissolved in CB5OCB are plotted together with those of the analogous ether and methylene linked dimers (see figure 12), we find S_{ZZ}^{NI} =0.45 which is intermediate to S_{ZZ}^{NI} =0.4 and 0.48 of CBO4OCB and CB6CB respectively but the major order parameter of CB5OCB soon rises to 0.63 at a shifted temperature of 46° C which is more than 0.04 above that of CB6CB at an equivalent shifted temperature. This same qualitative trend is also seen for CB3OCB. The biaxial order parameters (S_{xx}-S_{yy}), start and finish at levels below those of either CBO4OCB or CB6CB coupled with a greater rate of decrease. This unexpected behaviour implies that CB5OCB becomes highly ordered as the freezing point is approached. Figure 13 shows the major and biaxial order parameters of CB6OCB plotted alongside those of CB7CB and CBO5OCB. Again S_{ZZ}^{NI} for CB6OCB lies between S_{ZZ}^{NI} for the symmetric dimers and continues to rise steadily as the temperature is decreased until the smectic phase is encountered when S_{ZZ}=0.45 whereafter the order decreases initially and then levels off until the sample freezes. The biaxial order parameters reflect the trends found in S_{ZZ} to a certain extent, however, (S_{xx}-S_{yy}) for CB7CB is markedly lower ($\approx$ 0.05) than (S_{xx}-S_{yy}) for CB6OCB and CBO5OCB which are effectively coincident over the entire mesophase range. It must not be forgotten, however, that throughout these investigations so far we have measured the order parameters of a probe molecule that has been assumed to mimic the order of the liquid crystal host. Such an assumption is considered acceptable for hosts containing just one aromatic site however for molecules of the CB(n-1)OCB type the aromatic sites are inequivalent albeit only a very subtle difference with no probable effect. This idea has been crudely tested by synthesising CB6OCB with deuterium in the aromatic sites ortho to the ether linkage.

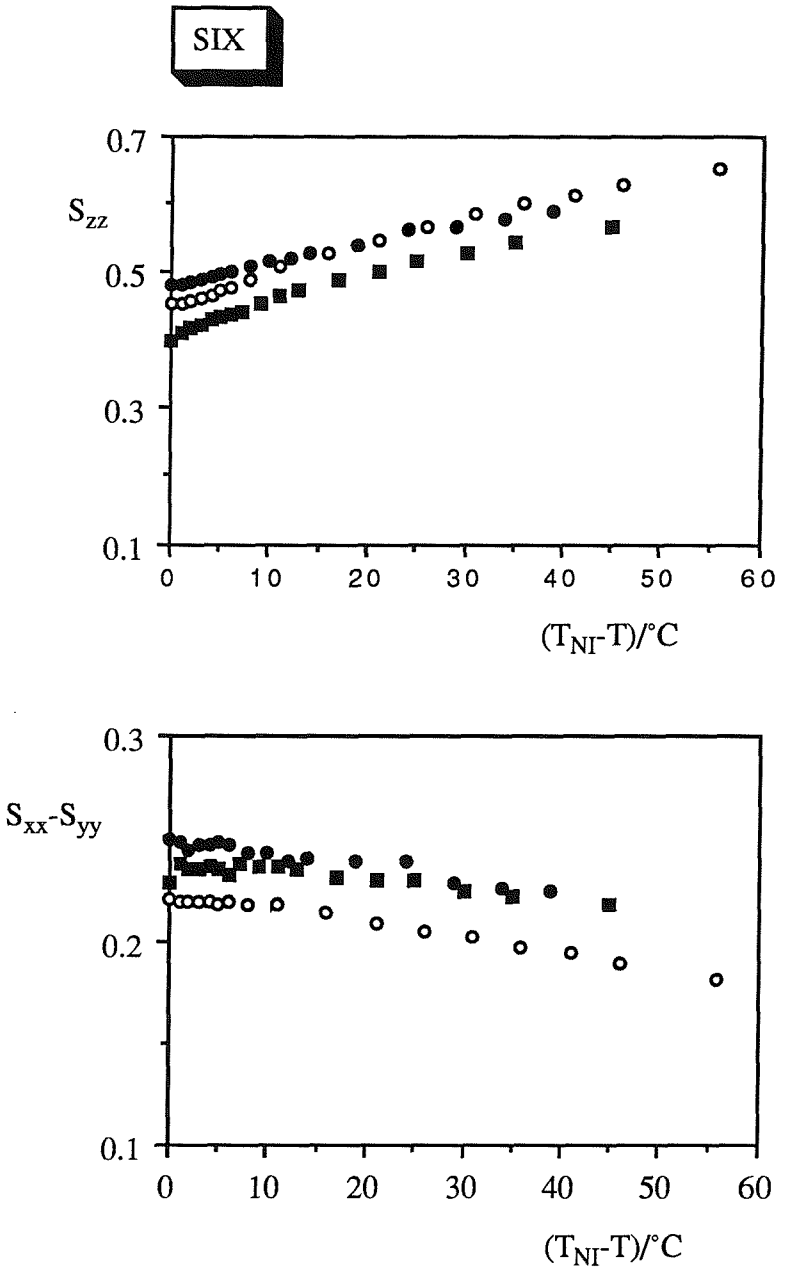

Figure 12. The dependence of the major (a) and biaxial order parameters (b) for anthracene-d_{10} dissolved in dimers with 6 units in the spacer chain where, CB6CB (●), CB5OCB (O) and CBO4OCB (■) on the shifted temperature T_{NI}-T.

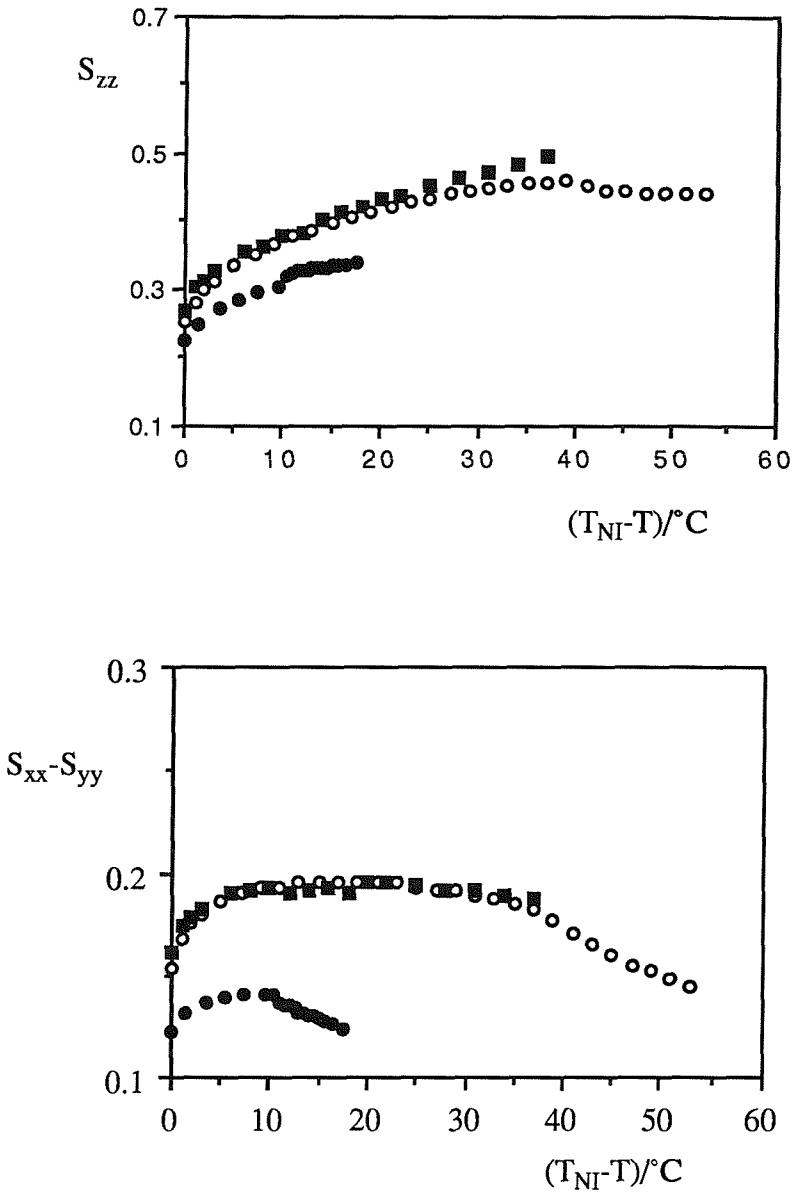

Figure 13. The dependence of the major (a) and biaxial order parameters (b) for anthracene-d_{10} dissolved in dimers with 7 units in the spacer chain where, CB7CB (●), CB6OCB (O) and CBO5OCB (■) on the shifted temperature T_{NI}-T.

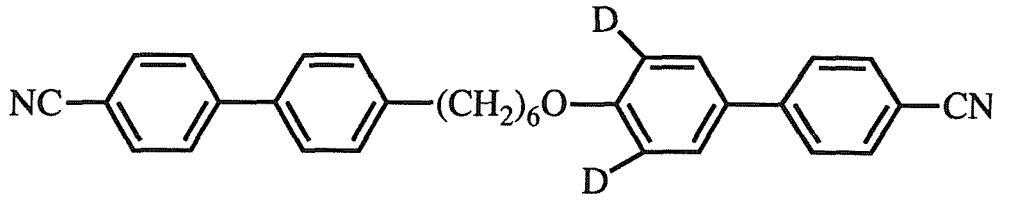

The ordering of this pure material was then measured over the entire mesogenic range. (n.b. the difference in the derivation of order parameters from an anthracene-d_{10} probe molecule and deuterium incorporated in the pure mesogen is outlined in the Chapter 2.) Figure 14 shows the major and biaxial order parameters of the mesogenic molecule and those obtained for the anthracene probe molecule. From this overlay of order parameters it is seen that the transition temperatures to the smectic phase are not quite coincident. This minor variation is due to the presence of anthracene-d_{10} in one of the samples and not in the other. More importantly is the difference between order parameters for the two samples. The major order parameters S_{zz} are effectively coincident until the smectic transition at which point the sample with the anthracene solute has values of approximately 0.07 higher than that of the pure phase. The greatest difference, however, is exhibited by the biaxial order parameters (S_{xx}-S_{yy}) in which although the temperature variation is essentially the same the values for the pure mesogen are consistently 0.1 lower than that of the probe. These differences are emphasised in figure 15 where S_{zz} is plotted directly against (S_{xx}-S_{yy}) . Such a difference is readily rationalised when we consider that the order parameters derived from the sample containing anthracene are a direct measure of the ordering of the probe and not of the solvent, although the solute is assumed to depend on the biaxiality of molecular shape of the liquid crystal host. The biaxiality of the molecular shape of anthracene is reflected in the larger values of (S_{xx}-S_{yy}) measured for it. Indeed the initial similarities in the values of S_{zz} for the two traces seem merely coincidental. These S_{zz} curves are very different from the continuous lineshapes observed for the other molecules. The transition to the

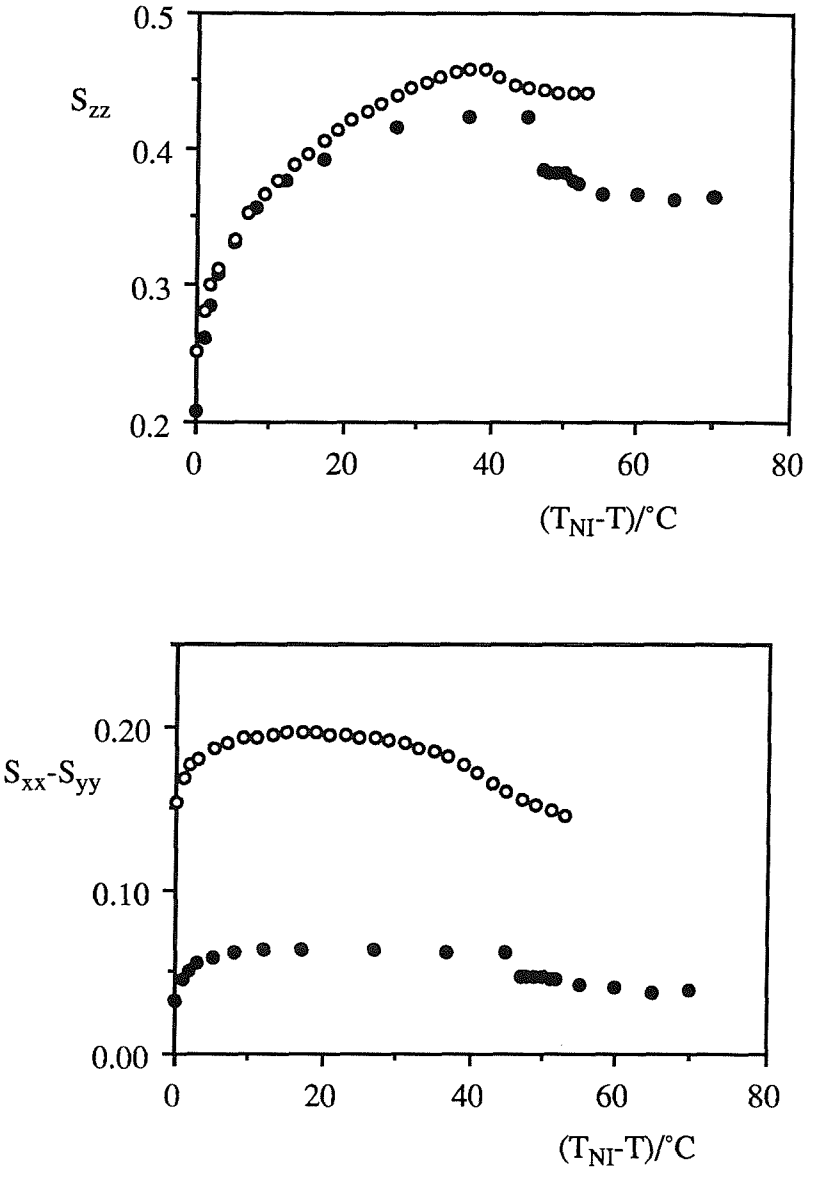

Figure 14. The dependence of the major (S_{zz}) and biaxial (S_{xx}-S_{yy}) order parameters for anthracene-d_{10} dissolved in CB6OCB (O) and those for CB6OCB-d_2 (●) on the shited temperature (T_{NI}-T).

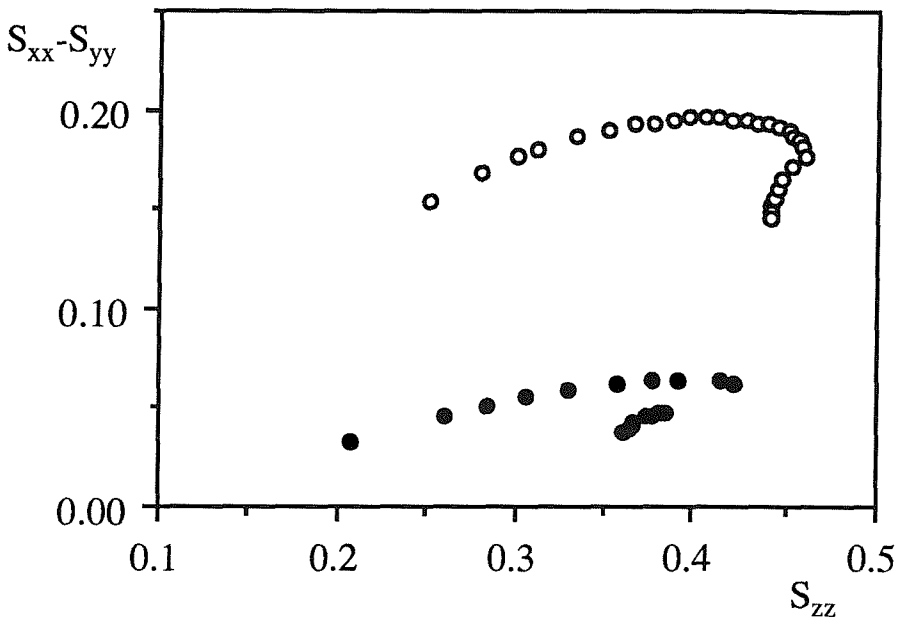

Figure 15. The variation of the biaxial order parameter (S_{xx}-S_{yy}) with the major order parameter S_{zz} for; anthracene-d_{10} dissolved in CB6OCB (O) and for the pure phase (●).

smectic phase in the pure sample appears to be discontinuous which would indicate a first order transition albeit very weak. The temperature was scanned at 2°C intervals which is large enough to effectively mask the order of the transition, hence a re-run of the sample in the region of the transition at temperature intervals of 0.5°C should elucidate the nature of the transition. Figure 16 shows the dependence of S_{zz} and S_{xx}-S_{yy} on temperature and a plot of S_{zz} versus (S_{xx}-S_{yy}) of this magnified region. Here the transition still appears very weakly first order although the DSC records a clear second order 'jump'. Examination of the NMR peak lineshapes shows no discernible coexisting phases at the transition so we may conclude that the transition to the smectic phase occurs between the temperature intervals and is essentially discontinuous for this pure material, where, for the solute experiment the transition appears continuous and therefore second order due to the phase blurring of the anthracene impurity. It is difficult to draw conclusions from such a comparison because several assumptions are made in the derivation of the order parameters from the quadrupolar and dipolar splitting data and these vary according to the position of deuterium and the geometry of the molecule under examination within the sample.

A much more interesting feature of the data is the drop in both S_{zz} and (S_{xx}-S_{yy}) when the smectic phase is encountered. All known smectic phases are, by definition, more ordered than a nematic under comparable conditions and yet decrease in order is observed. In a previous study [12] on this dimer using an anthracene probe two explanations of this anomaly have been proposed;

(i) The exclusion of the solute molecules to a less ordered inter-layer position, or the diffusion of the probe between these layers.

(ii) The smectic phase is made up of rippled layers creating a larger angular distribution of the local directors as sketched.

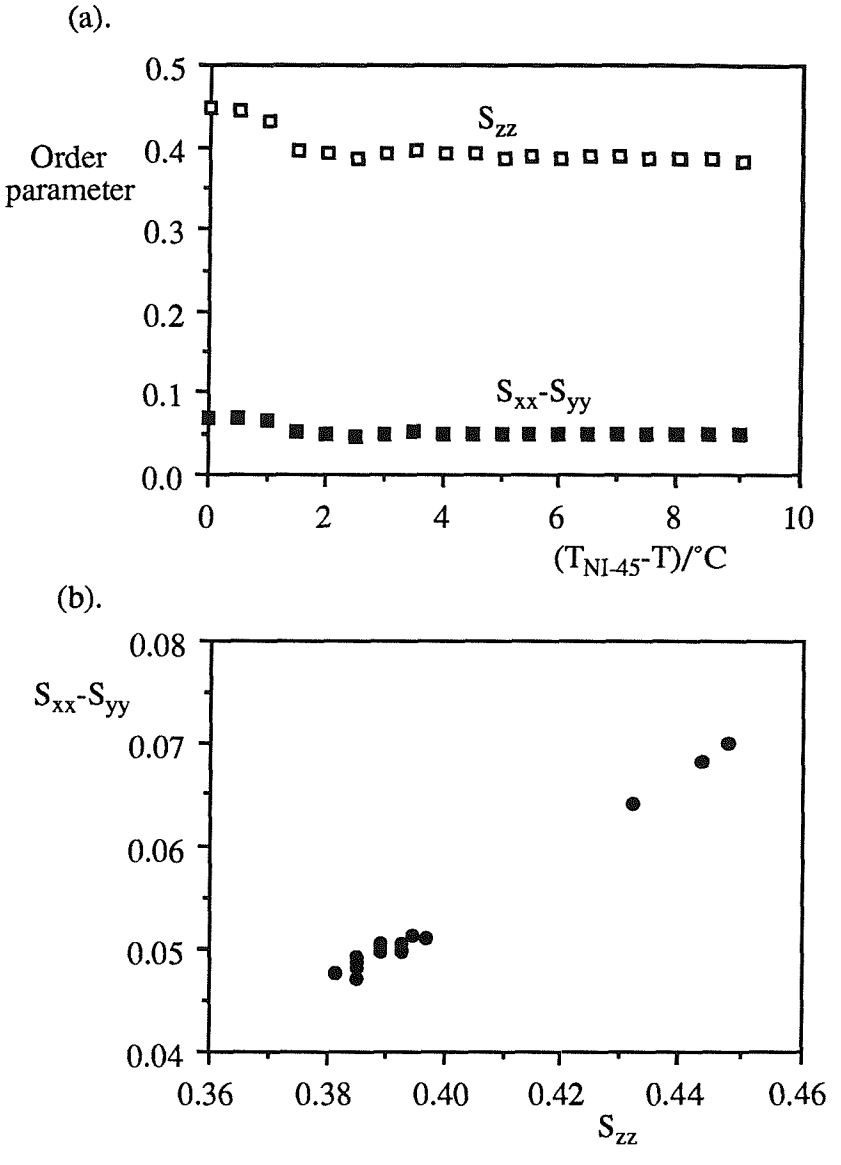

Figure 16. Magnified region of the smectic transition in CB6OCB-d_2 measured at 0.5°C intervals showing (a) the dependence of the order parameters on the shifted temperature and (b) the variation of S_{zz} with $(S_{xx}-S_{yy})$.

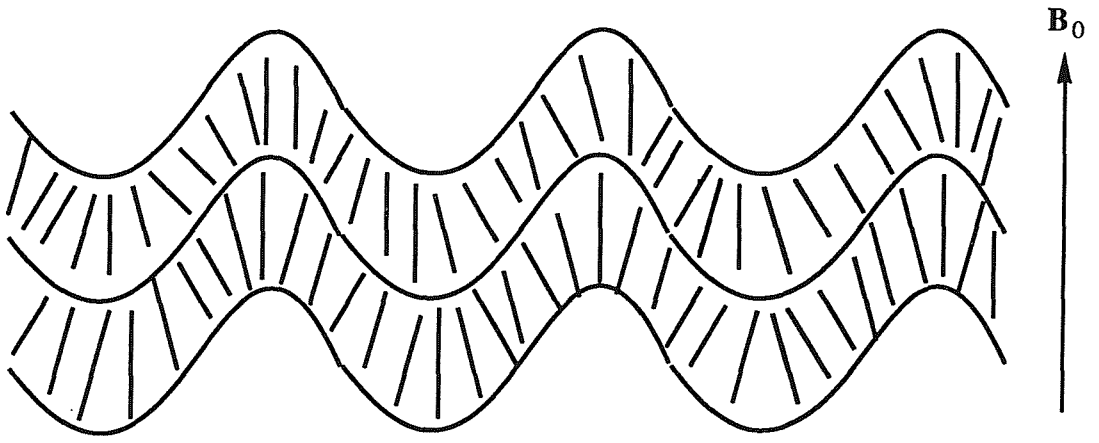

We have found that a similar drop in the order is experienced in the pure phase so proposal (i) can be disregarded. This leaves the ripple theory although there may be others. It was stated at the start of this section that this smectic phase is optically similar to that observed in the dimer CB7CB and also on supercooling CB5CB and CB4OCB, however the transient nature of the smectic phase in the latter two compounds restricted further studies to CB6OCB and CB7CB. In another study of CB7CB [6] this smectic phase is not noted.

5. Studies of the smectic phase of CB7CB

5.1 Optical microscopy

Plate 1 shows photographs of the textures of CB7CB where (a) is nematic at 105°C, (b) is smectic at 100°C (2°C below T_{NS}) and (c) shows the texture of this smectic phase at 83°C (T_{NS}-19°C).

On cooling from the schlieren texture of the nematic phase into the smectic phase, bands of a poorly defined focal conic fan texture are seen. Pretreatment of the microscope slide with an aligning agent allows areas of homeotropic texture to be observed when sheared. This suggests a smectic A phase. On cooling deeper into

Plate 1.

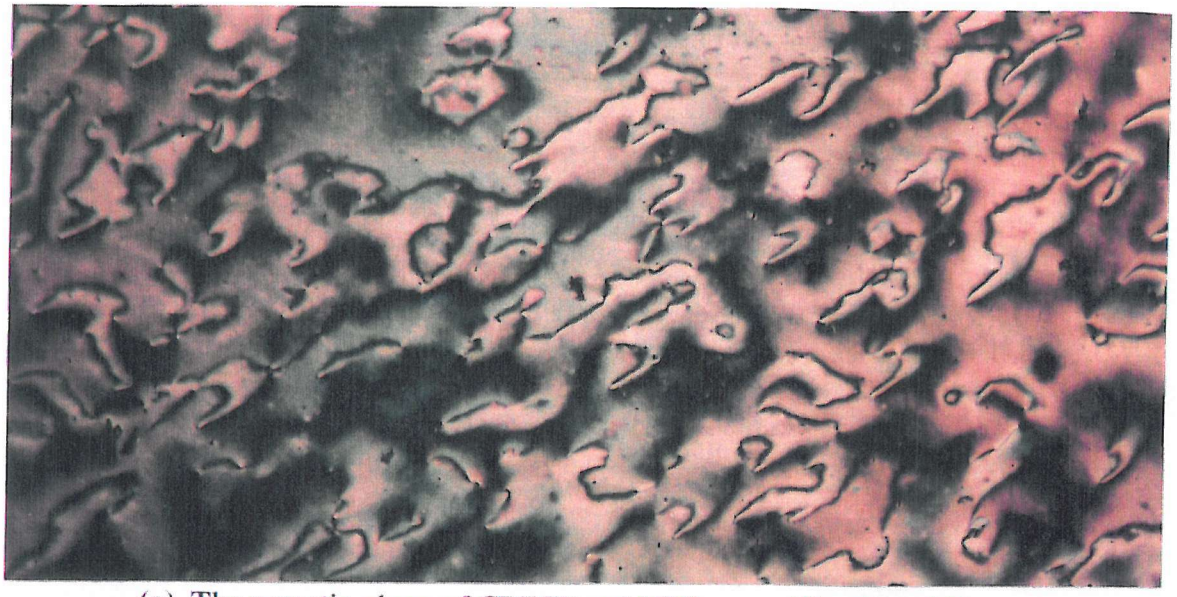

(a). The nematic phase of CB7CB at 105°C, magnification x100.

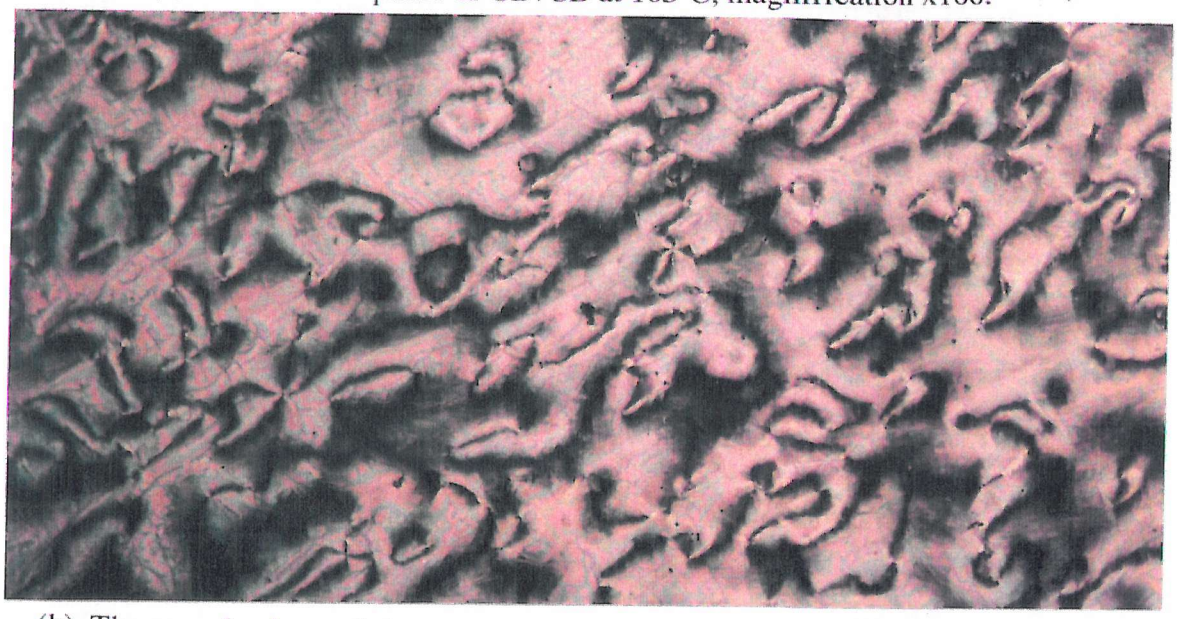

(b). The smectic phase of CB7CB at 100°C (T_{NS}-2°C), magnification x100.

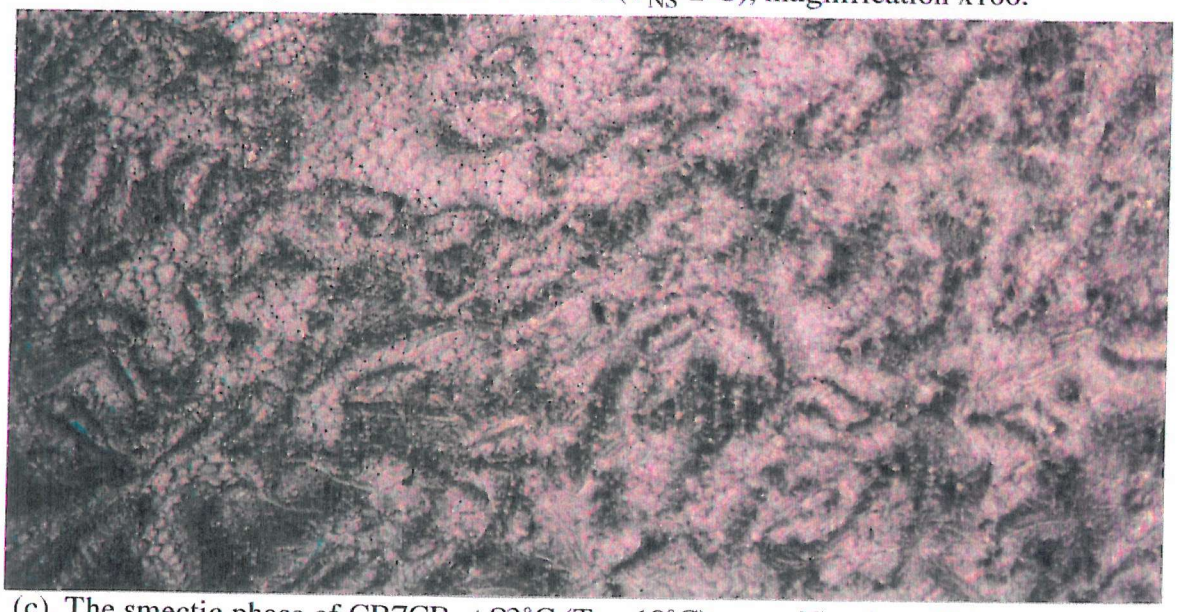

(c). The smectic phase of CB7CB at 83°C (T_{NS}-19°C), magnification x100.

the still fluid smectic phase, rows of small, drop-like parabolic defects develop to produce the sandy texture shown in plate 1(c). The delineations in the schlieren texture of the nematic phase are visible throughout.

5.2 Differential calorimetry

The small entropy of the smectic-nematic transition for CB7CB ($\Delta S/R=0.31$) would lend support to the designation of the smectic phase as a smectic A, however, the strength of an S_A-N transition depends to a certain extent on the length of the nematic range. McMillan [11] has extended the Maier-Saupe model of the nematic phase to include a smectic A phase by the introduction of a density wave. The resulting McMillan ratio T_{SAN}/T_{NI} predicts that the strength of the smectic A-nematic transition will steadily decrease to zero and become second order when the value of this ratio is <0.87. If we evaluate this ratio, bearing in mind that it was designed specifically for the smectic A - nematic transition, then CB7CB has a McMillan ratio T_{SAN}/T_{NI} of 0.89 and for the longer nematic range of CB6OCB, $T_{SAN}/T_{NI} = 0.70$ hence second order. This goes some way in explaining why the orders of the S-N transition for two compounds which we propose to exhibit the same phase are different.

5.3 X-ray diffraction

Preliminary X-ray studies of the smectic phase in CB7CB have proven inconclusive. In the diffraction pattern only wide angle scattering is observed, with no low angle scattering that would indicate a layered structure. This is in accord with the results of similar studies of CB6OCB. The same diffraction pattern was obtained when the sample was rotated which excludes the possibility that the sample had formed a monodomain.

5.4 Deuterium NMR

The major and the biaxial order parameters of both CB7CB and CB6OCB increase up to limiting values with decreasing temperature until the transition to the smectic phase is encountered whereupon a discontinuity is observed (see fig.13). The expected jump in S_{zz} is noted for CB7CB, however, for CB6OCB S_{zz} shows a sharp decrease at the transition and then remains constant until the freezing point. This is a surprising result. We have seen in this chapter that the order parameters for anthracene-d_{10} dissolved in CB6OCB are greater than those for CB7CB and that S_{zz} appears to have reached a low temperature limiting value in the nematic phase for CB6OCB whereas for CB7CB it has not. Additionally, we expect the anthracene probe to lie parallel to the mesogenic groups which in odd dimers such as these is the local director which makes a significant angle with the global director. The measurement of order parameters along a local director which is not coincident with the global director serves to reduce the magnitude of these order parameters. Hence if the local director made an increasingly large angle with the global director then the decrease in the values of the major order parameters for CB6OCB could be rationalised.

5.5 Electron spin resonance studies (ESR)

The temperature dependent behaviour of a cholestane spin probe dissolved in CB7CB shows qualitatively similar results to a previous experiment on CB6OCB using the same probe [12]. Figure 17 shows a stacked plot of ESR spectra of cholestane dissolved in CB7CB measured at temperature intervals of 1°C starting at the isotropic-nematic transition and decreasing into the page. In the nematic phase a three line spectrum is observed which indicates the sample has formed a good monodomain. Once the smectic phase is encountered the three line spectrum continues for a short temperature range of 5°C when two further lines start to

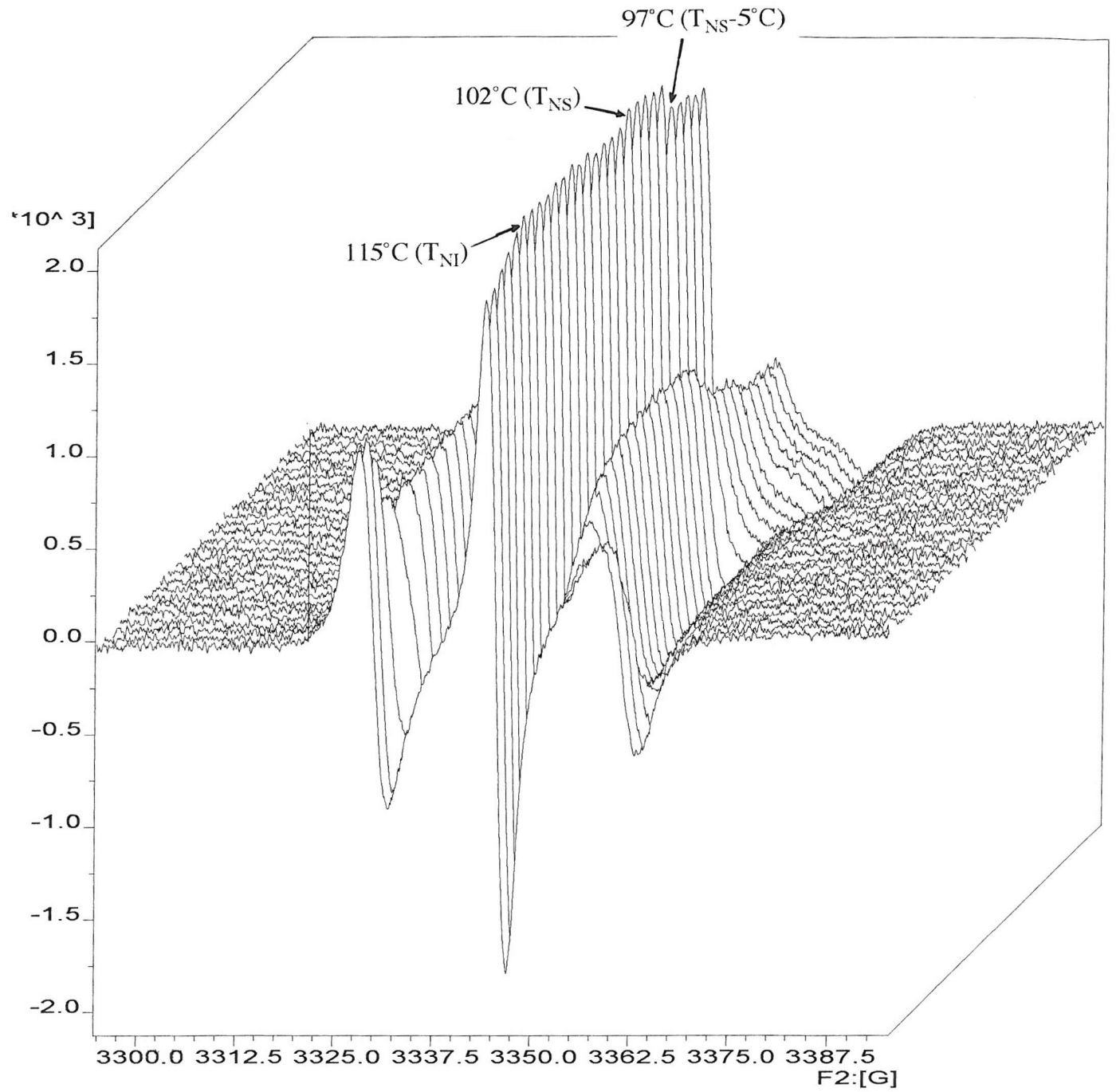

Figure 17. The ESR spectra of cholestane in CB7CB showing lineshapes accumulated at 1°C intervals cooling from the isotropic phase into the smectic phase. At T_{NS}-5°C an additional set of outer lines begin to develop.

develop which are associated with the director lying perpendicular to the magnetic field. This effect is consistent with the ripple theory stated earlier in which the smectic phase generates rippled layers, the wavelengths of which decrease with decreasing temperature. This effect is not observed in our NMR experiments because the high magnetic field is sufficient to maintain director alignment in the smectic phase whereas the relatively low magnetic field employed in the ESR experiment is not. In addition, the fast time scale in the NMR experiment mean that we observe director motions whereas for ESR we can study the molecular fluctuations within the phase.

6. Conclusions

We have seen in this Chapter that the nature of the linking group joining the aliphatic chain to the mesogenic group in liquid crystal dimers has a profound effect upon their transitional properties. These differences in the properties of ether and methylene linked dimers have been attributed to the change in the geometry of the mesogenic group with respect to the spacer. This strong dependence on the topology of the link is mirrored in the major and biaxial order parameters of anthracene-d10 dissolved in these dimers.These results have been rationalised, at least qualitatively, by drawing on the concept of global and local directors. In even dimers the local directors of the mesogenic groups are, on average, parallel to the global or phase director. In contrast, the local directors in the odd dimers are tilted with respect to the global director. This serves to reduce the order parameters which are measured with respect to the global director. This effect is greatest for the more biaxial odd methylene linked dimers.

Dimers containing one methylene and one ether link exhibit properties intermediate to solely methylene and ether linked dimers.

A smectic phase was observed in odd dimers possessing a methylene link. Studies of 1,7-bis(4'-cyanobiphenyl-4-yl)heptane in this phase indicate it to be a smectic A phase which generates a rippled layer structure as the freezing point is approached.

References

[1]. Emsley J.W., Luckhurst G.R., Shilstone G.N. and Sage I., 1984, *Mol. Cryst liq. Cryst Lett.*, **102**, 223.

[2]. Toyne K.J., Chapter 2, Liquid Crystal Behaviour in Relation to Molecular Structure. *Thermotropic Liquid Crystals* (Biddles), 1987.

[3]. Emerson A.P.J., Luckhurst G.R., 1991, *Liq. Crystals*, **10**, 861.

[4]. Kursanov, D.N., Parnes, D.N., and Loim, N.M., 1974, *Synthesis*, 663.

[5]. Coates, D., and Gray, G.W., 1976, *J. Chem. Soc. Perkin 2*, 863.

[6]. Kimara, T., Toriumi, H., and Wanatabe, H., 1988, *Preprints 14th Liquid Crystal Conference Japan*, **14**, 238. Toriumi, H., Photinos, D.J., and Samulski, E.T., 1989, *First Pacific Polymer Conference Preprints*, **1**, 285.

[7]. Emsley, J.W., Luckhurst, G.R., and Timimi, B.A., 1985, *Chem. Phys. Lett.*, **114**, 19.

[8]. Luckhurst, G.R., Zannoni, C., Nordio, P.L., and Segre, U., 1975, *Molec. Phys.*, **30**, 1345.

[9] Emsley, J.W., Hashim, R., Luckhurst, G.R., Rumbles, G.N., and Viloria, F.R., 1983, *Molec. Phys.*, **49**, 1321.

[10]. Heeks, S.K., and Luckhurst, G.R., 1993, *J. Chem. Soc. Faraday Trans.* **89**(17), 3289.

[11] McMillan W.L., 1971, *Phys. Rev.*, **4**, 1238.

[12]. Chui, F.S.M., 1985, *Third Year Project Report*, Southampton University, Chap. 2.

CHAPTER 4

Carbonate dimers

1. Introduction

The chemistry of the chloroformates has been well documented in organic chemistry [1]. However, the inclusion of a chloroformate synthon into the structure of liquid crystals as a carbonate group has attracted much more limited interest. Although carbonate group in monomeric liquid crystals has been studied as a linking group between a mesogenic group and a terminal alkyl chain. The study of some alkyl carbonato terminally substituted anils by Criswell et al in 1972 [2] provide some information concerning the basic trends of terminal carbonate inclusion. Schiffs bases of the form

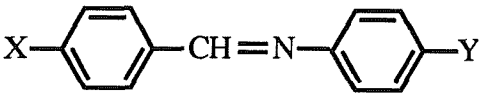

have been studied in which X and/or Y are an n-alkyl carbonato chain.

For the two series

A 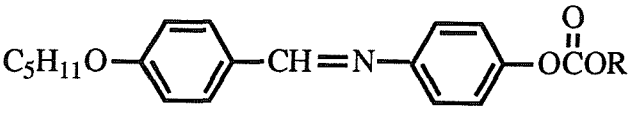

B 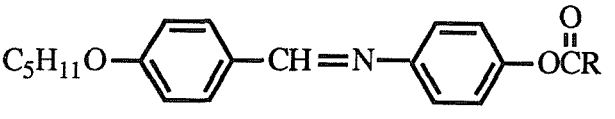

it was found that the presence of the carbonate group in series A not only lowered the nematic-isotropic transition temperatures when compared to the acyloxy link in series B for all R, but also broadened the nematic range, see figure 1. This result was examined further by fixing the length of the alkyl carbonato chain and the acyloxy chain adjusted so that the number of atoms in the 'backbone' of the chain were the same, and varying the alkyloxy chain length, i.e. for the compounds

C 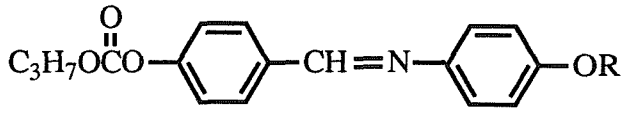

D 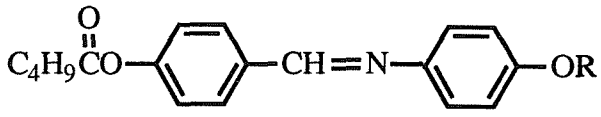

Figure 2 shows a similar lowering in the nematic-isotropic transition temperatures of the molecule containing the carbonate link. No explanation and no data other than the transition temperatures were offered to consolidate these empirical results.

In general, it was found that for a carbonate link, compared to alkyloxy, acyl and acyloxy links, produced the lower T_{NI} and broader mesogenic range. This was thought potentially useful at a time when there were very few room temperature liquid crystals, however the discovery of cyanobiphenyl mesogens shortly afterwards rather pushed these interesting molecules out of the limelight for several years until Abe and co-workers synthesised some alkylcarbonate linked polymers and compared them to some polyether and some alkyloxy linked polymers [3].

Their paper, published in 1986, reports the role of the spacer, more specifically the spacer-mesogenic group linkage, in the conformational analysis of successive rigid cores. They found that the angle, θ, defined by unit vectors attached to consecutive rigid cores was critically dependent on the type of linkage used and were therefore able to conclude that the odd-even oscillation in various thermodynamic quantities

Figure 1.

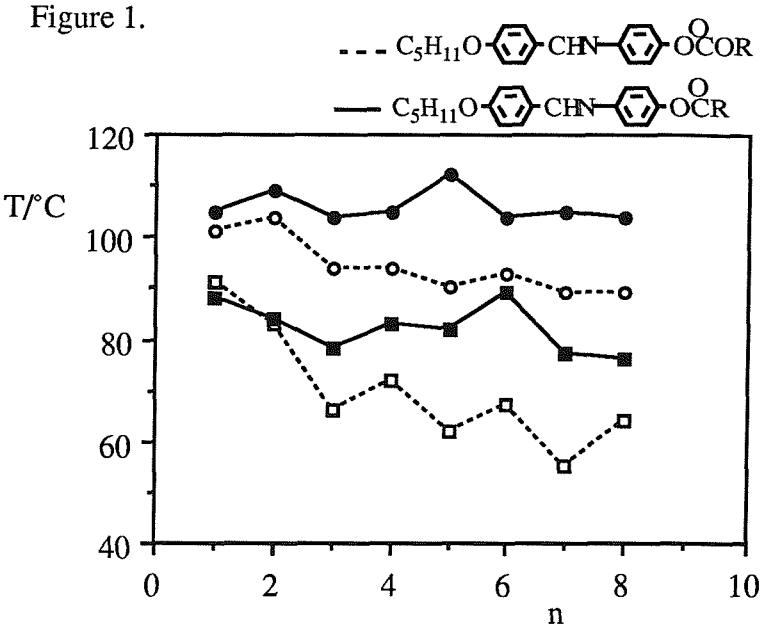

Figure 2.

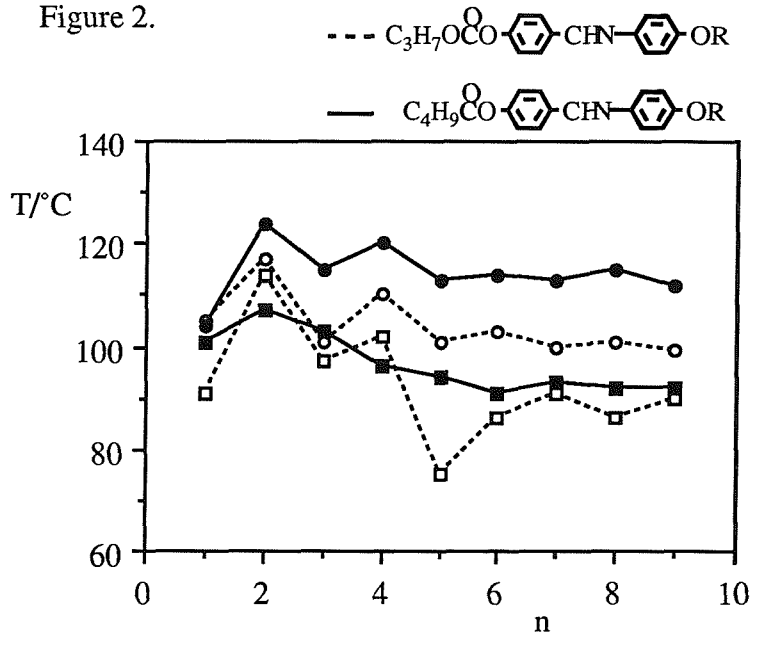

Figures 1 and 2. Comparing the carbonate link to the acyl link in terms of liquid crystallinity. The nematic-isotropic temperatures are represented by circles and the melting points by squares. Where n is the number of carbon atoms in the terminal chain R.

such as T_{NI}, and ΔS_{NI} with the chain length n was found to be explicable in terms of the geometrical characteristics of the chain. Of the linking groups studied, the carbonate link produced the lowest value of θ. No reference, however, was made to the nature of the mesogenic units.

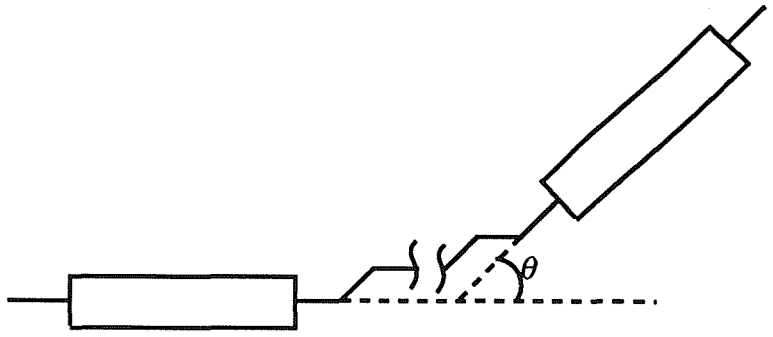

Further work by the same researchers [4] outlines the properties of some carbonate linked dimers constructed from cyanobiphenyl, di-Schiffs base and aromatic di-ester mesogens

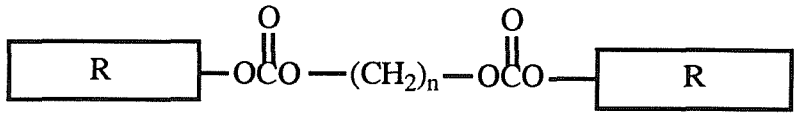

R = 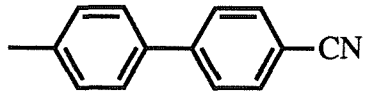 - CBC-n

R = 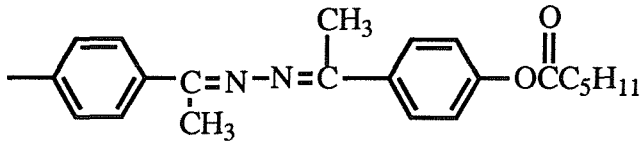 - DA-n

R = 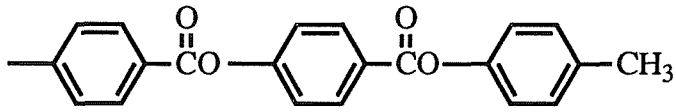 - 3MP-n

These all showed very little odd-even effect in their nematic-isotropic transition temperatures and transitional entropies.

With this phenomenon in mind, this chapter reports the synthesis of some carbonate dimers and the effect the inclusion of this group has upon the mesogenic properties compared to previously prepared liquid crystals of similar construction.

2. Experimental

Nine homologous members of the carbonate-linked dimers were prepared where the number of carbon atoms in the alkyl chain spacer varied from 4 to 12 inclusive.

2.1 Synthesis of bis-(4,4'-cyanobiphenyl)alkane dicarbonates

Synthesis of α,ω-alkanedichlorocarbonate

The synthetic route outlined in this section follows a procedure outlined by Abe [4]. 0.053 mol of α,ω-alkanediol was dissolved in anhydrous toluene (50ml) and trichloromethylchloroformate (20ml) was added. The solution was stirred at 40°C for 3 h. The toluene and excess trichloromethylchloroformate was removed under reduced pressure and pure α,ω-alkanedichlorocarbonate was distilled off under vacuum by means of a Kugelrohr apparatus to give a pungent smelling oil. Care was needed throughout the handling of trichloromethylchloroformate which is highly toxic and a potent lachrymator.

IR υ cm^{-1} loss of OH peak, appearance of C=O stretch at 1816cm^{-1}.

Synthesis of bis-(4,4'-cyanobiphenyl)alkane dicarbonate

4-hydroxy-4'-cyanobiphenyl (1g) was dissolved in dry pyridine (30ml). To this, a solution of 1,2 dichloroethane (20ml) containing α,ω-alkanedichlorocarbonate

(0.7g) was added dropwise at 0°C under vigorous stirring over approximately 2h. After stirring for a further 12h at room temperature the 1,2 dichloroethane was removed under reduced pressure. The remaining solution was neutralised by the addition of cold, dilute HCl solution. The resulting precipitate was collected by filtration, washed several times with water, and dried. The dry white solid was further purified by chromatography and recrystallisation from toluene. Yield 40%.
For the 9 homologue,

IR υ 2229cm^{-1} CN stretch, 1797cm-1 C=O stretch.
^{1}H NMR ($CDCl_3$, δ) 1.1 - 1.9 (m, 7H), 4.1 - 4.4 (t, 2H), 7.1 - 7.9 (m, 8H).
^{13}C NMR 25.82, 28.72, 29.25, 29.47, 69.34, 111.29, 118.98, 121.96, 127.86, 128.56, 132.83, 137.19, 144.70, 153.69, 153.76. 15 inequivalent carbons.
MS (EI, 70ev), (M^+ 602, 8%), (194 $C_{13}H_8NO$, 100%).

Reaction scheme

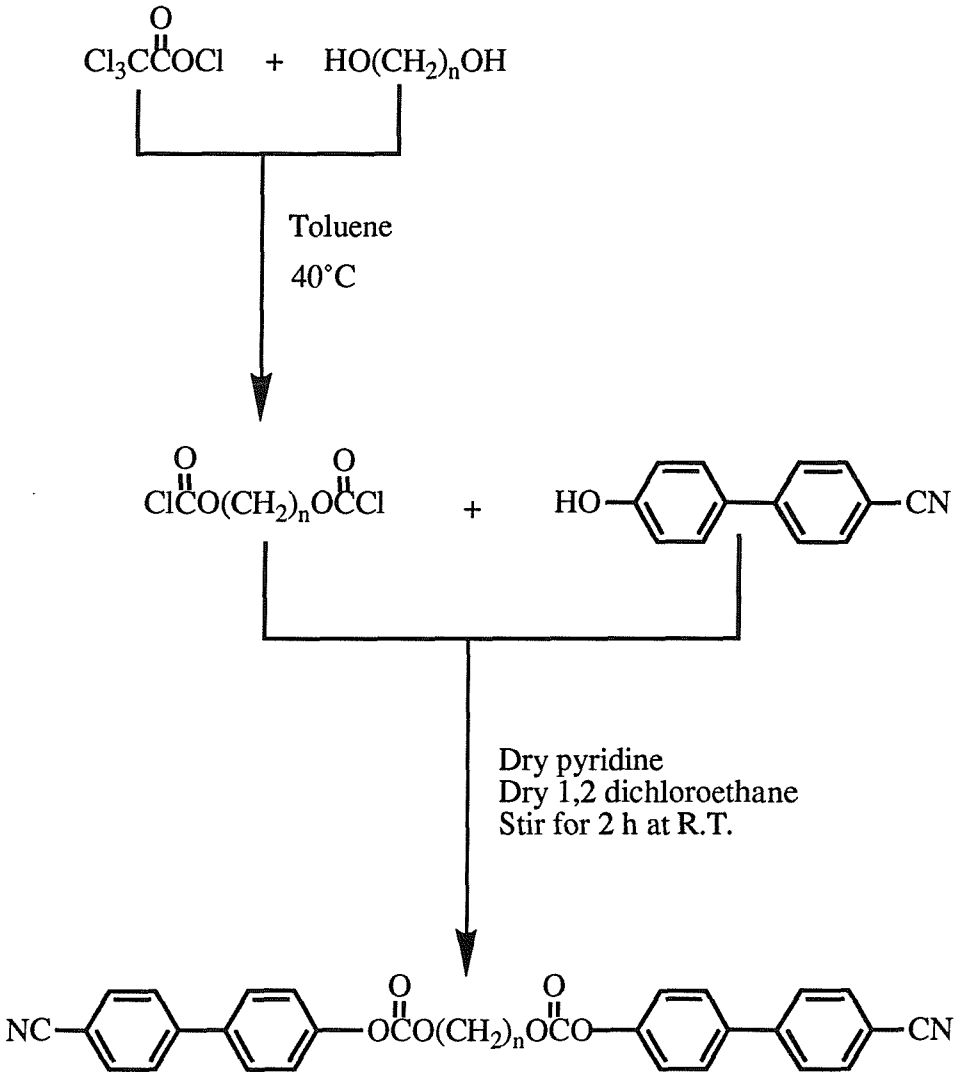

3. Results and discussion

The liquid crystal phase observed in all the compounds prepared was classified as a nematic from the schlieren texture with homeotropic regions that flashed when mechanically stressed when viewed through a polarising microscope. The transitional data for our carbonate dimers are given in table 1 and graphically represented in figure 3. The transition temperatures obtained by Abe are included for comparison. A study of the two data sets reveals some differing results, by as much as 12°C in places for T_{NI} and up to 50°C for T_{CN} . If, however, we overlay Abe's transition temperatures onto ours where we replace T_{CN} with T_{NC}, then the data points are almost coincident we therefore assume that Abes results were taken whilst cooling, this is seen in the lower plot of figure 3. We cannot speculate as to why the data from Abe is so different, however the underlying pattern of both data sets remains the same. The immediately striking feature is the virtual absence of an odd-even effect in the nematic-isotropic transition temperatures,T_{NI}s, often associated with dimeric liquid crystals linked through an alkyl chain, n.b. some oligomeric mesogens containing siloxane chains for example, do not exhibit an odd-even effect as the number of links is sequentially increased [5]. The alternation in the entropic data, $\Delta S_{NI}/R$, (see figure 4) remains but to a much lesser extent than most dimers coupled with a certain degree of attenuation, again, a feature not generally associated with dimers on the whole.

An obvious comparison to make is the α,ω-bis(4,4'-cyanobiphenyloxy)alkanes [6], this well documented series of mesogens is structurally similar. Figure 4 depicts the nematic-isotropic transitional data versus the total number of atoms in the spacer backbone for both the alkyloxy and the alkylcarbonato cyanobiphenyl series. From this we can see that the T_{NI}s for the carbonate dimers closely follow the locus of the even members of the alkyloxy dimers. This suggests that the carbonate link is disguising the parity effect in some way. The large reduction of the nematic range

n	T_{CN}/°C	T_{NC}/°C	T_{NI}/°C	T_{CN}/°C (Abe)	T_{NI}/°C (Abe)	ΔH_{CN}/ kJmol^{-1}	ΔH_{NI}/ kJmol^{-1}	$\Delta S_{CN}/R$	$\Delta S_{NI}/R$
4	197	187	203	-	-	60.13	6.73	15.4	1.70
5	183	168	190	161	192	50.04	5.77	13.2	1.50
6	180	167	186	159	198	65.91	6.60	17.5	1.73
7	172	122	182	125	171	59.57	5.75	16.1	1.52
8	166	131	178	139	175	51.10	6.45	14.0	1.72
9	160	111	172	115	164	54.92	5.85	15.2	1.58
10	143	122	164	-	-	56.72	5.96	16.4	1.64
11	136	96	157	-	-	55.43	5.51	16.3	1.54
12	130	91	152	-	-	57.96	5.69	17.3	1.61

Table. 1 The transitional properties of the carbonate dimers. The results from Abe [4] are included for comparison. Here, n indicates the number of carbon atoms in the alkyl chain.The uncertainties in the transition temperatures are ±1°C, and the entropies and enthalpies of transition ±5%.

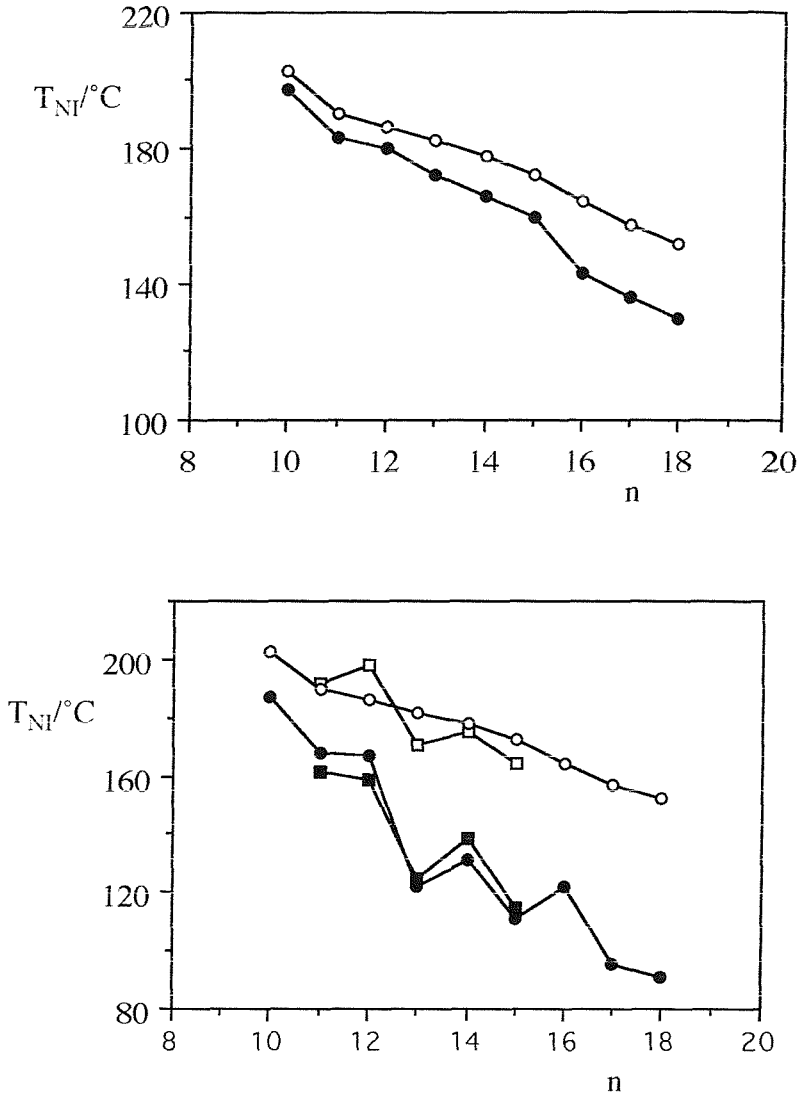

Figure 3. The nematic-isotropic (O) and crystal-nematic (●) transition temperatures for the carbonate dimers versus the total no. of atoms in the spacer backbone. Abes' results [4] are overlayed in the lower graph for comparison, T_{NI} (□), T_{CN} (■).

leads us to consider the symmetry and the ease of rotational freedom of the molecules within the phase.

If we consider both the alkyloxy and the carbonate link using molecular geometry data from Abe [3],

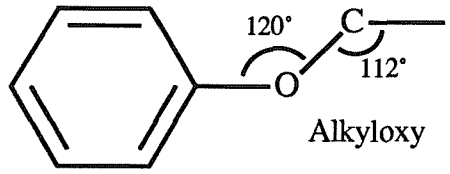

Alkyloxy

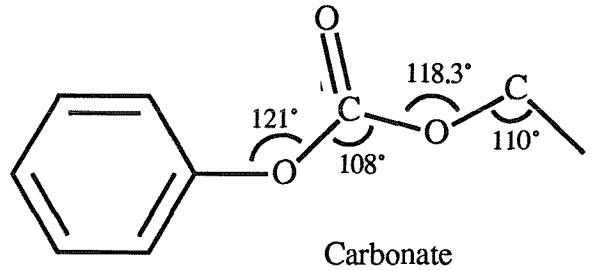

Carbonate

It is immediately apparent that the bond angle sequence C_{ph}-O-C_{ket}-O-C_{alk}-C of the carbonate linked dimers acts to reduce the staggering effect that the alkyl chain imparts upon the molecule by effectively fixing the geometry of the first and last four atoms in the spacer backbone in an arrangement that is much more in line with the long axis of the mesogenic groups than the alkoxy link. Indeed, for the 2-dimensional representation of the links shown above, the angle of elevation to the first carbon atom in the flexible alkyl chain is 60° for the alkoxy link and only 35° for the carbonate link. To demonstrate this fact some energy minimised molecular models of two carbonates, one odd and one even, have been computer generated together with two alkyloxy dimers of similar backbone length. From the pictures displayed in plates 1 to 4 it is apparent that the carbonate linkages cushion the parity effect of the alkyl chain to such an extent that the mesogenic groups lie virtually parallel to one another in both the odd and the even dimers, this is in contrast to the alkyloxy analogues that show a definite 'zig-zag' for the even and a 'bent'

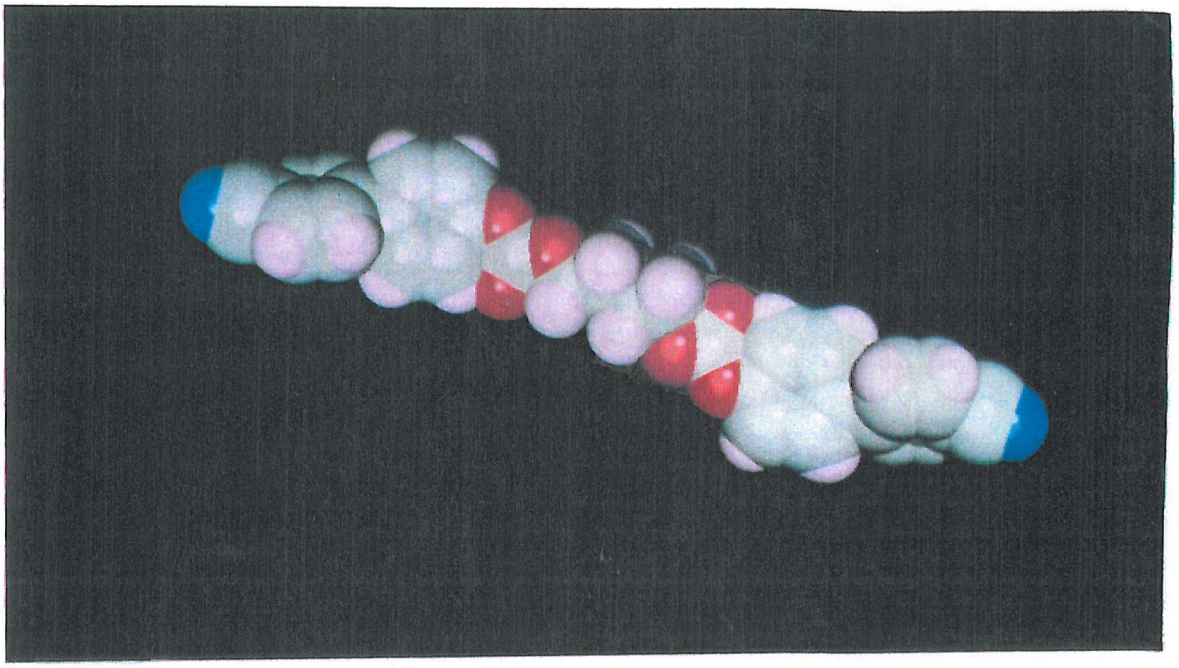

Plate 1. The linear all trans model of a carbonate 4 dimer molecule.

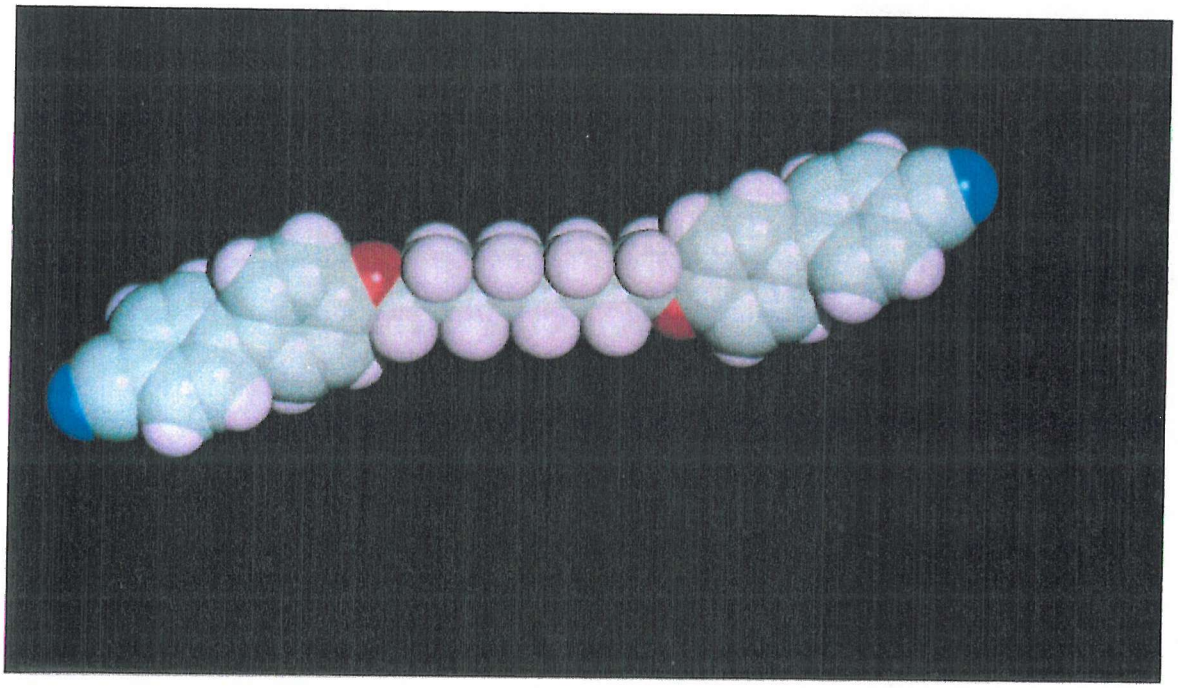

Plate 2. The zig-zag shape of the all trans model of a CBO8OCB molecule.

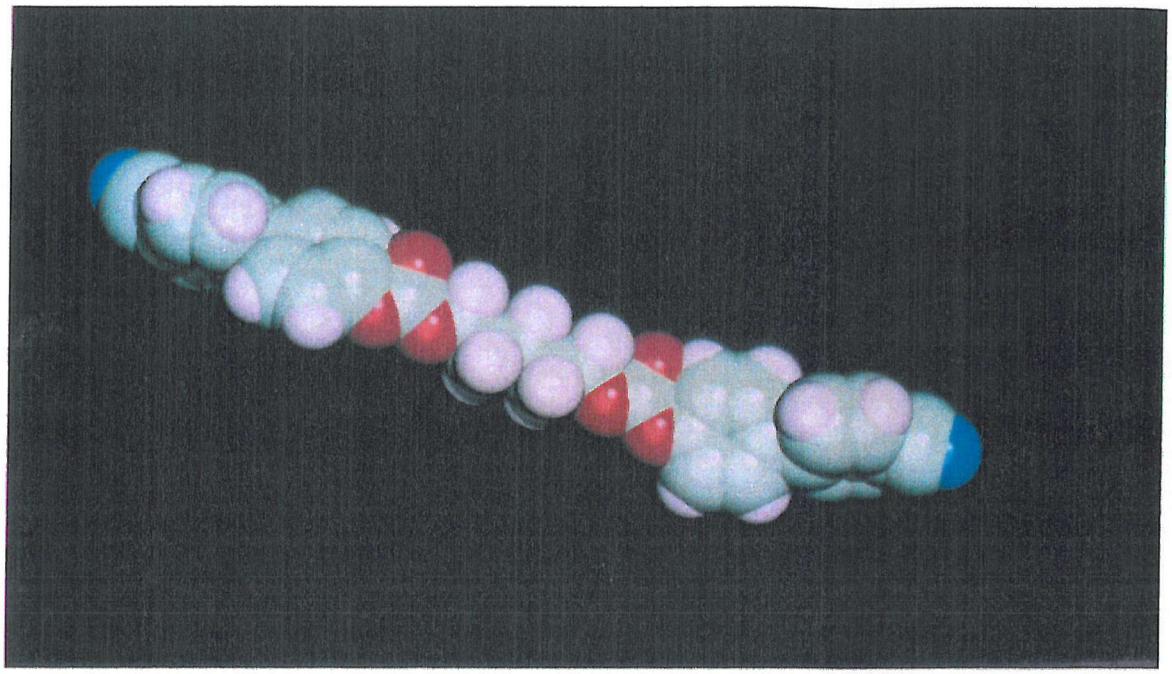

Plate 3. The linear all trans model of the carbonate 5 dimer molecule.

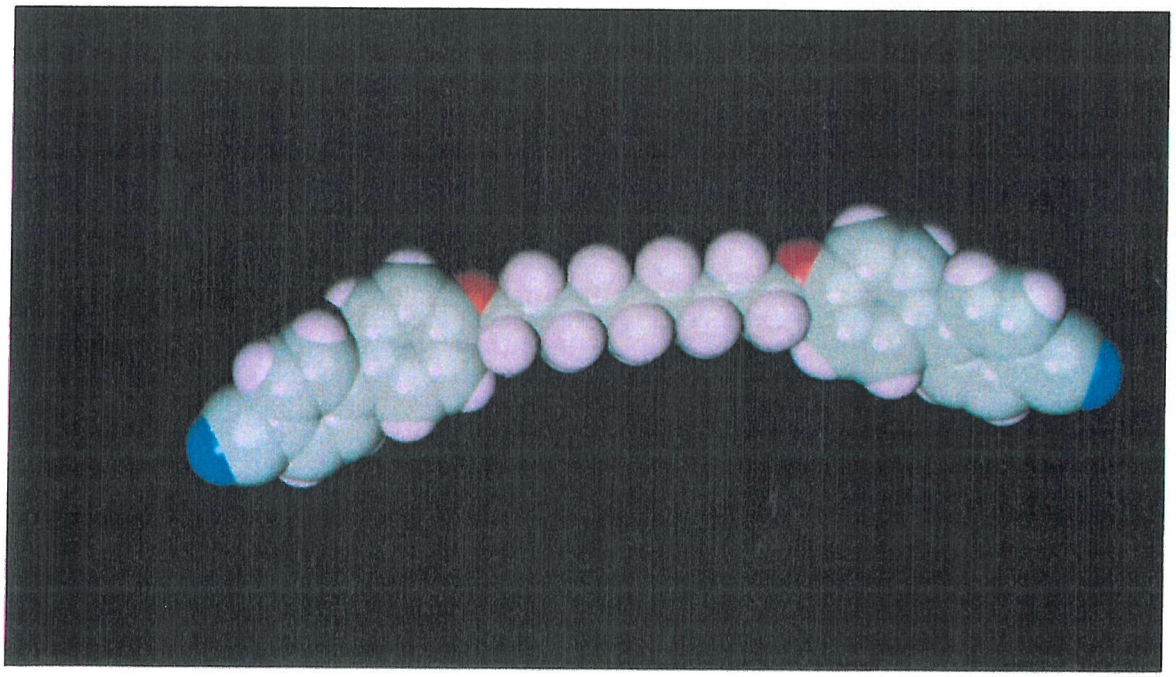

Plate 4. The bent shape of the all trans model of a CBO9OCB molecule.

construction for the odd chains. This is in compliance with a similar suggestion made by Abe [3].

A feature that must be considered when comparing the carbonate dimers to the alkyloxy dimers is the presence of an additional four atoms in the spacer backbone over and above the purely alkyl content. The dotted line in figure 4 anticipates that the alternation in T_{NI}s for the alkyloxy dimers will completely attenuate when n reaches 16 or thereabouts, at a temperature that is comparable to the corresponding carbonate dimer.

The decreased mesogenicity of the carbonate dimers relative to many other cyanobiphenyl based dimers is a little less straightforward to rationalise. Indeed the alkyl carbonato-Schiffs base materials reviewed in the introduction exhibit a broader mesogenic range than either alkyloxy or acyloxy links. This could be due to the presence of the C=O groups which can be thought of as lateral substituents which hinder intermolecular rotation while increasing the possibility of hydrogen bonding in turn raising the melting points while permitting substantial monotropic behaviour.

If we now turn our attention to the entropic data for the nematic-isotropic transition, a clear odd-even effect remains albeit greatly reduced with respect to the alkyloxy dimers. This implied similar level of order for both odd and even carbonate dimers is consistent with our proposal that, for the all-trans conformers, the geometry of both odd and even are very similar. The levels of the entropy data lie approximately intermediate to those for the alkyloxy dimers, this is a little more difficult to rationalise. We might have expected little alternation in the entropic data but at values similar to those for the even alkyloxy dimers. The reduced entropy values suggest that gauche links in the chain severely disrupt the molecular organisation.

A major by-product of the synthetic route shown in the reaction scheme was found to be strongly mesogenic with consistent transitional data for each of the dimers

(i).

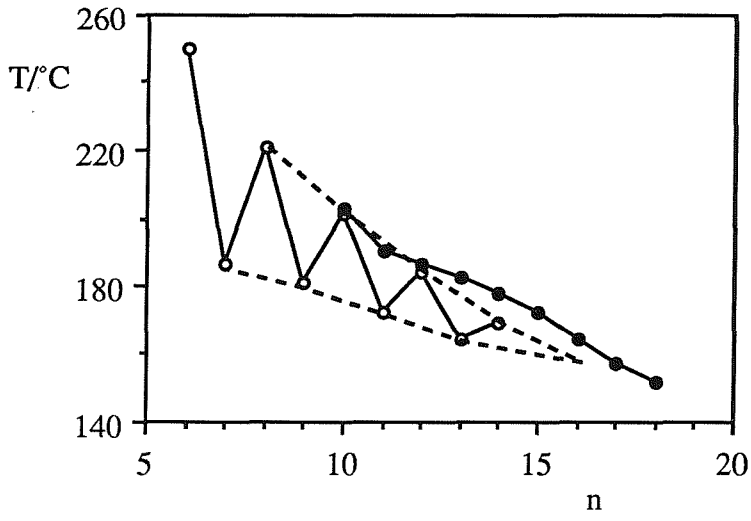

(ii).

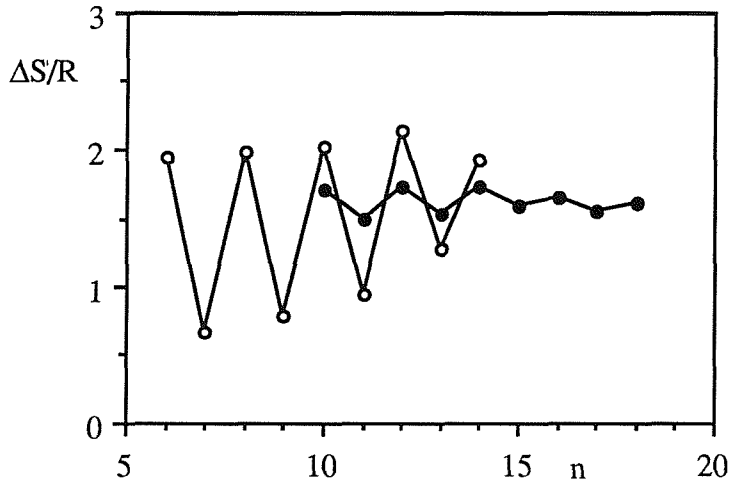

Figure 4. The dependence of (i) the nematic-isotropic transition temperatures and (ii) the entropies of transition on n, the total no. of atoms in the spacer backbone for the carbonate dimers (●) and the alkyloxydimers (○).

prepared. Subsequent spectroscopy eluded the structure of this compound to be two cyanobiphenyl units joined via a single carbonate linkage thus

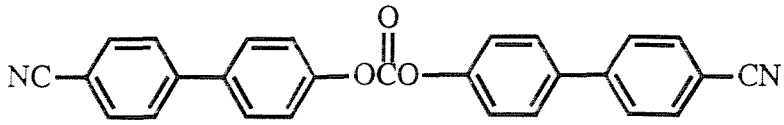

T_{CN} 235°C T_{NI} 320°C

$\Delta S_{CN}/R$ 8.31 $\Delta S_{NI}/R$ 0.73

IR υ 2226cm^{-1} CN stretch, 1803cm^{-1} C=O stretch.

^{1}H NMR ($CDCl_3$, δ) 7.4 - 7.5 (m, 2H), 7.6 - 7.7 (m, 4H) 7.75 - 7.8 (m, 2H).

^{13}C NMR ppm 111.48, 118.88, 121.73, 127.88, 128.69, 132.85, 137.68, 144.60, 151.40, 152.04. 10 inequivalent carbon atoms in aromatic spectral region.

MS (EI, 70ev) (M^+ 416, 54%), (194 $C_{13}H_8NO$, 100%).

This by-product reveals something interesting in itself. If, as before, we compare this carbonate dimer to the equivalent alkyloxy dimer, i.e. just one methyl group in the alkyl chain, there is a vast difference in transition temperatures for compounds with such a similar molecular shape. The situation found earlier is now completely reversed.

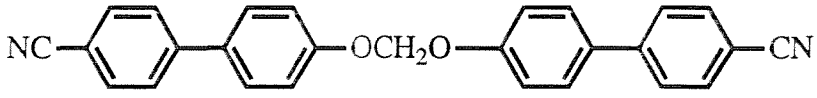

T_{CI} 144°C T_{IN} 124°C

This demonstrates our proposal that the tetrahedral nature of a methyl unit instils a kink sufficiently large to disrupt enantiotropic behaviour completely whereas the 'flat' carbonate link as a whole creates a linear molecule and hence a very effective liquid crystal. However, it is not clear as to why there is such an enormous difference between the transition temperatures of these two compounds.

4. Conclusions

The results reported in this chapter have demonstrated that dimeric molecules whose flexible spacers are joined through a carbonate link are more or less linear in shape for the all-trans conformer which maintains a parallelism between the two mesogenic groups over all spacer lengths, n, studied, both odd and even. This translates to the nematic-isotropic transition temperatures as a steadily decreasing smooth line as the alkyl spacer lengthens. This is opposed to most other dimers which tend to develop a strong alternation in transition temperatures as n changes from odd to even. The reduction in mesogenic behaviour is a little more difficult to explain, however, the presence of the C=O bond in the carbonate linkage is proposed to interfere with the efficient management of the phase. In addition to this, the entropy values of the nematic-isotropic transitions imply that the order within both odd and even dimers is very similar.

A dichotomy is introduced when we see that a by-product of the reaction is very strongly mesogenic with a 100°C nematic range while the equivalent alkyloxy dimer is only monotropic. We propose that the carbonate link 'locks' the geometry in a way that sustains a highly efficient nematogenic material.

References

[1] Matzner M., Kurkjy R.P., Cotter R.J., 1964, *Chem. Rev.*, **64(6)**, 645.

[2] Criswell T.R., Klanderman B.H., Batesky D.C., 1973, *Mol. Cryst. Liq. Cryst.*, **22**, 211.

[3] Abe A., Furuya H., 1986, *Soc. Polym. Science Japan*, **43**, 247.

[4] Abe A., 1988, *'Ekisho Kobunshi'*, **2**, 11. Eds. K Iimura, T. Asada and A. Abe, Shigumu Pub., Tokyo (in Japanese).

[5] Acquilera C., Bernai L., 1984, *Polymer Bulletin*, **12**, 383.

[6] Emsley J.W., Luckhurst G.R., Shilstone G.N., Sage I., 1984, *Mol. Cryst. Liq. Cryst.*, **102**, 223.

CHAPTER 5

Orientational order of liquid crystal trimers

1. Introduction

Liquid crystal formation is governed by the anisotropy of molecular shape, however, not all molecules that deviate from spherical symmetry will form a liquid crystalline phase. Indeed the majority of molecules that satisfy this condition do not exhibit liquid crystallinity simply because they crystallise at a temperature higher than that at which a mesophase would otherwise be formed. Any potential mesophase 'hidden' by the high melting point of a rigid molecule can often be accessed by supercooling, a change of pressure or simply by the introduction of a flexible alkyl chain. A basic example of this is seen in the 4-n-alkyloxy-4'-cyanobiphenyls (nOCBs) where the basic mesogenic unit, 4-hydroxy-4'-cyanobiphenyl, melts to an isotropic liquid at 210°C and the nOCBs, in which a terminal alkyl chain of length n is added, where n varies from 1 to 12, all exhibit a liquid crystal phase in the temperature range 60° to 90°C. It is understood that the rigid (frequently aromatic) core enhances the anisotropic intermolecular interactions and therefore increases the liquid crystal-isotropic transition temperature while the alkyl chains tend to depress the freezing point, although certain other effects on the transition temperatures may be seen as well. The precise role of such pendant alkyl chains was largely ignored in early molecular theories of liquid crystals due to the inherent complications associated with the many different conformations that an alkyl chain can adopt. Any theory that is developed to simulate the role of the flexible chain and hence the liquid crystal as a whole necessarily contains certain approximations and assumptions due to the seemingly infinite number of forces and influences over the

constituent molecules. The development of theoretical work and the improvement of the approximations contained in these over the course of time are well documented for flexible molecules [1] and, more pertinent to this Thesis, the cyanobiphenyl mesogenic unit and attached alkyl chains [2,3]. Comparison between the predictions of these theories and experimental NMR results is similarly well studied [4,5].
The aforementioned citations detail the theory and parameters involved in the development of the computer modelling, but here we will just describe a brief synopsis of the basic concepts and relate these to larger molecules containing two and three mesogenic groups.
For flexible molecules, the conformational distribution needs to be described . This formidable task is greatly simplified if all internal modes except rotations about the C-C or O-C bonds are ignored. The rotameric state model of Flory [6] can be applied in which bond lengths and angles are fixed to leave the energy of each chain segment dependant only on the dihedral angle. The three minimum energy states resulting from this model are the lowest energy trans (t) conformer and the two higher energy gauche (g±) conformers. The rotameric state model assumes that only these conformations are allowed, which permits any single conformer of an alkyl chain to be described as a sequence of trans and gauche links. For monomeric liquid crystals two interaction tensors X_c and X_a are introduced where X_c is the interaction tensor for a carbon-carbon bond and X_a for a mesogenic group, these determine the orientational energy resulting from the molecular field. Also supplied to the program is E_{tg}/RT, the energy difference between a trans and a gauche link scaled with the temperature. To generate a conformer these interaction tensors are combined with the rotameric state model constrained by a diamond lattice which restricts the carbon-carbon bond angles to the tetrahedral value of 109°28', and the dihedral angle for a gauche arrangement to ±60°. For a given chain , conformers are generated sequentially and averages of properties such as the internal energy and the order parameters are accumulated (conformations that contain 4 alternate g+ g- repeats generate six membered rings and are eliminated). Use of the geometric mean

rule to simplify the thermodynamic equations then allows the free energy and entropy to be calculated together with the scaled temperature, T^*.

Eigenvectors resulting from the diagonalisation of the interaction tensors, X, can give the order parameters for individual segments in the molecule. This is particularly useful along a C-D bond direction which can be compared directly with experimental NMR results. Dimeric molecules composed of two rigid mesogenic segments linked through an alkyl or an alkyloxy chain can be readily simulated by setting the strength parameter of the final segment in the flexible chain to be X_a rather than X_c. Calculations then proceed as for monomers but with the modification of a volume factor to accommodate the extra space occupied the second mesogenic unit. The qualitative trends in the transitional data obtained from theory agree well with experiment.

A similar adaptation is employed for the simulation of trimeric liquid crystals. Here the interaction parameter of the central carbon-carbon bond in a dimer is set as X_a with the volume factor adjusted accordingly. Again qualitative trends are in good agreement with experiment. In this particular simulation [7] however, a significant difference between the ordering of the end and the middle mesogenic units have been predicted, especially for short length trimers. It is this difference that will now be experimentally investigated with the aid of deuterium NMR spectroscopy.

This Chapter focuses on NMR studies of two specifically deuteriated short chain length trimers, where n=3 and 5, previously unstudied on account of their high transition temperatures. A comparison with the trimer of n=4 would have been desirable, however, the very high nematic-isotropic transition temperature at which point the material started to decompose made this compound unsuitable to study.

2. The NMR experiment

Two members from the symmetric trimeric series, 4,4'-bis(4'-cyanobiphenyloxyalkyloxy)-biphenyls, specifically deuteriated in the aromatic sites ortho to the chain for the end and middle mesogenic groups were synthesized and their orientational order was investigated using deuterium NMR spectroscopy. Strictly these compounds are not trimers for the middle biphenyl group is not identical to the end cyanobiphenyl group; however the difference is not sufficiently great to change from this convenient terminology to something which while more accurate would inevitably be more cumbersome. The physical properties of this trimeric series have been investigated and were found to be very similar qualitatively to those observed for the analogous dimeric CBOnOCB series although the magnitude of the odd-even effects for both the nematic-isotropic transition temperature and the entropy of transition are consistently more accentuated [8]. In an attempt to further our understanding of this fascinating behaviour in terms of the molecular organisation within the nematic phase we have studied the orientational order of the end and middle mesogenic groups, again by using deuterium NMR spectroscopy.

2.1 Deuterium NMR measurements

The deuterium NMR spectra of all the compounds were measured using a Bruker MSL 200 fourier transform spectrometer operating at 30.7 MHz. The probe head had a 10mm diameter receiver/transmission solenoid coil mounted horizontally and the samples were contained in 5mm o.d. tubes. Since the transition temperatures of the materials are so high, up to 214 °C, it was necessary to use a pre-heated air supply which was exhausted from the bore of the superconducting magnet by means of a glass tube connected to a small suction pump. The spectra were obtained typically by averaging 10,000 transients following a 90° quadrature echo pulse sequence of 5.5ms duration, a delay between pulses of 50ms was used to ensure a

full recovery of the magnetisation especially along the direction of the magnetic field, Z. A spectral width of 125 kHz accumulated into 8K of computer memory was used which gives a spectral resolution of 30 Hz which is within the accuracy to which peak definition estimates could be made (approx ±50 Hz) because of the large spectral linewidths.

Sample preparation was based on a total of approximately 200mg of material contained in an NMR tube, this was heated until the contents were just isotropic to ensure the removal of air then contained using a small teflon plug to prevent leakage.

3. Experimental

3.1. Synthesis of 4,4'-bis(4'-cyanobiphenyloxyalkyloxy)-biphenyls, n=3,5

Both trimers were prepared in the following way according to the procedure outlined in the reaction scheme.

4-hydroxy-4'-cyanobiphenyl (1g, 1equiv.) together with α,ω-dibromoalkane (11g, 10 equiv.) were dissolved in dry acetone and anhydrous potassium carbonate (5.5g, 7.25 equiv.) was added; the mixture was stirred under reflux for 18 h. The mixture was filtered while hot and the acetone removed under reduced pressure. The excess α,ω-dibromoalkane was recovered by distillation under vacuum and the crude 4-bromo-n-alkyloxy-4'-cyanobiphenyl was recrystallised from methanol and dried. Yield 85%.

4-bromo-n-alkyloxy-4'-cyanobiphenyl (1g, 2.1 equiv.) and biphenol (0.22g, 1 equiv.) were dissolved in dry dimethyl formamide (30 ml) and K_2CO_3 (1.7g, 5 equiv.) was added, this was heated under reflux for 5 h, allowed to cool and then

Reaction scheme

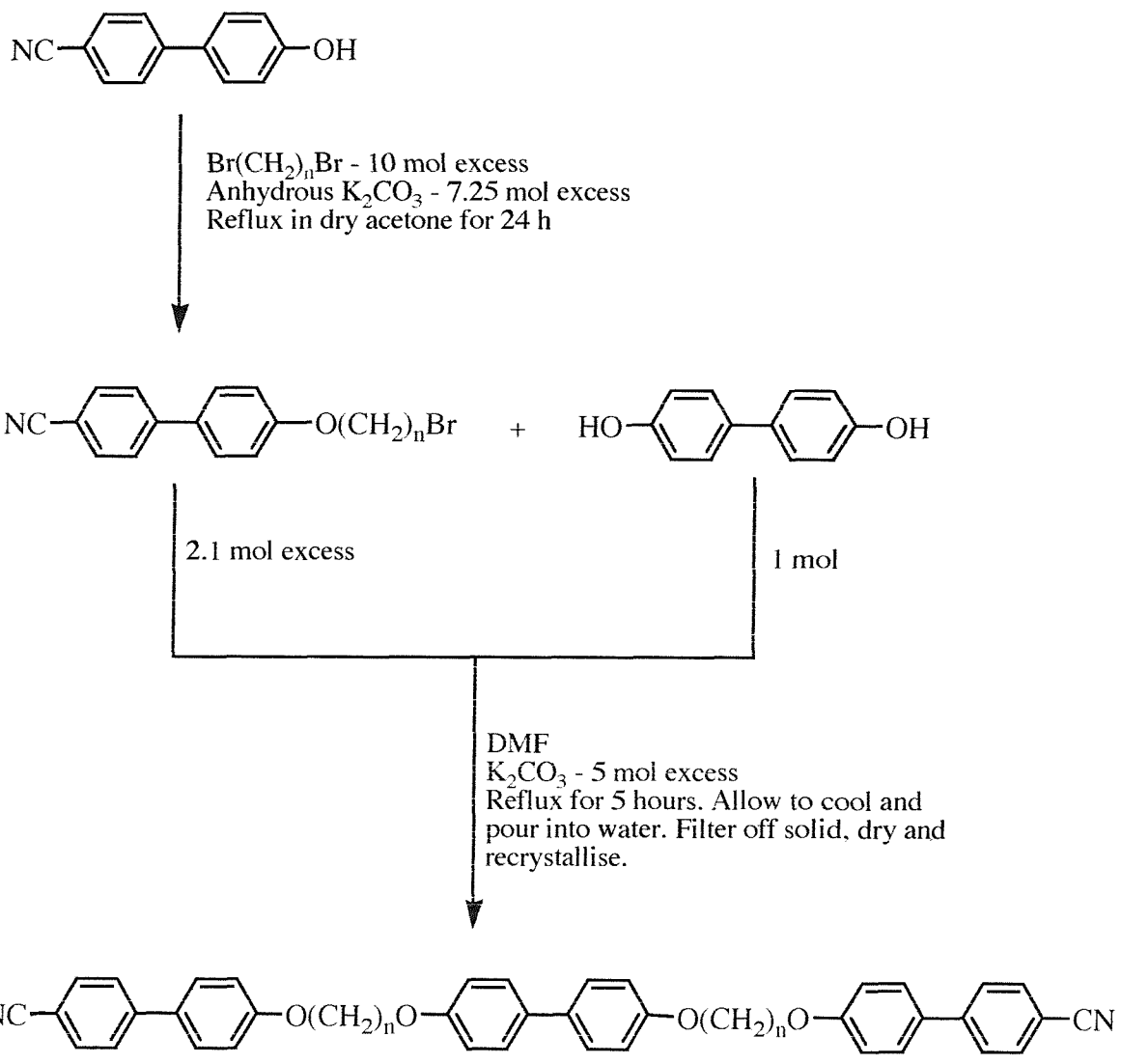

poured into water (200ml). The white precipitate was filtered off and dried. After drying the sparingly soluble crude product was refluxed in sufficient toluene to effect dissolution. This was then filtered hot to remove any undissolved impurities, allowed to cool, and filtered once again to give pure material in 60% yield.

3.1.1. Deuteriation technique

Deuteriation of 4-hydroxy-4'-cyanobiphenyl

The deuteriation of 4-hydroxy-4'-cyanobiphenyl, (OCB), was acheived by employing the following procedure described by Emsley et al.[9].

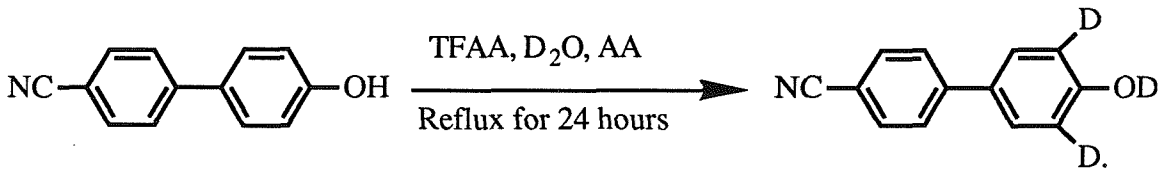

Trifluoroacetic anhydride (20ml) was added slowly with cooling to D_2O (10ml) this produces the very strongly acid, trifluoroacetic acid-d_1, to this acetic anhydride (15ml) and 4-hydroxy-4'-cyanobiphenyl (2.0g) were added and the mixture refluxed for 24 hours. The reaction mixture was allowed to cool and then shaken with water (200ml), the white solid thus recipitated was filtered off, washed well with water and filtered off. The major component (≈70%) of the crude product was 4-(3,5-d_2-4-hydroxyphenyl)benzamide which results from the hydrolysis of the cyano group under such strongly acidic conditions. This unwanted component was removed by refluxing the solid in dichloromethane (400ml) and methanol (4ml) for two hours, standing overnight and filtering off the insoluble amide. After the evaporation of the solvent the slightly yellow colour was removed using decolourising charcoal and then recystallised from 20% v/v aq. methanol (150ml) to

Figure 1. ^1H NMR Spectra of (a) OCB, and (b) OCB-d_2.

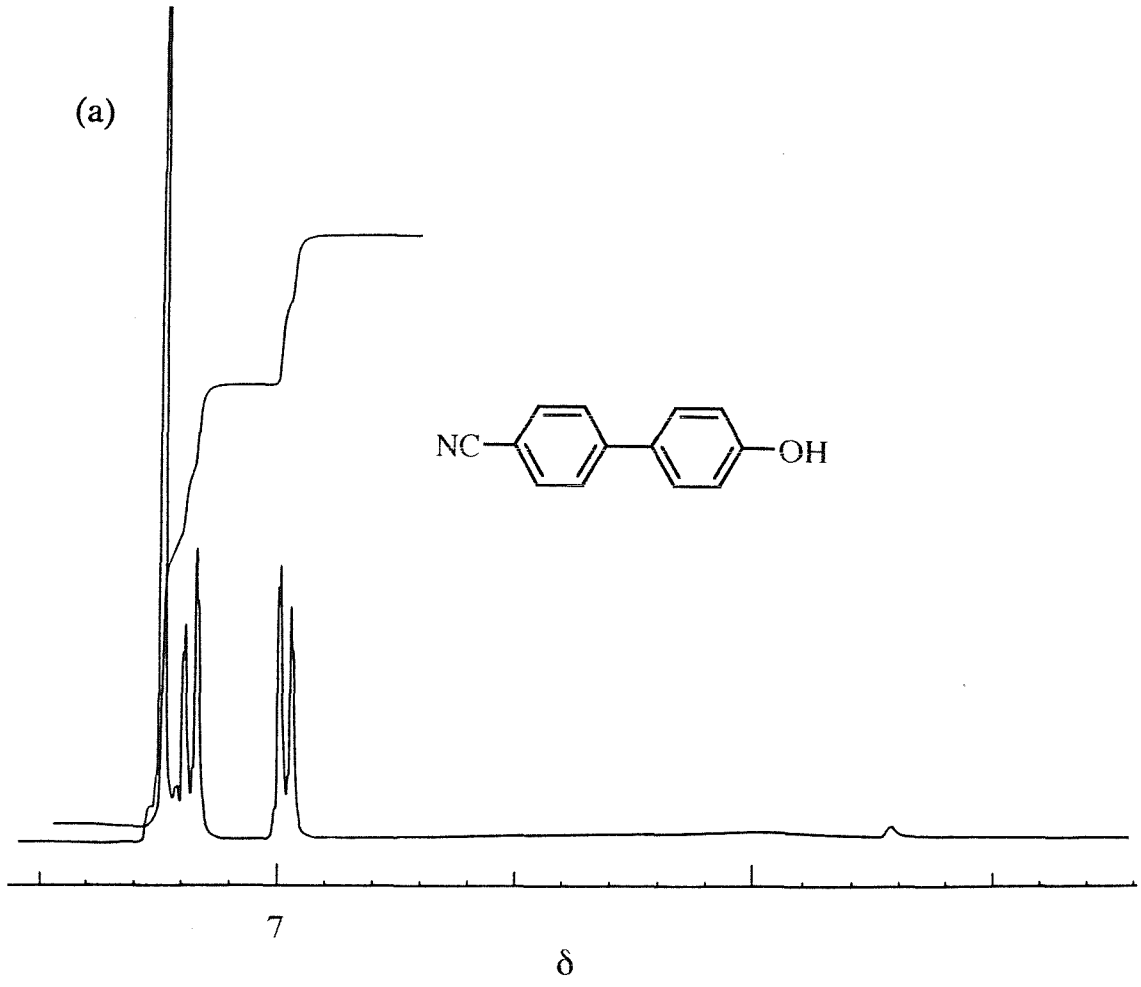

give pure 4-hydroxy-3,5-d_2-4'-cyanobiphenyl (OCB-d_2) crystals with a yield of 30%.

Comparison between the ^1H NMR spectra of OCB and OCB-d_2 showed a virtual disappearance of the peaks attributed to the 3,5-hydrogens for OCB. By comparing the integrals of the peaks the product was estimated to have >90% incorporation of deuterium (see figure 1).

In addition the nitrile can be recovered from the amide. The amide produced from hydrolysis of the cyano group may be dehydrated back to the nitrile by employing thionyl chloride ($SOCl_2$). This technique involves dissolving the amide (10 mmol) in DMF (20ml), adding $SOCl_2$ (80 mmol) and heating with stirring at 80°C for 1 h. This was allowed to cool and then poured carefully onto iced sodium bicarbonate solution (1 molar) This procedure is extremely effervescent with the evolution of much SO_2, CO_2, HCl and froth. Once settled the precipitate is filtered and washed well with water and then purified in the same manner as described above. This recovery process gives a yield of 90% with minimal loss of the deuterium content.

Deuteriation of biphenol

The partial deuteriation of biphenol was achieved using a similar method to that described for 4-hydroxy-4'-cyanobiphenyl.

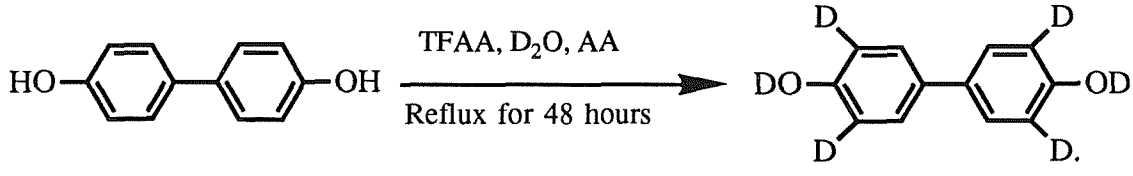

Trifluotroacetic anhydride (40ml) was added slowly with cooling and shaking to D_2O (15ml). Acetic anhydride (25ml) and biphenol (5g) were then added and the mixture refluxed for 48 hours. After shaking the cooled reaction mixture with water (200ml), the white solid was filtered off, washed well with water, and dried. The

solid was readily recrystallised from ethanol to give 3,3',5,5'-d_4-biphenol in 95% yield. ^{1}H NMR showed a decrease in peak area of ≈90% for the 3,5-H's (see figure 2).

Deuteriation of trimers

The specific incorporation of deuterium was achieved by using OCB-d_2 and biphenol-d_2 in place of their non-deuteriated analogues, in the manner described previously.

MS; (EI, 70eV) Trimer 3-d_{ends} 196(100%), 422, 660(M^+).

Trimer 3-d_{middle} 194(100%), 424, 660(M^+).

Trimer 5-d_{ends} 196(100%), 450, 660(M^+).

Trimer 5-d_{middle} 194(100%), 452, 660(M^+).

The figures given below show the trimers and the position of deuterium incorporation within them.

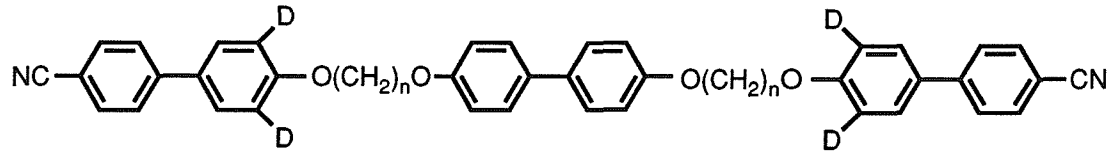

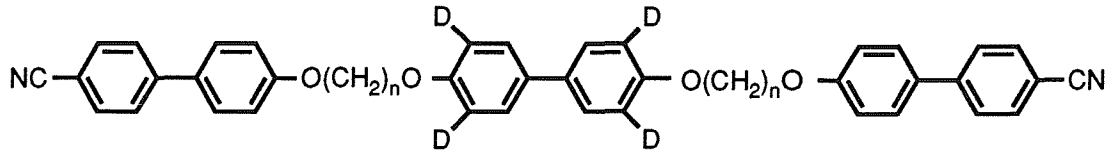

Characterisation of the trimers was difficult because of their extremely low solubility. The introduction of deuterium into the 3,5 sites of the mesogenic biphenyl groups was observed not to alter their mesogenic properties to any

Figure 2. ^{1}H NMR Spectra of (a) Biphenol, and (b) Biphenol-d_4.

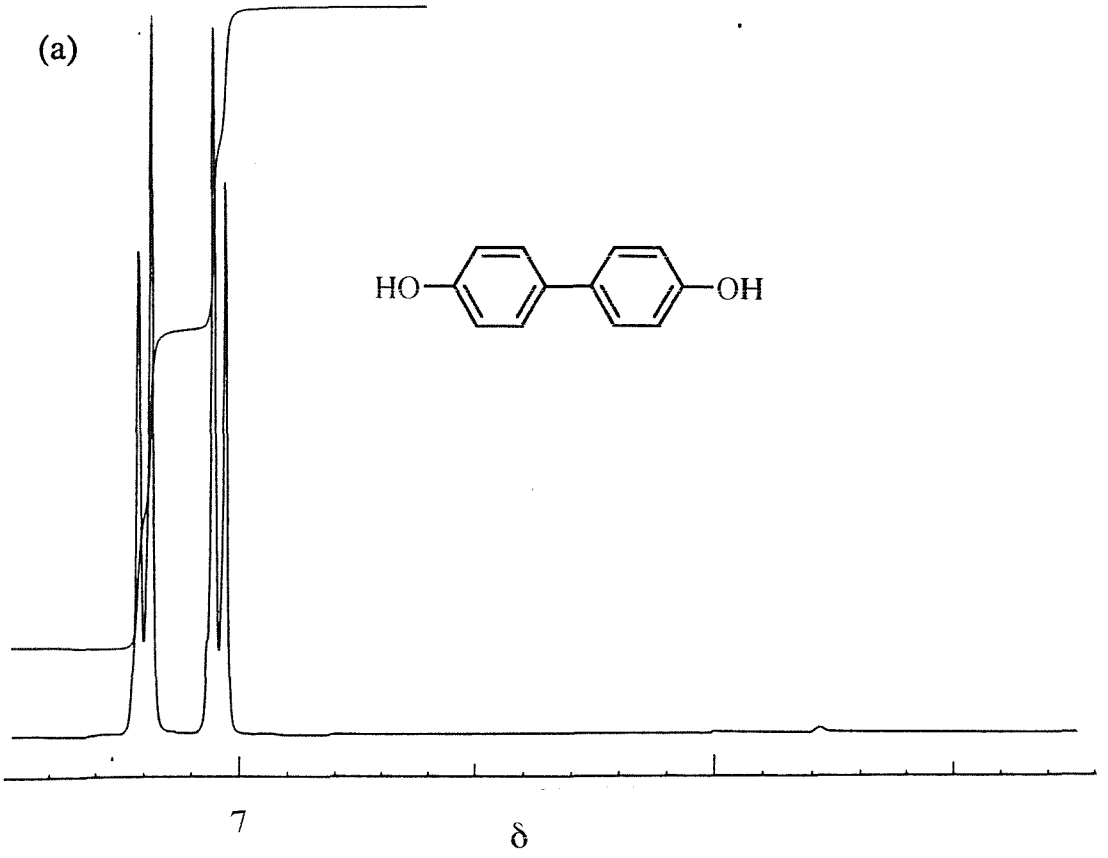

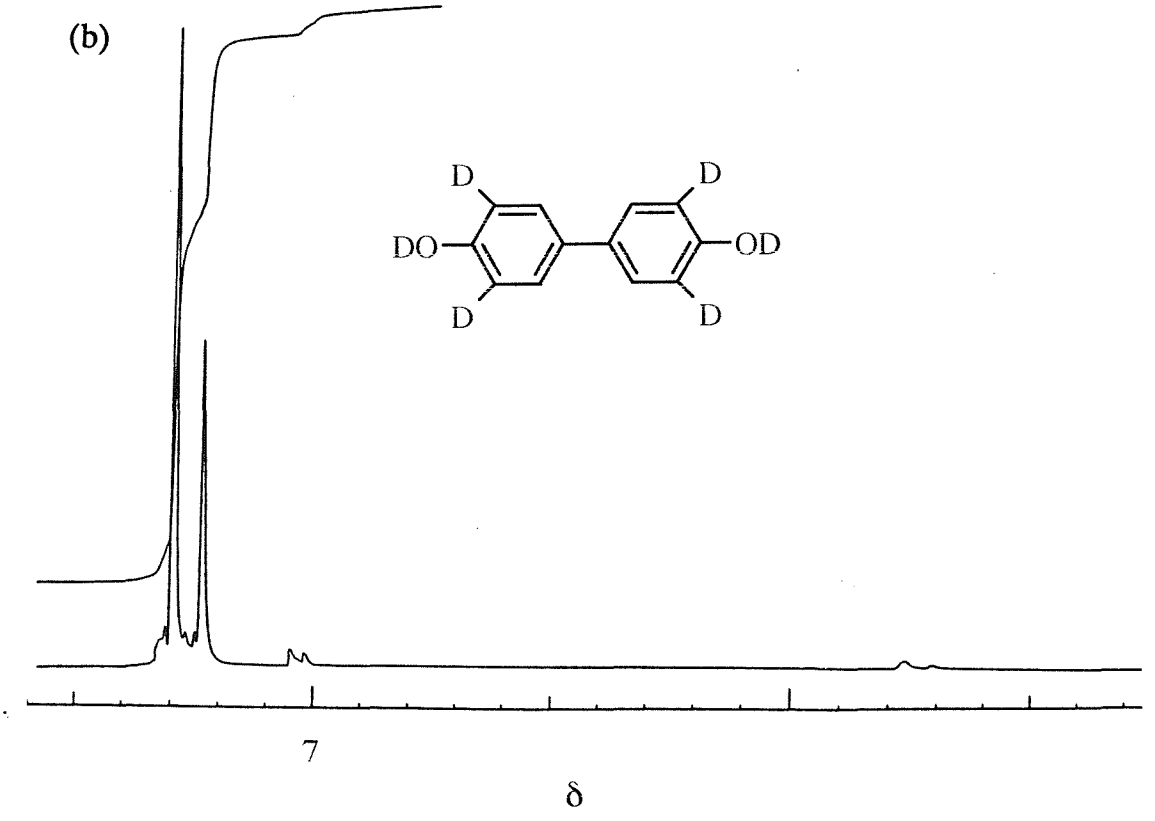

significant extent hence allowing a direct comparison with the previous study and the theoretical predictions for the protonated analogues which does not distinguish between isotopes of atoms. The data tabulated below shows the transitional properties of the deuteriated trimers to be in good agreement with that of the previously prepared protonated analogues (within 1.1°C for T_{NI}) further supporting the identity and purity of these compounds.

	Trimer 3		Trimer 5	
	T_{CN}/°C	T_{NI}/°C	T_{CN}/°C	T_{NI}/°C
d- Ends	169.2	195.5	161.8	207.9
d-Middle	171.6	197.4	162.9	208.7
Non-d	171.4	196.4	164.8	209.0

4. Results and discussion

A study of the orientational behaviour of anthracene-d_{10} dissolved in the homologous series of trimers has been carrried out [10] from which a fairly good understanding of the orientational properties of the series has been obtained. However, unlike the symmetric dimers in which just one type of mesogenic site exists, in the symmetric trimers there are two i.e. the end cyanobiphenyl groups and the central biphenyl link. These might be expected to be ordered to different extents. A symmetric probe molecule such as anthracene-d_{10} is assumed to lie parallel to the local director of molecules within its liquid crystal solvent . In a molecule where there are theoretically two different local directors such a probe is unlikely to distinguish between them and if it did there would be no way of knowing to which group it would preferably align. Selective deuteriation of these mesogenic units makes the distinction between these two groups and hence allows access to the ordering details of each individually and therefore a direct comparison with the

theoretical predictions that the end and middle mesogenic groups are ordered to different extents for short length trimers.

The results for the quadrupolar splittings and hence the order parameters for the end and middle mesogenic groups found for the trimers with odd and even spacers follows the trends outlined in the theory outlined earlier for mesogens composed of flexible molecules. Given the aforementioned approximations it is possible to calculate the nematic-isotropic transition temperatures and the order parameters as a function of the spacer length. The input parameters required for these calculations are E_{tg}/RT and X_c/X_a. Here E_{tg} is the energy difference between a trans and a gauche link while X_c and X_a are the interaction tensors for a carbon-carbon bond and the mesogenic group respectively. For simplicity the interaction parameters for the end and middle mesogenic groups are taken to be the same. This appears to be a reasonable assumption for the trimers which have been studied. The ratio X_c/X_a was set equal to 0.2, which, is a value obtained by fitting the order parameter profiles for 4-n-alkyloxy-4'-cyanobiphenyls to the theory [8]. Finally E_{tg}/RT was given the value of 1.0 which is reasonable and gives a good fit to the order parameter profiles. These values were used to obtain the results given in the table for the scaled nematic-isotropic transiton temperature (T_{NI}^*) and the order parameters for the para axes of the end (P_2^e) and the middle (P_2^m) mesogenic groups at the transition. The results have been obtained for spacers containing 1 to 7 methylene groups. The general trends of an odd-even effect are readily discernable and are seen to be in agreement with experiment. Thus for spacers with an even number of methylene groups in the spacer the order parameters for the end and middle groups are essentially the same; in fact the order of the middle group is predicted to be slightly larger than for the end group. In contrast there is a marked difference for the early odd spacers with the ordering of the end mesogenic group being greater than for the middle. This can visualised in the following way; the end groups tend to be parallel to the director but because of the geometrical constraint imposed by the spacers the middle mesogenic group tends to be inclined with respect to the end groups and hence to the director.

As the length of the odd spacer increases so the predicted difference between the order parameters of the end and middle mesogenic groups decreases. Indeed extrapolation of the results suggest that for the nine spacer the difference would be negligible. This suggests that as the chain length is increased the angular correlations between the three mesogenic groups are lost and they become essentially independent of one another. The theory also predicts that the order parameters for the para axes of the mesogenic groups are larger for the even than the odd spacers, again in agreement with experiment.

Theoretical work does indeed show a difference in ordering between the end and middle mesogenic groups. This difference is most pronounced for odd members of the series and is as high as 0.3 for n=1 and decreases steadily as n increases. In the table, T^* is the scaled temperature, P_2^e is the order parameter of the end mesogenic group, P_2^m is the order parameter for the middle group and P_2^e-P_2^m is the difference between the them.

n	T^*	P_2^e	P_2^m	P_2^e-P_2^m
1	0.1645	0.3351	0.0313	0.3035
2	0.1353	0.5746	0.6203	-0.0457
3	0.1574	0.4116	0.1661	0.2455
4	0.2595	0.6874	0.7258	-0.0358
5	0.1650	0.5068	0.3387	0.1681
6	0.2303	0.7392	0.7672	-0.0280
7	0.1708	0.5814	0.4800	0.1014

Preliminary experimental studies to test this theory indicate that there may indeed exist a difference in the ordering of the end and middle mesogenic groups within this class of molecules [11]. However, this work was carried out on two trimers with

n = 8 and 9 to which, due to the prohibitively large amount of computational time required to simulate the behaviour of these molecules with such long chain lengths, only the extrapolated trends could be compared. A small difference in ordering for these sites was observed in accord with predictions but due to the poor quality of spectra, with no resolved dipolar splitting for trimer 9, this difference lay within experimental error and hence was somewhat inconclusive.

The temperature dependence of the major order parameter S_{zz} of the two trimers with chain lengths of 3 and 5 methyl groups specifically deuteriated in the end and middle mesogenic units are shown in figure 3.

The results for these trimers, as expected, do show a marked difference in ordering between the end and middle mesogenic groups but not as large as the simulations predict.

			Experimental	Theoretical
n	P_2^e	P_2^m	P_2^e-P_2^m	P_2^e-P_2^m
3	0.3205	0.1928	0.1277	0.2455
5	0.3383	0.2645	0.0740	0.1681

Indeed the experimental difference for P_2^e-P_2^m is approximately half that predicted by theory. The order parameters for the end groups are predicted to be much larger than those experimentally observed.

4.1 Error in the Measurement of Dipolar Coupling

It was stated earlier that the alignment of the molecules in the nematic phase to a common direction gives rise to two peaks in the NMR spectrum symmetric about the spectral centre. Dipolar coupling between the nearby aromatic protons and

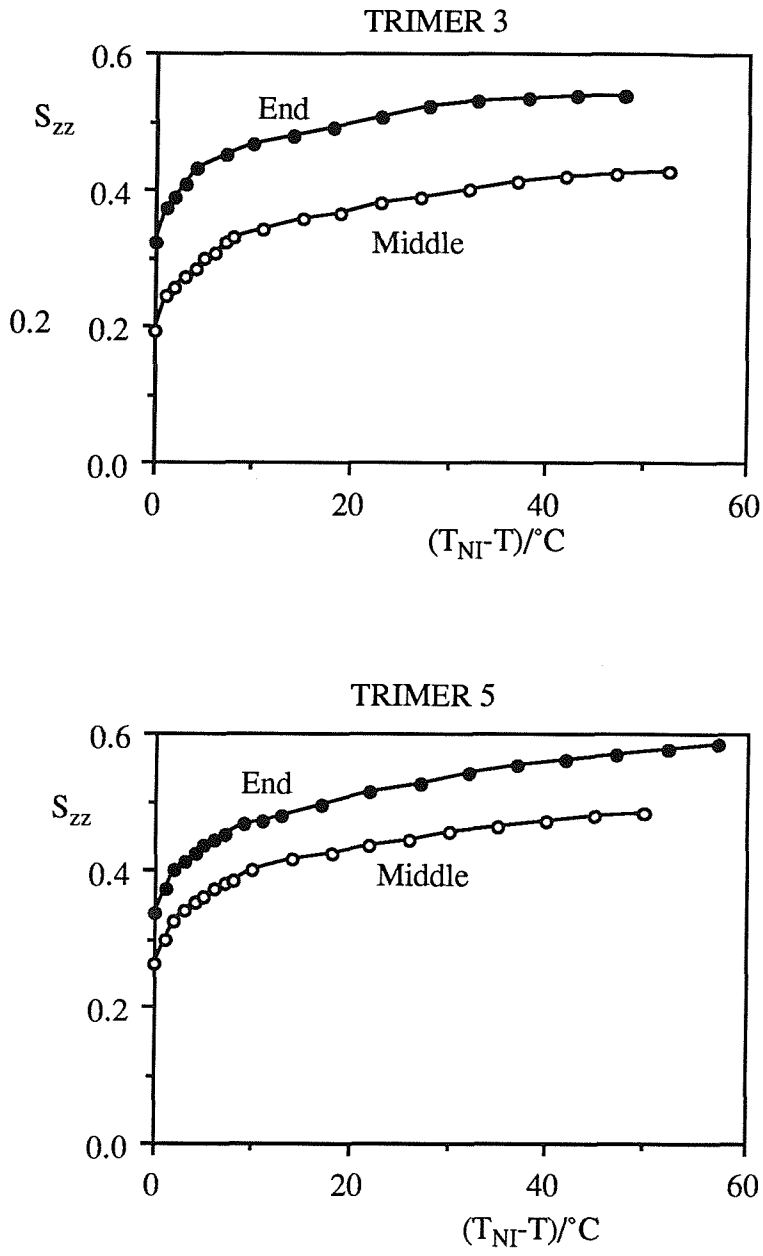

Figure 3. The dependence of the major order parameters (S_{zz}) of the end and middle mesogenic groups on the shifted temperature (T_{NI}-T) for both trimers.

deuterons further split these two peaks into four (sample NMR spectra of end and middle deuteriated trimer 5 at T_{NI} and T_{NI}-25°C are given in figure 4). The resolution of this extra splitting depends on several factors:-

(i) Temperature fluctuations, especially at higher temperatures, as the order of the phase depends critically on the temperature.

(ii) Dipolar coupling with other protons in the molecule.

(iii) Position and % incorporation of deuterium into the sample; the less deuterium, the lower the signal : noise ratio.

(v) The number of accumulated scans, to improve the signal : noise ratio.

(vi) The purity and viscosity of the sample.

And many other factors controlled by the pulsing sequence and processing parameters of the spectrometer will also affect the resolution, although these were optimised at the start of the experiment.

Bearing these considerations in mind and looking at the varying degrees of resolution and the linewidth of the anisotropic signal compared with that of the isotropic phase signal observed in the spectra, it can perhaps be said that the main influences over this resolution are the high temperatures involved and the position of deuterium within the molecule. It is seen that the best resolution is obtained for deuterons in the end group and at lower temperatures where the order is higher. As the resolution decreases so does the accuracy to which the true splitting can be measured since when two signals overlap tthe peaks are effectively 'drawn' together which offsets the true splitting and introduces error into the measurement which can be substantial. The amount of convergence and hence error incurred can be estimated by means of a simple peak simulation routine. From inspection of the spectral lineshapes they are seen to be gaussian. The ratios of the valley height to the maximum peak height were measured for a selection of spectra and this data was entered into a simulation program which simulated two overlapping gaussian lineshapes with a valley:maxima ratio similar to that experimentally measured. The computer calculated the extent the two peaks were brought together by the effect of

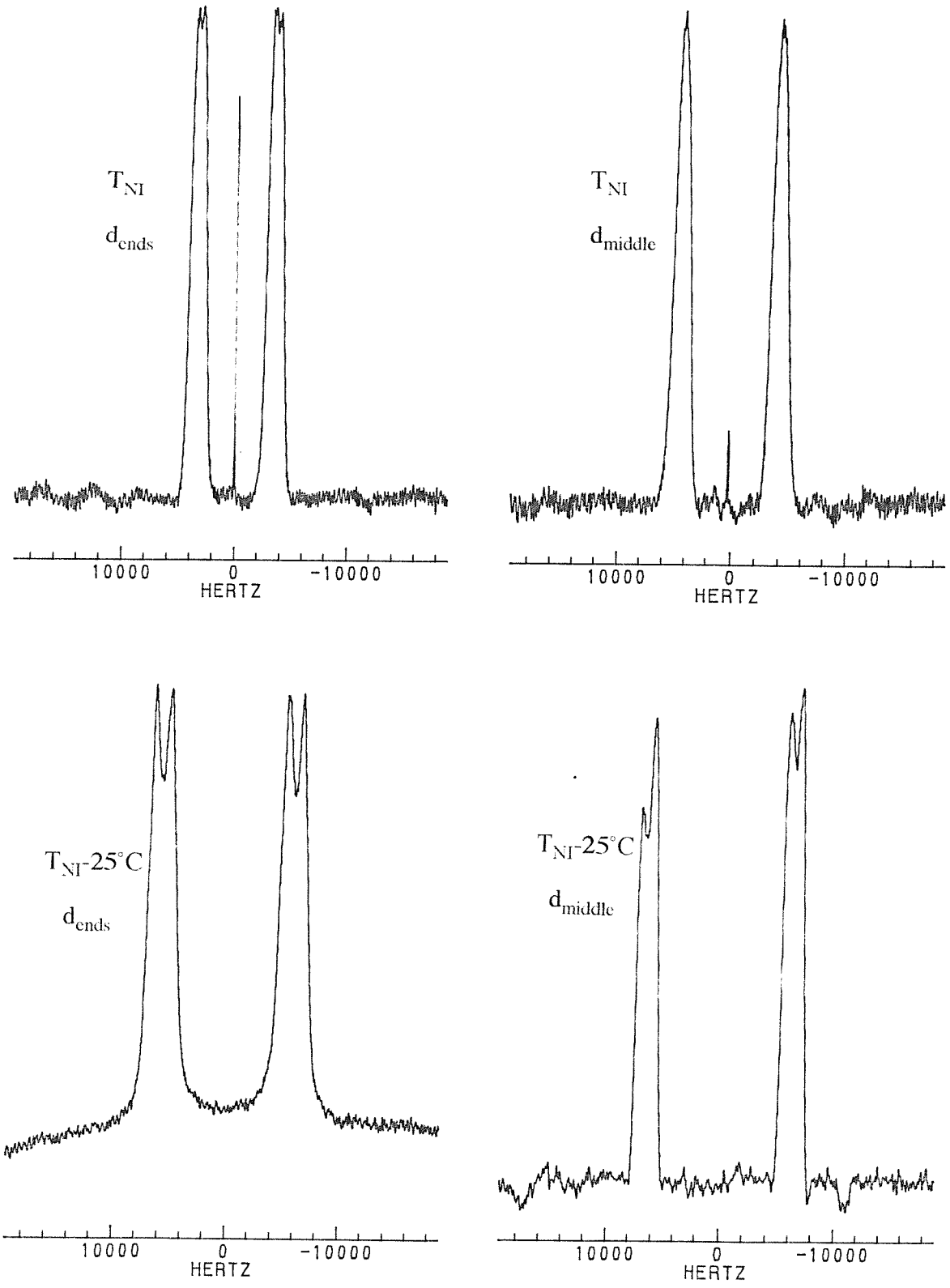

Figure 4. Deuterium NMR spectra of trimer 5 at T_{NI} and at T_{NI}-25°C.

the overlap which was measured as the ratio of the valley height to the total peak height. This was then displayed as a percentage error for each of the valley:peak height measurements taken, allowing a graph to be constructed so that any valley depth could be read off as a % error of the true distance between the two maxima. From the simulated spectra an error band of 3% to 27% was found. The latter figure was deemed unacceptably high. The error was reduced to an estimated ±5% by the multiplication of the observed maximum splitting by $(1+ {}^{\%error}/_{100})$. The correction factor in this equation was continually assessed according to the valley:maxima ratio measured from the observed spectra and relating this to the graph shown below.

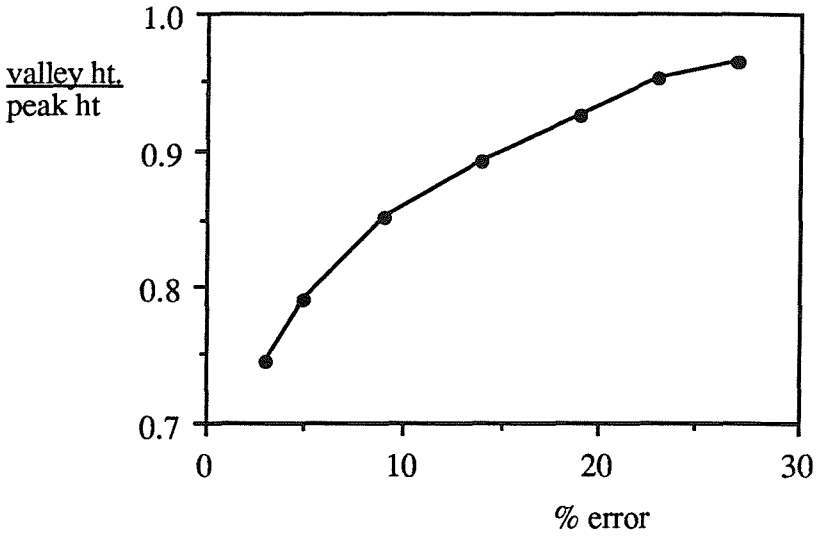

This was estimated to reduce the error in the splitting measurement to ±5%.

The deuterium NMR spectra of molecules deuteriated in this way give two quadrupolar signals symmetric about the spectral centre which are further split by dipolar coupling.The H-D direction is essentially parallel to the para axis of the mesogenic group which means that the order parameter S_{HD} can be compared directly to theory which predicts the order parameters along the same axes of the mesogenic groups.

The dipolar splitting is much less than the quadrupolar splitting (≈ a factor of 10), however, the fact that the dipolar interaction is approximately along the para axis for the mesogenic group which means that the angle β between the H-D vector and the para axis is close to 0° and is therefore insensitive to the magic angle of 54.7° (i.e.when $(3\cos^2\beta-1)/2 = 0$). If we consider the quadrupolar splitting, or any splitting resulting from an interaction along a bond vector that makes an angle close to 54.7° (±10° say) with the director which, in this case is assumed to be the para axis of the mesogenic group, then from the basic representation of $P_2(\cos\beta)$ visualised below it is seen that a small change in the angle β will have a dramatic effect on the splitting and hence on the calculation of the order parameter for the para axis derived from it. The measurement of the quadrupolar splitting is inherently more accurate than the measurement of the much smaller dipolar splitting, but because the quadrupolar interaction in these trimers is at approximately 60° to the director, this proximity to the magic angle makes magnitude of the splitting very sensitive to small fluctuations in β and hence magnifies the smaller error associated with the measurement of this larger splitting.

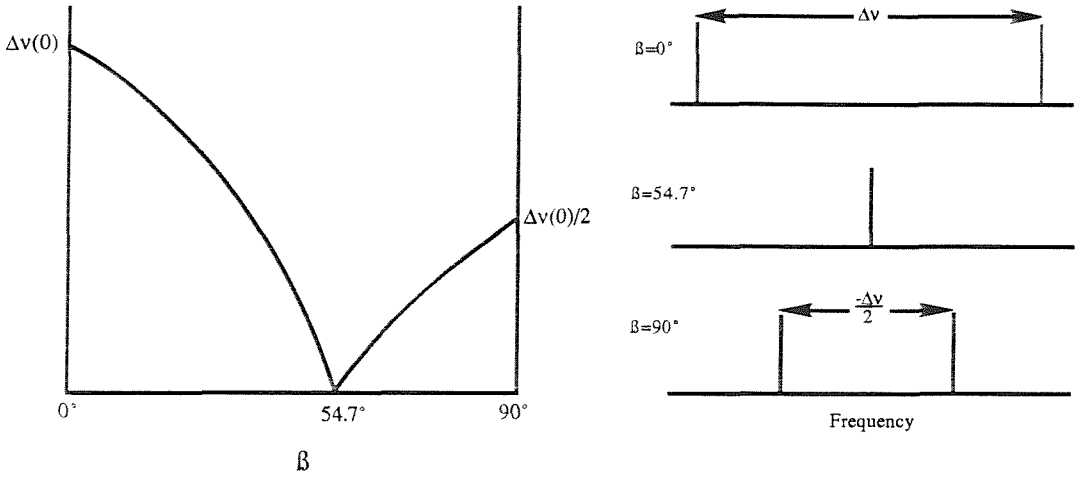

The quadrupolar splittings for the deuterons in this system, however, are by no means worthless and we now describe how valuable information can be gained from them.

The raw splitting data as taken directly from the NMR spectrometer can, via the calculations outlined in the introduction, be converted into the major and biaxial order parameters, S_{zz} and S_{xx}-S_{yy}, these, however, are directly proportional to the original splittings, hence a qualitative picture of the order within a system may be gained from a plot of the splitting data versus shifted temperature.

The quadrupolar splittings shown in figure 5 show some slightly unexpected results. Both sets of data for trimer 5 are greater than those for trimer 3 which is mirrored in the dipolar (hence major order parameter) results and predicted by theory. However, close to T_{NI} for both trimers the difference between the end and middle mesogenic groups is very small for trimer 3, and even the reverse of what is expected from theory and indeed experimentally shown in the dipolar results, for trimer 5. This situation is rectified somewhat as we go deeper into the nematic phase and approach the freezing point. As the temperature is lowered the quadrupolar splittings of the end groups increase at a greater rate than those of the middle groups in both trimers, to leave the end groups of trimer 5 at a slightly higher level than the middle group at the freezing point. The splitting for the end groups of trimer 3 attain a splitting some 2,000 Hz higher than that achieved by the middle group as the temperature is lowered. This is in accord with a decrease in energy causing the anisotropic forces of the molecules to induce a greater alignment of the cyanobiphenyl end groups. These splittings, although a little unexpected close to T_{NI} do produce, at least qualitatively, the same results as those predicted by theory and found experimentally through the dipolar splittings.

The quadrupolar splittings do not tell us much about the ordering within the sysem as they stand because they only give information on the ordering along the C-D bond direction. If we assume that the partially deuteriated phenyl ring rotates freely about the para axis of the mesogenic group and has C_{3v} rotational symmetry, the order parameters along the C-D bond direction and the para axis can now be related

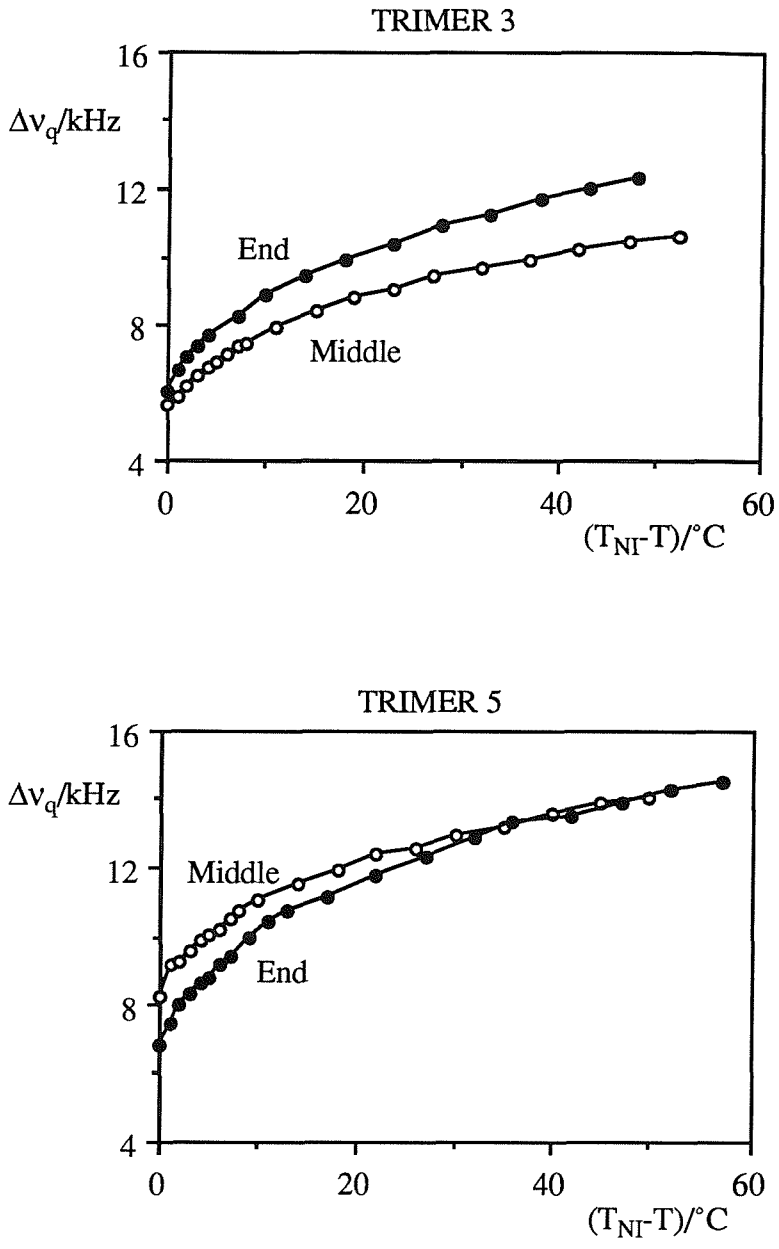

Figure 5. The dependence of the the quadrupolar splittings ($\Delta\nu_q$) of the end and middle mesogenic groups on the shifted temperature (T_{NI}-T) for both trimers.

by

$$S_{CD} = S_{zz}P_2(\cos\beta),$$

where β is the angle between the C-D bond and the para axis. As we know the angle β is expected to be very close to 60° and therefore we can crudely test our model by calculating the values of β from the experimental data of S_{CD} and S_{zz} and comparing them with 60°. We only expect the angles calculated in this way to approximate to 60° because we have not taken the biaxiality of the mesogenic groups into account. Figure 6 shows the values of calculated from S_{CD} and S_{zz} for the four trimers over the total mesogenic temperature range. It is seen that to a large extent the calculated values of are indeed very close to 60°.

We can utilise the quadrupolar splittings together with S_{zz} obtained from the dipolar splittings can be used to ontain the previously ignored molecular biaxiality by employing the equation,

$$\Delta\nu_q = (3/2)\langle q_{zz}\rangle + (1/2)(S_{xx}\text{-}S_{yy})(\langle q_{zz}\rangle))(\langle q_{xx}\rangle - \langle q_{yy}\rangle),$$

where <q> denotes the components of the quadrupolar tensor in the local frame averaged over the motion of the phenyl group. They are related to the principal components of the quadrupolar tensor by

$$\langle q_{xx}\rangle = q_{bb}\sin^2\gamma + q_{cc}\cos^2\gamma,$$
$$\langle q_{yy}\rangle = q_{aa}$$
$$\langle q_{zz}\rangle = q_{bb}\cos^2\gamma + q_{cc}\sin^2\gamma,$$

where a is orthogonal to the phenyl group, b is parallel to the C-D bond and γ is the angle between this and the Z axis, and $\gamma = 60°$, q_{aa} = -90.2 kHz, q_{bb} = 186 kHz and q_{cc}= -95.8 kHz.

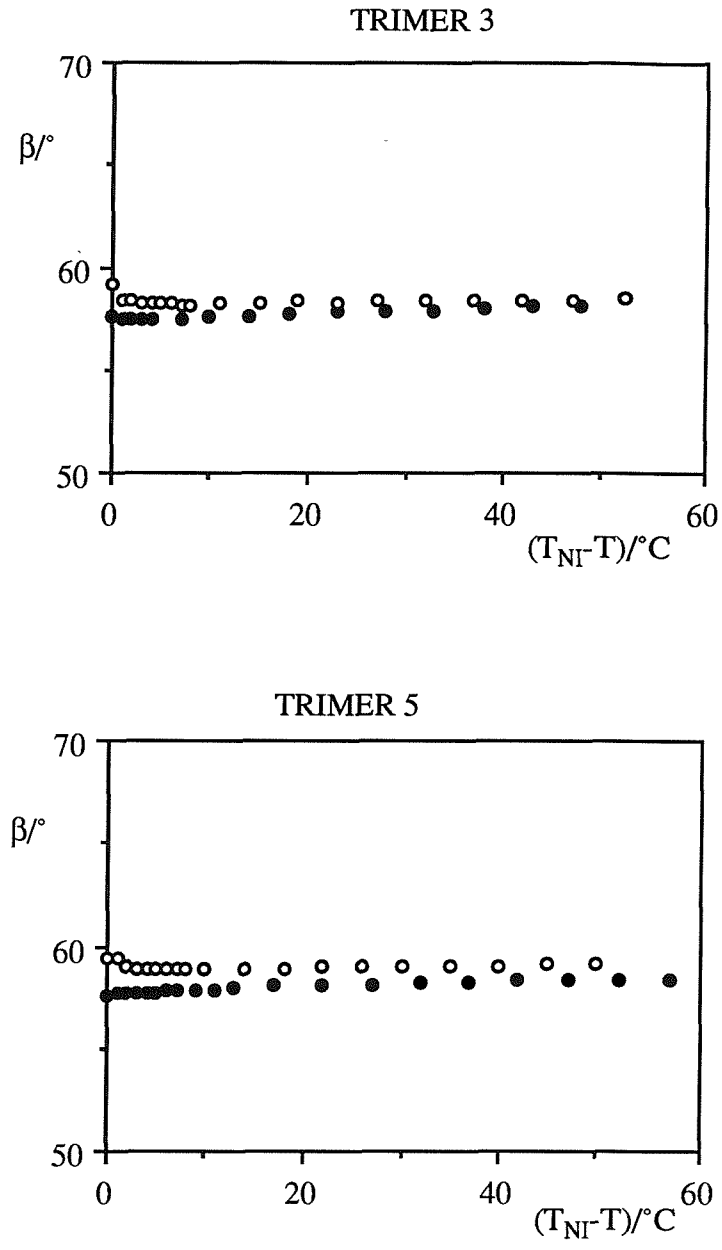

Figure 6. An approximation of the angle β for the end (●) and middle (O) mesogenic groups as a function of the shifted temperature (T_{NI}-T) for both trimers.

Figure 7 shows a plot of shifted temperature versus biaxiality (S_{xx}-S_{yy}), which here depends critically on the value of γ, for each of the trimers. It is seen that the end groups are more biaxial than the middle groups in both trimers and also that trimer 3 is more biaxial than trimer 5 overall. This result fits in with our general theory that the trimer 3 is an inherently less ordered system than trimer 5, i.e. the shorter chain length in trimer 3 has fewer degrees of freedom available to align the mesogenic groups in a minimum energy conformation together with the overall lower length to breadth ratio.

The biaxiality values are low, about 8% for the end groups, and approximately 9% for the middle groups. A low biaxiality for these mesogenic units does not necessarily mean a low average molecular biaxiality, especially for the odd membered trimers discussed here. This is because the biaxiality is measured with respect to a local axis system and is therefore a measure of the difference between the local x and y axes, which is small for a biphenyl group (especially a cyanobiphenyl group) relative to its length.

Figure 8 shows plots of the major order parameter, S_{zz}, versus the biaxiality, S_{xx}-S_{yy}, of each mesogenic unit for both trimers. The points do not lie on an ideal curve due to the experimental error but when extrapolated in the form of a parabola can be envisaged to pass through the origin and to reach a maximum as S_{zz}=0.5 which, by definition for a nematic, it must.

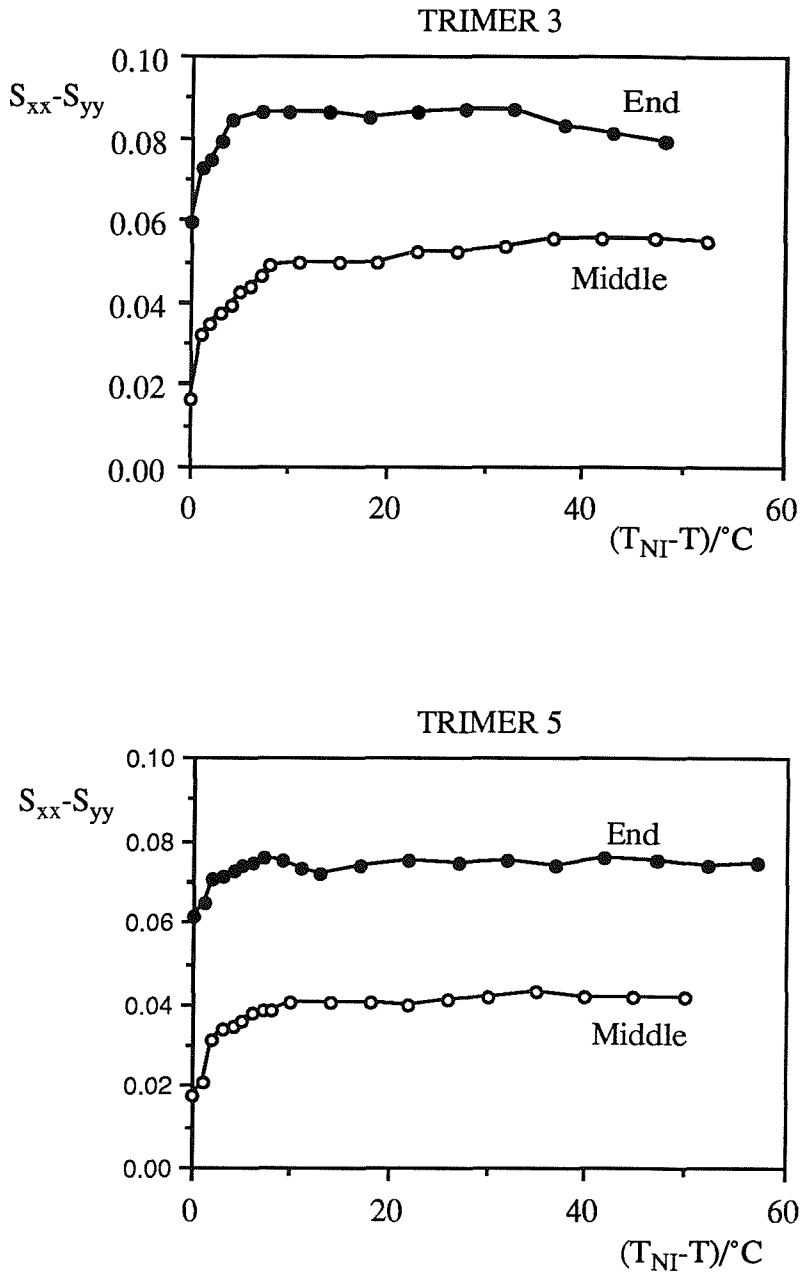

Figure 7. The dependence of the biaxial order parameters (S_{xx}-S_{yy}) of the end and middle mesogenic groups on the shifted temperature (T_{NI}-T) for both trimers.

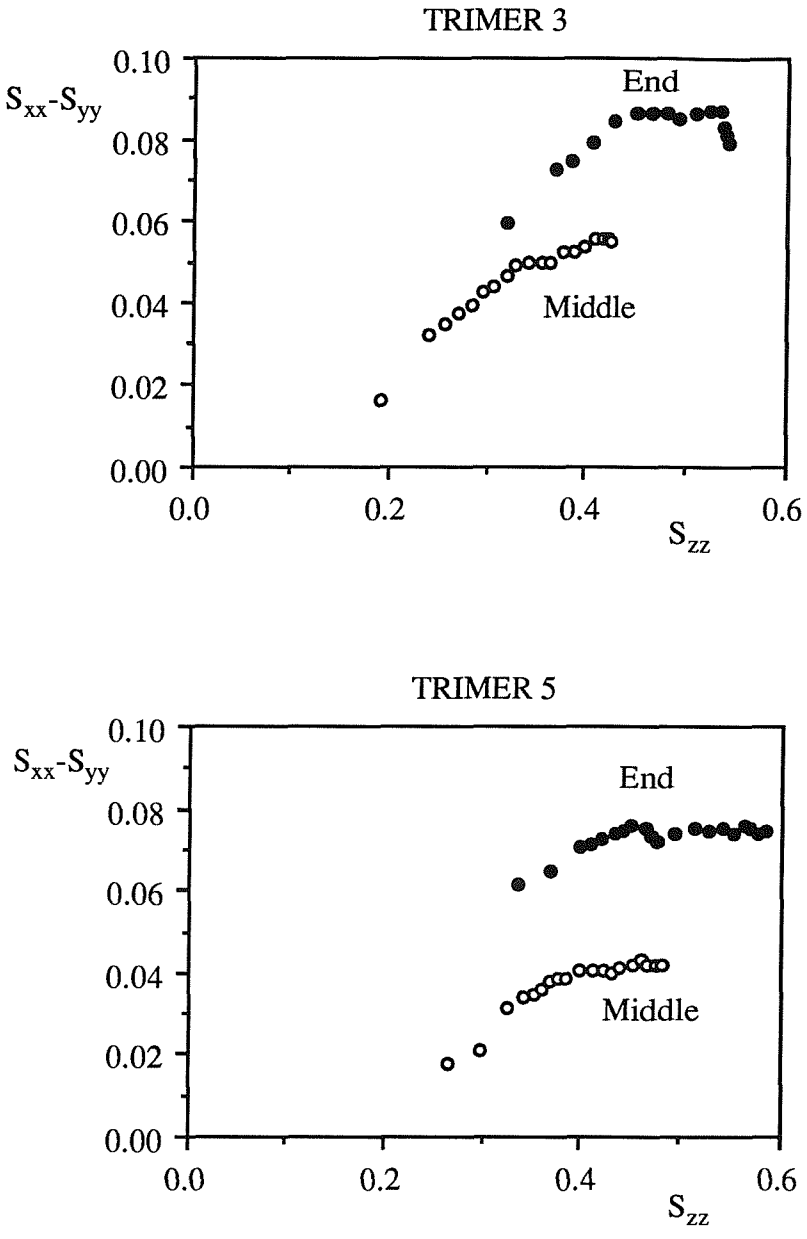

Figure 8. The variation of the biaxial order parameters (S_{xx}-S_{yy}) with the major order parameters (S_{zz}) for the end and middle mesogenic groups of both trimers.

5. Conclusions

The theory behind liquid cystalline oligomers developed initially by Marcelja and later improved by Emsley, Luckhurst and Stockley has been adapted by Emerson to specifically take account of trimers. This theory not only predicts the odd-even effect in the thermodynamic data but suggests that there exists a difference in the ordering of the middle and end mesogenic groups, more specifically for trimers with odd membered alkyl chain spacers whose mesogenic units cannot, for low energy conformations, simultaneously align in a parallel manner. This difference is predicted to become significant as the spacer length is decreased.

We have tested this theory with the aid of specific deuteriation techniques and NMR spectroscopy. In this Chapter we have described the synthesis of four trimers of alkyl chain lengths 3 and 5, chosen to show best the predicted difference between the order parameters mesogenic groups within these molecules, with deuterium incorporated into the end or middle mesogenic groups, and the subsequent determination of the order parameters of these groups. Deuterium NMR spectroscopy has has been used to measure the orientational properties of these two short-length trimers.

The experimental results show that the theory predicted trend, of the end mesogenic units to become more ordered than the middle as the length of the odd spacer is decreased, is followed but not to the same magnitude as the model suggests, hence we may conclude that where the theory seems to fail on a quantitative level it suceeds in predicting the order within trimers on a semi-qualitative scale.

References

[1] Marcelja S., 1974, *J. Chem. Phys.*, **60**, 3599.

[2] Emsley J.W., Luckhurst G.R. and Stockley C.P., 1981, *Molec. Phys.*, **44**, 565.

[3] Counsell C.J.R., 1983, *Ph.D. Thesis*, University of Southampton, U.K.

[4] Counsell C.R.J., Emsley J.W., Heaton N.J., Luckhurst G.R., 1985, *Molec. Phys.*, **54**, 847.

[5] Emsley J.W., Fung B.M., Heaton N.J., Luckhurst G.R., 1987, *J. Chem. Phys.*, **87**, 3099.

[6] Flory P.J.,1969, *Statistical Mechanics of Chain Molecules*, (Interscience).

[7] Emerson A.P.J., *Unpublished work*, The University of Southampton, U.K.

[8] Counsell C.R.J., Emsley J.W., Luckhurst G.R. and Sachdev H.S., 1988, *Mol. Phys.*, **63**, 33.

[9] Emsley J.W., Hamilton K., Luckhurst G.R., Sundholm F., Timimi B.A., Turner D.L.,1984, *Chem. Phys. Lett.*, **104**, 136.

[10] Fan S.M., 1992, *Ph.D Thesis*, Southampton University, U.K.

[11] Barnes P.J., 1991, *M.Phil. Thesis*, Southampton University, U.K.

CHAPTER 6

Non-symmetric trimers

1. Introduction

The liquid crystals termed trimers tend to fall into two categories:-

(i) Star-shaped, where three mesogenic groups are each attached through a flexible spacer chain to a central linking group that allows the mesogenic groups to lie in the corners of a triangular boundary [1].

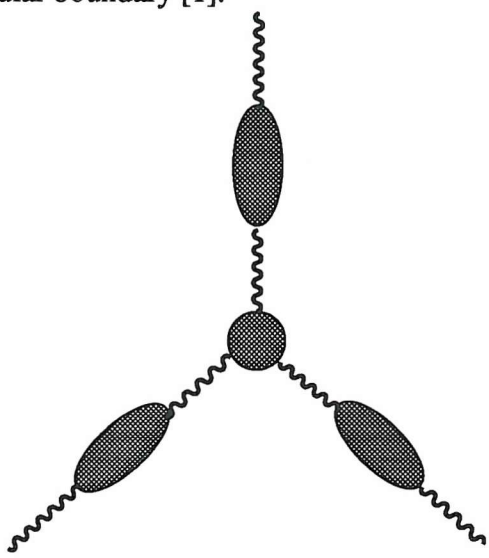

(ii) Linear, where three mesogenic groups are bound by two flexible linking chains in a continuous manner.

In effect a mesogen that contains three mesogenic groups connected through flexible spacers may be classed as a trimer.

In keeping with the rest of this Thesis, this Chapter will be concerned with the linear class of trimers. Symmetric trimers, a term that describes a molecule with three mesogenic units in which, if a bisecting line were drawn through the middle mesogenic group, both halves would superimpose and not necessarily one containing three identical mesogenic units have been previously reported.

Furuya et al.[2] synthesised four members of the trimeric 1,4-bis(ω-4,4'-cyanobiphenyloxyalkoxy)benzene series,

with n=4 to 8. They found some rather unexpected results. The members with even chain lengths gave a nematic phase but those of odd parity were not liquid crystalline. In these molecules the low axial ratio of the central phenyl unit was regarded as a part of the flexible spacer. They proposed that the number of methylene units between the terminal cyanobiphenyl units was 2n and therefore always even overall. Hence, enantiotropic compounds with a diminished odd-even effect were predicted since both terminal mesogenic groups could align in a parallel manner assuming a low energy conformation without drastically altering the length to breadth ratio. They prepared two members of the 1,4-bis(ω-4,4'-cyanobiphenyloxyalkoxy)-biphenyl series with n=5 and 6 for comparison. Both exhibited large enantiotropic phases and it was concluded that the central biphenyl unit was sufficiently anisotropic to take part in the formation of a mesophase. Attard and Imrie [3] proposed that the decreased liquid crystallinity of the compounds prepared by Furuya et al. containing a central phenyl ring was due to their high melting points rather than a low T_{NI}. They had synthesised a series of compounds that incorporated a lateral alkyl chain of variable length in the central phenyl unit. Such an addition to mesogens is known to lower melting points as well as changing T_{NI} and access hidden liquid crystal phases [4]. All of these compounds were observed to be nematic with additional smectic phases identified for shorter lateral chain lengths.

A complete series of the 1,4-bis(ω-4,4'-cyanobiphenyloxyalkoxy)-biphenyl class of trimers has been synthesised and characterised by Imrie[5] and theit orientational orders examined by Fan [6] and is also described elsewhere in this Thesis. They show an enhanced odd-even effect in both transitional temperatures and entropies in comparison with the analogous dimeric α,ω-bis(-4'-cyanobiphenyl-4-oxy)alkanes, see figure 1.

In a continuation of this trimeric theme this introduction introduces several novel classes of molecules that can be termed non-symmetric trimers, trimeric molecules loosely based on the symmetric 1,4-bis(ω-4,4'-cyanobiphenyloxyalkoxy)-biphenyls, in which the two halves either side of the mid-point in the molecule are inequivalent. We will then go on to study in greater detail the mesogenic behaviour of a class of trimers in which the non-symmetry is introduced by two different length flexible spacers in the same molecule.

We have synthesised some individual non-symmetric trimeric materials and noted the difference this has made to the transition temperatures by comparison with analogous symmetric trimers. The nature of the link between the flexible alkyl chain and the central aromatic group has been shown to be a non-trivial factor which affects the liquid crystal range of the trimer quite considerably. The replacement of an oxygen atom by a sulphur link into the centre of 1,4-bis(4-4,4'-cyanobiphenyloxybutyloxy)benzene reduces the liquid crystal range by 34°C.

T_{CN} 171°C T_{NI} 196°C

T_{CN} 164°C T_{NI} 233°C

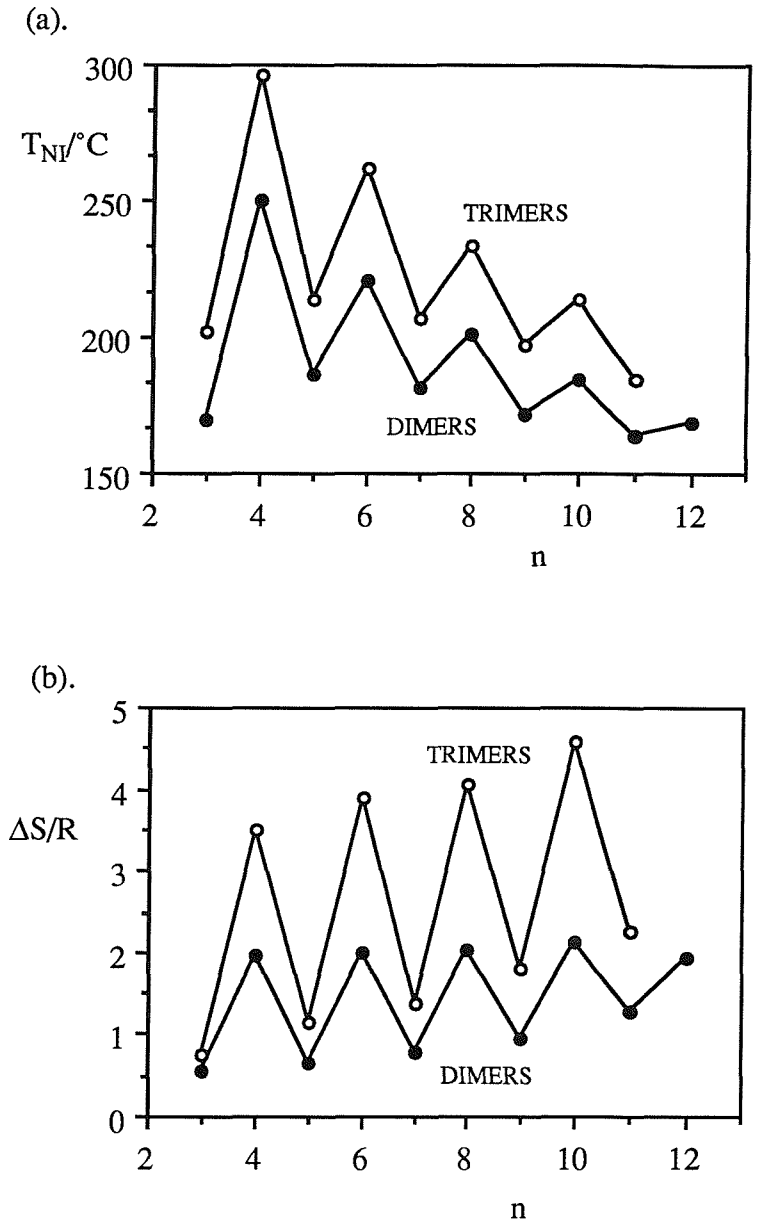

Figure 1. (a). The nematic-isotropic transition temperatures for the homologous 1,4-bis(ω-4,4'-cyanobiphenyloxyalkyloxy)-biphenyl series together with the values of the corresponding dimers and (b). The variation of entropy for the nematic-isotropic transition with n, the alkyl chain length, for the two series is also shown.

If the asymmetry is now incorporated into the end mesogenic group for example by replacing one of the terminal cyanobiphenyl groups in 1,4-bis(6-4,4'-cyanobiphenyloxyhexyloxy)-biphenyl with a cyanophenyl group the transition temperatures are intermediate to those of the centrally biphenyl linked and phenyl linked symmetric trimers of similar spacer length as might be expected. The nematic range is extended,

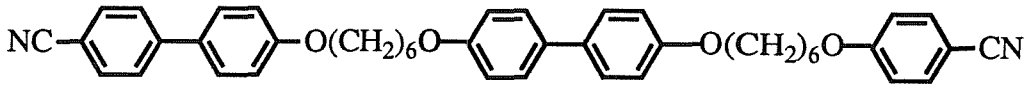

T_{CN} 186°C T_{NI} 230°C

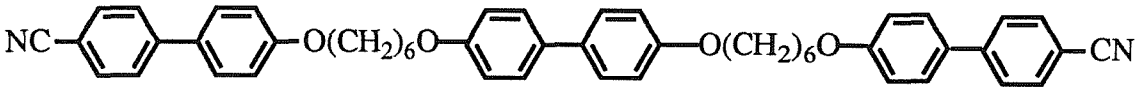

T_{CN} 215°C T_{NI} 257°C

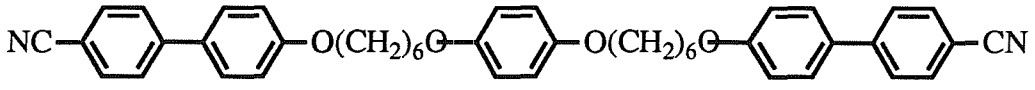

T_{CN} 150°C T_{NI} 192°C

This mesophase extension does not translate to the exchange of both terminal cyanobiphenyl groups for cyanophenyl units. Indeed 1,4-bis(6-4,4'-cyanophenyloxyhexyloxy)benzene is strongly monotropic

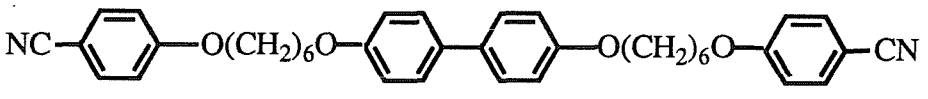

T_{CI} 170°C T_{IN} 144°C T_{NC} 138°C

The terminal cyano group has a profound effect upon the melting point and hence the mesogenicity. The substitution of one terminal cyano-group for a bromine atom raises the melting point by almost 70°C

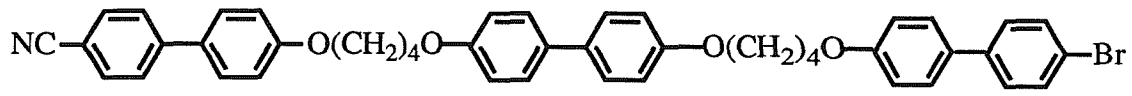

T_{CN} 282°C T_{NI} 291°C

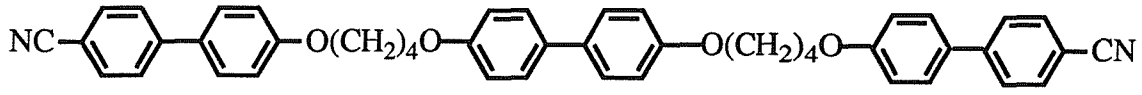

T_{CN} 215°C T_{NI} 294°C

The trimeric molecule can be made completely non-symmetric by the exchange of the terminal cyanoaromatic group for a Schiffs base group with a pendant alkyl chain. It was hoped that the cyanobiphenyl, Schiffs base and alkyl chain combination would produce a rich polymorphism [7] that tends to be lacking in liquid crystals containing purely cyanobiphenyl mesogenic units. Unfortunately only a nematic phase was observed.

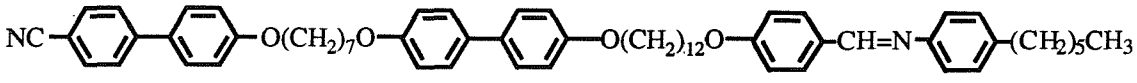

T_{CN} 156°C T_{NI} 187°C

This disappointing result coupled with the multistep chemistry needed to make this material led us back to the known symmetric cyanobiphenyl type trimers. In an attempt to pursue the role of the flexible spacer and the effect it has upon the mesogenic properties, a novel variant of the 4,4'-bis(ω-4,4'-cyanobiphenyloxyalkoxy)-biphenyls is the synthesis of non-symmetric trimers, where the mesogenic groups are connected through alkyl chains of differing length. These trimers might be expected to exhibit unusual liquid-crytstalline behaviour because the different chain lengths within each molecule could affect the intermolecular organisation of the mesophase. Four series have been produced, each series had one fixed length spacer, n, and one that varied from m=4 to 12 where n and m are the number of methylene units in the two chains.

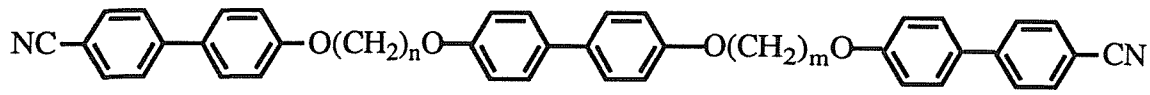

All compounds were found to form enantiotropic nematic phases, however, monotropic smectic A phases were observed on supercooling some of the trimers.

2. Experimental

The synthesis of the non-symmetric trimers required a route that could produce a product of known identity and high purity. A substantial amount of time was spent trying to exploit a synthetic route based on a boronic acid coupling technique which if successful could be expanded to include lateral chains and other groups in the central mesogenic unit. This process involved a multistage synthesis and, although eventually unsuccessful, it includes some chemistry useful to non-symmetric oligomer synthesis. Reaction scheme 1 illustrates the synthetic route to the non-symmetric trimers involving the boronic acid coupling technique.

Problems were encountered trying to form the grignard reagent necessary for the production of the boronic acid, this was attributed to low solubility and incomplete reaction of the reagents involved. The low yields from this stage of the process were all but lost in the cleavage of the benzyl protecting group. Analysis of the products from this stage revealed either no de-protection or the destruction of molecule depending on the concentration of HBr employed. This route was eventually abandoned in favour of the somewhat cruder but very successful biphenol method detailed in this section and in reaction sheme 2.

The synthetic route for the preparation of the non-symmetric trimers involves three steps; the reaction of 4-hydroxy-4'-cyanobiphenyl with an excess of an α,ω-dibromoalkane to produce the monomeric 4-cyano-4'-(ω-bromoalkoxy)biphenyl. This in turn was reacted with excess biphenol to produce the dimeric α-(4-cyanobiphenyl-

Reaction Scheme 1

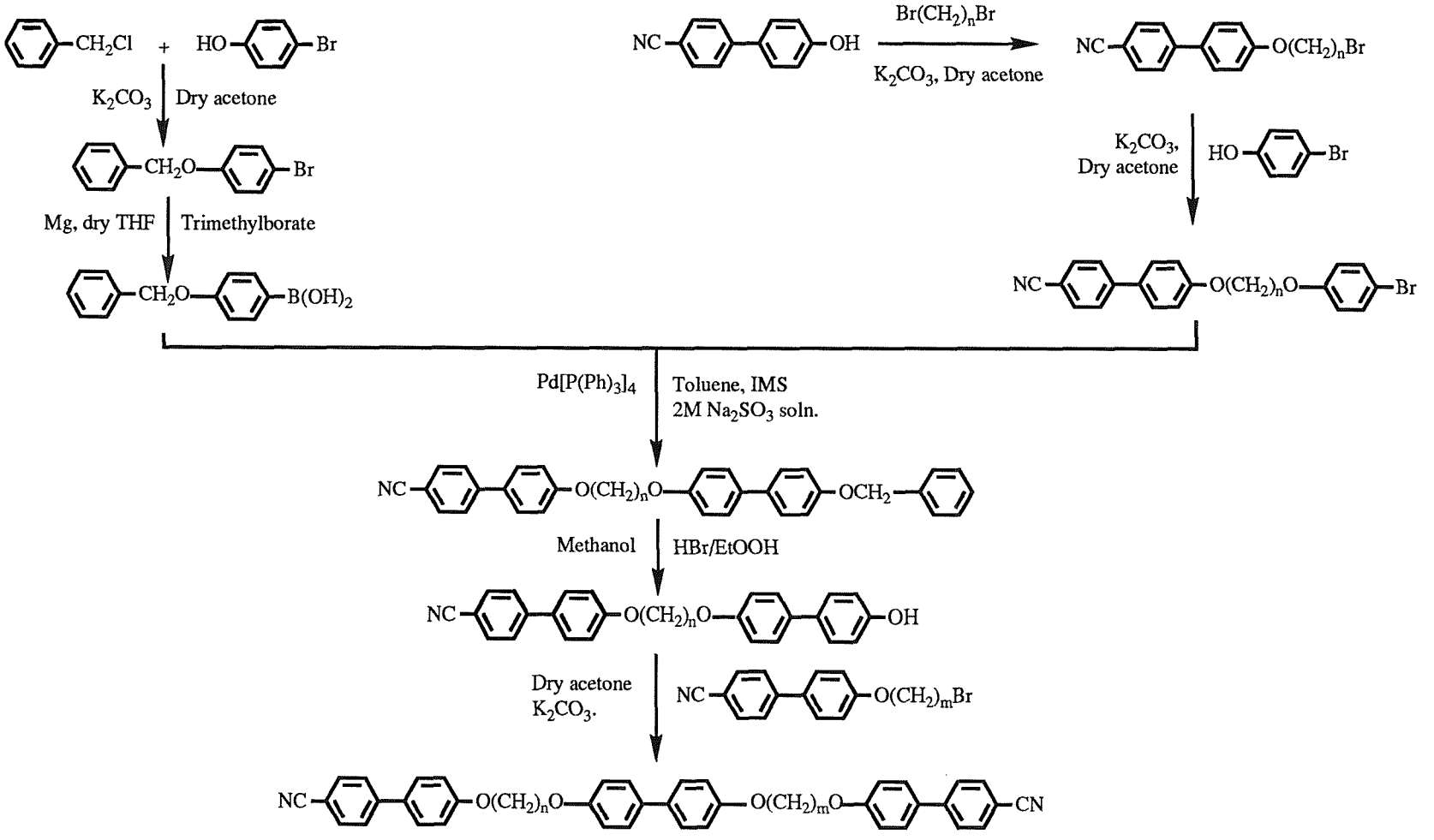

4'-oxy)-ω-(4,-hydroxybiphenyl-4'-oxy)alkane. From the reaction of a specific monomer with a dimer we were able to produce four consecutive series of non-symmetric trimers. In this section we detail the synthesis of the 4,5 trimer, however, the same basic procedure was used for the manufacture of all trimers.

2.1 Synthesis of [1,-(ω-4,4'-cyanobiphenyloxybutyloxy)-4-(ω-4,4'-cyanobiphenyloxypentyloxy)]-biphenyl.

Synthesis of 4-bromo-n-butyloxy-4'-cyanobiphenyl

4-hydroxy-4'-cyanobiphenyl (15g, 1 equiv.) was dissolved in dry acetone to which 1,4-dibromobutane (166g, 10 equiv. to minimise dimerisation) and anhydrous potassium carbonate (K_2CO_3,80g, 7.25 equiv.) were added. The mixture was stirred under reflux for 18 h. The mixture was filtered hot and the residual inorganics rinsed with hot acetone. The acetone was removed under reduced pressure The excess 1,4-dibromobutane was distilled off under vacuum and the crude 4-bromo-n-butyloxy-4'-cyanobiphenyl was recrystallised from ethanol and dried. Yield 85%.

IR υ cm-1 Loss of OH peak.
1HNMR ($CDCl_3$, δ) 1.8-2.2 (2H, m), 3.4-3.6 (1H, t), 3.9-4.1 (1,H, t), 6.9-7.1 (1H, m), 7.4-7.8 (3H, m) ppm.

Synthesis of 1-(4-cyanobiphenyl-4'-oxy)-4-(4,-hydroxybiphenyl-4'-oxy)butane

4-bromo-n-butyloxy-4'-cyanobiphenyl (15g, 1 equiv.) together with biphenol (42g, 5 equiv.) were dissolved in ethanol (200ml.) made alkaline by the addition of potassium hydroxide (1g). K_2CO_3 (31g, 5 eqiuv.) was added. This mixture was stirred under reflux for 18 h.The reaction mixture was filtered hot and the solids were washed with hot ethanol (100ml) and hot, dilute potassium hydroxide solution (100ml.) to remove

any unreacted 4-bromo-n-butyloxy-4'-cyanobiphenyl and biphenol. The solids were then added to water (400ml) acidified with hydrochloric acid (10ml). This served to dissolve the K_2CO_3 and so leave the crude 1-(4-cyanobiphenyl-4'-oxy)-4-(4,-hydroxybiphenyl-4'-oxy)butane as a solid. This was filtered off and dried. The product was recrystallised twice from toluene (100ml) which was filtered hot to remove any undissolved symmetric trimer biproduct to leave pure 1-(4-cyanobiphenyl-4'-oxy)-4-(4,-hydroxybiphenyl-4'-oxy)butane in 50% yield.

IR; υ 3500-3100 cm^{-1} OH peak.

^1H NMR ($CDCl_3$, δ) 1.8-2.1 (t, 2H), 3.9-4.3 (t, 2H), 6.9-7.7 (m, 4H).

Transition temperatures of the α-(4-cyanobiphenyl-4'-oxy)-ω-(4,-hydroxybiphenyl-4'-oxy)alkanes.

n	T_{CI}/°C	T_{IN}/°C	T_{NC}/°C
4	262	256	236
5	197	181	172
6	238	228	215
7	193	159	145

Synthesis of [1,-(ω-4,4'-cyanobiphenyloxybutyloxy)-4-(ω-4,4'-cyanobiphenyloxypentyloxy)]-biphenyl.

1-(4-cyanobiphenyl-4'-oxy)-4-(4,-hydroxybiphenyl-4'-oxy)butane (0.5g, 1 equiv.) and 4-bromo-n-pentyl-4'-cyanobiphenyl (0.3g, 1.1 equiv.)were dissolved in dry dimethyl formamide (20ml) to which K_2CO_3 (0.8g, 5 equiv.) was added. This was stirred under

reflux for 5h. After cooling the reaction mixture was added to water and the precipitate was filtered off and dried. Recystallisation from toluene left the pure trimer product in typically 70% yield.

IR; υ cm^{-1} loss of OH peak.

^1H NMR; ($CDCl_3$, δ), 1.87-1.97 (3H, m), 2.01-2.10 (2H, m), 4.03-4.17 (4H, m), 6.93-7.05 (4H, m), 7.45-7.60 (4H, m), 7.63-7.73 (4H, m) ppm.

MS (EI 70eV); 698 (M+, 18%), 434, 194 (100%).

Elemental analysis of the two equivalent non-symmetric trimers made by different routes show satisfactory results. The results for two symmetric trimers made via the route detailed are shown for comparison. Calculated values are given in parentheses.

Compound	C	N
4,5	81.12% (80.77%)	4.07% (4.01%)
4,4	80.57% (80.68%)	4.12% (4.09%)
5,4	81.22% (80.77%)	4.04% (4.01%)
5,5	81.35% (80.87%)	4.00% (3.93%)

Reaction Scheme 2

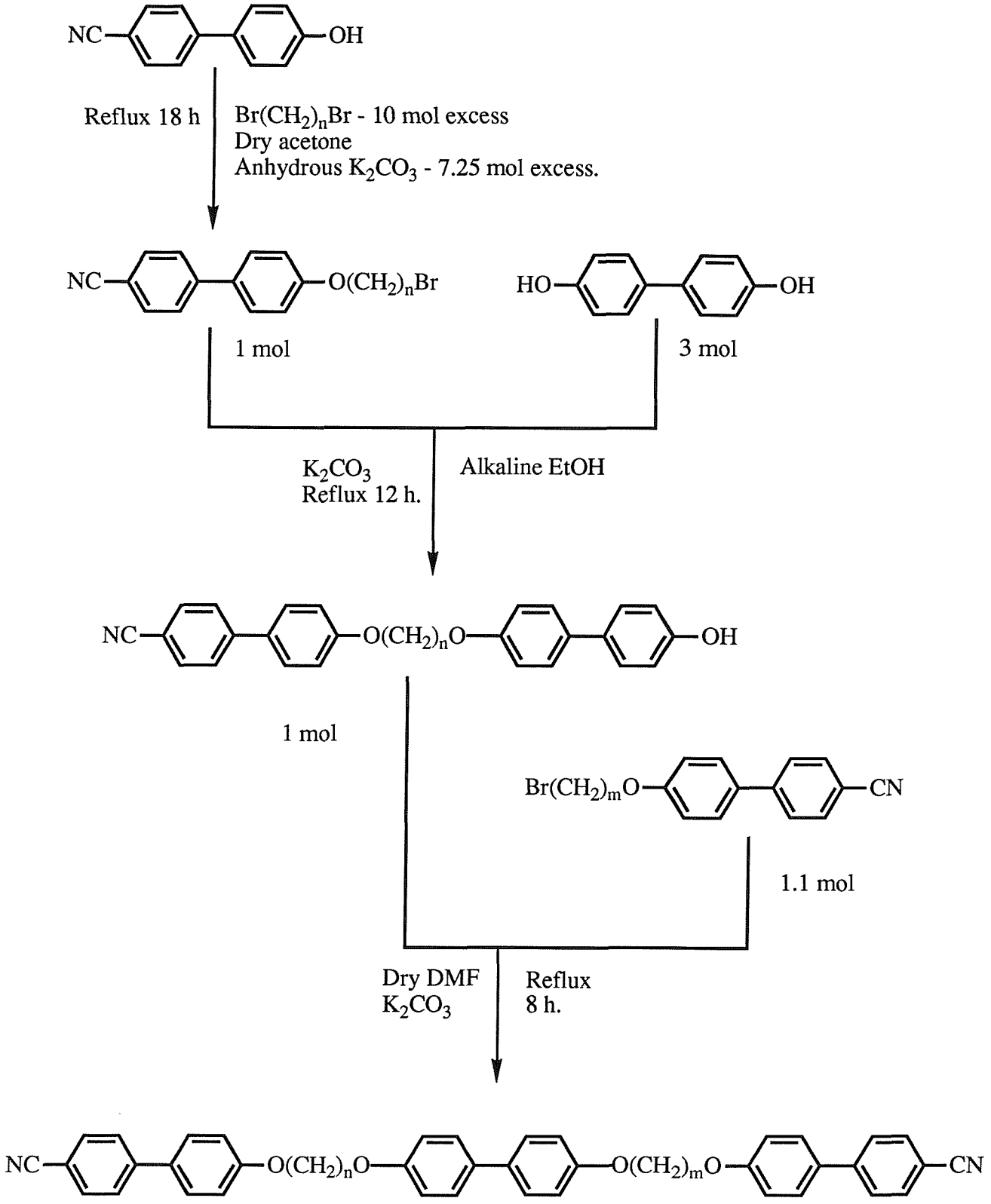

3. Results and Discussion

The transitional properties of the four homologous series abbreviated to CB*n*B*m* CB are given in tables 1 to 4. Phase identifications were performed from optical textures viewed through a polarising microscope. Nematic textures were assigned from their schlieren and homeotropic textures which flashed when subjected to mechanical stress. A typical nematic schlieren texture is shown in plate 1. Smectic A phases have been assigned from optical textures in which regions of focal conic fan and homeotropic patterns coexist, an example of the focal conic texture is shown in plate 2. Confirmation of these monotropic smectic A phases with X-ray diffraction was not possible due to their transient monotropic nature.

Each series exhibits a classical odd-even effect in both the nematic-isotropic transition temperatures and the entropies of transition which attenuates as *m* increases. In addition the whole of each series alternates in a regular fashion as *n*, the fixed length term increases. This is concisely portrayed in figures 2 and 3 which depict each series as a cluster of increasing *m* and *n* . The dotted line on both graphs joins the point in each series that represents the analogous symmetric trimer i.e. where $n = m$. These four points for the symmetric trimers lie completely in in accord within each series which indicates that the ordering within the phase is not unduly affected when the two alkyl chains joining the mesogenic groups are dissimilar. The odd-even alternation in each series is approximately half that of the symmetric trimeric series in both T_{NI} and $\Delta S/R$. This reduced alternation is comparable with the odd-even effect exhibited by the α,ω-bis(4'-cyanobiphenyl-4-yloxy)-alkanes.

Another way of presenting the results is if we now sum the number of methylene units in each trimer (i.e $n+m=X$), and select those values of *X* that are common to each series and compare them we see some interesting trends.

These data are listed in table 5 and plotted in figures 4 and 5. It is seen that T_{NI} and $\Delta S/R$ alternate in a regular manner as each column is descended i.e as the chains n and

FOUR				
m	T_{CN}/°C	T_{NI}/°C	$\Delta S_{CN}/R$	$\Delta S_{NI}/R$
4	215	294	12.03	3.50
5	187	257	10.40	2.20
6	212	278	10.77	3.48
7	167	253	12.11	2.86
8	174	260	16.13	3.83
9	160	243	14.28	3.12
10	170	246	18.56	4.10
11	155	233	18.43	3.20
12	167	238	19.28	4.26

Table 1. Transitional data for the *4,m* series.

FIVE					
m	T_{CN}/°C	T_{NI}/°C	T_{NSA}/°C	$\Delta S_{CN}/R$	$\Delta S_{NI}/R$
4	187	257	-	12.03	2.20
5	161	212	-	11.16	1.11
6	154	233	-	13.09	2.21
7	135	207	-	13.51	1.18
8	172	220	-	13.86	2.21
9	141	202	(119)	14.85	1.20
10	148	205	-	15.20	2.26
11	130	193	(116)	15.29	1.34
12	109	196	-	16.07	2.20

Table 2. Transitional data for the *5,m* series. ( ) represents a monotropic transition.

SIX					
m	T_{CN}/°C	T_{NI}/°C	T_{NSA}/°C	$\Delta S_{CN}/R$	$\Delta S_{NI}/R$
4	212	278	-	10.77	3.48
5	154	234	-	13.09	2.21
6	215	257	-	14.15	3.44
7	178	232	(145)	12.07	2.67
8	193	244	(169)	13.42	3.61
9	140	220	(130)	14.12	2.80
10	182	231	(150)	16.62	3.76
11	151	217	-	16.08	2.90
12	196	223	-	14.37	3.89

Table 3. Transitional data for the *6,m* series. ( ) indicate a monotropic transition.

SEVEN					
m	T_{CN}/°C	T_{NI}/°C	T_{NSA}/°C	$\Delta S_{CN}/R$	$\Delta S_{NI}/R$
4	167	253	-	12.11	2.86
5	135	207	-	12.60	1.18
6	178	232	-	12.07	2.67
7	164	204	-	12.89	1.38
8	175	219	(149)	12.39	2.60
9	130	196	-	14.02	1.61
10	138	200	-	13.61	2.80
11	123	188	-	16.27	1.58
12	125	190	-	15.73	2.60

Table 4. transitional data for the *7,m* series. ( ) indicates a monotropic transition.

Transition temperatures are ±1°C, enthalpies and entropies of transition ±5%.

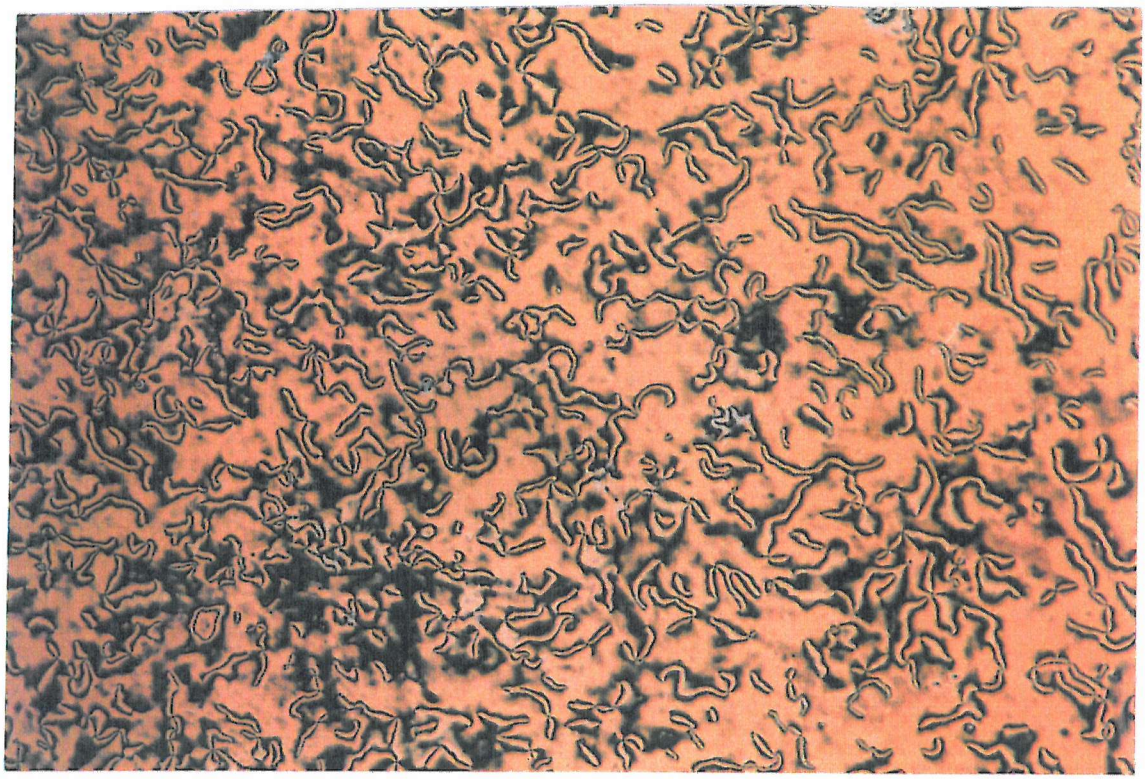

Plate 1. The schlieren texture of the nematic phase of trimer *6,9* at 200°C. Magnification x100.

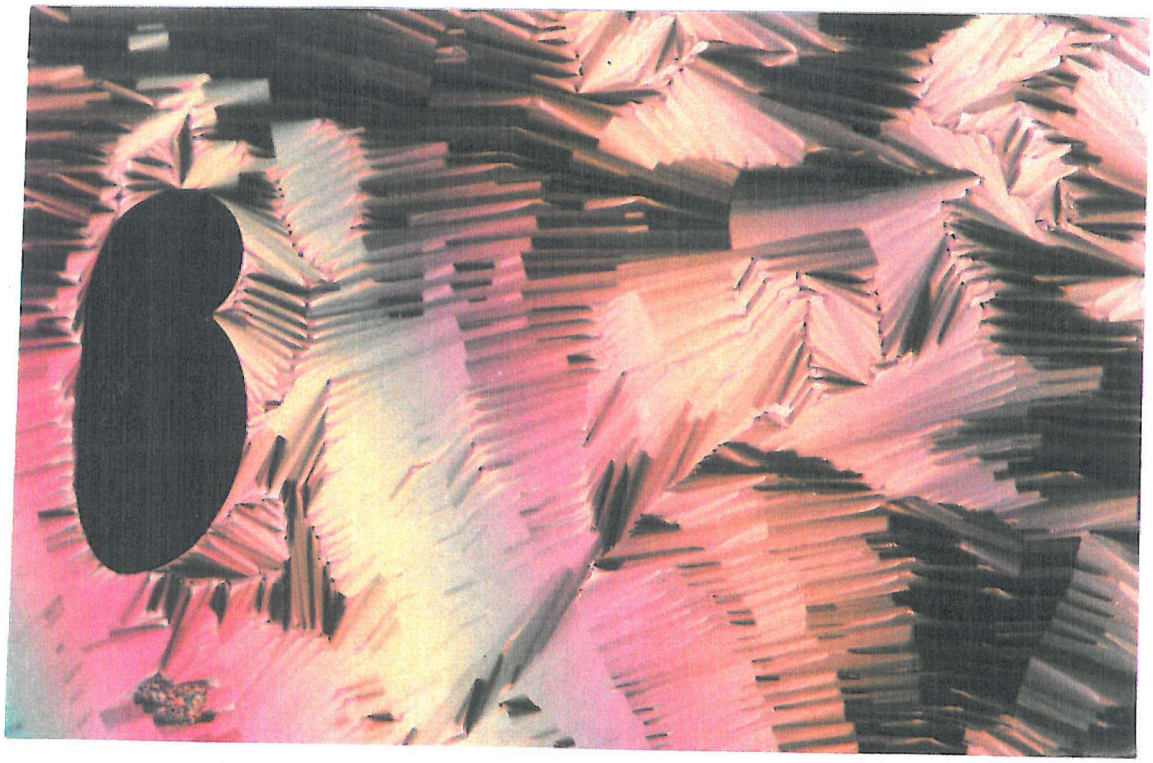

Plate 2. The focal conic fan texture of the monotropic smectic A phase of trimer *6,9* at 128°C. Magnification x100.

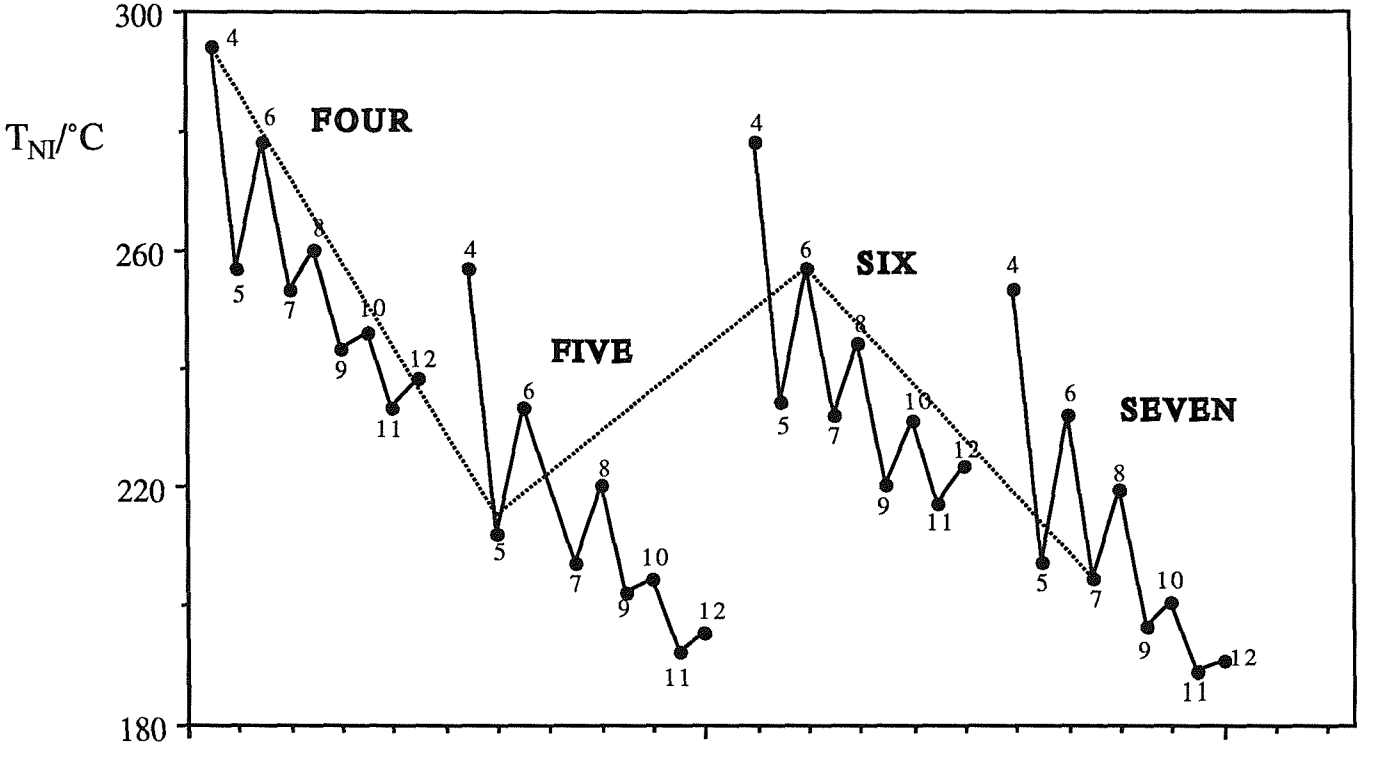

Figure 2. The variation of the nematic-isotropic transition temperatures for the non-symmetric trimers with the number of units in the spacer chains *n* and *m*.

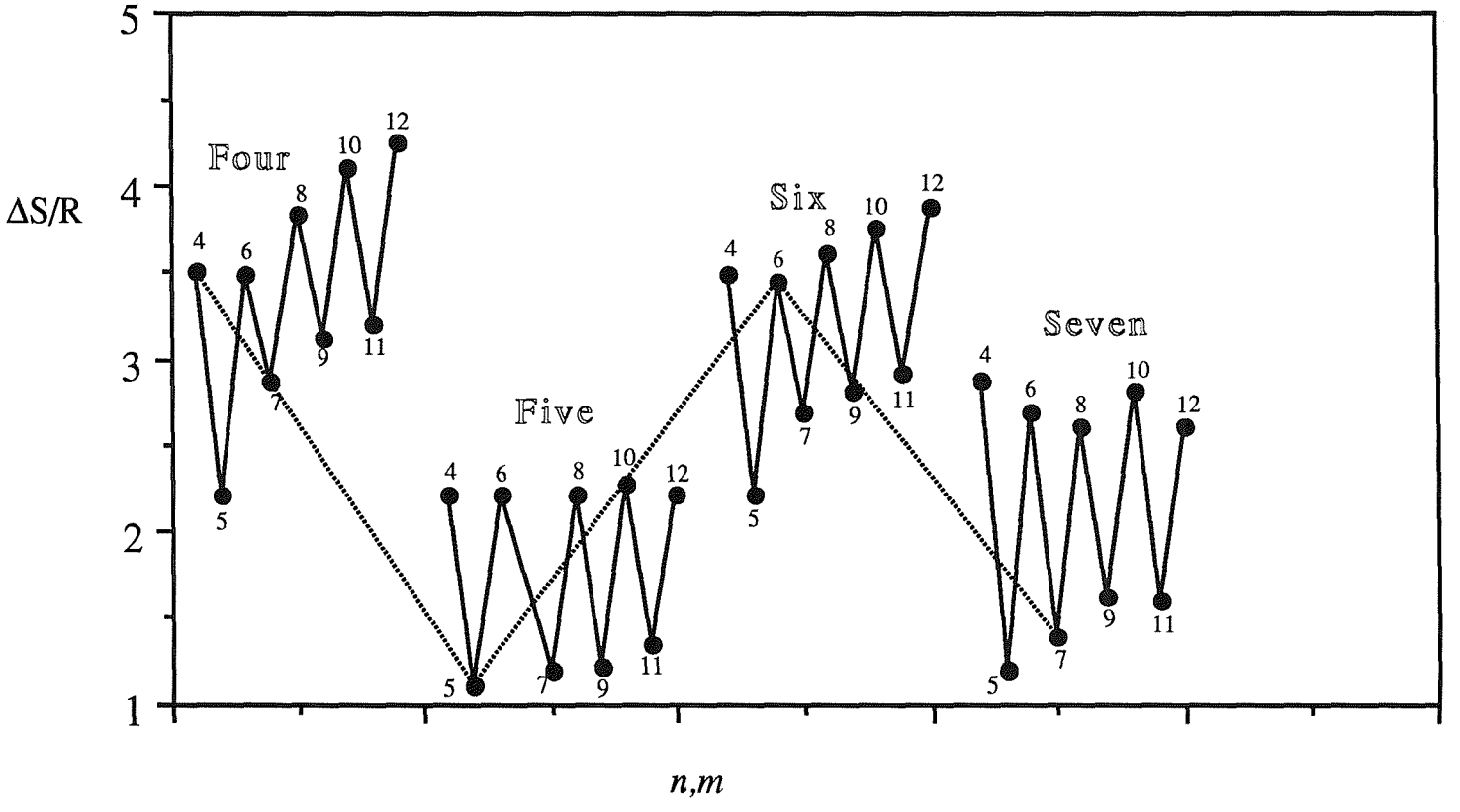

Figure 3. The dependence of the entropy change at the nematic-isotropic transition , $\Delta S_{NI}/R$, for the non-symmetric trimers on the number of methylene units in the spacer chains *n* and *m*..

Table 5. Nematic-isotropic transition data taken from tables 1 to 4 that represent the total number of methylene units, *X*, in the non-symmetric trimers as 14, 15 and 16.

X=14	T_{NI}/°C	$\Delta S_{NI}/R$	*X*=15	T_{NI}/°C	$\Delta S_{NI}/R$	*X*=16	T_{NI}/°C	$\Delta S_{NI}/R$
4,10	246	4.1	*4,11*	233	3.2	*4,12*	238	4.26
5,9	202	1.2	*5,10*	205	2.26	*5,11*	193	1.34
6,8	244	3.61	*6,9*	220	2.8	*6,10*	232	3.76
7,7	204	1.38	*7,8*	219	2.6	*7,9*	196	1.61
						8,8†	235†	4.06†

† represents data from Imrie [5].

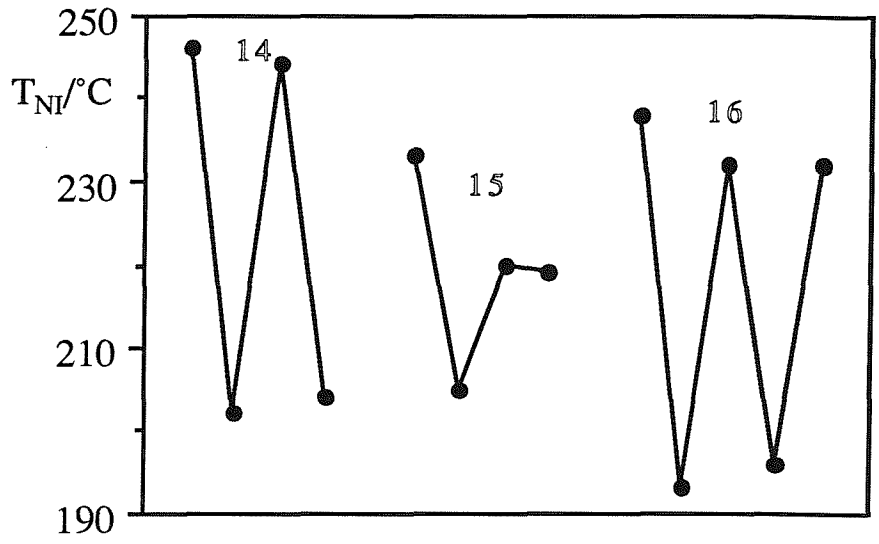

Figure 4. The variation of the nematic-isotropic transition temperatures with the total number of methylene units in the spacer chains for the trimers whose sum of units = 14,15 and16.

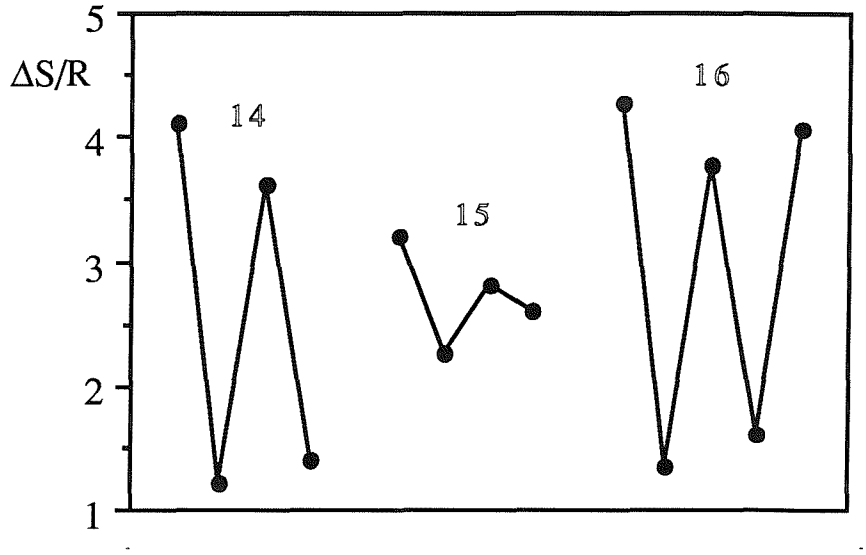

Figure 5. The dependence of the nematic-isotropic transition entropy on the total number of methylene units in the spacer chains for the trimers whose sum of units = 14,15 and16.

m become more similar in length. For X_{even} the largest values of T_{NI} and $\Delta S/R$ are observed for the trimers in which both *n* and *m* are even which enables all three mesogenic groups to align parallel with one another at least in the all trans configuration. Where *n* and *m* are are both odd, only the two terminal mesogenic groups can align with respect to a common direction. This is reflected in the lower values of T_{NI} and $\Delta S/R$. It is interesting to note that for X_{even} the trimers of the same overall length , for example *4,10* and *6,8*, have very similar nematic-isotropic transition temperatures of 246°C and 244°C respectively, and likewise for X_{odd}, see *5,9* and *7,7* whose T_{NI}s are 202°C and 204°C. This is contrast to the trimers of odd overall length i.e. *X*=15, where each of the trimers contain an odd and an even spacer. Here the clearing points lie intermediate to the overall even trimers and converge to 219°C - the nematic-isotropic transition temperature of *7,8*. In this column *7,8* is the trimer whose constituent alkyl chains are the most similar in length. These trends are reflected in the nematic-isotropic transitional entropy data. This presentation of the data suggests that the inclusion of one even length spacer in the trimer significantly raises the nematic-isotropic transition temperatures. Such a scenario permits a terminal and the central mesogenic groups to align to a common direction, while the remaining terminal group lies at an angle to both. These interesting conclusions are perhaps not that unexpected, it might be predicted that a trimer consisting of one odd and one even spacer would exhibit transitional properties intermediate to consecutive trimers containing two spacers of the same parity. For example

n,m	T_{NI}/°C	$\Delta S_{NI}/R$
4,4	294	3.50
4,5	255	2.20
5,5	212	1.11

However it was stated earlier that for trimers of the type n_{odd},m_{even} or vice versa, and n_{odd},m_{odd}, two of the three mesogenic groups are able to align to the same extent to the director.

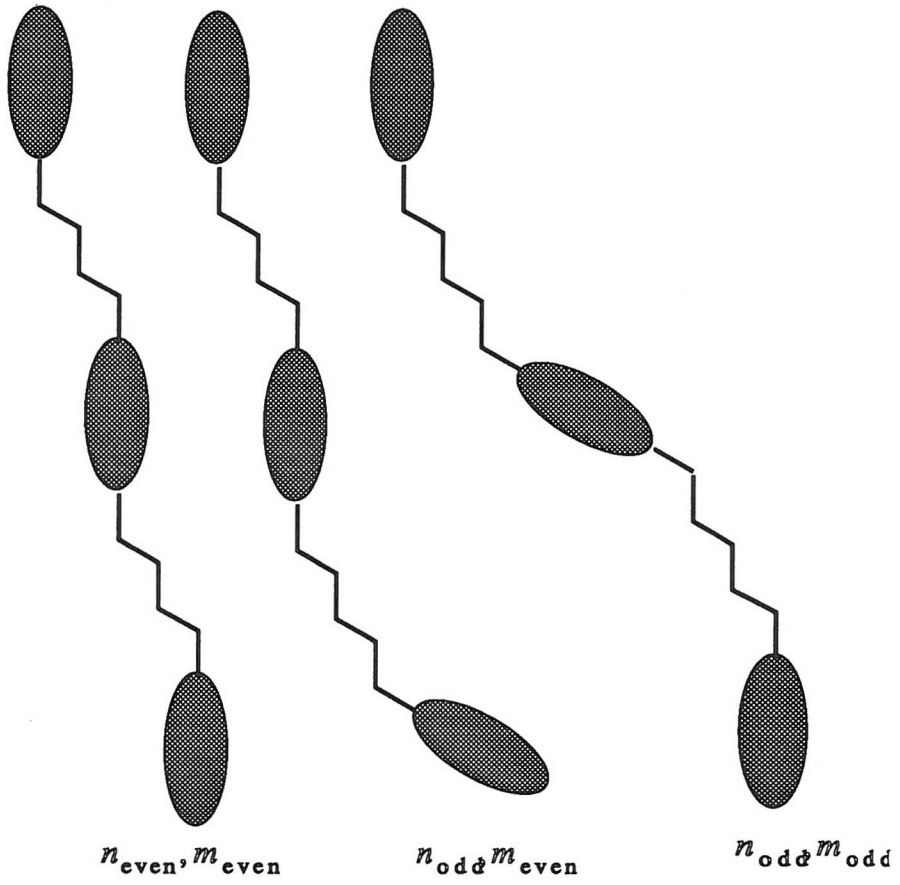

In trimers that consist of two odd spacers, however, the molecular biaxiality is substantially increased. For this reason the transitional data are lower.

The transitional data detailed in this results section illustrate the the regular odd-even trends often resolved for oligomeric and polymeric mesogens. The precise nature of the origin of this effect, however, is often interpreted by geometry and on packing efficiency. Theoretical simulations of dimeric liquid crystals have attained good agreement with experiment [8], this success does not, however, elucidate the physical origins of the unusual transitional behaviour of liquid crystal dimers and, by extrapolation, liquid crystal trimers. The idealised all-trans state of the alkyl chain is

clearly unrepresentative of a real molecule because of the many additional conformations resulting from possible gauche links. Current computational restrictions do not allow an unbiased simulation of the seemingly infinite amount of conformational and orientational freedom experienced by real molecules in a macroscopic sample. The simulation of true liquid crystal behaviour is therefore necessarily restricted to the presumption and exclusion of many conformations.

Ferrarini et. al. [9] have attempted to solve this problem by concentrating on the inclination of the mesogenic groups. They have realised that however many conformations the linking alkyl chain can adopt, tetrahedral symmetry of the alkyl chain dictates that, in both odd and even dimers, the mesogenic groups will always lie either parallel or bent with respect to one another. It is only the relative populations of these two states that controls the transition temperatures and strength of transition. The population of linear conformers is a minor percentage of the conformers as a whole for both odd and even dimers in the isotropic phase but is lowest for the odd dimer. On average, the linear conformers of an even dimer possess a higher internal energy than the bent conformer, this situation is reversed for odd dimers. The onset of long range orientational order required by a nematic phase increases the concentration of the linear component and this is reflected in the high transition temperatures and strength of transition exhibited by dimers with even spacers. For dimers with odd spacers, the concentration of linear conformers in the isotropic phase is below a critical concentration which no longer allows the interchange from bent to linear to occur. For this reason odd dimers have lower transition temperatures, because bent conformers depress T_{NI}, and entropies of transition than their even counterparts. Although this theory has been developed for dimers the qualitative trends are expected to remain for trimers.

Emerson [10] has conducted some preliminary simulation work on trimeric liquid crystals of a similar non-symmetric genus as those detailed in the mainstay of this chapter. The chain lengths of these are short because the large number of conformers requires a large amount of computational time, however, the basic trends can be related

to our empirical results. In this theoretical study the nature of the units in the spacer chains were identical with tetrahedral symmetry effectively eliminating the ether links present in the experimental trimers.The initial links were, however, set at trans allowing a comparison with experimental results to be made. The absolute lengths of the fixed length chains varied from 1 to 3 methylene units, and the variable chain from 4 to 10 methylene units. Because the naming system of our experimental results counts only the number of methylene units and ignores the ether linkages, the theoretical trimers will be referred to as n^*,m^* , where in terms of absolute length n^*,m^* is effectively equivalent to *n-2,m-2*. The scaled nematic-isotropic transition temperatures and transitional entropies are given in tables 6 to 8 and graphically represented in figures 6 and 7. From these theoretical data, it is seen that the trends observed for trimers whose spacers both contain more than one link are qualitatively similar to our experimental results. The trimer series 1^*, m^*whose fixed length consists of one linking unit exhibits a reversed parity effect. In both the scaled T_{NI} and values of $\Delta S/R$ the largest values are obtained when the length of the variable chain is odd. This apparent paradox can perhaps be rationalised if we relate some simple sketches to the Luckhurst odd-even effect proposal.

The mesogenic unit-single link- mesogenic unit structure in the 'fixed' half of the $1^*,m^*$ trimer can only adopt a bent configuration even in the isotropic phase unlike the odd dimers described in Ferrarinis' theory. This conformational restriction coupled with the close proximity of the end and the middle mesogenic groups to one another permits us to perceive the fixed half of this trimer series as one large, rather inefficient, mesogenic group. Now effectively a dimer, the long axis of this slightly skew 'new group' aligns in a more linear manner with the other when the parity of the variable spacer is odd rather than even. For this reason we see an apparently reversed odd-even effect, with the weaker, simulated transitional data resembling more a dimer than a trimer. This idea is sketched in figure 8.

Theoretical $1^*,m^*$ series		
m^*	T_{NI}	$\Delta S/R$
3	0.1934	0.384
4	0.1607	0.351
5	0.1773	0.622
6	0.1597	0.485
7	0.1688	0.181
8	0.1585	0.634
9	0.1633	0.966
10	0.1569	0.784

Table 6. Theoretical nematic-isotropic transition data for the $1^*,m^*$ series.

Theoretical $2^*,m^*$ series.		
m^*	T_{NI}	$\Delta S/R$
3	0.1957	1.270
4	0.2850	2.493
5	0.2132	1.806
6	0.2644	2.977
7	0.2200	2.121
8	0.2504	3.297
9	0.2218	2.410
10	0.2398	3.513

Table 7. Theoretical nematic-isotropic transition data for the $2^*,m^*$ series.

Theoretical $3^*,m^*$ series		
m^*	T_{NI}	$\Delta S/R$
4	0.1841	1.966
5	0.1732	1.121
6	0.1778	2.236
7	0.1703	1.422
8	0.1733	2.390
9	0.1679	1.701
10	0.1695	2.523

Table 8. Theoretical nematic-isotropic transition data for the $3^*,m^*$ series.

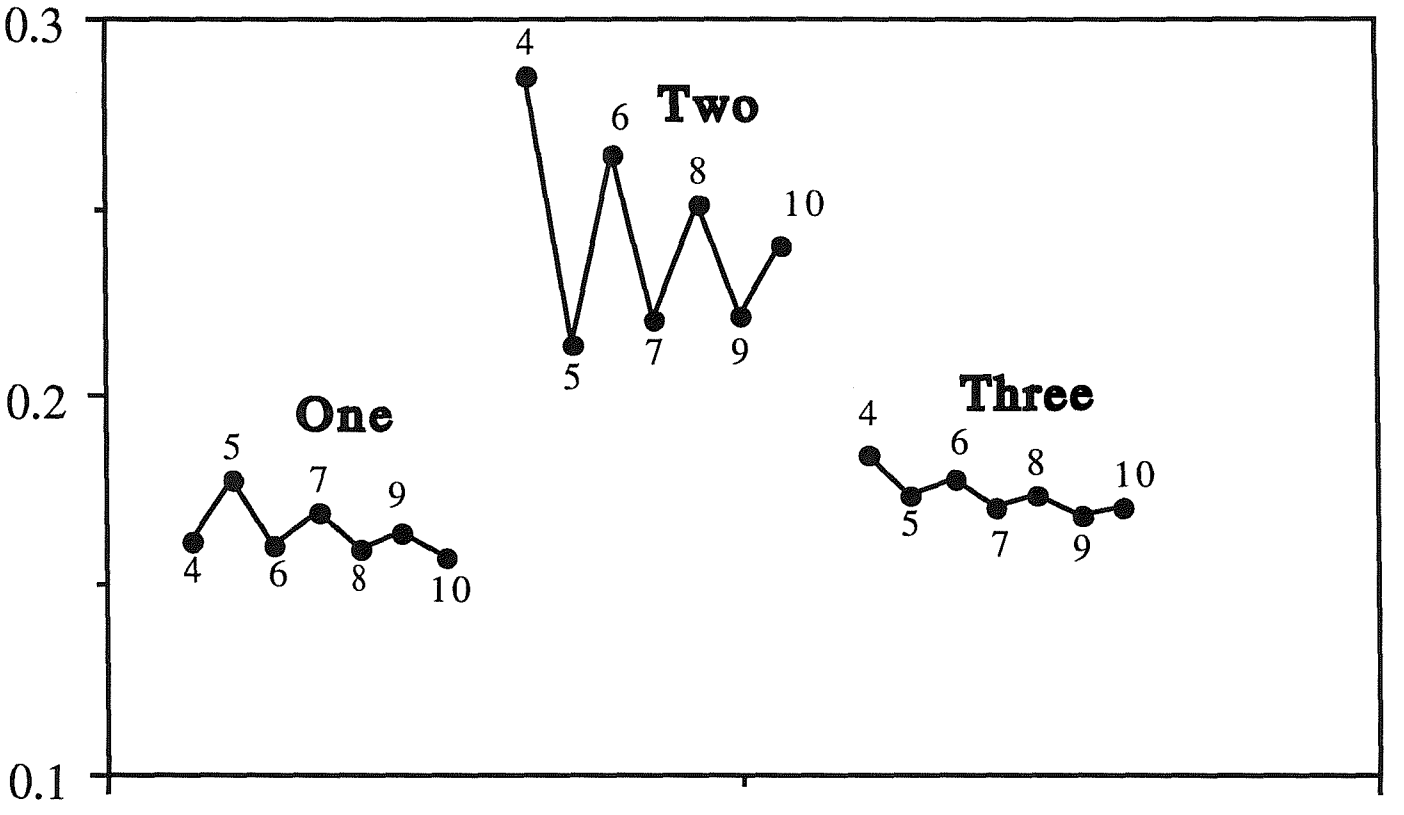

Figure 6. The variation of the scaled theoretical nematic-isotropic transition temperatures for the n^*,m^* trimers with the number of units in the spacer chains.

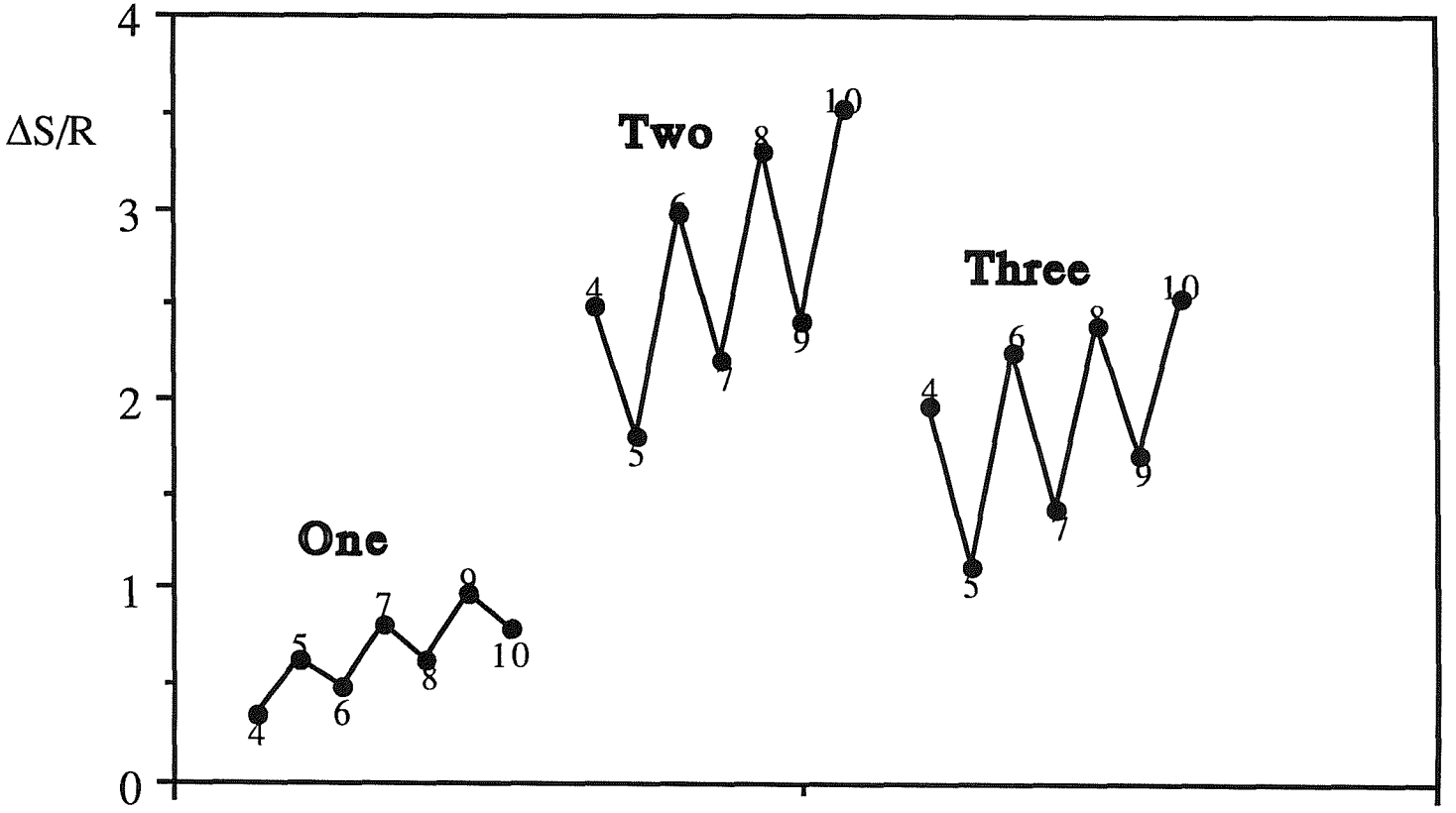

Figure 7. The variation of the theoretical nematic-isotropic entropy for the n^*, m^* trimers with the number of units in the spacer chains.

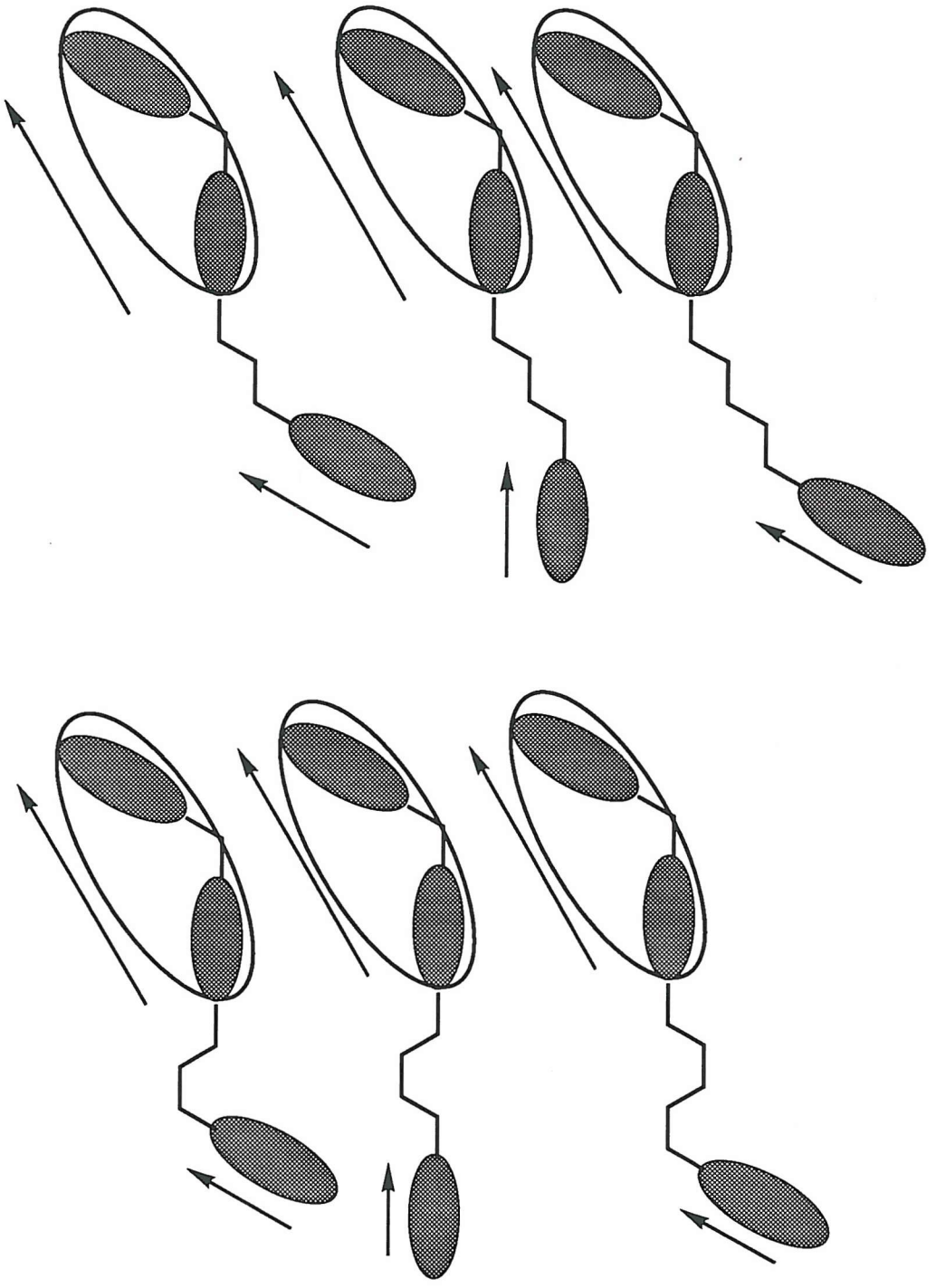

Figure 8. Caricatures of three early members of the $1^*,m^*$ series showing the enhanced anisotropy of molecular shape when the parity of m is odd (outer depictions). The arrows represent the long axes of the effective mesogenic groups.

4. Conclusions

The non-symmetric trimers described exhibit novel odd-even effects. The alternation in the transition temperature and entropy of transition is much smaller for the non-symmetric trimers than for their symmetric analogues, however they are in keeping with the symmetric dimers. Preliminary simulations of non-symmetric trimers show qualitative agreement with experiment [10], however, the simulation of the series of trimers in which the fixed length spacer is a single methylene group, shows a reversed odd-even effect. It has been proposed these trimers behave as dimers in which the long axes of the, now effectively, two mesogenic groups can align in a more parallel manner when the parity of the second chain is odd. Alternatively, theory could perhaps just fail. Transitional and such data will provide a valuable test-bed for molecular field theories for nematics formed from non-rigid molecules.

References

[1] Attard G.S., Douglass A.G., Imrie C.T., Taylor L., 1992, *Liq. Crystals*, **11**, 779.

[2] Furuya H., Asahi K., Abe A., 1986, *Polym. J.*, **18**, 779.

[3] Attard G.S., Imrie C.T., 1989, *Liq. Crystals*, **6**, 387.

[4] Toyne K.J., 1987, *Thermotropic Liquid Crystals*, Ed. Gray G.W., (John Wiley and sons) Chapter 2.

[5] Imrie C.T., *Unpublished work*, University of Southampton.

[6] Fan S., *Ph.D. Thesis*, 1992, University of Southampton.

[7] Attard G.S., Garnett S., Hickman C.G., Imrie C.T., Taylor L., 1990, *Liq. Crystals*, **7**, 495.

[8] Marcelja S., 1974, *J. Chem. Phys.*, **60**, 3599. Emsley J.W., Luckhurst G.R., Stockley C.P., 1982, *Proc. Roy. Soc. A.*, **381**, 117.

[9] Ferrarini A., Luckhurst G.R., Nordio P.L., Roskilly S.J., 1993, *Chem. Phys. Lett.*, **214**, 409.

[10] Emerson A., *Unpublished work*, University of Southampton.

CHAPTER 7

Naphthalene trimers

1. Introduction

The disubstituted naphthalene system was clearly shown to be conducive to the formation of liquid crystals in the 1950s in the case of the 6-n-alkoxy-2-naphthoic acids [1] (see figure 1). However, rather few other liquid crystal systems which incorporate this aryl unit were reported until 1976 when the relative merits of some 2,6-disubstituted naphthalene esters and 4,4'-disubstituted biphenyl ester systems both with terminal cyano groups were compared [2]. It was found that the naphthalene compounds generally had lower transition temperatures coupled with a reduced mesophase thermal stability.

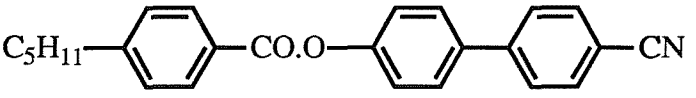

C 109°C N 238°C I

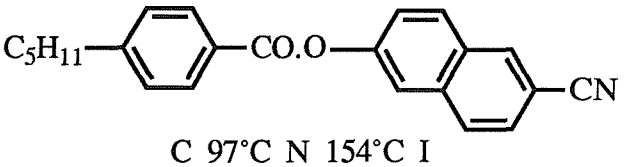

C 97°C N 154°C I

This effect was greatest when the naphthalene group was not part of the terminal cyano unit.

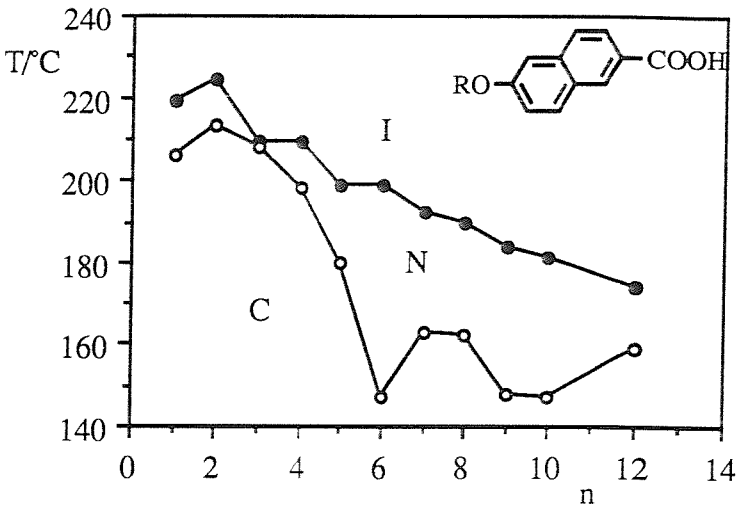

n	TCN/°C	TNI/°C
1	206	219
2	213	224
3	208	209
4	198	209
5	180	199
6	147	199
7	163	192
8	162	190
9	148	184
10	147	181
12	159	174

Figure 1. The transition temperatures for the 6-n-alkoxy-2-naphthoic acids.

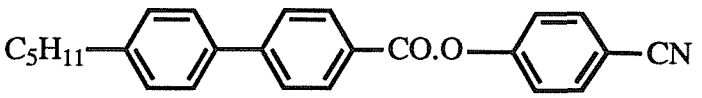

C 111°C N 229°C I

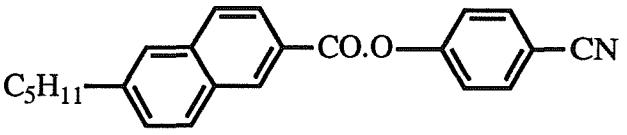

C 85°C N 140°C I

This lower liquid crystallinity was explained in terms of the naphthalene system being shorter and broader than the biphenylene system.

Mesogens that combine naphthalene and biphenylene ring systems exhibit very high nematic-isotropic transition temperatures, T_{NI}s, often decomposing before the clearing points are reached

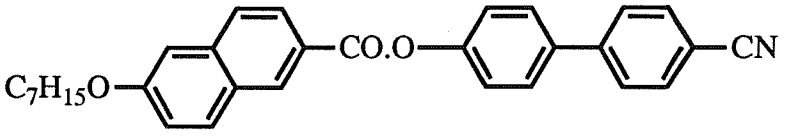

C 136°C N 304°C(d) I

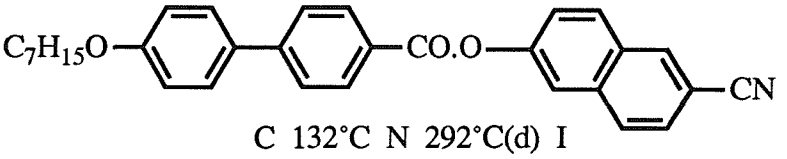

C 132°C N 292°C(d) I

Two biphenyl units produce still higher transition temperatures whereas two naphthalene units lower the clearing points considerably.

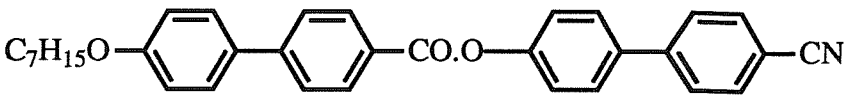

C 128°C N >3000°C(d) I

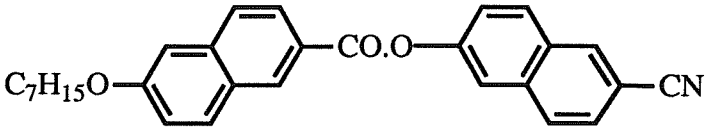

C 110°C N 216°C I

The enormous impact of the discovery of the 4-n-alkyl-4'-cyanobiphenyls and 4-n-alkyl-4"-cyano-p-terphenyls [3] on the display industry proved that the central linking group was not essential for the formation of liquid crystal phases. The 4-n-alkyl-4"-cyano-p-terphenyls have very high T_{NI} values and are excellent additives for increasing the clearing points of mesogenic mixtures, but these compounds also have high melting points and rather low solubilities which are less than desirable features. With this in mind Gray and Lacey [4] looked at the replacement of two of the phenyl rings with a naphthalene unit with a view that an overall advantage might be gained as a result of lowering the melting points. They found, as they had expected, that the mesogenic properties of a naphthalene group lay intermediate to those of a biphenyl and phenyl group .

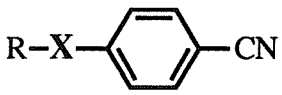

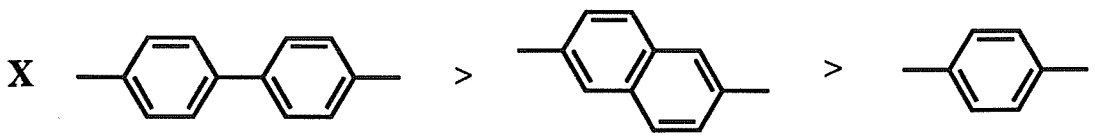

More recently the potential of technological applications has lead researchers to look more closely at naphtholenic mesogens [5]. Their very high optical anisotropy combined with ethynyl linking groups to increase the polarisability along the molecular

long axis has been shown to produce liquid crystals with a very high birefringence coupled with lower melting points that could possibly replace terphenyls in advanced display device applications.

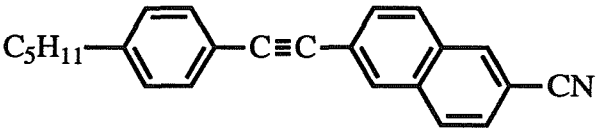

C 79.5°C N 164°C I

Birefringence - 0.40

The inclusion of a 2,3-disubstituted naphthalene group into a liquid crystal has been shown to promote both nematic and smectic A phases more than a single 1,2-phenyl ring for some Schiffs base-benzoate derivatives [6]. For the Schiffs base-benzoate derivative molecule shown below the substitution of a 1,2-phenyl group for the 2,3-naphthyl unit promoted the nematic phase by 85°C and the smectic A phase by 60°C.

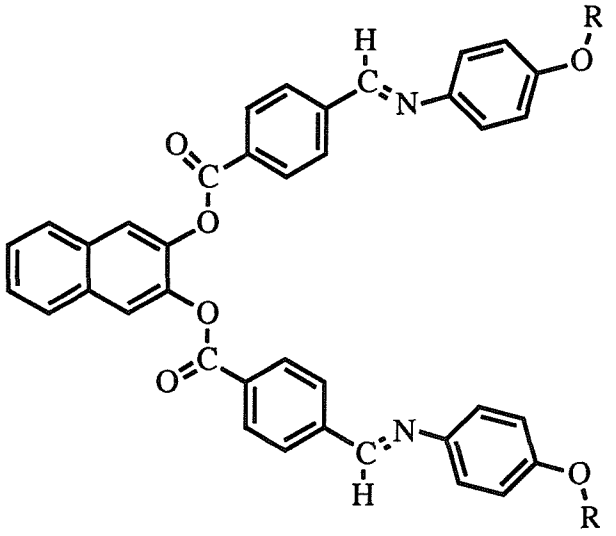

2,3-Naphthylene bis[4-(4-alkoxyphenyliminomethyl)benzoate.

The researchers also found, however, that the inclusion of naphthalene in the shorter 2,3-naphthalene bis(4-alkoxybenzoates) resulted in a reduction in liquid crystalline behaviour when compared to the 1,2-phenyl analogous series.

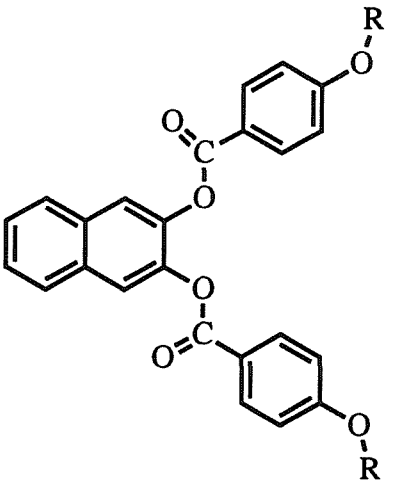

In contrast to the enantiotropic 1,2 phenyl bis(4-alkoxybenzoates), all members of this series were found to be monotropic

In the course of this study, no reference has been found that cites the naphthyl moiety as anything other than an extension of a mesogenic unit. To try and establish if a sole naphthalene group has any mesogenic ability in its own right this chapter reports the placement of a naphthyl unit into the centre of an essentially cyanobiphenyl terminated trimer connected through flexible alkyl spacers.

2. Experimental

Two series of trimers containing a central naphthyl group were prepared using; the 2,6 and the 2,7 sites of attachment, also one member of the 1,5 series was prepared, this however displayed only very monotropic properties and so no other members from this series were made. In keeping with the rest of this Thesis trimers containing the 1,8 and 2,3 disubstituted naphthyl unit were not synthesised as these would not produce elongated linear materials

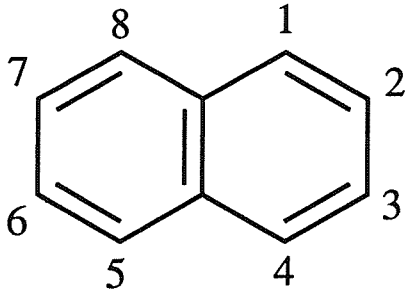

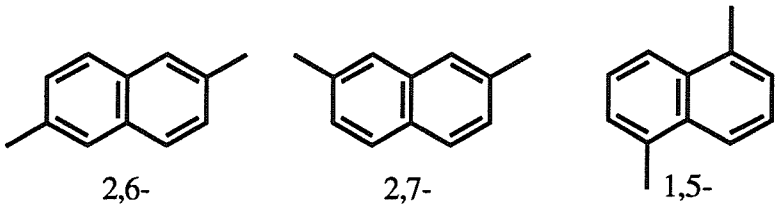

2,6- 2,7- 1,5-

The synthetic procedure and the reaction scheme show the synthesis of the 2,6-naphthalene trimers, however the same procedure was used for all three classes of trimer with a similar level of yield for each. The following synthetic route describes the addition of the alkyl chains initially to the naphthyl group and then the subsequent addition of the terminal cyanobiphenyl units. This order is reversed for trimers of similar construction described elsewhere in this thesis, however, for the naphthalene trimers this method was found to give a cleaner product in greater yield.

2.1 Synthesis of 2,6-bis(4'-cyanobiphenyl-4-butyloxy)naphthalene

Synthesis of 2,6-bis(ω-bromobutyloxy)naphthalene

2,6-dihydroxynaphthalene (1g, 0.0063mol) was dissolved in dry butanone. To this 1,4-dibromobutane (27g, 0.125mol) and anhydrous potassium carbonate, K_2CO_3, (6g, 0.04mol) were added. Following 8 h of stirring at reflux the mixture was filtered hot and the butanone was removed under reduced pressure. The excess 1,4-dibromobutane was recovered by distillation under vacuum to leave a crude white solid that was recrystallised twice from ethanol to leave pure 2,6-bis(ω-bromobutyloxy)naphthalene in 85% yield.

IR; loss of OH peak

^{1}H NMR; ($CDCl_3$, δ), 1.8-2.2 (4H, m), 3.3-3.6 (2H, q), 3.9-4.2 (2H, q), 7.0-7.2 (2H, m), 7.5-7.7 (1H, m).

Synthesis of 2,6-bis(4'-cyanobiphenyl-4-butyloxy)naphthalene

2,6-bis(ω-bromobutyloxy)naphthalene (1g, 0.0023mol) and 4-hydroxy-4'-cyanobiphenyl (0.95g, 0.0049mol) were dissolved in dry dimethyl formamide and K_2CO_3 (4g, 0.03mol) was added, this mixture was stirred at 120°C for 5 h. After cooling the reaction mixture was poured into cold water and the resulting precipitate filtered off and dried. The crude product was recrystallised from toluene and then passed through a flash silica column using dichloromethane as eluent. A final recrystallisation from toluene gave a material that produced a single spot on a thin layer chromotography plate in 50-60% yield.

IR; υ 2224 cm^{-1} (cyanide).

^{1}H NMR; ($CDCl_3$, δ) 1.6-2.1 (4H, m), 3.9-4.3 (4H, q), 6.9-7.2 (3H, m), 7.4-7.8 (8H, m) ppm

MS (EI, 70eV) 658 (M^+, 29%), 194 ($C_{13}H_8O$, 100%)

Reaction Scheme

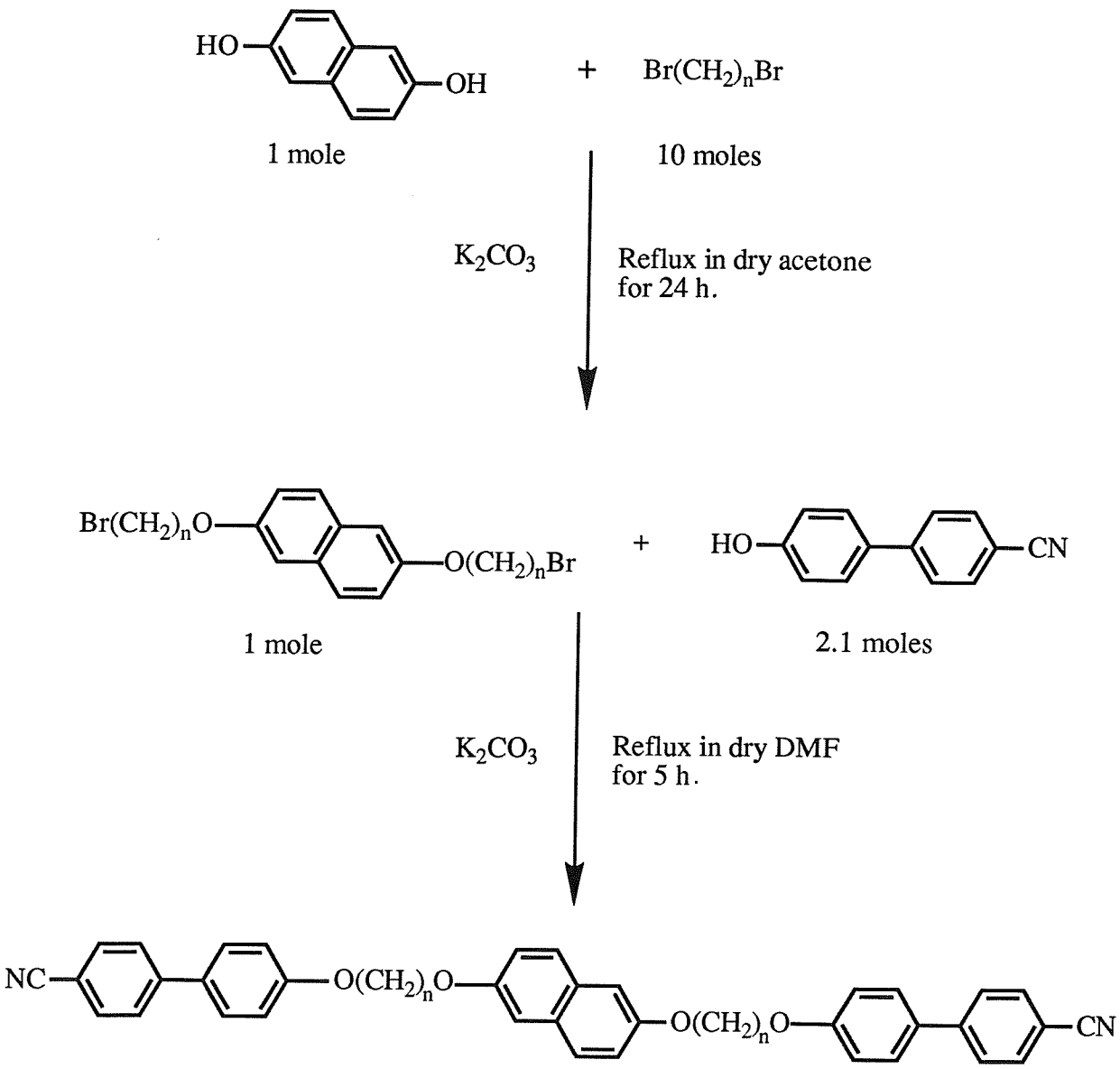

3. Results and discussion

The liquid crystal phase exhibited by all the materials discussed in this Chapter was classified as nematic, based on a typical 2 and 4 brush schlieren pattern and a homeotropic texture that flashed with mechanical stress, when viewed through a polarising microscope.

The transitional data for the two naphthalene trimer series are detailed in tables 1 and 2. It is seen from figure 2 that for the 2,6 series all but the 5 homologue exhibits an enantiotropic nematic phase. This contrasts with the 2,7 series in which only the 10 homologue shows an enantiotropic character. However, if we concentrate on just the nematic-isotropic transition temperatures (or isotropic-nematic), both series exhibit a classical odd-even effect which attenuates as n increases. The nematic-isotropic trnasition temperatures for the 2,7 series are consistently 60-70°C lower than those for the 2,6 series over all values of n and this is reflected in the entropy data depicted in figure 3 where the values of the 2,6 series are also consistently larger. The values of $\Delta S_{NI}/R$ again exhibit a classical odd-even effect, but here the level of alternation is considerably greater for the 2,6 series with generally smaller values for the 2,7 series.

It was mentioned in the introduction to this chapter that the 2,6 naphthyl unit was found to lie intermediate between the phenyl and biphenyl groups in promoting nematic thermal stability in some cyanophenyl terminated liquid crystal monomers. To explore whether this order holds true for the central unit of a trimeric liquid crystal we have superimposed the T_{NI}s (or T_{IN}s) of the trimers that have a central phenyl group [7] and those that have a central biphenyl group [8] onto a plot of the transition temperatures of the naphthalene trimers. From figure 4 it is apparent that the influence of the 2,6 naphthyl group on T_{NI} does indeed lie intermediate to the phenyl and biphenyl groups. The 2,7 series however, has transition temperatures significantly below those of all the aforementioned three series which indicates that the 2,7 naphthyl group actually inhibits liquid crystal formation or rather that the overall shape of the resulting trimer does.

Table 1. The transitional data for the 2,6-bis(4'-cyanobiphenyloxyalkyloxy)-naphthalenes.

n	T_{CN}/°C	T_{NI}/°C (T_{IN}/°C)	ΔH_{NI}/kJmol^{-1}	ΔS_{NI}/R
4	237	252	13.14	3.01
5	207	(195)	7.31	1.88
6	186	222	13.21	3.21
7	179	(179)	6.99	1.86
8	175	196	13.30	3.41
9	159	176	7.47	2.00
10	153	184	13.72	3.61
11	150	170	7.81	2.12
12	152	175	13.33	3.58

The uncertainties in the measurement of the transition temperatures are ±1°C, and the enthalpies and entropies of transition ±5%.

Table 2. The transitional data for the 2,7-bis(4'-cyanobiphenyloxyalkyloxy)-naphthalenes.

n	T_{CN}/°C	T_{NI}/°C (T_{IN}/°C)	ΔH_{NI}/kJmol^{-1}	ΔS_{NI}/R
4	181	(169)	4.26	1.16
5	153	(126)	2.45	0.74
6	158	(154)	4.79	1.35
7	132	(111)	2.62	0.82
8	133	(126)	4.61	1.39
9	123	(103)	2.79	0.89
10	110	116	5.40	1.67
11	104	(95)	3.05	1.00
12	105	(100)	5.12	1.65

The uncertainties in the measurement of the transition temperatures are ±1°C, and the enthalpies and entropies of transition ±5%.

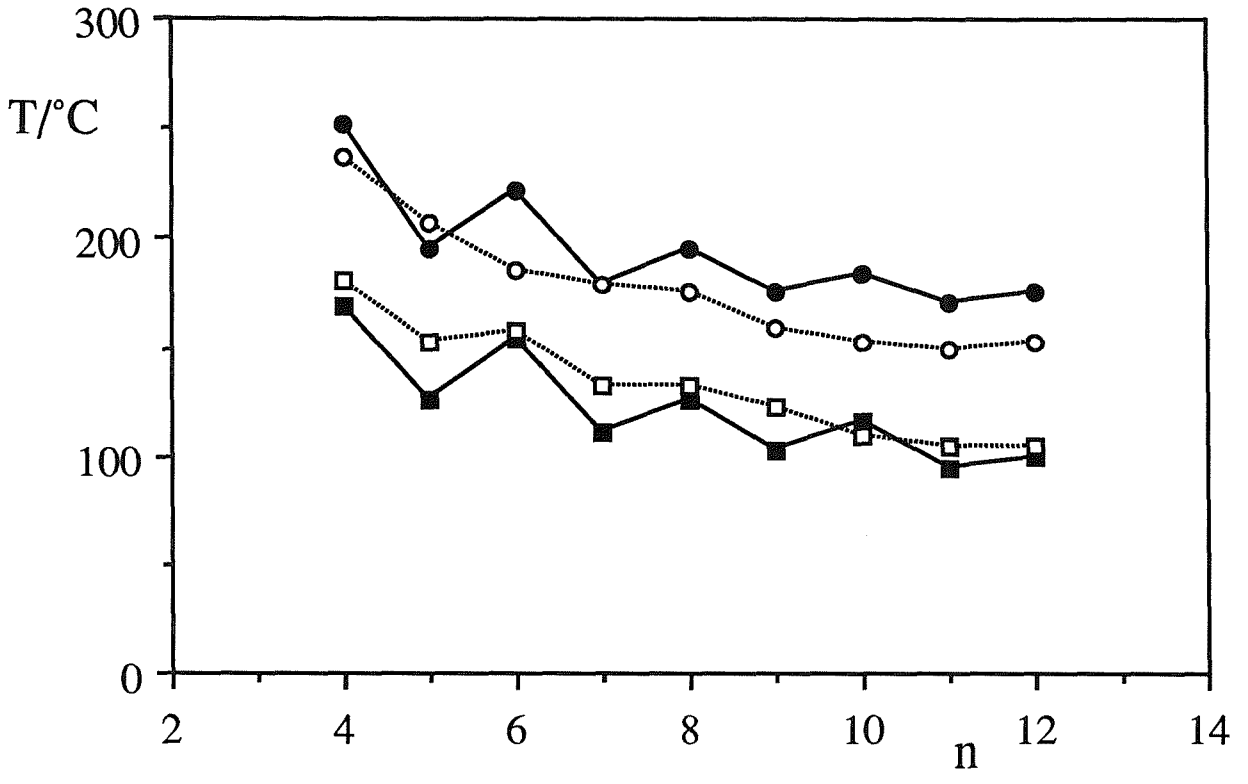

Figure 2. The nematic-isotropic (or isotropic-nematic) transition temperatures for the 2,6 series (●) and the 2,7 series (■). The crystal-nematic (or crystal-isotropic) transition temperatures are indicated by open symbols of the same shape connected through dotted lines. n is the number of methylene groups in each spacer.

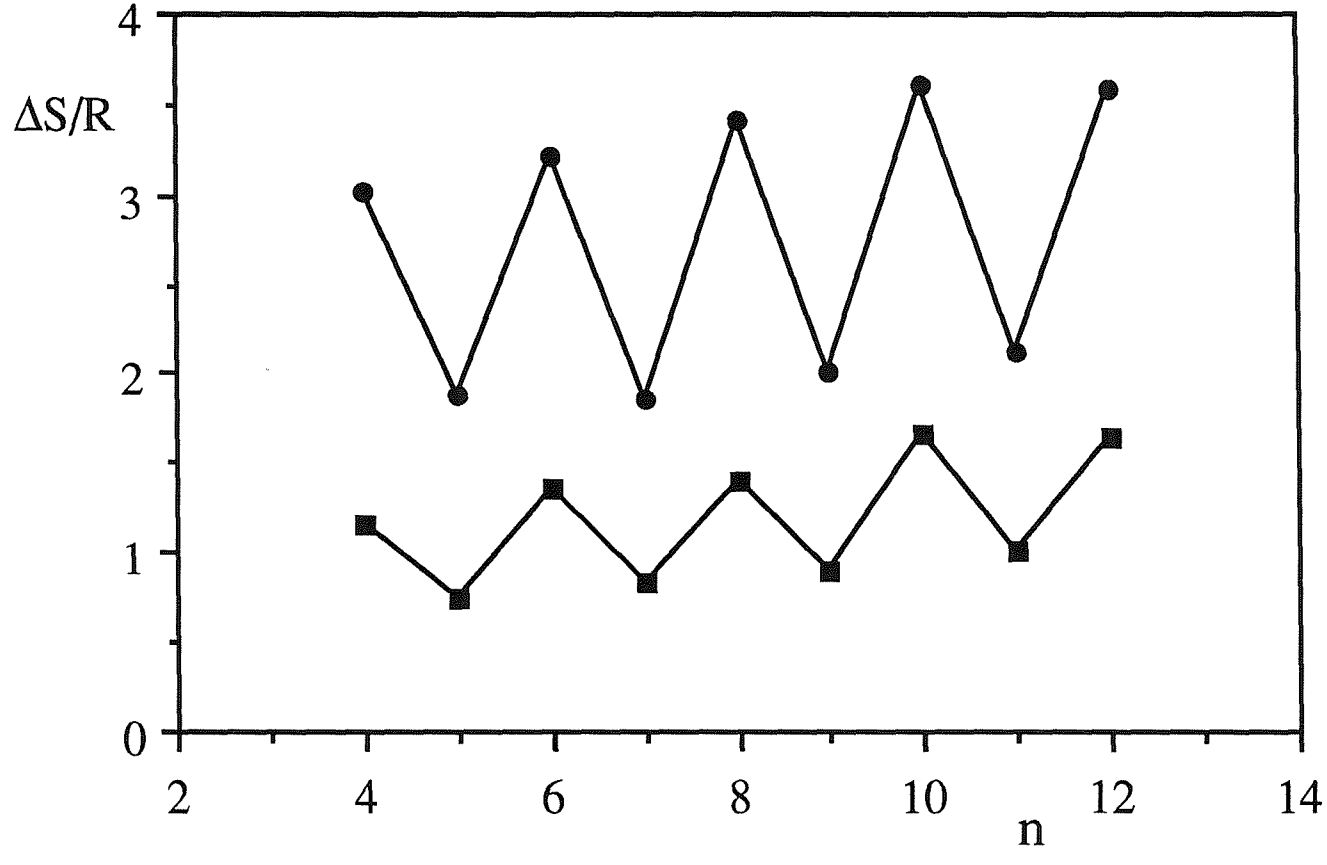

Figure 3. The nematic-isotropic (or isotropic-nematic) transitional entropies for the 2,6 series (●) and the 2,7 series(■). n is the number of carbon atoms in each alkyl chain.

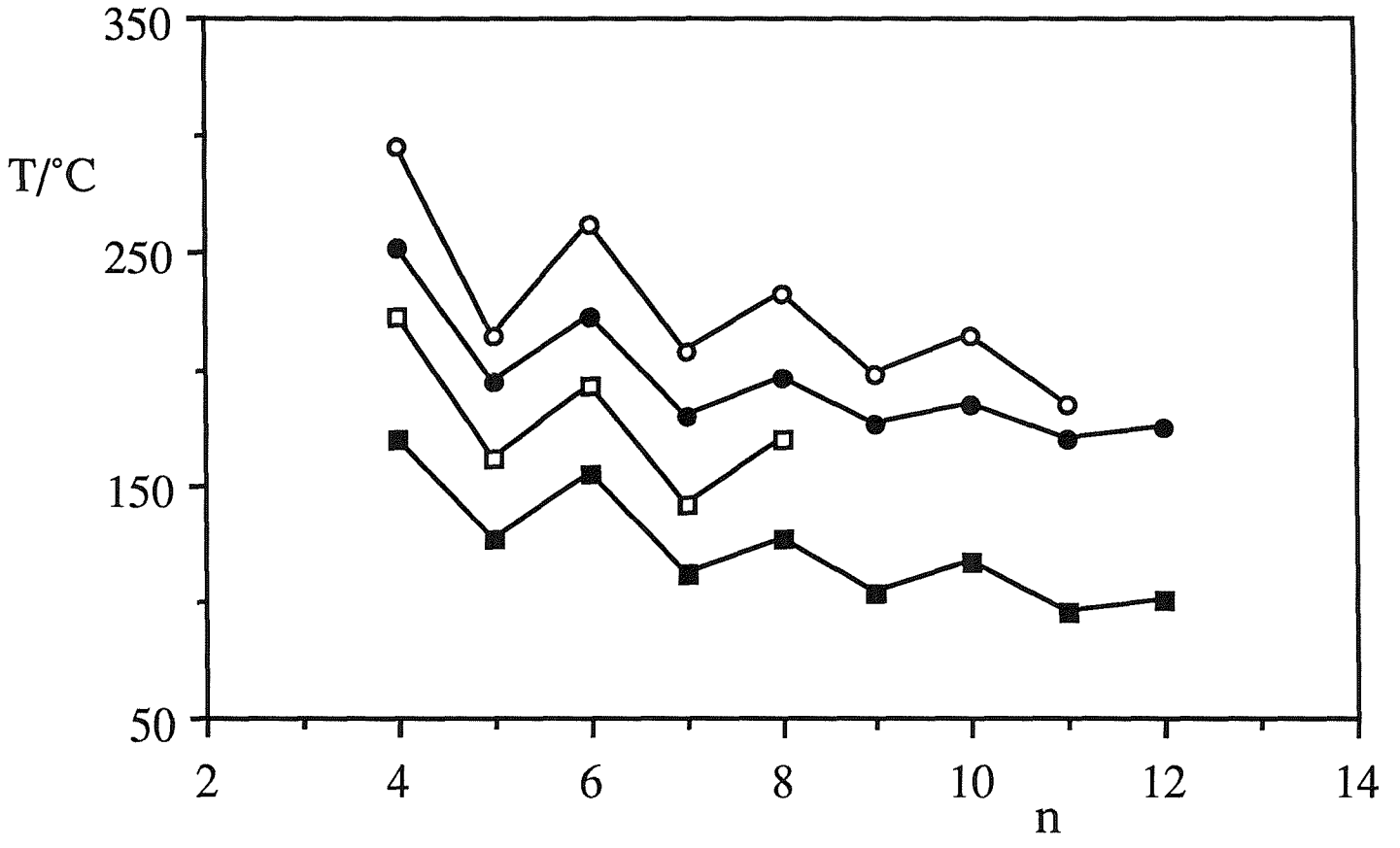

Figure 4. The nematic-isotropic (or isotropic-nematic) transition temperatures for the four series of cyanobiphenyl terminated trimers whose central mesogenic units are in descending order; 4,4'-biphenyl (○), 2,6-naphthyl (●), 1,4-phenyl (□), and 2,7-naphthyl (■).

If we consider the all-trans caricatures of the 2,6 and 2,7 naphthalene trimers in figure 5 we see that for the 2,6 series the two terminal cyanobiphenyl groups always lie parallel to one another for both odd and even spacers, although the anisotropy of the molecule as a whole is reduced when the spacer is odd as the long axis of the naphthyl unit makes a greater angle with that of either long axis for the terminal groups. The two sketches for each molecule exaggerate the change in molecular shape for two conformers which differ only in the direction the initial link of the alkyl chain takes from the oxygen atom adjacent to the naphthyl group, these two conformers are expected to be equally populated at any one time. The caricatures of the 2,7 series on the other hand suggest that none of the three mesogenic units align parallel to one another for the idealised all trans state depicted here. The second of the 2,7 odd drawings however, displays the terminal groups as aligning in a parallel fashion but this highly unanisotropic shape is not thought to aid liquid crystal formation. The reduced alternation in the values of $\Delta S_{NI}/R$ for the 2,7 series might be an effect of the similarity in shape of the odd and the even trimers.

If we now introduce the only 1,5 naphthalene trimer prepared we can see that it is barely liquid crystalline

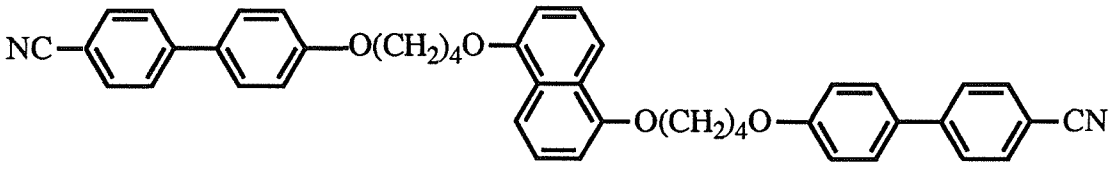

T_{CI} - 210°C T_{IN} - 144°C T_{NC} - 142°C

As we saw for the 2,6 naphthalene trimers the terminal mesogenic units of this series can align parallel to one another, this is reflected in the relatively high melting point, however the large perpendicular step this group introduces into the molecule virtually destroys any liquid crystalline character although the 70°C hysteresis of crystallisation suggests that a certain degree of anisotropy does exist within the molecule .

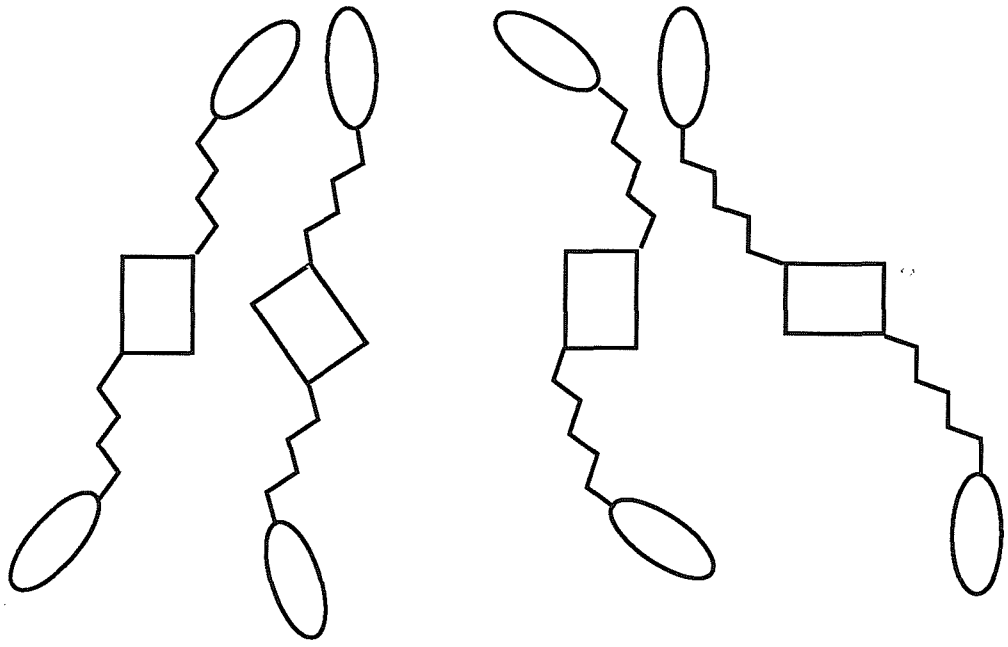

2,6 even

2,6 odd

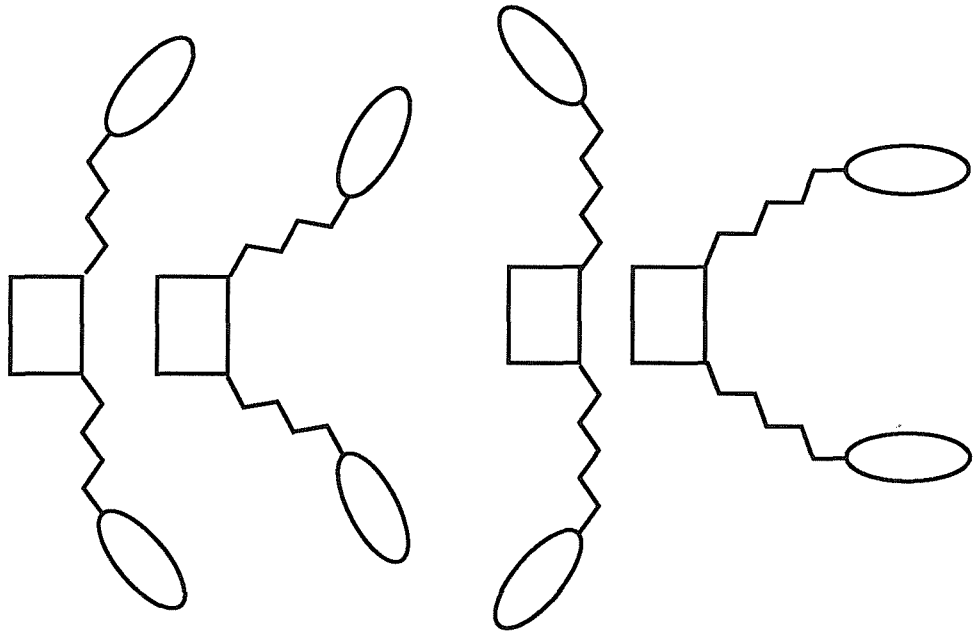

2,7 even

2,7 odd

Figure 5. Diagram of some all-trans caricatures for the 2,6 and 2,7 naphthalene trimers with both odd and even spacers emphasising the diversity of shape depending on the direction the alkyl chain takes when coming from the central naphthyl unit, which here is emphasised as a biaxial box.

The reduction in both the transition temperatures and the nematic ranges of the naphthalene trimers compared to their biphenyl counterparts cannot be explained solely on a geometric level, the naphthyl unit can be thought of as a highly biaxial group that broadens the structure

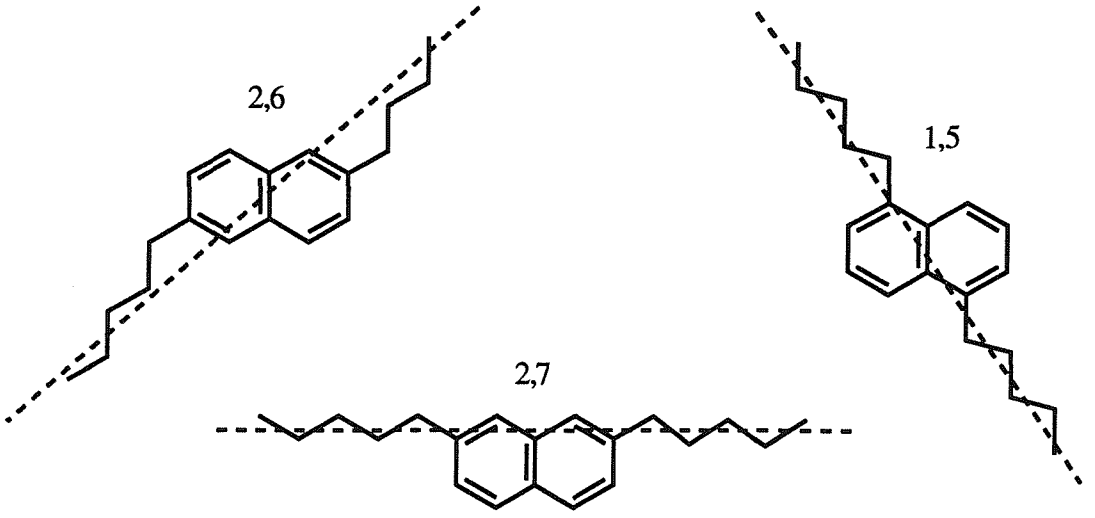

The dotted lines represent pathways through the naphthyl units if they were considered as alkyl chains, here, for an idealised all-trans conformation. It is apparent from these drawings that, to varying degrees, part of each naphthyl unit is superfluous to requirements and just serves to broaden the chain. This is particularly pronounced in the 1,5 and 2,7 moieties. However, we envisage the presence of gauche± links to reduce the redundant area of the naphthyl unit more in the 2,7 system than the 1,5 system.

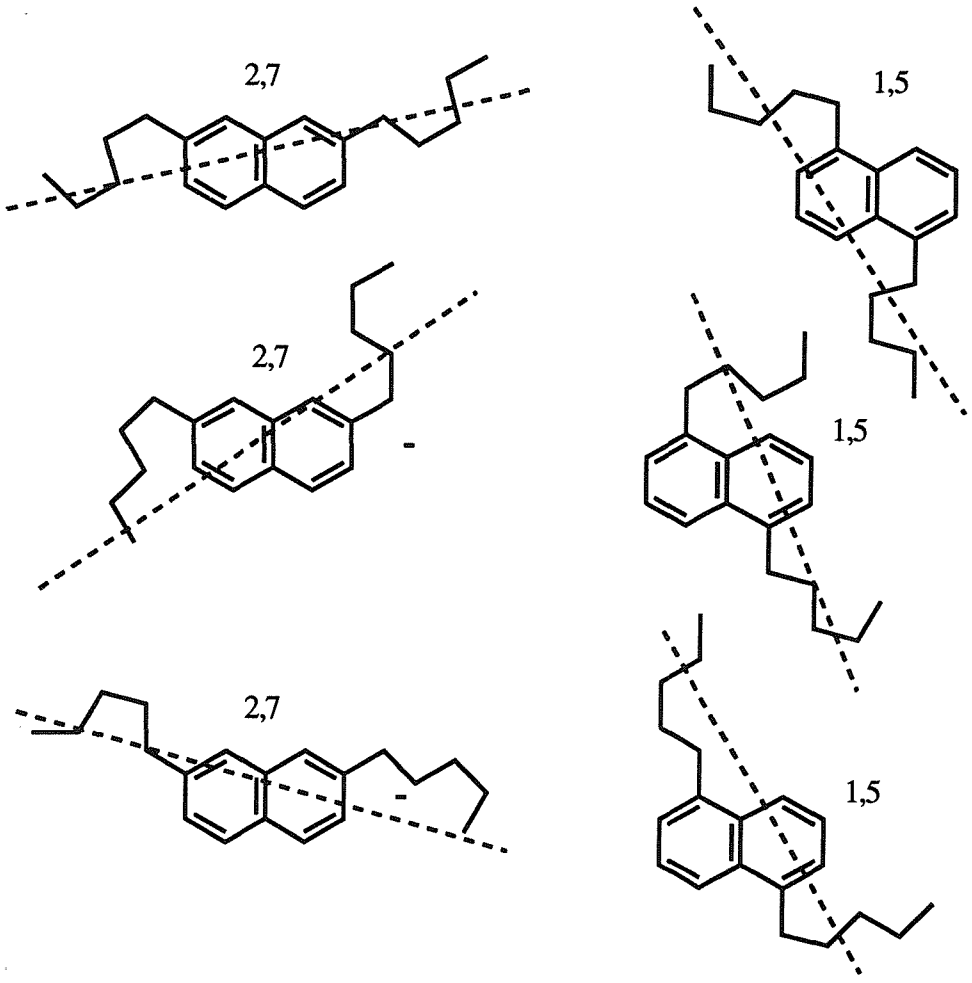

Hence we can argue that the 1,5 unit is the most biaxial of the three naphthalene groups studied.The off axis bonds of the 2,6 and the 2,7 disubstituted naphthalene unit serve to increase the number of permutations in molecular shape that the trimers can adopt. The trimer comprising the axially symmetric 4,4'-biphenyl unit maintains the same level of anisometry which ever way the all-trans alkyl chain joins the central unit. This extra degree of freedom, coupled with the relatively high biaxiality of the naphthyl group, reduces the transition temperatures and the liquid crystallinity of this class of compounds.

If we now return to the entropy data, in particular the high values of the 2,6 series. We have seen that for the even trimers, the mesogenic groups can align parallel to one another, the level of these entropy data are significantly greater than those of the 2,7 series for both odd and even spacers. This high level of order within the 2,6 trimers is

consistent with a theory that proposes that, within a liquid crystal, there is a coupling between the conformational distribution and the long range orientational order [9]. In the isotropic liquid there is a proportion of linear conformers in both odd and even trimers. The coupling results in the more elongated conformers being favoured over the bent ones within a liquid crystal phase and that the strength of the nematic-isotropic transition depends upon the extent of interconversion between these linear and bent conformers at the transition. For the 2,6 trimers, the large difference in the strength of transition on going from an odd to an even trimer is dependent on the mole fraction of linear conformers in each trimer. For an even trimer, the relatively high concentration of the linear component in the isotropic phase is further increased with the orientational order brought about by entry into the nematic phase. This produces a high entropy of transition. In an odd trimer, the concentration of the linear component in the isotropic phase is less than for the even such that the orientational order in the nematic phase cannot produce such a large change in this concentration, therefore, the entropy of transition for the odd trimer is relatively low. The essence of high entropy (and hence order) is the presence of bent conformers which depress T_{NI} for the system of linear conformers. At the transition to the nematic phase the onset of orientational order changes the bent to linear conformers, this necessarily increases T_{NI} and hence the order and the entropy. Such changes can, however, only occur if the concentration of the linear component in the isotropic phase is neither too large or too small. These changes account for the high entropy of the 2,6 series where the concentration of linear conformers is expected to be higher than that for the 2,7 series.

4. Conclusions

This chapter has shown us that a disubstituted naphthalene unit employed as the central mesogenic group in a liquid crystal trimer reduces both the transition temperatures and the mesogenic range of the trimer relative to a 4,4'-biphenyl unit. The 2,6 naphthyl group lies intermediate to the 4,4'-biphenyl and the 1,4 phenyl in terms of mesogenic ability whereas the 2,7 naphthyl group is a poorer liquid crystal than all the above three. By sketching some idealised all-trans molecular shapes of these novel mesogens we have shown that the step the naphthalene group introduces into the structure coupled with the broadening effect of this biaxial group results in trimers whose mesogenic groups cannot all align simultaneously. In addition the increased number of low energy conformations that result in poorly anisotropic shapes further hinders the formation of a large, stable nematic range such as is seen for the analogous 4,4'-biphenyl trimers. The formation of an enantiotropic phase depends on T_{NI} and T_{CN}, where T_{NI} is high but T_{CI} is higher then it will seem as if the group does not promote liquid crystalline behaviour. This effect is particularly accentuated in the 1,5 trimer and the 2,7 series.
The difference in the entropy levels for the two series has been discussed in terms of the concentration of the linear component in the 2,6 series being higher than that for the 2,7 series.

References

[1] Gray G.W., Jones B., 1954, *J. Chem. Soc.*, 683, and 236 (1955).

[2] Coates D., Gray G.W., 1976, *Mol. Cryst. Liq. Cryst.*, **37**, 249.

[3] Gray G.W., Harrison K.J., Nash J.A., 1974, *Liquid Crystals and Ordered Fluids*, (Eds., Johnson J.F. and Porter R.S.), Plenum Press, New York, vol. **2**, 617.

[4] Gray G.W., Lacey D., 1983, *Mol. Cryst. Liq. Cryst.*, **99**, 123.

[5] Hird M., Toyne K.J., Gray G.W., Day S.E., McDonnell D.G., 1993, *Liq. Crystals*, **15**, 123.

[6] Matsuzaki H., Matsunaga Y., 1993, *Liq. Crystals*, **14**, 105.

[7] Furuya H., Asahi K., Abe A., 1986, *Polym. J.* **18**, 779.

[8] Fan S.M., Emerson A., Heeks S.K., Imrie C.T., Luckhurst G.R., 1990, Presented at the 13th International Liquid Crystal Conference, Vancouver.

[9] Ferrarini A., Luckhurst G.R., Nordio P.L., Roskilly S.J., 1993, *Chem. Phys. Lett.*, **214**, 409.

Appendix A

The splittings and order parameters obtained for anthracene-d_{10} dissolved in dimeric liquid crystal solvents and those obtained from CB6OCB-d_2 as detailed in Chapter 3.

Table 1. Anthracene-d_{10} in CBO4OCB.

$(T_{NI}-T)/°C$	$\Delta\nu_{\alpha,\gamma}$ / Hz	$\Delta\nu_{\beta}$ / Hz	S_{zz}	$S_{xx}-S_{yy}$
0	21801	79760	0.398	0.228
1	22167	82177	0.410	0.237
2	23242	83325	0.417	0.235
3	24218	84399	0.423	0.234
4	24707	85351	0.428	0.236
5	25585	86401	0.434	0.235
6	26465	86938	0.437	0.232
7	26489	88037	0.442	0.237
9	28198	90136	0.454	0.236
11	29443	91796	0.464	0.236
13	30761	93041	0.471	0.234
17	33349	95776	0.487	0.231
21	35449	98339	0.501	0.230
25	37475	100592	0.514	0.229
30	39965	103077	0.529	0.224
35	42236	105323	0.542	0.221
45	46264	109644	0.567	0.217

Table 2. Anthracene-d_{10} in CBO5OCB.

$(T_{NI}-T)$ / °C	$\Delta\nu_{\alpha,\gamma}$ / Hz	$\Delta\nu_{\beta}$ / Hz	S_{zz}	$S_{xx}-S_{yy}$
0	54037	13581	0.268	0.161
1	60474	16205	0.302	0.174
2	62570	17243	0.312	0.178
3	65281	18371	0.327	0.183
6	70367	21056	0.353	0.190
8	71846	21941	0.361	0.192
10	74740	23895	0.377	0.193
12	76563	24963	0.382	0.190
14	78967	26691	0.400	0.192
16	81001	28105	0.412	0.193
18	83036	29784	0.423	0.190
20	84823	30975	0.433	0.196
22	85903	31920	0.439	0.196
25	88213	33874	0.452	0.194
28	90124	35644	0.463	0.192
31	91850	37200	0.473	0.191
34	93731	38970	0.484	0.189
37	95642	40740	0.495	0.187

Table 3. Anthracene-d_{10} in CB6CB.

$(T_{NI} - T)$ / °C	$\Delta\nu_{\alpha,\gamma}$ / Hz	$\Delta\nu_{\beta}$ / Hz	S_{zz}	$S_{xx} - S_{yy}$
0	95001	29754	0.479	0.249
1	95459	30243	0.482	0.248
2	95978	31219	0.485	0.244
3	96588	31311	0.488	0.247
4	97442	32074	0.493	0.246
5	98412	32475	0.498	0.248
6	98877	33172	0.501	0.246
8	100006	34454	0.508	0.243
10	101287	35675	0.515	0.242
12	101990	36713	0.520	0.239
14	103424	37689	0.528	0.240
19	105743	39611	0.541	0.239
24	109528	42511	0.562	0.239
29	110076	44769	0.567	0.228
34	111907	46539	0.578	0.226
39	113830	48339	0.589	0.224

Table 4. Anthracene-d_{10} in CB7CB.

$(T_{NI}$ -T)/ °C	$\Delta\nu_{\alpha,\gamma}$ / Hz	$\Delta\nu_{\beta}$ / Hz	S_{zz}	S_{xx} -S_{yy}
0	44738	13092	0.224	0.122
1.5	49713	15411	0.250	0.131
3.5	53894	17547	0.273	0.137
5.5	56396	19134	0.286	0.139
7.5	58380	20416	0.297	0.140
9.5	59692	21515	0.304	0.140
10.5	62835	23956	0.321	0.140
11	63079	24627	0.323	0.137
11.5	63324	25024	0.326	0.135
12	63629	25268	0.327	0.135
12.5	63812	25665	0.329	0.134
13	63934	26000	0.330	0.132
13.5	64208	26306	0.331	0.132
14	64361	26672	0.332	0.130
14.5	64442	26763	0.333	0.130
15	64605	27038	0.334	0.129
15.5	64667	27374	0.335	0.128
16.5	65032	27893	0.337	0.126
17.5	65124	28259	0.338	0.124

Table 5. Anthracene-d_{10} in CB3OCB

$(T_{NI}-T)$/ °C	$\Delta\nu_{\alpha,\gamma}$ / Hz	$\Delta\nu_{\beta}$ / Hz	S_{zz}	$S_{xx}-S_{yy}$
0	23986	83587	0.428	0.231
5	25909	86700	0.445	0.233
10	28900	90423	0.467	0.232
15	31491	93475	0.485	0.230
20	33841	96252	0.501	0.228
30	38513	101257	0.431	0.223
40	41931	105285	0.554	0.220
50	45837	109039	0.577	0.214
60	49224	112640	0.599	0.210
70	52551	115692	0.617	0.201
80	56243	119018	0.638	0.196
90	59753	121887	0.656	0.188
100	63323	124603	0.674	0.179

Table 6. Anthracene-d_{10} in CB4OCB.

$(T_{NI}-T)$/ °C	$\Delta\nu_{\alpha,\gamma}$ / Hz	$\Delta\nu_{\beta}$ / Hz	S_{zz}	$S_{xx}-S_{yy}$
0	11669	33200	0.173	0.079
1	13476	42607	0.220	0.110
2	15405	44897	0.233	0.109
4	18457	51538	0.269	0.120
7	21386	56909	0.298	0.127
10	25219	65257	0.343	0.141
14	27172	68286	0.359	0.143
18	28784	70898	0.374	0.145

Table 7. Anthracene-d_{10} in CB5OCB.

$(T_{NI}-T)$/ °C	$\Delta\nu_{\alpha,\gamma}$ / Hz	$\Delta\nu_{\beta}$ / Hz	S_{zz}	$S_{xx}-S_{yy}$
0	28533	87280	0.451	0.220
1	28747	87310	0.452	0.219
2	29235	87921	0.455	0.219
3	29907	88867	0.461	0.219
4	30700	89904	0.467	0.219
5	31555	90911	0.473	0.218
6	32226	91949	0.478	0.219
8	33843	93902	0.490	0.218
11	36133	96801	0.506	0.217
16	39276	100616	0.529	0.215
21	42755	103790	0.548	0.209
26	45868	107110	0.568	0.205
31	48523	109860	0.585	0.210
36	51269	112510	0.601	0.197
41	53649	114960	0.615	0.194
46	56396	117460	0.631	0.188
56	60028	120810	0.651	0.182

Table 8. Anthracene-d_{10} inCB6OCB

$(T_{NI}-T)$/ °C	$\Delta\nu_{\alpha,\gamma}$ / Hz	$\Delta\nu_{\beta}$ / Hz	S_{zz}	$S_{xx}-S_{yy}$
0	13477	48926	0.251	0.154
1	15723	54635	0.281	0.168
2	17188	58105	0.300	0.176
3	18408	60400	0.312	0.180
5	20556	64453	0.334	0.186
7	22413	67627	0.352	0.190
9	24073	70166	0.366	0.193
11	25439	72070	0.377	0.193
13	26757	74121	0.388	0.195
15	27925	75634	0.397	0.196
17	29150	77247	0.406	0.196
19	30224	78564	0.414	0.196
21	31396	79883	0.422	0.195
23	32421	81055	0.428	0.195
25	33446	82031	0.434	0.193
27	34375	82958	0.440	0.192
29	35254	83789	0.445	0.191
31	36132	84521	0.450	0.189
33	36914	85058	0.453	0.187
35	37647	84958	0.456	0.185
37	38281	85791	0.458	0.182
39	39013	85693	0.459	0.177
41	39013	84327	0.452	0.171
43	39209	83301	0.447	0.165
45	39551	82666	0.445	0.160
47	39941	82275	0.443	0.155
49	40332	81983	0.442	0.152
51	40674	81885	0.442	0.149
53	41211	81738	0.442	0.145

Table 9. CB6OCB-d_2

$(T_{NI}-T)$/ °C	$\Delta\nu_{dip}$ / Hz	$\Delta\nu_{quad}$ / Hz	S_{zz}	$S_{xx}-S_{yy}$
0	500	4460	0.207	0.033
1	629	5155	0.261	0.046
2	685	5671	0.284	0.050
3	741	6019	0.307	0.055
5	798	6516	0.331	0.059
8	863	7174	0.358	0.063
12	910	7803	0.377	0.064
17	948	8451	0.393	0.063
27	1004	9221	0.416	0.064
37	1023	9746	0.424	0.062
45	1023	9812	0.424	0.061
47	985	9746	0.385	0.048
48	957	9652	0.383	0.048
49	957	9662	0.381	0.047
50	957	9634	0.383	0.048
51	957	9626	0.377	0.046
52	929	9615	0.375	0.045
55	873	9624	0.367	0.042
60	873	9690	0.367	0.042
65	873	9831	0.362	0.038
70	880	9906	0.365	0.039

Table 10. Magnified region of CB6OCB-d_2 close to the smectic transition.

$(T_{NI-45}-T)$/ °C	$\Delta\nu_{dip}$/Hz	$\Delta\nu_{quad}$/Hz	S_{zz}	S_{xx} -S_{yy}
0.0	1080	9821	0.448	0.070
0.5	1070	9859	0.444	0.068
1.0	1042	9840	0.432	0.064
1.5	957	9831	0.397	0.051
2.0	948	9840	0.393	0.050
2.5	929	9803	0.385	0.047
3.0	948	9840	0.393	0.050
3.5	957	9821	0.395	0.051
4.0	948	9803	0.393	0.050
4.5	948	9756	0.393	0.050
5.0	929	9709	0.385	0.048
5.5	939	9699	0.389	0.050
6.0	929	9634	0.385	0.049
6.5	939	9634	0.389	0.050
7.0	939	9615	0.389	0.050
7.5	929	9587	0.385	0.049
8.0	929	9596	0.385	0.049
8.5	929	9596	0.385	0.049
9.0	920	9605	0.381	0.048

Appendix B

The splittings and order parameters obtained for specifically deuteriated trimers detailed in Chapter 5.

Table 1. End deuteriated trimer 3.

$(T_{NI}-T)/°C$	$\Delta\nu_{dip}/Hz$	$\Delta\nu_{quad}/Hz$	S_{zz}	$S_{xx}-S_{yy}$
0	773	6042	0.320	0.060
1	895	6652	0.371	0.072
2	935	7059	0.388	0.074
3	984	7385	0.408	0.079
4	1037	7710	0.430	0.084
7	1091	8280	0.452	0.086
10	1125	8870	0.466	0.086
14	1156	9379	0.479	0.086
18	1184	9847	0.491	0.085
23	1220	10355	0.506	0.086
28	1258	10864	0.522	0.087
33	1281	11230	0.531	0.087
38	1289	11718	0.534	0.083
43	1295	12023	0.537	0.081
48	1300	12349	0.539	0.079

Table 2. Middle deuteriated trimer 3.

$(T_{NI}-T)/°C$	$\Delta\nu_{dip}/Hz$	$\Delta\nu_{quad}/Hz$	S_{zz}	$S_{xx}-S_{yy}$
0	465	5671	0.193	0.016
1	582	5878	0.241	0.032
2	619	6206	0.257	0.035
3	657	6507	0.272	0.037
4	685	6779	0.284	0.039
5	715	6929	0.296	0.042
6	741	7155	0.307	0.044
7	772	7380	0.320	0.047
8	793	7683	0.329	0.049
11	826	7925	0.342	0.050
15	858	8385	0.356	0.050
19	881	8779	0.365	0.050
23	914	9033	0.379	0.052
27	939	9399	0.389	0.053
32	962	9662	0.399	0.053
37	989	9850	0.410	0.056
42	1010	10225	0.419	0.055
47	1023	10394	0.424	0.056
52	1030	10620	0.427	0.055

Table 3. End deuteriated trimer 5

$(T_{NI}-T)/°C$	$\Delta\nu_{dip}/Hz$	$\Delta\nu_{quad}/Hz$	S_{zz}	$S_{xx}-S_{yy}$
0	816	6516	0.388	0.062
1	895	7446	0.371	0.065
2	967	7962	0.401	0.071
3	993	8328	0.412	0.071
4	1020	8620	0.423	0.073
5	1051	8948	0.436	0.074
6	1072	9211	0.444	0.075
7	1091	9380	0.452	0.076
9	1121	9925	0.465	0.075
11	1138	10404	0.472	0.073
13	1153	10761	0.478	0.072
17	1188	11099	0.493	0.074
22	1236	11784	0.512	0.075
27	1271	12348	0.527	0.075
32	1305	12845	0.541	0.075
37	1330	13352	0.551	0.074
42	1354	13521	0.561	0.076
47	1370	13869	0.568	0.075
52	1390	14282	0.576	0.074
57	1408	14545	0.584	0.074

Table 4. Middle deuteriated trimer 5

$(T_{NI}-T)/°C$	$\Delta\nu_{dip}/Hz$	$\Delta\nu_{quad}/Hz$	S_{zz}	$S_{xx}-S_{yy}$
0	638	8216	0.265	0.018
1	721	9209	0.299	0.021
2	788	9221	0.327	0.031
3	827	9568	0.343	0.034
4	852	9850	0.353	0.035
5	873	10056	0.362	0.036
6	895	10206	0.371	0.038
7	915	10488	0.379	0.038
8	931	10732	0.386	0.038
10	963	11033	0.399	0.040
14	998	11549	0.414	0.040
18	1023	11944	0.424	0.041
22	1046	12385	0.434	0.040
26	1067	12563	0.442	0.041
30	1095	12977	0.454	0.042
35	1117	13192	0.463	0.043
40	1132	13549	0.469	0.042
45	1150	13850	0.477	0.042
50	1164	14075	0.483	0.042